frontiers | Research Topics

Cannabidiol treatment in neurotherapeutic interventions, volume II

Edited by
Gustavo Gonzalez-Cuevas, Jorge Manzanares, Maria S. Garcia-Gutierrez, Francisco Navarrete and Giordano de Guglielmo

Published in
Frontiers in Pharmacology

ISSN 1664-8714
ISBN 978-2-83251-860-1
DOI 10.3389/978-2-83251-860-1

About Frontiers

Frontiers is more than just an open access publisher of scholarly articles: it is a pioneering approach to the world of academia, radically improving the way scholarly research is managed. The grand vision of Frontiers is a world where all people have an equal opportunity to seek, share and generate knowledge. Frontiers provides immediate and permanent online open access to all its publications, but this alone is not enough to realize our grand goals.

Frontiers journal series

The Frontiers journal series is a multi-tier and interdisciplinary set of open-access, online journals, promising a paradigm shift from the current review, selection and dissemination processes in academic publishing. All Frontiers journals are driven by researchers for researchers; therefore, they constitute a service to the scholarly community. At the same time, the *Frontiers journal series* operates on a revolutionary invention, the tiered publishing system, initially addressing specific communities of scholars, and gradually climbing up to broader public understanding, thus serving the interests of the lay society, too.

Dedication to quality

Each Frontiers article is a landmark of the highest quality, thanks to genuinely collaborative interactions between authors and review editors, who include some of the world's best academicians. Research must be certified by peers before entering a stream of knowledge that may eventually reach the public - and shape society; therefore, Frontiers only applies the most rigorous and unbiased reviews. Frontiers revolutionizes research publishing by freely delivering the most outstanding research, evaluated with no bias from both the academic and social point of view. By applying the most advanced information technologies, Frontiers is catapulting scholarly publishing into a new generation.

What are Frontiers Research Topics?

Frontiers Research Topics are very popular trademarks of the *Frontiers journals series*: they are collections of at least ten articles, all centered on a particular subject. With their unique mix of varied contributions from Original Research to Review Articles, Frontiers Research Topics unify the most influential researchers, the latest key findings and historical advances in a hot research area.

Find out more on how to host your own Frontiers Research Topic or contribute to one as an author by contacting the Frontiers editorial office: frontiersin.org/about/contact

Cannabidiol treatment in neurotherapeutic interventions, volume II

Topic editors

Gustavo Gonzalez-Cuevas — Idaho State University, United States
Jorge Manzanares — Miguel Hernández University of Elche, Spain
Maria S. Garcia-Gutierrez — Miguel Hernández University of Elche, Spain
Francisco Navarrete — Miguel Hernández University of Elche, Spain
Giordano de Guglielmo — University of California, San Diego, United States

Citation

Gonzalez-Cuevas, G., Manzanares, J., Garcia-Gutierrez, M. S., Navarrete, F., de Guglielmo, G., eds. (2023). *Cannabidiol treatment in neurotherapeutic interventions, volume II*. Lausanne: Frontiers Media SA.
doi: 10.3389/978-2-83251-860-1

Table of contents

frontiers | Frontiers in Pharmacology

TYPE Editorial
PUBLISHED 23 February 2023
DOI 10.3389/fphar.2023.1163991

OPEN ACCESS

EDITED AND REVIEWED BY
Nicholas M. Barnes,
University of Birmingham,
United Kingdom

*CORRESPONDENCE
Gustavo Gonzalez-Cuevas,
gonzgust@isu.edu

SPECIALTY SECTION
This article was submitted to Neuropharmacology, a section of the journal Frontiers in Pharmacology

RECEIVED 11 February 2023
ACCEPTED 14 February 2023
PUBLISHED 23 February 2023

CITATION
Gonzalez-Cuevas G, Navarrete F, Garcia-Gutierrez MS, de Guglielmo G and Manzanares J (2023), Editorial: Cannabidiol treatment in neurotherapeutic interventions, volume II.
Front. Pharmacol. 14:1163991.
doi: 10.3389/fphar.2023.1163991

Editorial: Cannabidiol treatment in neurotherapeutic interventions, volume II

Gustavo Gonzalez-Cuevas[1,2]*, Francisco Navarrete[3,4,5], Maria S. Garcia-Gutierrez[3,4,5], Giordano de Guglielmo[6] and Jorge Manzanares[3,4,5]

[1]Department of Clinical Psychopharmacology, College of Pharmacy, Idaho State University, Meridian, ID, United States, [2]Department of Psychological Science, Boise State University, Boise, ID, United States, [3]Instituto de Neurociencias, Universidad Miguel Hernández-CSIC, San Juan de Alicante, Alicante, Spain, [4]Redes de Investigación Cooperativa Orientada a Resultados en Salud (RICORS), Red de Investigación en Atención Primaria de Adicciones (RIAPAd), Instituto de Salud Carlos II, MICINN and FEDER, Madrid, Spain, [5]Instituto de Investigación, Sanitaria y Biomédica de Alicante (ISABIAL), Alicante, Spain, [6]Department of Psychiatry, University of California San Diego, La Jolla, CA, United States

KEYWORDS

CBD, cannabidiol, neurotherapeutics, psychiatric disorders, Alzheimer's disease, Parkinson's diseae, acetaminophen, mood disorders, autism spectrum disorder (ASD)

Editorial on the Research Topic
Cannabidiol treatment in neurotherapeutic interventions, volume II

In this Research Topic, "Cannabidiol Treatment in Neurotherapeutic Interventions, Volume II", we have compiled a new series of case and research reports and original research articles written by world-renowned experts in the field of neuropsychopharmacology. These publications provide scientifically sound evidence in the evaluation of cannabidiol (CBD) as a potential pharmacotherapeutic tool for the treatment of mood disorders such as anxiety and depression and diseases such as Alzheimer's and Parkinson's in animal and human studies. Furthermore, a wide variety of methodologies, ranging from novel analytical and computational techniques to a medical case, also cast light on CBD's underlying action mechanisms, therapeutic monitoring, and potential side effect profile.

In a 3-month follow-up observational and clinical trial study, Souza et al. reported the anxiolytic effects of CBD in frontline healthcare professionals that lasted up to a month after treatment discontinuation. In newborn piglets, Barata et al. demonstrated that CBD can prevent hypoxia–ischemia-induced mood disturbances by acting on 5-hydrotryptamine 1A ($5HT_{1A}$) receptors. In aged rats, Hernandez-Hernandez and Garcia-Fuster demonstrated a dose-dependent antidepressant-like response for CBD. In a female Alzheimer's disease mouse model, Chesworth et al. showed a beneficial effect of long-term CBD on learning and anxiety. Regarding the role of CBD in Parkinson's disease, Patricio et al. demonstrated that intrapallidal injection of CBD had inhibitory effects on G protein-coupled receptor 55 (GPR55) receptors in the external globus pallidus, seemingly related to GABAergic overactivation in hemiparkinsonism, and Morash et al. showed that minimum essential therapeutic mixtures from the cannabis plant extracts, including CBD, had the greatest therapeutic potential for treating Parkinson's disease using *in silico*, *in vitro*, and medium *in vivo* experimental systems. Using computational models, Davila et al. found interacting loci in the

binding sites of the GPR55 and the CB1 receptors that may be responsible for the differential functional features of CBD.

Moreover, Franco et al. reported a new and simple liquid chromatography–mass spectrometry method (LC–MS/MS) for the determination of CBD and its active metabolite 7-hydroxy-cannabidiol (7-OH-CBD) in human serum and saliva, which may be used as a therapeutic tool for drug monitoring and pharmacokinetic studies. Lastly, in a case report, Souza et al. warned of the adverse side effect of skin rash after ongoing CBD use and outlined recommendations for its simultaneous consumption with other drugs that can affect its potential side effect profile.

Additionally, we conducted a basic bibliometric analysis of the publications on CBD, revealing possible trends. Publications dating up to 2022 were retrieved from the PubMed database using the key search terms: "cannabidiol" -or- "CBD" -and- "psychiatric disorders". A total of 1,161 articles were found within the included years between 1973 and 2022. The increasing exponential trend in the number of scholarly journal publications, also shared with broader cannabinoid research (see, for example, Ng and Chang, 2022), has been especially steep since the year 2015 (42 results in this year alone). However, a plateau effect (or deacceleration) might be currently occurring, as the total of publications in 2022 (154) were inferior to those in the year 2021 (168). Nonetheless, an impressive total number of 52 review articles were published on the related research topic of cannabidiol and psychiatric disorders. We invite our readers to update their general views by reading, for example, the following review papers by Kirkland et al. (2022) and Bilbao and Spanagel (2022). Remarkably, the majority of these reviews published in 2022 (about 15%) discuss the therapeutic role of CBD in autism spectrum disorders (ASD), revealing an emerging trend (Aishworiya et al., 2022; Babayeva et al., 2022; Brignell et al., 2022; Colizzi et al., 2022; de Camargo et al., 2022; Dias-de Freita et al., 2022; Pedrazzi et al., 2022; Silva et al., 2022).

Important considerations about the therapeutic use of CBD should be particularly relevant to the treatment of populations with mental disorders, since psychiatric patients receive ubiquitous polypharmaceutical treatments (Stassen et al., 2022). In conjunction with the therapeutic promises of CBD and its ever-increasing uses, multiple drug interactions between CBD and other therapeutic drugs in psychiatric populations should be critically assessed by clinicians (Graham et al., 2022). In addition, the growing popularity of CBD use in the general public also raises serious concerns about its potential interactions with common medications, such as acetaminophen (Balachandran et al., 2021). Interestingly, both acetaminophen and CBD share a common mechanism of action by inhibiting fatty acid hydrolase (FAAH), the enzyme that degrades the endogenous cannabinoid anandamide (AEA) (Schultz, 2010), and are commonly perceived by the public as safe drugs with limited side effects. However, the consumption of these two widely consumed over-the-counter anti-inflammatory and non-opioid analgesic drugs during pregnancy may increase the risk of neurodevelopmental disorders such as autism spectrum disorder (ASD) (Corsi et al., 2020; Smith et al., 2020; Alemany et al., 2021; Bührer et al., 2021). The potential perils of CBD use need to be considered. For instance, will widespread CBD use further contribute to the pandemic of neurodevelopmental disorders in years to come? Let sound scientific research on CBD answer the question, sooner rather than regrettably later.

Author contributions

All authors listed have made a substantial, direct, and intellectual contribution to the work and approved it for publication.

Conflict of interest

The authors declare that the research was conducted in the absence of any commercial or financial relationships that could be construed as a potential conflict of interest.

Publisher's note

References

Aishworiya, R., Valica, T., Hagerman, R., and Restrepo, B. (2022). An update on psychopharmacological treatment of autism spectrum disorder. *Neurother. J. Am. Soc. Exp. Neurother.* 19 (1), 248–262. doi:10.1007/s13311-022-01183-1

Alemany, S., Avella-García, C., Liew, Z., García-Esteban, R., Inoue, K., Cadman, T., et al. (2021). Prenatal and postnatal exposure to acetaminophen in relation to autism spectrum and attention-deficit and hyperactivity symptoms in childhood: Meta-analysis in six European population-based cohorts. *Eur. J. Epidemiol.* 36 (10), 993–1004. doi:10.1007/s10654-021-00754-4

Babayeva, M., Assefa, H., Basu, P., and Loewy, Z. (2022). Autism and associated disorders: Cannabis as a potential therapy. *Front. Biosci. (Elite Ed.* 14 (1), 1. doi:10.31083/j.fbe1401001

Balachandran, P., Elsohly, M., and Hill, K. P. (2021). Cannabidiol interactions with medications, illicit substances, and alcohol: A comprehensive review. *J. General Intern. Med.* 36 (7), 2074–2084. doi:10.1007/s11606-020-06504-8

Brignell, A., Marraffa, C., Williams, K., and May, T. (2022). Memantine for autism spectrum disorder. *Cochrane database Syst. Rev.* 8 (8), CD013845. doi:10.1002/14651858.CD013845.pub2

Bührer, C., Endesfelder, S., Scheuer, T., and Schmitz, T. (2021). Paracetamol (Acetaminophen) and the developing brain. *Int. J. Mol. Sci.* 22 (20), 11156. doi:10.3390/ijms222011156

Colizzi, M., Bortoletto, R., Costa, R., Bhattacharyya, S., and Balestrieri, M. (2022). The autism-psychosis continuum conundrum: Exploring the role of the endocannabinoid system. *Int. J. Environ. Res. public health* 19 (9), 5616. doi:10.3390/ijerph19095616

Corsi, D. J., Donelle, J., Sucha, E., Hawken, S., Hsu, H., El-Chaâr, D., et al. (2020). Maternal cannabis use in pregnancy and child neurodevelopmental outcomes. *Nat. Med.* 26 (10), 1536–1540. doi:10.1038/s41591-020-1002-5

de Camargo, R. W., de Novais Júnior, L. R., da Silva, L. M., Meneguzzo, V., Daros, G. C., da Silva, M. G., et al. (2022). Implications of the endocannabinoid system and the

therapeutic action of cannabinoids in autism spectrum disorder: A literature review. *Pharmacol. Biochem. Behav.* 221, 173492. doi:10.1016/j.pbb.2022.173492

Dias-de Freitas, F., Pimenta, S., Soares, S., Gonzaga, D., Vaz-Matos, I., and Prior, C. (2022). The role of cannabinoids in neurodevelopmental disorders of children and adolescents. *Rev. Neurol.* 75 (7), 189–197. doi:10.33588/rn.7507.2022123

Graham, M., Martin, J. H., Lucas, C. J., Murnion, B., and Schneider, J. (2022). Cannabidiol drug interaction considerations for prescribers and pharmacists. *Expert Rev. Clin. Pharmacol.* 15 (12), 1383–1397. doi:10.1080/17512433.2022.2142114

Ng, J. Y., and Chang, N. (2022). A bibliometric analysis of the cannabis and cannabinoid research literature. *J. Cannabis Res.* 4, 25. doi:10.1186/s42238-022-00133-0

Pedrazzi, J. F. C., Ferreira, F. R., Silva-Amaral, D., Lima, D. A., Hallak, J. E. C., Zuardi, A. W., et al. (2022). Cannabidiol for the treatment of autism spectrum disorder: Hope or hype? *Psychopharmacology* 239 (9), 2713–2734. doi:10.1007/s00213-022-06196-4

Schultz, S. T. (2010). Can autism be triggered by acetaminophen activation of the endocannabinoid system? *Acta neurobiol. Exp.* 70 (2), 227–231.

Silva, E. A. D., Junior, Medeiros, W. M. B., Torro, N., Sousa, J. M. M., Almeida, I. B. C. M., et al. (2022). Cannabis and cannabinoid use in autism spectrum disorder: A systematic review. *Trends psychiatry psychotherapy* 44, e20200149. doi:10.47626/2237-6089-2020-0149

Smith, A., Kaufman, F., Sandy, M. S., and Cardenas, A. (2020). Cannabis exposure during critical windows of development: Epigenetic and molecular pathways implicated in neuropsychiatric disease. *Curr. Environ. health Rep.* 7 (3), 325–342. doi:10.1007/s40572-020-00275-4

Stassen, H. H., Bachmann, S., Bridler, R., Cattapan, K., Herzig, D., Schneeberger, A., et al. (2022). Detailing the effects of polypharmacy in psychiatry: Longitudinal study of 320 patients hospitalized for depression or schizophrenia. *Eur. archives psychiatry Clin. Neurosci.* 272 (4), 603–619. doi:10.1007/s00406-021-01358-5

frontiers | Frontiers in Pharmacology

CASE REPORT
published: 19 May 2022
doi: 10.3389/fphar.2022.881617

Case Report: Cannabidiol-Induced Skin Rash: A Case Series and Key Recommendations

José Diogo S. Souza[1], Maíra Fassoni-Ribeiro[2], Rayssa Miranda Batista[3], Juliana Mayumi Ushirohira[1], Antonio W. Zuardi[1,4], Francisco S. Guimarães[4,5], Alline C. Campos[5], Flávia de Lima Osório[1,4], Daniel Elias[3], Cacilda S. Souza[3], AndRea A. Fassoni[6], Jaime E. C. Hallak[1,4] and José Alexandre S. Crippa[1,4]*

[1]Department of Neurosciences and Behavior, Ribeirão Preto Medical School, University of São Paulo, Ribeirão Preto, Brazil, [2]Department of Dermatology, São Paulo Federal University, São Paulo, Brazil, [3]Division of Dermatology, Department of Internal Medicine, Ribeirão Preto Medical School, University of São Paulo, Ribeirão Preto, Brazil, [4]National Institute of Science and Technology—Translational Medicine, Ribeirão Preto, Brazil, [5]Department of Pharmacology, Ribeirão Preto Medical School, University of São Paulo, Ribeirão Preto, Brazil, [6]Anatomed Laboratory, Bauru, Brazil

Cannabidiol (CBD) is a non-psychotomimetic constituent of the *Cannabis* plant, with potential therapeutic properties for many physical and neuropsychiatric conditions. Isolated CBD has been suggested to have favorable safety and tolerability. Although CBD-related rash is described, few case reports are well documented in the literature, and usually, CBD was used concomitantly with other medications. Thus, we report four women who presented a skin rash after ongoing CBD use. Other causes of these skin rashes were ruled out after conducting an extensive viral and serological detection panel, and three patients had their lesions biopsied. Two patients were re-exposed to the vehicle (MCT) without developing a new skin rash. Therefore, clinicians must be aware of this potential adverse effect of CBD use.

Keywords: cannabidiol, drug interaction, side effects, skin rash, case report, case series

OPEN ACCESS

Edited by:
Gustavo Gonzalez-Cuevas, Idaho State University, United States

Reviewed by:
Robert B. Laprairie, University of Saskatchewan, Canada
Franjo Grotenhermen, Nova Institut GmbH, Germany

****Correspondence:***
José Diogo S. Souza
jose.diogo.souza@usp.br

Specialty section:
This article was submitted to Neuropharmacology, a section of the journal Frontiers in Pharmacology

Received: *22 February 2022*
Accepted: *25 March 2022*
Published: *19 May 2022*

Citation:
Souza JDS, Fassoni-Ribeiro M, Batista RM, Ushirohira JM, Zuardi AW, Guimarães FS, Campos AC, Osório FL, Elias D, Souza CS, Fassoni AA, Hallak JEC and Crippa JAS (2022) Case Report: Cannabidiol-Induced Skin Rash: A Case Series and Key Recommendations. Front. Pharmacol. 13:881617. doi: 10.3389/fphar.2022.881617

INTRODUCTION

Cannabidiol (CBD) is a non-psychotomimetic phytocannabinoid with potential therapeutic properties across many physical and neuropsychiatric conditions (Crippa et al., 2018). CBD is generally well tolerated and has few serious adverse effects (Chesney et al., 2020). There is an increasing requirement in many countries for patients to legally use this cannabinoid to treat sleep disorders, addiction, pain, and anxiety and, more broadly, promote their health and wellbeing (Crippa et al., 2018). However, only the isolated CBD Epidiolex® (GW-Pharm, United Kingdom) has been licensed for two rare childhood epilepsies in some Western countries. Some of the most common side effects of Epidiolex® include sleepiness, decreased appetite, diarrhea, increase in liver enzymes, sleep problems, and cutaneous rash (EPIDIOLEX, 2022). Although this skin condition is documented as a common side event, the trials that reported it had used CBD formulations as an adjuvant treatment to other drugs (Devinsky et al., 2018).

We report here four women, three patients without comorbidities and one with diabetes using daily medications, who presented a skin rash between 6 h and 11 days after starting CBD use. The subjects were volunteers in the Brazilian clinical trial and follow-up study to evaluate the anxiolytic effects of CBD in healthcare frontline workers during the current COVID-19 pandemic, between June and November 2020. Part of these results has been published (Crippa et al., 2021). The subjects

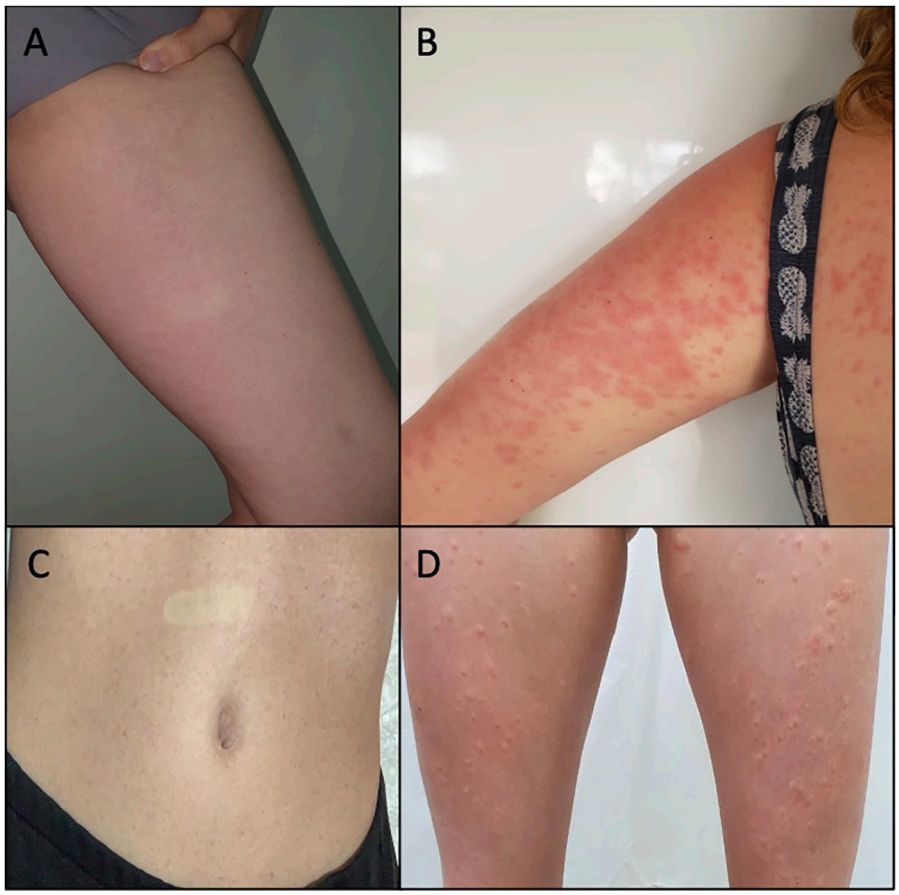

FIGURE 1 | (A) Case 1: rash on the inner side of the left thigh after 6 h of CBD use. The disappearance of the lesion on digital pressure is observed. **(B)** Case 2: confluent erythematous papules on the trunk and left arm after 8 days of CBD use. **(C)** Case 3: abdominal rash after 5 days of CBD use. The disappearance of the lesion on digital pressure is observed. **(D)** Case 3: evolution of rash to erythematous papules, surrounded by a hypochromic halo, on the lower limbs, after 10 days of CBD use.

received isolated oral CBD (99.6% purity with no other cannabinoid; PurMed Global; United States) dissolved in medium-chain triglyceride oil (150 mg/ml) at a daily dose of 300 mg (150 mg twice per day) for 4 weeks. To the best of our knowledge, these are the first case reports with multiple individuals not using other medications, with an extensive investigation to exclude other clinical causes (Pettit et al., 2018; Singh and Antimisiaris, 2020). Half of the patients were exposed only to the vehicle (medium-chain triglyceride (MCT) oil) to confirm that the adverse effect was specifically related to CBD use.

CASE DESCRIPTION

Case 1

A 34-year-old woman, without comorbidities or medication use, after 6 h of CBD use, noticed the emergence of a skin rash in the cervical region, trunk, and abdomen, with progression to the upper and lower limbs (**Figure 1A**). She reported an associated feeling of abdominal distension that improved after taking symptomatic medication, Simethicone. She had no fever or any other systemic symptoms. She presented a morbilliform exanthem on the face, neck, trunk, abdomen, upper limbs, and thighs, sparing the face and palmoplantar region, without mucosal lesions. There were no abnormalities in the blood count, and the broad investigation of viral infections and syphilis by RT–PCR or serology was negative for recent or active infections (**Table 1**). CBD withdrawal resulted in the involution of all lesions after 5 days, without any topical or systemic therapy. The patient voluntarily agreed to be exposed to the CBD vehicle (medium-chain triglyceride (MCT) oil). After 5 days of use, there was no recurrence or emergence of new rashes.

Case 2

A female subject, 33 years old, diabetic using metformin, sibutramine, and semaglutide, 7 days after starting CBD use, reported the appearance of erythematous and pruritic papules on the trunk, abdomen, and thighs, with an increase in the lesions and progression to the arms after 1 day. She had no fever or other systemic symptoms associated with the skin condition. A physical examination showed coalescing erythematous papules on the limbs, trunk, and abdomen (**Figure 1B**) without affecting

other areas such as the face, and the palmoplantar and mucosal regions. There was a complete remission of the lesions after 6 days of CBD suspension, without the need for any topical or systemic therapy. There was no change in the blood count (before and after CBD use), and the broad investigation of viral infections and syphilis by RT–PCR or serology was negative for recent or active infections (**Table 1**).

Case 3

A 34-year-old woman without comorbidities or medication use developed a rash on the abdomen after 5 days of CBD use (**Figure 1C**). The patient chose to continue using CBD, and after 5 days, the skin condition worsened, with progression to erythematous lesions on the buttocks and limbs, which were not pruritic but sensitive. She presented associated headaches and myalgia without fever or other systemic complaints. On physical examination, monomorphic erythematous papular lesions with a hypochromic halo were observed on the trunk, back, buttocks, lower limbs, and upper limbs (**Figure 1D**), sparing the face and the palmoplantar region, and without mucosal lesions. Withdrawal of CBD resulted in the involution of all lesions after 7 days, without the need for any topical or systemic therapy. There was no change in the blood count (before and after CBD use), and the broad investigation of viral infections and syphilis by RT-PCR or serology was negative for recent or active infections (**Table 1**). The patient voluntarily agreed to be exposed to the CBD vehicle (MCT), and after 5 days of use, there was no recurrence or emergence of new rashes.

Case 4

A female subject, 28 years old, without comorbidities or medication use, reported erythematous and pruritic lesions on the trunk and abdomen with evolution to arms and legs after 9 days of CBD use. She had associated diarrhea but did not present fever or other systemic symptoms. The physical examination showed monomorphic urticarial lesions (**Figure 2A**) that evolved after 2 days, with coalescence in the trunk, abdomen, and the upper and lower limbs (**Figure 2B**), even after discontinuing CBD in the period. Lesions spared the face and the palmoplantar and mucosal regions. There was a complete improvement of the lesions after 11 days of discontinuation of CBD, and it was necessary to initiate oral corticosteroid therapy (prednisone 0.5 mg/kg/day). There was no change in the blood count (before and after CBD use). The broad investigation of viral infections and syphilis by RT–PCR or serology was negative for other active or recent infections (**Table 1**), except for IgM positivity for Epstein–Barr.

DISCUSSION

Adverse drug reactions focus on clinical studies to connect possible side effects and the studied compound. Skin lesions often herald these reactions because this body organ can be quickly evaluated and confirmed to be immunologically active. These aspects make it particularly relevant in this and other clinical contexts. However, the skin condition itself can be highly non-specific, and it is always necessary to rule out other possible clinical causes, especially viral infections and drug vehicle allergies.

These skin reactions can be considered pharmacologically mediated (type A) or allergic or non-allergic hypersensitivity reactions (type B) (Böhm et al., 2018). Type A reactions, as they are generally dose dependent, can be resolved with changes in therapy and allow for the maintenance of treatment. On the other hand, Type B reactions constitute the minority, although they are more unpredictable than type A. Moreover, these responses can lead to severe conditions, such as Stevens–Johnson syndrome (SJS), toxic epidermal necrolysis (TEN), or drug reaction with eosinophilia and systemic symptoms (DRESS). In these cases, re-exposure to the potentially causative drug is strictly not recommended.

The most common form of drug rash is morbilliform or maculopapular (Hoetzenecker et al., 2016). Nonetheless, the

TABLE 1 | Laboratory findings for investigation of infections in the four patients with skin rash using cannabidiol.

Exams	Case 1	Case 2	Case 3	Case 4
PCR				
Multiplex for dengue, Zika virus, and chikungunya	(–)	(–)	(–)	(–)
Herpes simplex- type I	(–)	(–)	(–)	(–)
Herpes simplex- type II	(–)	(–)	(–)	(–)
Herpes simplex- type IV	(–)	(–)	(–)	(–)
Cytomegalovirus	(–)	(–)	(–)	(–)
Parvovirus	(–)	(–)	(–)	(–)
Enterovirus	(–)	(–)	(–)	(–)
SARS-CoV-2 (PCR)	(–)	(–)	(–)	(–)
Anti-SARS-CoV-2 antibodies	IgM -/IgG -	IgM -/IgG -	IgM -/IgG -	IgM -/IgG -
ELISA				
Rubella	IgM -/IgG +	IgM -/IgG +	IgM -/IgG +	IgM -/IgG +
Cytomegalovirus	IgM -/IgG +	IgM -/IgG +	IgM -/IgG +	IgM -/IgG +
Epstein–Barr	IgM -/IgG +	IgM -/IgG +	IgM -/IgG +	IgM +/IgG +
Anti-HIV	(–)	(–)	(–)	(–)
Serologies				
Syphilis (VDRL)	(–)	(–)	(–)	(–)
Hepatitis B and C	(–)	(–)	(–)	(–)

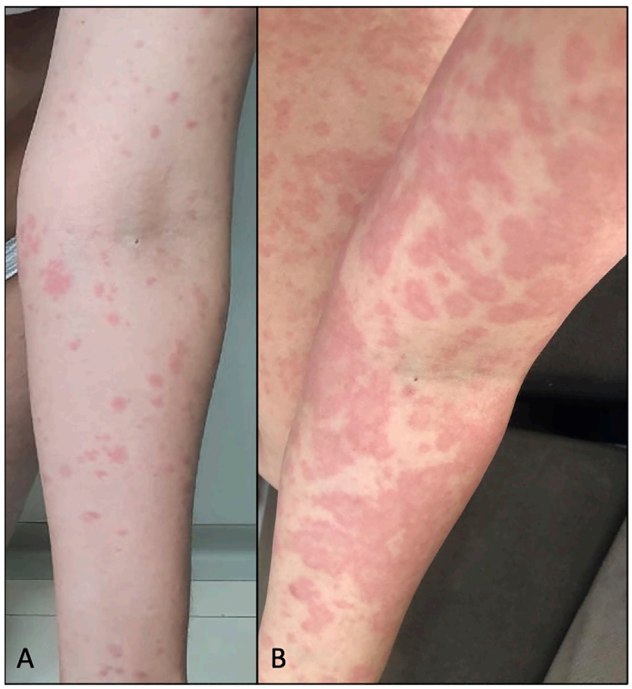

FIGURE 2 | (A) Case 4: erythematoedematous papules on the left upper limb after 9 days of CBD use. **(B)** Evolution of the lesions after 2 days, after medication discontinuation, and initiation of oral prednisone.

same drug can cause different patterns of dermatological manifestation since the pathogenesis of pharmacodermia is multifactorial and may involve genetic factors, lymphocyte activation, metabolic enzyme defects, eosinophilia, herpes virus activation, among others. Regarding DRESS cases, it is believed that an allergic immune response to a particular drug can stimulate T cells and induce viral reactivation (Husain et al., 2013). In one of the present study cases, even though it was a mild skin reaction, positive IgM and IgG for Epstein–Barr may suggest a relationship between pharmacodermia and reactivation of herpes virus 7 (HHV-7).

We report four women, three patients without comorbidities, and one with diabetes using daily medications, who presented with skin rashes between 6 h and 9 days after starting CBD use. The experimental CBD studied was pharmaceutical grade with no other compound than the MCT oil vehicle. In total, 100 participants (79 women and 21 men) received CBD oil, with four skin reactions related to the medication use (4% of volunteers). Three main patterns were observed: exanthematous, monomorphic erythematous papular lesions, and urticarial pattern, on the trunk and abdomen, with centrifugal progression to the limbs, sparing the face and palmoplantar regions, which were pruritic or sensitive to touch. There was an association with headache and myalgia in one case and abdominal symptoms in two other cases. The suspension of CBD resulted in the involution of the lesions between 5 and 11 days, without any topical or systemic therapy for three of the patients and prednisone 0.5 mg/kg for 5 days for one of the patients. Subsequent re-exposure to CBD vehicle (MCT) for 5 days in two of the patients did not induce a recurrence of the rash.

A broad investigation of viral infections and serology for syphilis and hepatitis was carried out, which were negative, except for one of the patients who had positive serology for the Epstein–Barr virus. The relevance of research on arboviruses is worth noting since they are prevalent in the study region and on SARS-CoV-2, given the context of the COVID-19 pandemic. In addition, lesions were biopsied from three patients (cases 1, 3, and 4). The histopathological pattern showed skin with mild hyperkeratosis, dermal edema, focal vacuolar degeneration of the basal layer, and lymphohistiocytic infiltrate with sparse eosinophils predominantly in the perivascular and periadnexal locations (**Figure 3**). Given such clinical, laboratory, and anatomopathological findings, the four cases can be diagnosed as skin rashes induced by CBD use. To the best of our knowledge, these are the first case reports with multiple individuals not using other medications, with an extensive investigation to exclude other clinical causes and half of the patients being exposed only to the MCT vehicle afterward (Pettit et al., 2018; Singh and Antimisiaris, 2020).

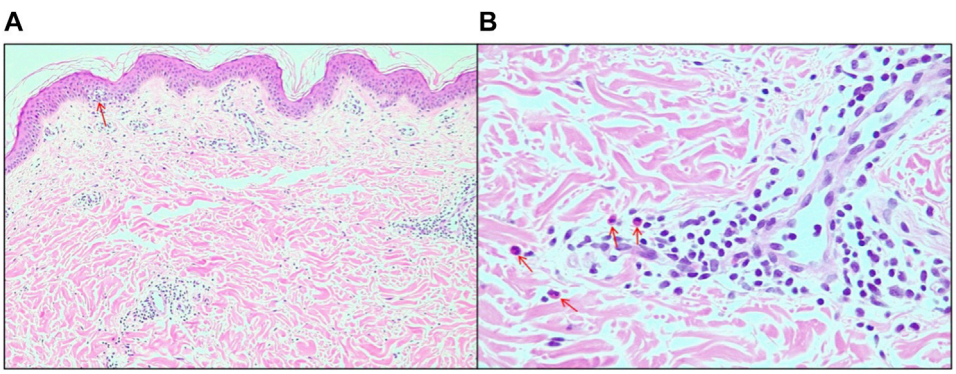

FIGURE 3 | (A) Edema of the papillary dermis and focal area of vacuolar degeneration of the basal layer of the epidermis (arrow), 10x magnification. **(B)** Details for the presence of eosinophils (arrows), 20x magnification.

An individual analysis of CBD plasma levels was only possible in two of the subjects since the other two withdrew from the trial before measurement. These two subjects showed levels that reached the upper 95% percentile of the whole study (levels of 98 and 179 ng/ml, respectively). This finding suggests that the reported pharmacodermia could be associated with high plasma levels of CBD. However, this possibility should be seen with caution, considering the low number of subjects. Also, the cutaneous rash did not occur in five other subjects that also reached similar high CBD plasma levels. CBD is extensively metabolized by CYP450 isoenzymes. The extent to which genetic polymorphisms in these isoenzymes would affect CBD plasma levels and their side effects remains poorly explored and should be a focus of future research.

Cannabis products are widely employed worldwide, and their use has been illegalized in several countries (Bonomo et al., 2018). After legalizing medicinal and recreational cannabis in some countries, its use highly increased (Wen et al., 2015; Martins et al., 2016; Hasin et al., 2017). In the United Kingdom, for instance, it is estimated that over a million people are using non-legally sourced cannabis for self-medication of diagnosed conditions (Schlag et al., 2021). CBD has gained special attention for its therapeutic potency for several neuropsychiatric and general medical conditions, including a trend as a new ingredient for skincare products. However, apart from epilepsy, much of the available data are from preclinical studies and lack the support of robust human, randomized, placebo-controlled, double-blind studies (Jhawar et al., 2019; Baswan et al., 2020).

While there is a growing demand in many countries for legal CBD use to treat various mental and physical health problems, determining the best regulatory response to these demands is a significant challenge. It occurs because most CBD products come in multiple formulations and routes of administration, and the great majority is prepared in an artisanal manner, without the necessary manufacturing, quality control, labeling, and pharmaceutical-grade production. In addition, there is a paucity of data to support the therapeutic use of many of the indications consumed by this tremendous global demand. The clinical use of CBD needs to be aligned with many other pharmaceutical products to ensure efficacy and safety for patients, given its interactions with other drugs and its potential side effect profile. Therefore, through evidence-based medicine, an exhaustive framework to guarantee the quality and safety of the CBD product is urgently needed to protect the consumers and minimize possible harm.

CONCLUSION

We report four cases who presented with a skin rash between 6 h and 11 days after starting CBD use. Considering the clinical, laboratory, and anatomopathological findings, the four cases can be diagnosed as skin rashes induced by this cannabinoid. This finding reinforces the proposal that CBD use should be guided by evidence-based medicine, being necessary to balance the benefits with potential adverse and undesired effects when making decisions regarding its use.

DATA AVAILABILITY STATEMENT

The raw data supporting the conclusions of this article will be made available by the authors if requested, without undue reservation.

ETHICS STATEMENT

The studies involving human participants were reviewed and approved by the research ethics committee of the Ribeirão Preto Medical School University Hospital and the National Council on Research Ethics as part of the 'Burnout and Distress Prevention With Cannabidiol in Front-line Healthcare Workers Dealing With COVID-19 (BONSAI)' trial. The patients/participants provided their written informed consent to participate in this study. Written informed consent was obtained from the individual(s) for the publication of any potentially identifiable images or data included in this article.

AUTHOR CONTRIBUTIONS

Assessment and support of study patients: JS, RB, JU, and JC. Drafting of the manuscript: JS, MF-R, and RB. Critical revision of the manuscript: JS, MF-R, RB, JU, AZ, FG, AC, FO, DE, CS, AF, JH, and JC. Anatomopathological analysis: AF. Funding: JH and JC. Supervision: AZ, FG, DE, CS, and JC.

FUNDING

This work was supported by a grant (2020/12,110-9) from the Fundação de Amparo à Pesquisa do Estado de São Paulo and a grant (2008/09,009-2) from the Instituto Nacional de Ciência e Tecnologia Translational em Medicina.

ACKNOWLEDGMENTS

The authors thank PurMed Global (Delray Beach, Florida) for donating cannabidiol and ANATOMED Laboratory (Bauru, Brazil) for their anatomopathological analysis at no cost.

REFERENCES

Baswan, S. M., Klosner, A. E., Glynn, K., Rajgopal, A., Malik, K., Yim, S., et al. (2020). Therapeutic Potential of Cannabidiol (CBD) for Skin Health and Disorders. *Clin. Cosmet. Investig. Dermatol.* 13, 927–942. doi:10.2147/CCID.S286411

Böhm, R., Proksch, E., Schwarz, T., and Cascorbi, I. (2018). Drug Hypersensitivity. *Dtsch Arztebl Int.* 115 (29-30), 501–512. doi:10.3238/arztebl.2018.0501

Bonomo, Y., Souza, J. D. S., Jackson, A., Crippa, J. A. S., and Solowij, N. (2018). Clinical Issues in Cannabis Use. *Br. J. Clin. Pharmacol.* 84 (11), 2495–2498. doi:10.1111/bcp.13703

Chesney, E., Oliver, D., Green, A., Sovi, S., Wilson, J., Englund, A., et al. (2020). Adverse Effects of Cannabidiol: a Systematic Review and Meta-Analysis of Randomized Clinical Trials. *Neuropsychopharmacology* 45 (11), 1799–1806. doi:10.1038/s41386-020-0667-2

Crippa, J. A., Guimarães, F. S., Campos, A. C., and Zuardi, A. W. (2018). Translational Investigation of the Therapeutic Potential of Cannabidiol (CBD): Toward a New Age. *Front Immunol.* 9, 2009. doi:10.3389/fimmu.2018.02009

Crippa, J. A. S., Zuardi, A. W., Guimarães, F. S., Campos, A. C., de Lima Osório, F., Loureiro, S. R., et al. (2021). Efficacy and Safety of Cannabidiol Plus Standard Care vs Standard Care Alone for the Treatment of Emotional Exhaustion and Burnout Among Frontline Health Care Workers during the COVID-19 Pandemic: A Randomized Clinical Trial. *JAMA Netw. Open* 4 (8), e2120603. doi:10.1001/jamanetworkopen.2021.20603

Devinsky, O., Patel, A. D., Thiele, E. A., Wong, M. H., Appleton, R., Harden, C. L., et al. (2018). Randomized, Dose-Ranging Safety Trial of Cannabidiol in Dravet Syndrome. *Neurology* 90 (14), e1204–11. doi:10.1212/WNL.0000000000005254

EPIDIOLEX (2022). *EPIDIOLEX® (Cannabidiol).* https://www.epidiolex.com (Acessed Feb 19, 2022).

Hasin, D. S., Cerdá, M., Keyes, K. M., Stohl, M., Galea, S., et al. (2017). US Adult Illicit Cannabis Use, Cannabis Use Disorder, and Medical Marijuana Laws: 1991-1992 to 2012-2013. *JAMA Psychiatry* 74 (6), 579–588. doi:10.1001/jamapsychiatry.2017.0724

Hoetzenecker, W., Nägeli, M., Mehra, E. T., Jensen, A. N., Saulite, I., Schmid-Grendelmeier, P., et al. (2016). Adverse Cutaneous Drug Eruptions: Current Understanding. *Semin. Immunopathol* 38 (1), 75–86. doi:10.1007/s00281-015-0540-2

Husain, Z., Reddy, B. Y., and Schwartz, R. A. (2013). DRESS Syndrome: Part I. Clinical Perspectives. *J. Am. Acad. Dermatol.* 68 (5), 693–698. e1–14; quiz 706–8. doi:10.1016/j.jaad.2013.01.033

Jhawar, N., Schoenberg, E., Wang, J. V., and Saedi, N. (2019). The Growing Trend of Cannabidiol in Skincare Products. *Clin. Dermatol.* 37 (3), 279–281. doi:10.1016/j.clindermatol.2018.11.002

Martins, S. S., Mauro, C. M., Santaella-Tenorio, J., Kim, J. H., Cerda, M., Keyes, K. M., et al. (2016). State-level Medical Marijuana Laws, Marijuana Use and Perceived Availability of Marijuana Among the General U.S. Population. *Drug Alcohol Depend* 169, 26–32. doi:10.1016/j.drugalcdep.2016.10.004

Pettit, C., Massick, S., and Bechtel, M. (2018). Cannabidiol-Induced Acute Generalized Exanthematous Pustulosis. *Dermatitis* 29 (6), 345–346. doi:10.1097/DER.0000000000000422

Schlag, A. K., O'Sullivan, S. E., Zafar, R. R., and Nutt, D. J. (2021). Current Controversies in Medical Cannabis: Recent Developments in Human Clinical Applications and Potential Therapeutics. *Neuropharmacology* 191, 108586. doi:10.1016/j.neuropharm.2021.108586

Singh, J., and Antimisiaris, M. F. (2020). Epidiolex-induced Skin Rash. *Epileptic Disord.* 22 (4), 511–514. doi:10.1684/epd.2020.1189

Wen, H., Hockenberry, J. M., and Cummings, J. R. (2015). The Effect of Medical Marijuana Laws on Adolescent and Adult Use of Marijuana, Alcohol, and Other Substances. *J. Health Econ.* 42, 64–80. doi:10.1016/j.jhealeco.2015.03.007

Conflict of Interest: AZ reported receiving grants from the National Institute of Translational Science and Technology in Medicine and personal fees from the National Council for Scientific and Technological Development during the conduct of the study, being a co-owner of a patent for fluorinated cannabidiol compounds (licensed to Phytecs), and having a patent pending for a cannabinoid-containing oral pharmaceutical composition outside the submitted work. FG reported receiving grants from Prati-Donaduzzi, being a co-owner of a patent for fluorinated cannabidiol compounds (licensed to Phytecs), and having a patent pending for a cannabinoid-containing oral pharmaceutical composition outside the submitted work. AC reported having a patent pending for a cannabinoid-containing oral pharmaceutical composition outside the submitted work. CS is a consultant and/or has received speaker fees and/or sits on the advisory board and/or receives research funding from Abbvie, Novartis, Janssen-Cilag, and Boehringer Ingelheim. JH reported receiving grants from Prati-Donaduzzi, travel support and personal fees from BioSynthesis Pharma Group, being a co-owner of a patent for fluorinated cannabidiol compounds (licensed to Phytecs), and having a patent pending for a cannabinoid-containing oral pharmaceutical composition outside the submitted work. JC reported receiving grants from the São Paulo Research Foundation and the National Institute of Translational Science and Technology in Medicine and personal fees from the National Council for Scientific and Technological Development and receiving travel support and personal fees from BioSynthesis Pharma Group; serving as a member of the international advisory board of the Australian Centre for Cannabinoid Clinical and Research Excellence, National Health and Medical Research Council; being a co-owner of a patent for fluorinated cannabidiol compounds (licensed to Phytecs); and having a patent pending for a cannabinoid-containing oral pharmaceutical composition outside the submitted work.

The remaining authors declare that the research was conducted in the absence of any commercial or financial relationships that could be construed as a potential conflict of interest.

frontiers | Frontiers in Pharmacology

ORIGINAL RESEARCH
published: 22 June 2022
doi: 10.3389/fphar.2022.915004

On-Line Solid Phase Extraction High Performance Liquid Chromatography Method Coupled With Tandem Mass Spectrometry for the Therapeutic Monitoring of Cannabidiol and 7-Hydroxy-cannabidiol in Human Serum and Saliva

Valentina Franco[1,2], Michela Palmisani[2], Roberto Marchiselli[1], Francesca Crema[1], Cinzia Fattore[2], Valentina De Giorgis[2], Costanza Varesio[2,3], Paola Rota[4], Vincenza Flora Dibari[5] and Emilio Perucca[6,7]*

[1]*Department of Internal Medicine and Therapeutics, Clinical and Experimental Pharmacology Unit, University of Pavia, Pavia, Italy,* [2]*IRCCS Mondino Foundation, Pavia, Italy,* [3]*Department of Brain and Behavioral Sciences, University of Pavia, Pavia, Italy,* [4]*Department of Biomedical, Surgical and Dental Sciences, University of Milan, Milan, Italy,* [5]*B.S.N. Srl R&D Laboratory, Castelleone, Italy,* [6]*Department of Medicine, Austin Health, The University of Melbourne, Melbourne, VIC, Australia,* [7]*Department of Neuroscience, Monash University, Melbourne, VIC, Australia*

Cannabidiol is a novel antiseizure medication approved in Europe and the US for the treatment of seizures associated with Lennox-Gastaut syndrome, Dravet syndrome and tuberous sclerosis complex. We describe in this article a new and simple liquid chromatography-mass spectrometry method (LC-MS/MS) for the determination of cannabidiol and its active metabolite 7-hydroxy-cannabidiol in microvolumes of serum and saliva (50 µl), to be used as a tool for therapeutic drug monitoring (TDM) and pharmacokinetic studies. After on-line solid phase extraction cannabidiol, 7-hydroxy-cannabidiol and the internal standard cannabidiol-*d3* are separated on a monolithic C18 column under gradient conditions. Calibration curves are linear within the validated concentration range (10–1,000 ng/ml for cannabidiol and 5–500 ng/ml for 7-hydroxy-cannabidiol). The method is accurate (intraday and interday accuracy within 94–112% for cannabidiol, 91–109% for 7-hydroxy-cannabidiol), precise (intraday and interday precision <11.6% for cannabidiol and <11.7% for 7- hydroxy-cannabidiol) and sensitive, with a LOQ of 2.5 ng/ml for cannabidiol and 5 ng/ml for 7-hydroxy-cannabidiol. The stability of the analytes was confirmed under different storage conditions. Extraction recoveries were in the range of 81–129% for cannabidiol and 100–113% for 7-hydroxy-cannabidiol. The applicability of the method to TDM was demonstrated by analysis of human serum and saliva samples obtained from patients with epilepsy treated with cannabidiol.

Keywords: cannabidiol, 7-hydroxy-cannabidiol, antiseizure medications, HPLC-MS/MS, saliva, serum, on-line solid phase extraction

OPEN ACCESS

Edited by:
Gustavo Gonzalez-Cuevas, Idaho State University, United States

Reviewed by:
Guillermo Moreno-Sanz, Khiron Life Sciences Corp, Colombia
Paula Schaiquevich, Garrahan Hospital, Argentina
Federica Pigliasco, Giannina Gaslini Institute (IRCCS), Italy

****Correspondence:***
Valentina Franco
valentina.franco@unipv.it

Specialty section:
This article was submitted to Neuropharmacology, a section of the journal Frontiers in Pharmacology

Received: *02 March 2022*
Accepted: *29 April 2022*
Published: *22 June 2022*

Citation:
Franco V, Palmisani M, Marchiselli R, Crema F, Fattore C, De Giorgis V, Varesio C, Rota P, Dibari VF and Perucca E (2022) On-Line Solid Phase Extraction High Performance Liquid Chromatography Method Coupled With Tandem Mass Spectrometry for the Therapeutic Monitoring of Cannabidiol and 7-Hydroxy-cannabidiol in Human Serum and Saliva. Front. Pharmacol. 13:915004. doi: 10.3389/fphar.2022.915004

INTRODUCTION

Cannabidiol (CBD) is a new antiseizure medication (ASM) recently approved in Europe and the US for the treatment of seizures associated with Lennox-Gastaut syndrome, Dravet syndrome and tuberous sclerosis complex (Epidyolex, 2019; Epidiolex, 2020). The mechanisms by which CBD exerts antiseizure effects are unclear. CBD shows low affinity for the cannabinoid CB1 and CB2 receptors at therapeutic concentrations, and its antiseizure effects may be related to other actions such as inhibition of adenosine reuptake, G protein–coupled receptor 55 (GPR55) antagonism and desensitization of vanilloid type 1 (TRPV1) channels (Perucca, 2017; Franco and Perucca, 2019; Franco et al., 2021). CBD bioavailability is low and very variable (around 6% on average) due to extensive first-pass metabolism (Bialer et al., 2018), and increases 4-fold when the compound is taken with a high-fat meal (Taylor et al., 2018). CBD is highly bound to plasma proteins (>94%) and is extensively metabolized by cytochrome P450 (CYP) enzymes, mainly CYP3A4 and CYP2C19, and glucuronosyltransferases. The conversion of CBD to the primary pharmacologically active metabolite 7-hydroxy-CBD is mediated by CYP2C19, while the conversion of 7-hydroxy-CBD to the inactive 7-carboxy-CBD metabolite is mediated by CYP3A4 (Mazur et al., 2009; Jiang et al., 2011; Zendulka et al., 2016; Epidyolex, 2019; Morrison et al., 2019). CBD pharmacokinetics show prominent variability within and across patients, which is likely to contribute to large individual differences in clinical response (Franco and Perucca, 2019).

For many therapeutic agents, measurement of serum drug levels can be valuable in facilitating dose optimization. In the case of CBD, the relationship between serum levels of the parent drug and its active 7-hydroxy-metabolite and clinical effects have not been evaluated. Identification of the serum concentration at which an individual patient shows an optimal response can be used as a reference to guide dose adjustments should pharmacokinetic changes over time lead to loss of seizure control or appearance of adverse effects in a given individual (Patsalos et al., 2008). In the present article, we describe the development and validation of a novel on-line solid phase extraction high performance liquid chromatography-mass spectrometry (HPLC-MS/MS) micromethod for the simultaneous determination of CBD and 7-hydroxy-CBD in human serum and in saliva, which is suitable for pharmacokinetic studies and therapeutic drug monitoring (TDM). Although the correlation between serum and salivary CBD levels has not been investigated to date, the feasibility of using saliva samples for TDM purposes is worth exploring as most patients with Lennox-Gastaut and Dravet syndrome are children in whom avoidance of repeated venepunctures would be desirable.

EXPERIMENTAL SECTION

Chemicals and Reagents

CBD and the internal standard (IS) deuterated CBD (CBD-*d3*) were purchased from Merck (Merck, Darmstadt, Germany). 7-hydroxy-CBD was purchased from Toronto Research Chemicals (TRC, Toronto, Canada) (**Figure 1**). Ultrapure water for the preparation of solutions and eluents was obtained with a Millipore-Q-plus system (Millipore, Milan, Italy). LC-MS grade methanol, acetonitrile, isopropanol, 99% formic acid and 99% ammonium formate for the preparation of the mobile phase were obtained from VWR (VWR International, Milan, Italy). Drug-free human serum and saliva used for the preparation of quality control (QC) samples and calibrators were obtained from healthy adult donors and written informed consent was obtained.

Preparation of Stock Solutions, Calibrators and QC Samples

Stock solutions of CBD (1 mg/ml), 7-hydroxy-CBD (1 mg/ml) and IS (100 µg/ml) were prepared in methanol. Working standard solutions were prepared in methanol by diluting the stock solutions to obtain concentrations of 10, 20, 50, 100, 250, 500 and 1,000 ng/ml for CBD, and 5, 10, 25, 50, 125, 250 and 500 ng/ml for 7-hydroxy-CBD. The working IS solution was prepared at 170 ng/ml. Calibrators were prepared freshly for each run by mixing 50 µl of working solutions containing both CBD and 7-hydroxy-CBD, 50 µl of working solution of IS, 50 µl of blank matrix (human serum or saliva) and 100 µl of methanol. QCs of CBD (35, 350 and 750 ng/ml) and 7-hydroxy-CBD (17.5, 175 and 375 ng/ml) were prepared from separate stock solutions and analyzed as the unknown samples.

Sample Preparation

As for calibrators, QC samples of human serum or saliva (50 µl) were mixed with 50 µl of IS working solution (170 ng/ml), 50 µl of CBD and 7-hydroxy-CBD working solution and 100 µl of methanol. For the unknown samples, 50 µl of human serum or saliva were mixed with 50 µl of IS working solution (170 ng/ml) and 150 µl of methanol. After vortexing the mixture was centrifuged for 10 min at 4°C and 11,000 rpm using a Hettich Rotina 35R (model 1710) refrigerated centrifuge. 40 µl taken from the supernatant were injected into the HPLC-MS/MS system.

Instrumentation and HPLC-MS/MS Parameters

The HPLC-MS/MS apparatus consisted of a 3200 QTRAP® triple-quadrupole linear ion trap mass spectrometer fitted with a TurboIonSpray interface (Applied Biosystems Sciex, Darmstadt, Germany) and an HPLC ExionLC 100 integrated system equipped with a quaternary low pressure mixing pump, a column oven, an autosampler, a degasser and a controller (Applied Biosystems Sciex, Darmstadt, Germany). On-line clean-up and enrichment were performed on a perfusion column (POROS R1, 2.1 × 30 mm i.d., 20 µm, Thermo Fisher Scientific, Waltham, Massachusetts, United States). Chromatographic separation was achieved on a monolithic C18 column (Onyx, 100 × 3 mm i.d., Phenomenex, Bologna, Italy) heated at 25°C. A solution of water/methanol 98:2 v/v containing 10 mM ammonium formate and 0.1% formic acid was used as mobile phase A. Mobile phase B consisted of methanol/acetonitrile/isopropanol 80:10:10 v/v containing 8 mM ammonium

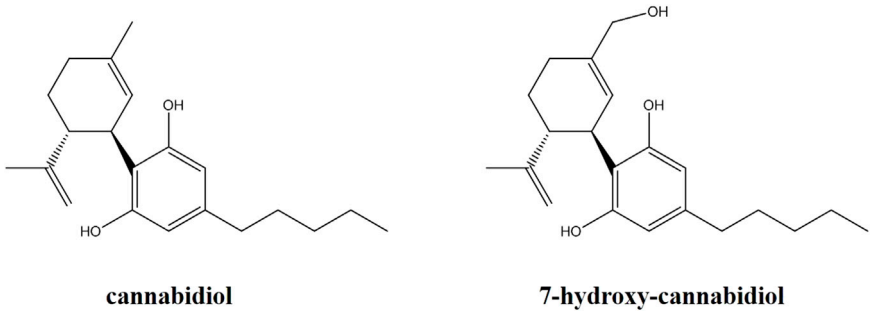

FIGURE 1 | Chemical structures of cannabidiol and its active metabolite 7-hydroxy-cannabidiol.

TABLE 1 | Mass spectrometry parameters for CBD, 7-hydroxy-CBD and IS.

Compounds	RT (min)	Q1 mass (m/z)	Q3 mass (m/z)	DP (V)	CE (V)	CXP (V)
CBD	4.8	315.2	193.2	38	30	4
7-hydroxy-CBD	3.9	313.2	201.1	57	28	4
CBD-*d3*	4.8	318.2	196.1	38	28	4

Abbreviations: CBD, cannabidiol; 7-hydroxy-CBD, 7-hydroxy-cannabidiol; CBD-d3, cannabidiol-d3; CE, collision energy; CXP, collision cell exit potential; DP, declustering potential; IS, internal standard; RT, retention time.

formate and 0.08% formic acid. Total runtime was 12 min. The TurboIonSpray source was kept at 550°C. Electrospray ionization was performed in positive ion mode for all analytes, using the multiple reaction monitoring measurement. Setting parameters are reported in **Table 1**. All HPLC-MS/MS components were controlled by Analyst software version 1.6.3. MultiQuant version 3.0.2 was used for data analysis (Applied Biosystems Sciex, Darmstadt, Germany).

On-Line Solid Phase Extraction

On-line solid phase extraction consisted of various automated steps. In the loading step 40 µl of sample were injected by the HPLC autosampler onto the perfusion column fitted into the loading position of the 10-port switching valve. This step lasted 1 min with a flow rate of 1.5 ml/min of a mixture of 99% A: 1% B. By using this procedure the sample matrix was diverted to the waste and the analytes were retained on the perfusion column. After completing this phase and switching-back the valve, the injection step was started and the analytes were transferred to the chromatographic column. In this step the flow rate was restored at 0.5 ml/min and a gradient was set to start at 20% A: 80% B ramped to 2% A: 98% B over 3 min and then maintained for 2 min. This step permitted the separation of the analytes in the analytical column and was followed by an additional cleaning step of 3 min with 0.6 ml/min of a mixture 1% B: 99% C (mobile phase C being pure methanol) before valve activation for re-equilibration of the perfusion column at 0.6 ml/min for 3 min (99% A: 1% B).

Method Validation

The validation of the method was performed according to the guidelines of the European Medicines Agency (EMA guidelines, 2011).

Calibration curves were obtained by evaluating the ratio between the area of the analyte peaks and the area of the IS peaks versus the corresponding concentrations of the calibrators. The curves were fitted using linear regression and the correlation coefficient was used as a measure of the goodness of fit. The concentrations of the unknown samples were calculated through the equation of the calibration line.

Precision and accuracy were investigated at four concentrations (limit of quantitation LOQ, low QC, medium QC and high QC). Precision data were expressed as coefficient of variation (CV%) with a limit of acceptability of less than 15% for QC samples and 20% for LOQ. Accuracy was calculated by comparing the means of the LOQ and QCs assay results with the nominal concentrations according to the formula [(measured value/theoretical value) x100].

Extraction recovery was determined by comparing the peak areas obtained from five different extracted QC and LOQ samples with the peak areas obtained after injection of known volumes of the non-extracted solutions containing the same concentration of CBD and 7-hydroxy-CBD. The stability of the analytes in extracted samples was evaluated by comparing the low, medium and high concentrations of fresh QC extracts with extracts at the same level of concentration stored at room temperature (24 h without protection from light), for one month at −20°C and after 3 freeze-thaw cycles.

Sensitivity was evaluated by determining the LOQ and the limit of detection (LOD). The LOQ was defined as the lowest concentration of calibrators with a signal-to-noise ratio of at least 10 with a CV% <20%. The LOD was defined as the concentration of calibrators with a signal-to-noise ratio of at least 3. Selectivity was assessed by evaluating the absence of interfering peaks at the retention time of CBD, 7-hydroxy-CBD

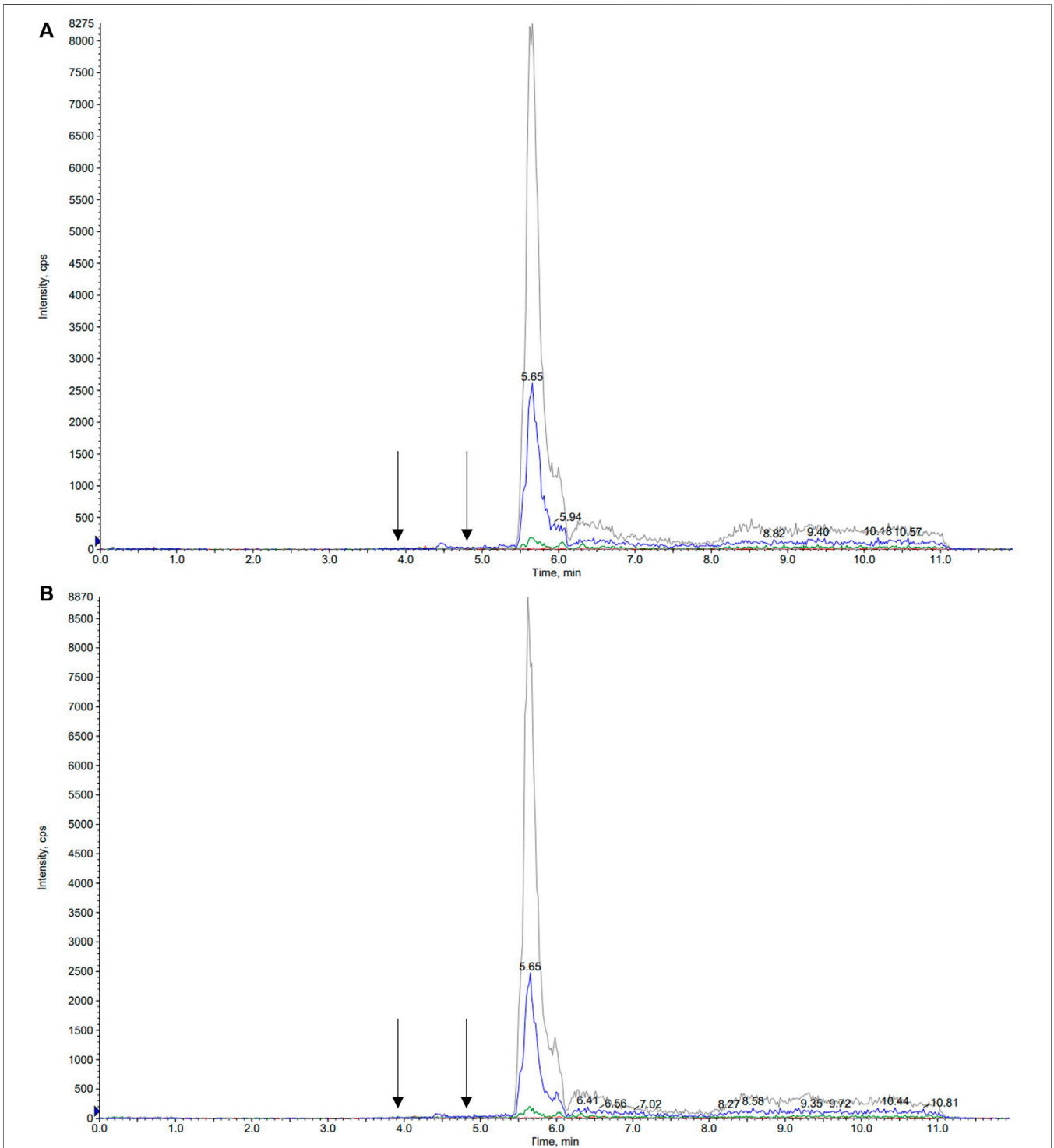

FIGURE 2 | Representative chromatograms of blank serum **(A)** and saliva **(B)** samples. Arrows correspond to the retention times of 7-hydroxy-cannabidiol, cannabidiol and the internal standard cannabidiol-*d3*, respectively.

and IS both in human serum and saliva from six different healthy individuals. Specificity was also assessed by assaying samples from individuals treated with a variety of ASMs different from CBD. Carry-over was determined by analyzing a blank solvent after the highest calibrator (six runs). Carryover was considered adequate when peak areas for CBD, 7-hydroxy-CBD and IS determined in extracted blank samples were lower than 20 and 5% than that associated with the calibration solution at the lowest concentration.

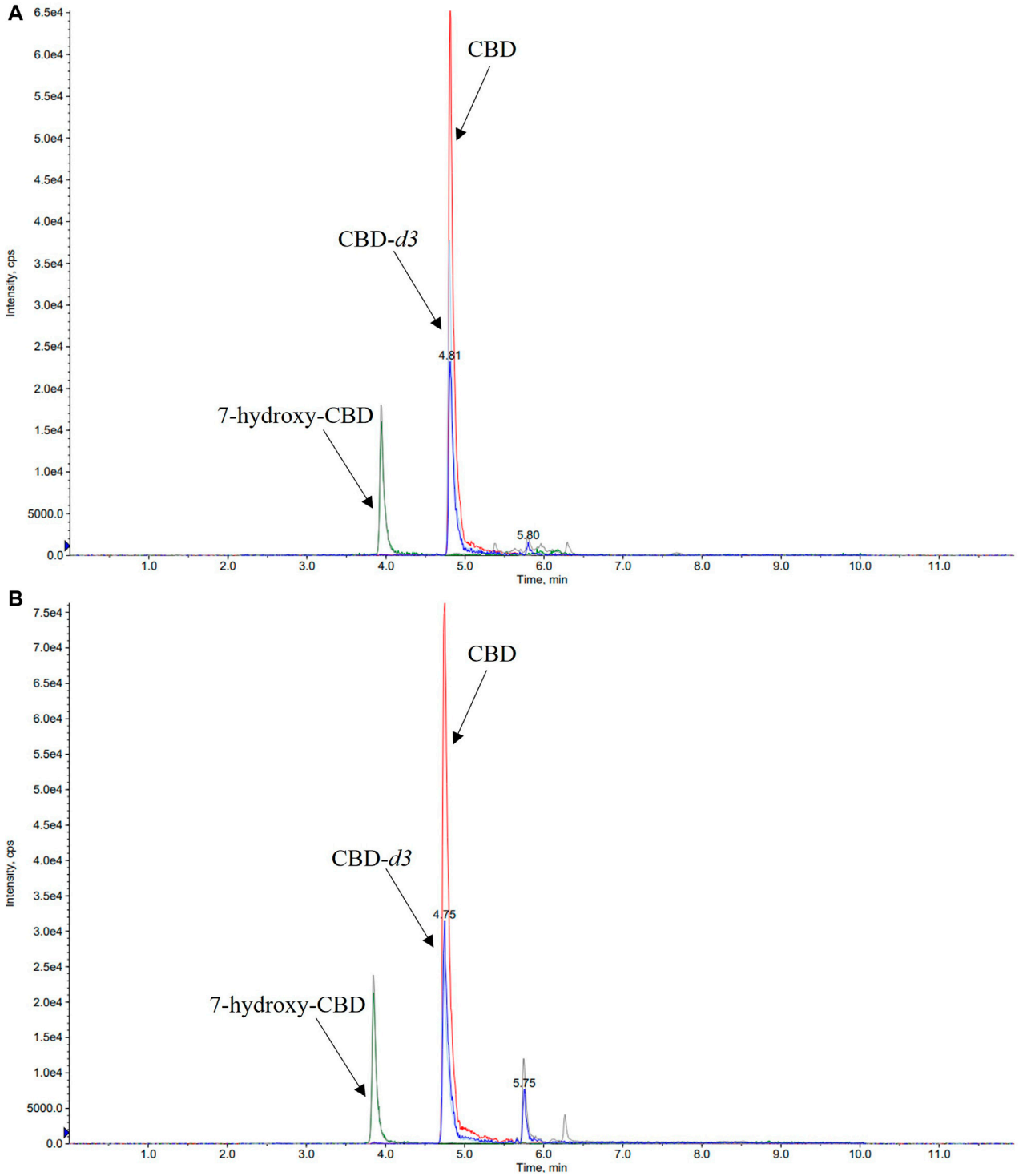

FIGURE 3 | Representative chromatograms of medium QC (quality control sample spiked with CBD 350 ng/ml, 7-hydroxy-CBD 175 ng/ml and cannabidiol-*d3* 170 ng/ml) serum **(A)** and saliva **(B)** samples. CBD, cannabidiol.

Application to Clinical Samples

The applicability of the method was tested on samples of serum and saliva collected simultaneously from 5 patients with Lennox-Gastaut syndrome receiving different dosing regimens of a liquid formulation of pharmaceutical-grade CBD (Epidiolex®, 100 mg/ml CBD solution), in combination with other ASMs (**Table 6**). All samples were collected at steady state about 16 h after the last dose of CBD, as part of the local

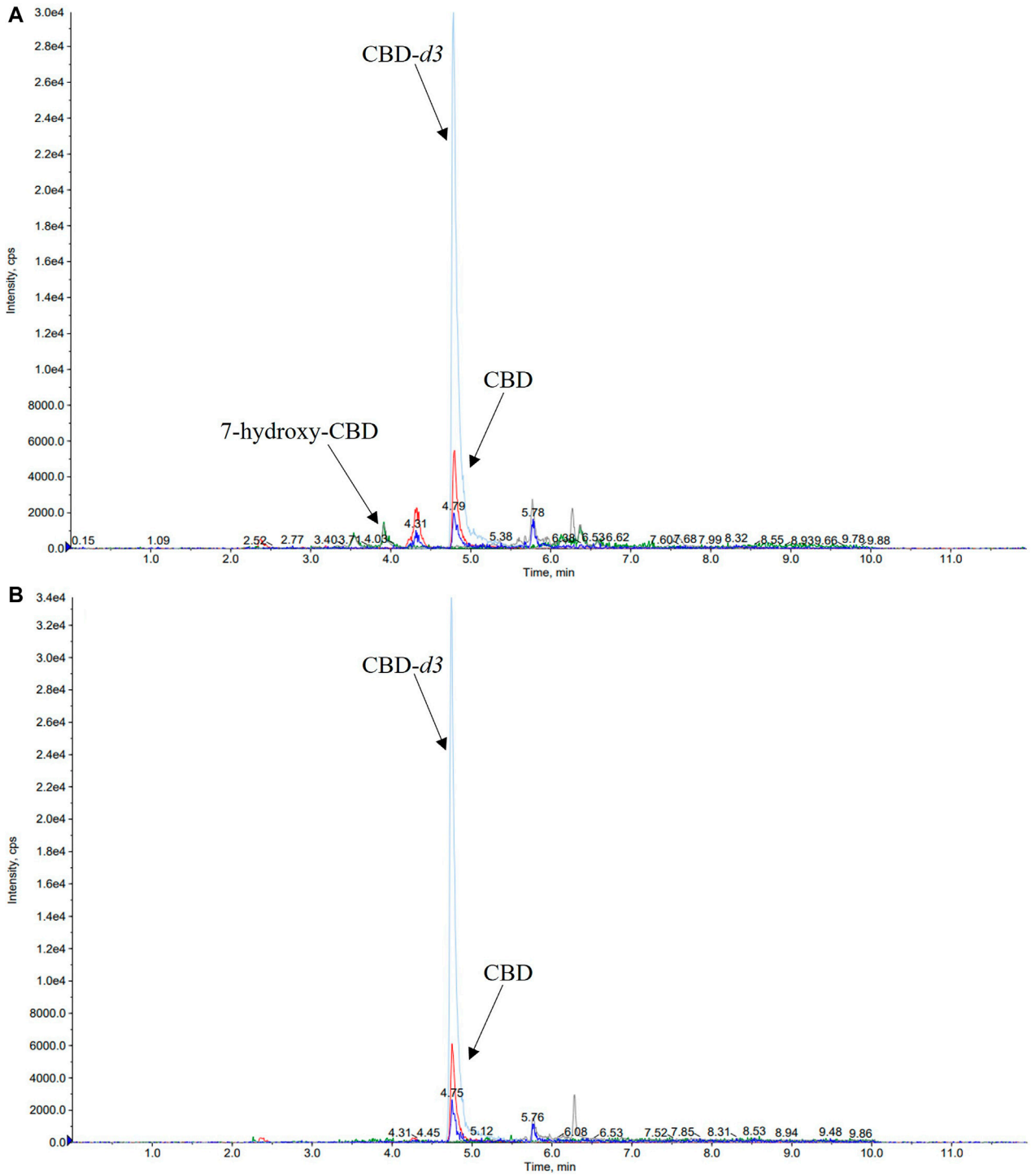

FIGURE 4 | Representative chromatograms of serum **(A)** and saliva **(B)** samples of a patient taking cannabidiol (CBD) at a dosage of 6.6 mg/kg/day. The serum concentration of 7-hydroxy-CBD and CBD was 11.2 ng/ml and 22.5 ng/ml, respectively. CBD salivary concentration was 23.2 ng/ml while 7-hydroxy-CBD was not detected.

TDM service. Unstimulated saliva samples were aspirated with a syringe from under the tongue, transferred into 1.5 ml polypropylene tubes and stored at −20°C until analysis. Subjects rinsed their mouths with plain water and did not drink or eat for 30 min before saliva collection (Patsalos and Berry 2013).

TABLE 2 | Intraday and interday precision and accuracy of CBD in human serum and saliva.

Spiked concentration (ng/ml)	Measured (ng/ml)	Precision (%)	Accuracy (%)	Measured (ng/ml)	Precision (%)	Accuracy (%)
Serum	Intraday (n = 5)			Interday (n = 12)		
2.5 (LOQ)	2.5 ± 0.3	11.6	101.6	2.6 ± 0.2	7.9	104.3
35 (CQ1)	35.9 ± 2.4	6.7	102.6	32.8 ± 2.9	8.9	93.7
350 (CQ2)	380.7 ± 12.1	3.2	108.8	365.6 ± 17.5	4.8	104.5
750 (CQ3)	843 ± 17.6	2.1	112.4	794.2 ± 66.8	8.4	105.9
Saliva	Intraday (n = 5)			Interday (n = 15)		
2.5 (LOQ)	2.7 ± 0.2	6.5	106.9	2.7 ± 0.2	5.7	109.7
35 (CQ1)	37.3 ± 0.6	1.7	106.6	37.5 ± 0.9	2.5	107.1
350 (CQ2)	358.4 ± 7.1	2.0	102.4	366.4 ± 9.8	2.7	104.7
750 (CQ3)	742.9 ± 25.8	3.5	99.1	758.7 ± 24.1	3.2	101.2

TABLE 3 | Intraday and interday precision and accuracy of 7-hydroxy-CBD in human serum and saliva.

Spiked concentration (ng/ml)	Measured (ng/ml)	Precision (%)	Accuracy (%)	Measured (ng/ml)	Precision (%)	Accuracy (%)
Serum	Intraday (n = 5)			Interday (n = 12)		
5 (LOQ)	4.7 ± 0.4	7.7	93.2	5.0 ± 0.6	11.7	100.6
17.5 (CQ1)	18.2 ± 1.6	8.9	104.1	16.3 ± 1.5	9.4	93.1
175 (CQ2)	177.1 ± 8.4	4.7	101.2	182.8 ± 12.1	6.6	104.5
375 (CQ3)	401.2 ± 30.8	7.7	107.0	407.3 ± 23.9	5.9	108.6
Saliva	Intraday (n = 5)			Interday (n = 15)		
5 (LOQ)	4.7 ± 0.3	6.6	94.7	4.5 ± 0.3	6.8	90.6
17.5 (CQ1)	17.6 ± 0.5	2.6	100.6	18.0 ± 0.7	4.1	102.6
175 (CQ2)	174.8 ± 4.3	2.5	99.9	176.0 ± 5.3	3.0	100.6
375 (CQ3)	377.4 ± 5.5	1.4	100.6	372.2 ± 11.4	3.1	99.2

Statistical Analysis

Concentrations of analytes are reported as ng/ml and expressed as means ± SD. Comparison of stability parameters was performed by repeated measures analysis of variance (ANOVA). A two-tailed p value ≤ 0.05 was considered statistically significant. Statistical analyses were performed using SPSS version 20.0 (SPSS, Inc. Chicago, United States).

RESULTS

Method Development

A number of different chromatographic columns were tested initially to separate the analytes, including a Zorbax (Agilent, United States) and a Kinetex column (Phenomenex, Bologna, Italy). However, only the monolithic column provided optimal peak shape and peak resolution. Under the described chromatographic conditions CBD and IS eluted at 4.8 min and 7-hydroxy-CBD eluted at 3.9 min. Representative chromatograms of extracted serum and saliva samples (blank sample, a medium QC sample and a sample from a patient receiving CBD) are shown in **Figures 2–4**.

Method Validation

Within-run and between-run precision and accuracy values are reported in **Tables 2** and **3**. All values met the acceptability criteria specified in international guidelines for the validation of analytical assays (EMA guidelines, 2011). Intraday and interday accuracy was within 93.7–112.4% for CBD and 93.1–108.6% for 7-hydroxy-CBD in serum, and within 99.1–109.7% for CBD and 90.6–102.6% for 7-hydroxy-CBD in saliva. Intraday and interday precision values were in the range of 2.1–11.6% for CBD and 4.7–11.7% for 7-hydroxy-CBD in serum, and 1.7–6.5% for CBD and 1.4–6.8% for 7-hydroxy-CBD in saliva (**Tables 2** and **3**).

Mean extraction recoveries for CBD were 81, 90, 87, 89% in serum samples and 129, 87, 100, 100% in saliva samples (LOQ, low QC, medium QC and high QC respectively). Mean extraction recoveries for LOQ, low QC, medium QC and high QC of 7-hydroxy-CBD were 113, 109, 109, 111% in serum and 108, 100, 109, 110% in saliva, respectively.

CBD and 7-hydroxy-CBD concentrations in serum and saliva were unaltered after samples storage for up to one month at −20°C and after three freeze–thaw cycles (**Tables 4** and **5**). Calibration curves were linear over the tested concentration range for both analytes (**Figure 5**). Coefficients of correlation of the curves were 0.998 and 0.999 for CBD in serum and saliva respectively, and 0.998 and 0.999 for 7-hydroxy-CBD in serum and saliva respectively. Mean slopes were 0.006 and 0.007 for CBD in serum and saliva respectively and 0.002 for 7-hydroxy-CBD in both serum and saliva. The LOQs in serum and saliva were 2.5 ng/ml for CBD and 5 ng/ml for 7-hydroxy-CBD. The LOD was 1.5 ng/ml for CBD and 7-hydroxy-CBD in both serum and saliva. No interfering peaks were detected around the retention times of CBD, 7-hydroxy-CBD and IS in serum and saliva samples. Carryover of blank injections after the highest calibrator was negligible for all the analytes.

TABLE 4 | Stability of CBD in human serum and saliva under different storage conditions.

Spiked concentration (ng/ml)	Fresh samples (ng/ml)	24 h at room temperature (ng/ml)	Three freeze–thaw cycles (ng/ml)	1 month at −20°C (ng/ml)
Serum				
35 (CQ1)	30.9 ± 0.8	31.4 ± 0.4	32.7 ± 1.7	37.4 ± 1.6
350 (CQ2)	344.6 ± 6.7	364.9 ± 2.3	367.6 ± 7.7	364.8 ± 19.5
750 (CQ3)	706.3 ± 12.9	819.0 ± 18.1	851.3 ± 11.2	831.7 ± 30.1
Saliva				
35 (CQ1)	37.5 ± 0.6	33.7 ± 1.7	35.4 ± 1.3	39.5 ± 0.9
350 (CQ2)	355.6 ± 3.7	347.3 ± 6.6	376.5 ± 13.9	367.1 ± 18.6
750 (CQ3)	732.3 ± 11.2	748.7 ± 31.4	796.3 ± 24.1	809.1 ± 28.3

TABLE 5 | Stability of 7-hydroxy-CBD in human serum and saliva under different storage conditions.

Spiked concentration (ng/ml)	Fresh samples (ng/ml)	24 h at room temperature (ng/ml)	Three freeze–thaw cycles (ng/ml)	1 month at −20°C (ng/ml)
Serum				
17.5 (CQ1)	15.7 ± 0.5	17.8 ± 0.9	15.2 ± 0.3	19.2 ± 1.1
175 (CQ2)	178.1 ± 14.8	191.1 ± 6.4	171.1 ± 4.3	179.6 ± 8.1
375(CQ3)	396.8 ± 11.0	415.5 ± 8.5	406.5 ± 22.3	413.0 ± 14.9
Saliva				
17.5 (CQ1)	17.6 ± 0.5	17.1 ± 0.6	17.3 ± 1.5	20.0 ± 0.2
175 (CQ2)	173.4 ± 3.5	190.6 ± 6.7	192.4 ± 5.8	192.6 ± 9.8
375 (CQ3)	376.0 ± 5.2	400.7 ± 5.9	392.7 ± 25.8	421.2 ± 10.4

TABLE 6 | Details of assay results in each of the patients receiving chronic CBD treatment. 7-hydroxy-CBD was not detected in any of the saliva samples. Abbreviations: ASMs, antiseizure medications; CBD, cannabidiol; CBZ, carbamazepine; CLB, clobazam; DLZ, delorazepam; F, female; LCM, lacosamide; LTG, lamotrigine; M, male; OXC, oxcarbazepine; PER, perampanel; PB, phenobarbital; RFN, rufinamide; TPM, topiramate; VPA, valproate.

Patient number	Age, y	Sex	Weigh, kg	Dose of CBD (mg/kg/day)	Concomitant ASMs	Serum CBD concentration (ng/ml)	Serum 7-Hydroxy-CBD concentration (ng/ml)	Saliva CBD concentration (ng/ml)
1	20	F	41	15	VPA, OXC	94.4	58.5	9.1
2	18	F	52	15	PB, LTG, TPM, PER	195.5	80.7	57.8
3	18	F	57	6.6	TPM, LCM, CBZ, DLZ	22.5	11.2	23.2
4	18	M	55	8	VPA, PB, CLB	33.6	20.9	12.6
5	18	M	87	10	RFN, OXC VPA, CLB	77.2	26.8	13.4

Clinical Application

Details of CBD and 7-hydroxy-CBD measurements in samples collected from 5 patients stabilized on CBD treatment are reported in **Table 6**. Serum CBD concentrations ranged from 22.5 to 195.5 ng/ml across patients while serum 7-hydroxy-CBD concentrations ranged from 11.2 to 80.7 ng/ml. CBD could be quantitated in all saliva samples (**Figure 4**). The ratio between saliva concentrations and serum concentrations was very variable (range, 9.6–103%). 7-hydroxy-CBD was below the LOQ in all saliva samples.

DISCUSSION

Several assays for determining CBD in different biological matrices such as peripheral capillary blood, plasma, serum, saliva, urine, breast milk and hair have been reported recently (Pérez Montilla et al., 2021; Sempio et al., 2021b; Cliburn et al., 2021; da Silva et al., 2020; Desrosiers et al., 2015; Cobo-Golpe et al., 2021; Reber et al., 2021). Although a few of these assays have also been validated for measuring the active metabolite 7-hydroxy-CBD in plasma or serum samples (Sempio et al., 2021a; Malaca et al., 2021), to our knowledge the present HPLC-MS/MS method is the first reported assay that permits the simultaneous determination of CBD and its active metabolite 7-hydroxy-CBD in both human serum and saliva. Performance characteristics are within acceptability standards recommended by current guidelines. The method required only 50 µl of biological fluid and retains a high sensitivity. Sample preparation involves a simple protein precipitation step

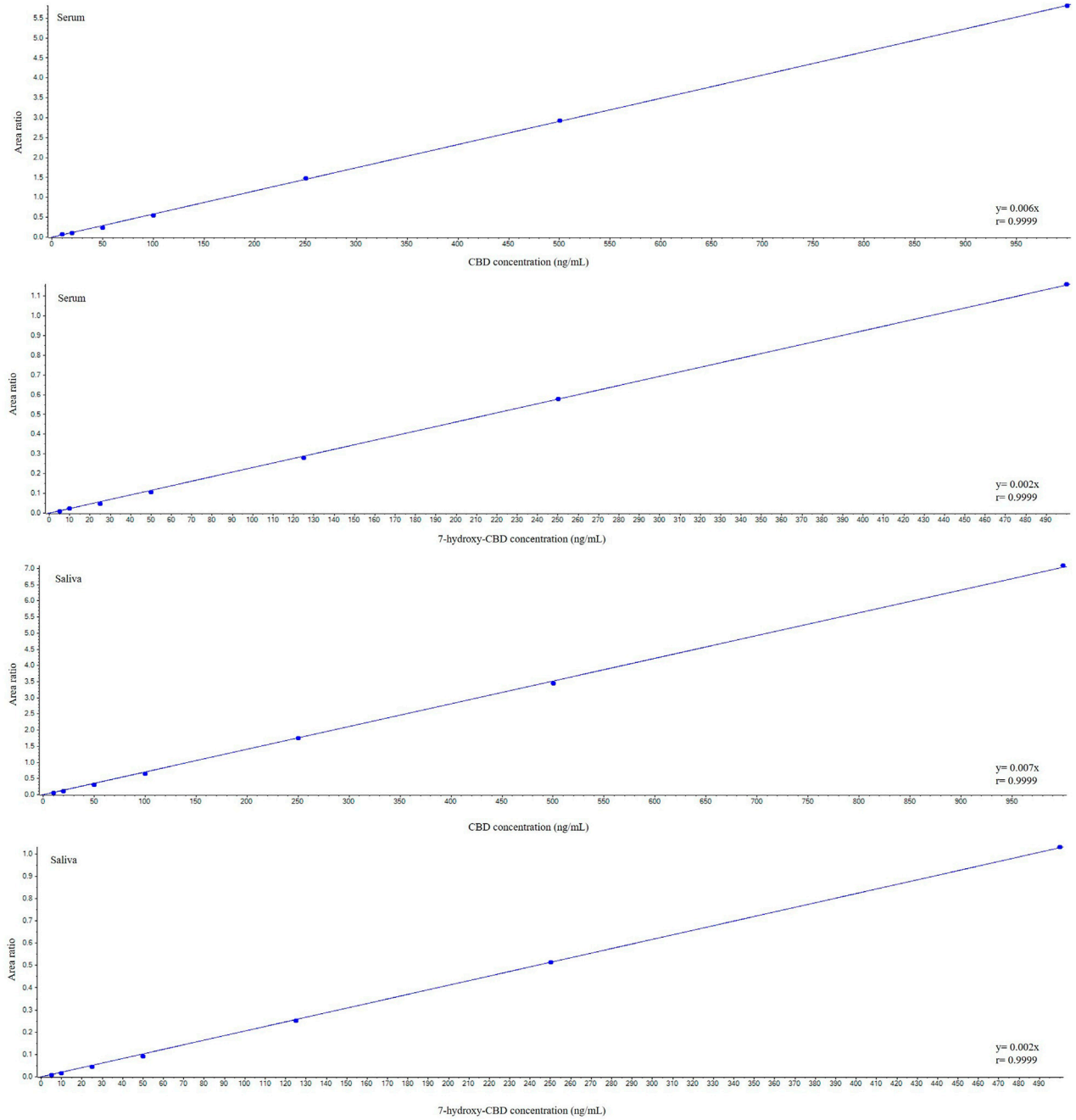

FIGURE 5 | Representative calibration curves for cannabidiol and 7-hydroxy-cannabidiol. CBD, cannabidiol.

followed by on-line extraction. Optimal separation of CBD and 7-hydroxy-CBD is achieved with a chromatographic run of 12 min. Use of an on-line solid phase extraction procedure associated with electrospray ionization is advantageous because it ensures optimal sensitivity/separation of the two analytes, reduces potential interferences/matrix effects and permits injection of a larger sample volume (40 µl versus standard volume of 5–10 µl) without overloading the analytical column while preserving optimal peaks shape and separation.

Our method is easy to implement in a clinical setting for several reasons. Processing and hands-on time is minimized due to absence of evaporation and/or concentration steps, without impacting on sensitivity. The assay involves direct injection of the sample in the HPLC-MS/MS system after a simple protein precipitation step with extremely low matrix effect, and automated on-line solid phase extraction avoids the time consuming process associated with off-line solid phase extraction. Stability of the analytes in samples kept at room

temperature for 24 h without protection from light exposure, after three freeze/thaw cycles and after 1 month storage at −20°C facilitates the handling of clinical samples prior to the assay.

The performance characteristics of the assay will facilitate its use for TDM as well as pharmacokinetic studies, including bioavailability investigations and studies designed to assess drug interactions affecting the pharmacokinetics of CBD and its active 7-hydroxy metabolite. For many ASMs, drug concentrations in saliva are highly correlated with concentrations in serum, allowing the use of salivary samples for TDM purposes (Patsalos et al., 2008). Salivary measurements are particularly convenient for children, who often experience discomfort with repeated venepunctures. The fact that CBD is mostly used in pediatric populations stimulated us to develop a CBD assay that could also be applied to salivary samples. Our preliminary observations suggest that 7-hydroxy-CBD concentrations in saliva are very low, and that CBD saliva to serum concentrations ratios are highly variable, and may not provide a reliable estimate of the drug concentration in serum. More studies, however, are required to confirm this finding. Further studies are also required to assess the relationship between serum CBD and 7-hydroxy-CBD concentrations, antiseizure response, and adverse effects. We believe that our assay will provide a useful tool to conduct such studies.

CONCLUSION

We described a novel simple, selective, sensitive and accurate on-line solid phase extraction HPLC-MS/MS method to measure CBD and 7-hydroxy-CBD in 50 µl samples of serum and saliva. The assay has been successfully validated according to existing guidelines. Fast on-line solid phase extraction on perfusion column combined with MS/MS detection enables to manage effectively background noise and matrix effect with sensitivity adequate for TDM and clinical pharmacokinetic studies.

DATA AVAILABILITY STATEMENT

The raw data supporting the conclusion of this article can be found in Zenodo (10.5281/zenodo.6520685).

AUTHOR CONTRIBUTIONS

VF: Assistance with study coordination, sample processing, analysis of the data, production of first draft of the manuscript MP, RM, PR, and VFD: sample processing, reviewing the manuscript for intellectual content FC, CF, VDG, and CV: data collection, reviewing the manuscript for intellectual content EP: Conceptualization of the study, coordination of the study, reviewing the manuscript for intellectual content.

FUNDING

This study was supported by grants from MIUR (Italian Ministry of Education, University and Research), the Italian Ministry of Health (Ricerca Corrente, IRCCS Mondino Foundation, Pavia, Italy) and the Regione Lombardia (Bando Innodriver-S3 2019 edition, fund POR FESR 2014–2020). This work was generated within the European Reference Network ERN-Epicare.

REFERENCES

Bialer, M., Johannessen, S. I., Koepp, M. J., Levy, R. H., Perucca, E., Tomson, T., et al. (2018). Progress Report on New Antiepileptic Drugs: A Summary of the Fourteenth Eilat Conference on New Antiepileptic Drugs and Devices (EILAT XIV). II. Drugs in More Advanced Clinical Development. *Epilepsia* 59 (10), 1842–1866. doi:10.1111/epi.14555

Cliburn, K. D., Huestis, M. A., Wagner, J. R., and Kemp, P. M. (2021). Identification and Quantification of Cannabinoids in Postmortem Fluids and Tissues by Liquid Chromatography-Tandem Mass Spectrometry. *J. Chromatogr. A* 1652, 462345. doi:10.1016/j.chroma.2021.462345

Cobo-Golpe, M., de-Castro-Ríos, A., Cruz, A., López-Rivadulla, M., and Lendoiro, E. (2021). Determination and Distribution of Cannabinoids in Nail and Hair Samples. *J. Anal. Toxicol.* 45 (9), 969–975. doi:10.1093/jat/bkaa164

da Silva, C. P., Dalpiaz, L. P. P., Gerbase, F. E., Muller, V. V., Cezimbra da Silva, A., Lizot, L. F., et al. (2020). Determination of Cannabinoids in Plasma Using Salting-Out-Assisted Liquid-Liquid Extraction Followed by LC-MS/MS Analysis. *Biomed. Chromatogr.* 34 (12), e4952. doi:10.1002/bmc.4952

Desrosiers, N. A., Scheidweiler, K. B., and Huestis, M. A. (2015). Quantification of Six Cannabinoids and Metabolites in Oral Fluid by Liquid Chromatography-Tandem Mass Spectrometry. *Drug Test. Anal.* 7 (8), 684–694. doi:10.1002/dta.1753

Epidyolex (2019). *Summary of Product Characteristics*. London: GW Pharma (International) B.V. https://www.ema.europa.eu/en/documents/product-information/epidyolex-epar-product-information_en.pdf (Accessed February 14, 2022).

Epidiolex (2020). *Full Prescribing Information*. United States: Greenwich Biosciences Inc. https://www.epidiolex.com/sites/default/files/pdfs/VV-MED-03633_EPIDIOLEX_(Cannabidiol)_USPI.pdf (Accessed February 14, 2022).

European Medicines Agency (2011). *Committee for Medicinal Products for Human Use: Guideline on Bioanalytical Method Validation*. London: EMA/CHMP/EWP. Retrieved from http://www.ema.europa.eu/docs/en_GB/document_library/Scientific_guideline/2011/08/WC500109686.pdf (Accessed February 14, 2022).

Franco, V., Bialer, M., and Perucca, E. (2021). Cannabidiol in the Treatment of Epilepsy: Current Evidence and Perspectives for Further Research. *Neuropharmacology* 185, 108442. doi:10.1016/j.neuropharm.2020.108442

Franco, V., and Perucca, E. (2019). Pharmacological and Therapeutic Properties of Cannabidiol for Epilepsy. *Drugs* 79, 1435–1454. doi:10.1007/s40265-019-01171-4

Jiang, R., Yamaori, S., Takeda, S., Yamamoto, I., and Watanabe, K. (2011). Identification of Cytochrome P450 Enzymes Responsible for Metabolism of Cannabidiol by Human Liver Microsomes. *Life Sci.* 89 (5–6), 165–170. doi:10.1016/j.lfs.2011.05.018

Malaca, S., Gottardi, M., Pigliasco, F., Barco, S., Cafaro, A., Amadori, E., et al. (2021). UHPLC-MS/MS Analysis of Cannabidiol and its Metabolites in Serum of Patients with Resistant Epilepsy Treated with CBD Formulations. *Pharmaceuticals* 14 (7), 630. doi:10.3390/ph14070630

Mazur, A., Lichti, C. F., Prather, P. L., Zielinska, A. K., Bratton, S. M., Gallus-Zawada, A., et al. (2009). Characterization of Human Hepatic and Extrahepatic UDP-Glucuronosyltransferase Enzymes Involved in the Metabolism of Classic Cannabinoids. *Drug Metab. Dispos.* 37 (7), 1496–1504. doi:10.1124/dmd.109.026898

Morrison, G., Crockett, J., Blakey, G., and Sommerville, K. (2019). A Phase 1, Open-Label, Pharmacokinetic Trial to Investigate Possible Drug-Drug Interactions between Clobazam, Stiripentol, or Valproate and Cannabidiol in Healthy Subjects. *Clin. Pharmacol. Drug Dev.* 8 (8), 1009–1031. doi:10.1002/cpdd.665

Patsalos, P. N., Berry, D. J., Bourgeois, B. F., Cloyd, J. C., Glauser, T. A., Johannessen, S. I., et al. (2008). Antiepileptic Drugs-Best Practice Guidelines for Therapeutic Drug Monitoring: a Position Paper by the Subcommission on Therapeutic Drug Monitoring, ILAE Commission on Therapeutic Strategies. *Epilepsia* 49 (7), 1239–1276. doi:10.1111/j.1528-1167.2008.01561.x

Patsalos, P. N., and Berry, D. J. (2013). Therapeutic Drug Monitoring of Antiepileptic Drugs by Use of Saliva. *Ther. Drug Monit.* 35 (1), 4–29. doi:10.1097/FTD.0b013e31827c11e7

Pérez Montilla, C. A., Schaiquevich, P. S., Cáceres Guido, P., Caraballo, R. H., Reyes Valenzuela, G., Cruz, C. V., et al. (2021). An Ultrafast Ultrahigh-Performance Liquid Chromatography Coupled with Tandem Mass Spectrometry Method for Cannabidiol Monitoring in Pediatric Refractory Epilepsy. *Ther. Drug Monit.* 43 (5), 712–717. doi:10.1097/FTD.0000000000000846

Perucca, E. (2017). Cannabinoids in the Treatment of Epilepsy: Hard Evidence at Last? *J. Epilepsy Res.* 7 (2), 61–76. doi:10.14581/jer.17012

Reber, J. D., Karschner, E. L., Seither, J. Z., Knittel, J. L., and Walterscheid, J. P. (2021). Screening and Confirmation Methods for the Qualitative Identification of Nine Phytocannabinoids in Urine by LC-MS/MS. *Clin. Biochem.* 98, 54–62. doi:10.1016/j.clinbiochem.2021.09.005

Sempio, C., Wymore, E., Palmer, C., Bunik, M., Henthorn, T. K., Christians, U., et al. (2021a). Detection of Cannabinoids by LC-MS-MS and ELISA in Breast Milk. *J. Anal. Toxicol.* 45 (7), 686–692. doi:10.1093/jat/bkaa142

Sempio, C., Almaraz-Quinones, N., Jackson, M., Zhao, W., Wang, G. S., Liu, Y., et al. (2021b). Simultaneous Quantification of 17 Cannabinoids by LC-MS-MS in Human Plasma. *J. Anal. Toxicol. Bkab030.* 46, 383–392. doi:10.1093/jat/bkab030

Taylor, L., Gidal, B., Blakey, G., Tayo, B., and Morrison, G. (2018). A Phase I, Randomized, Double-Blind, Placebo-Controlled, Single Ascending Dose, Multiple Dose, and Food Effect Trial of the Safety, Tolerability and Pharmacokinetics of Highly Purified Cannabidiol in Healthy Subjects. *CNS Drugs* 32 (11), 1053–1067. doi:10.1007/s40263-018-0578-5

Zendulka, O., Dovrtělová, G., Nosková, K., Turjap, M., Šulcová, A., Hanuš, L., et al. (2016). Cannabinoids and Cytochrome P450 Interactions. *Curr. Drug Metab.* 17 (3), 206–226. doi:10.2174/1389200217666151210142051

Conflict of Interest: EP received speaker and/or consultancy fees from Angelini, Arvelle, Biogen, Biopas, Eisai, GW Pharma, Sanofi group of companies, SKL Life Science, Takeda, UCB Pharma, Xenon Pharma, and Zogenix, and royalties from Wiley, Elsevier, and Wolters Kluwers. VDG received speaker and/or consultancy fees from GW Pharma, Neuraxpharm, Dr. Schar, Nutricia.

The remaining authors declare that the research was conducted in the absence of any commercial or financial relationships that could be construed as a potential conflict of interest.

Publisher's Note: All claims expressed in this article are solely those of the authors and do not necessarily represent those of their affiliated organizations, or those of the publisher, the editors and the reviewers. Any product that may be evaluated in this article, or claim that may be made by its manufacturer, is not guaranteed or endorsed by the publisher.

frontiers | Frontiers in Pharmacology

BRIEF RESEARCH REPORT
published: 01 July 2022
doi: 10.3389/fphar.2022.891842

Dose-Dependent Antidepressant-Like Effects of Cannabidiol in Aged Rats

Elena Hernández-Hernández[1,2†] *and M. Julia García-Fuster*[1,2*]

[1]IUNICS, University of the Balearic Islands, Palma, Spain, [2]Health Research Institute of Balearic Islands (IdISBa), Palma, Spain

Aging predisposes to late-life depression and since antidepressants are known to change their efficacy with age, novel treatment options are needed for our increased aged population. In this context, the goal of the present study was to evaluate the potential antidepressant-like effect of cannabidiol in aged rats. For this purpose, 19–21-month-old Sprague–Dawley rats were treated for 7 days with cannabidiol (dose range: 3–30 mg/kg) and scored under the stress of the forced-swim test. Hippocampal cannabinoid receptors and cell proliferation were evaluated as potential molecular markers underlying cannabidiol's actions. The main results of the present study demonstrated that cannabidiol exerted a dose-dependent antidepressant-like effect in aged rats (U-shaped, effective at the intermediate dose of 10 mg/kg as compared to the other doses tested), without affecting body weight. None of the molecular markers analyzed in the hippocampus were altered by cannabidiol's treatment. Overall, this study demonstrated a dose-dependent antidepressant-like response for cannabidiol at this age-window (aged rats up to 21 months old) and in line with other studies suggesting a beneficial role for this drug in age-related behavioral deficits.

Keywords: aging, late-life depression, antidepressants, rat, forced-swim test, hippocampus, CB receptors, neurogenesis

OPEN ACCESS

Edited by:
Maria S. Garcia-Gutierrez, Miguel Hernández University of Elche, Spain

Reviewed by:
Katarzyna Socała, Marie Curie-Sklodowska University, Poland
F. Khakpai, Islamic Azad University, Iran

***Correspondence:**
M. Julia García-Fuster
j.garcia@uib.es

***Present Address:**
Department of Pharmacology, University of the Basque Country (EHU/UPV), Leioa, Spain

Specialty section:
This article was submitted to Neuropharmacology, a section of the journal Frontiers in Pharmacology

Received: *08 March 2022*
Accepted: *20 May 2022*
Published: *01 July 2022*

Citation:
Hernández-Hernández E and García-Fuster MJ (2022) Dose-Dependent Antidepressant-Like Effects of Cannabidiol in Aged Rats. Front. Pharmacol. 13:891842. doi: 10.3389/fphar.2022.891842

INTRODUCTION

Aging is the strongest risk factor for most chronic disorders (e.g., Bektas et al., 2018), and in addition to changes in cognitive performance (Rosenzweig and Barnes, 2003; Mattson and Magnus, 2006), some other key features are particularly prone to decline, such as affective-like behavior, predisposing to the development of what is called late-life depression (McKinney and Sibille, 2013). In fact, the prevalence of depression in the population aged over 80 years has been shown to be around 15–20% (Stek et al., 2004), with the corresponding increased prescription of antidepressant drugs (Sonnenberg et al., 2008). Surprisingly, antidepressant-like treatments are known to change their efficacy with age [e.g., reviewed by Felice et al. (2015)]; however, not much research is focused on characterizing classical antidepressant-like responses and/or novel therapeutical options for this age group (see some representative recent preclinical studies: Fernández-Guasti et al., 2017; Mastrodonato et al., 2022), posing a health problem for our continuously increasing elderly population. In the clinic, the only approach taken with elderly patients includes lowering the doses to adjust for a slower metabolism. Remarkably, the described state of increased negative effect emerging with age can be modeled in naïve aging rodents (e.g., from middle-age and on; Hernández-Hernández et al., 2018 and references within; also Herrera-Pérez et al., 2008), providing a preclinical platform in which to test novel antidepressant drugs (e.g., Hernández-Hernández and García-Fuster, 2021).

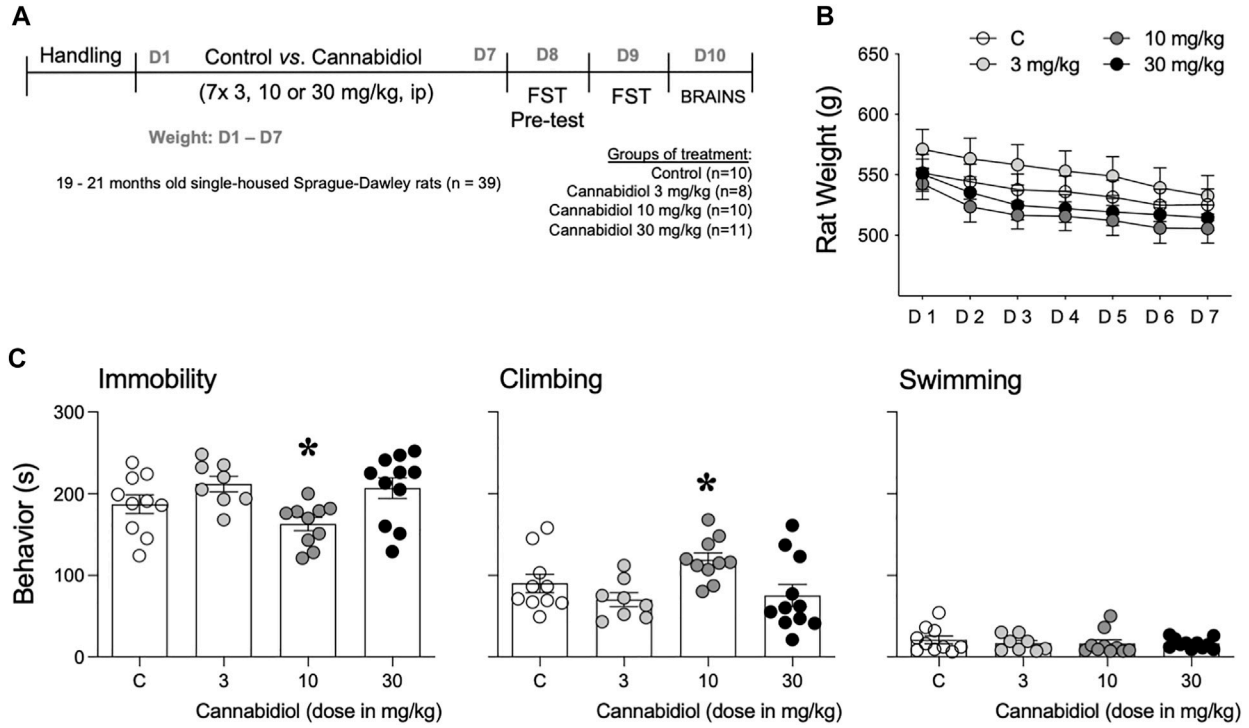

FIGURE 1 | (A) Experimental timeline. **(B)** Monitorization of body weight (g) during the experimental treatment. Data represent mean ± SEM of the body weight (g). A two-way repeated-measures ANOVA did not detect a significant effect of treatment. **(C)** Antidepressant-like effect as measured in the forced-swim test. Data represent mean ± SEM of the time spent (s) immobile, climbing, or swimming. Individual values are shown for each rat (symbols). One-way ANOVAs detected significant changes for immobility and climbing. Multiple comparisons were performed with Tukey's test: *$p < 0.05$ vs. the other doses tested, both 3 and 30 mg/kg of cannabidiol. Groups of treatment: control (C, $n = 10$) and cannabidiol (3 mg/kg, $n = 8$; 10 mg/kg, $n = 10$; and 30 mg/kg, $n = 11$).

In the context of characterizing novel treatment options, cannabidiol, a non-psychomimetic phytocannabinoid found in *Cannabis sativa*, has demonstrated a valuable role in ameliorating certain stress-related psychiatric symptoms in rodent models (e.g., Marco et al., 2011; Campos et al., 2016, 2017; Haney and Evins 2016; García-Gutiérrez et al., 2020; Gonzalez-Cuevas et al., 2021; Stanciu et al., 2021), with a great safety potential (Pisani et al., 2021). Interestingly, prior preclinical studies have reported that the antidepressant- and/or anxiolytic-like effects induced by cannabidiol [reviewed recently by García-Gutiérrez et al. (2020) and Melas et al. (2021)] are sex- (Silote et al., 2021; Ledesma-Corvi and García-Fuster, 2022; Martín-Sánchez et al., 2022), stress- (Shbiro et al., 2019; Bis-Humbert et al., 2021a; Ledesma-Corvi and García-Fuster, 2022), and/or age-related (e.g., different efficacy in adolescent vs. adult rats: Bis-Humbert et al., 2020), while studies reporting the potential beneficial effects in older populations are scarce (in addition to its anti-oxidant and anti-inflammatory potential; Dash et al., 2021 and references within). Against this background, the goal of this study was to evaluate whether cannabidiol could exert an antidepressant-like response as measured in the forced-swim test in aged rats.

Several studies have been centered on elucidating cannabidiol's actions on improving stress-related alterations, involving multiple targets (reviewed by Silote et al., 2019; García-Gutiérrez et al., 2020), such as a multimodal pharmacologic profile over the endocannabinoid system (Bisogno et al., 2001; Thomas et al., 2007; Pertwee, 2008; Campos et al., 2012; Laprairie et al., 2015; Martínez-Pinilla et al., 2017; Tham et al., 2019), an agonistic potential over TRPV1 receptors (Bisogno et al., 2001), as well as the regulation of other neurotransmitter systems [i.e., serotoninergic, opioidergic, and dopaminergic; reviewed in Silote et al. (2019)] or neuroprotective targets (i.e., hippocampal neurogenesis; Marchalant et al., 2009; Fogaça et al., 2018; Luján et al., 2018, 2020). For that reason, and since hippocampal function is altered with aging (Rosenzweig and Barnes, 2003), the current study evaluated the potential regulation of CB1 and CB2 receptors, as well as that of an early stage of neurogenesis (i.e., cell proliferation) following cannabidiol's treatment in the hippocampus of aged rats.

METHODS

Animals

For this study, 39 male Sprague–Dawley rats (bred in the animal facility at the University of the Balearic Islands) were used when they were 19–21 months old (**Figure 1A**). The rats were housed

under standard vivarium conditions (22°C, 70% humidity, and 12-h light/dark cycle, lights on at 8:00 a.m.) with *ad libitum* access to a standard diet and tap water. Following size requirements (animals housed per standard cage), the rats were individually housed for several months before testing started. All procedures were performed during the light period (between 8:00 h and 15:00 h), complied with ARRIVE guidelines (Percie du Sert et al., 2020), EU Directive 2010/63/EU for animal experiments, and Spanish Royal Decree 53/2013, and were approved by the Local Bioethical Committee and the Regional Government. All efforts were made to minimize the number of rats used and their suffering.

Repeated Cannabidiol Treatment

All rats were handled for 5 days prior to drug treatment, during which they were separated into four groups and received either a daily dose of cannabidiol (3, 10, or 30 mg/kg, i.p.; n = 8, 10, and 11, respectively) (purity ≥98%; THC Pharm, Germany) or vehicle (1 ml/kg of DMSO, control group; n = 10) for 7 days. The doses of cannabidiol were selected based on a prior study from our research group showing age- and dose-dependent antidepressant-like responses (i.e., different dose-efficacy during adolescence vs. adulthood in male naïve rats; Bis-Humbert et al., 2020). Body weight was daily monitored through the treatment process (D1–D7).

Forced-Swim Test

To ascertain cannabidiol's antidepressant-like response in aged rats we used the forced-swim test, since it is a standardized test for screening antidepressant-like responses under a stressful situation (Slattery and Cryan, 2012). For this purpose, and following prior well-established procedures in our group (Bis-Humbert et al., 2020; 2021b), rats were individually exposed to a 15 min pre-test on D8, and a 5-min test on D9 (**Figure 1A**) that was videotaped. The water tanks (41 cm high × 32 cm diameter) were filled with water up to 25 cm depth (25 ± 1°C) and were changed for each rat. Videos were coded and blindly analyzed using Behavioral Tracker Software (CA, United States) to calculate the time spent (s) immobile or active (climbing or swimming).

Hippocampal Neurochemical Correlation

All rats were sacrificed by rapid decapitation on D10 (**Figure 1A**), their brains were extracted, and both hemispheres were separated. On the one hand, the right hippocampus was freshly dissected and frozen in liquid nitrogen until the contents of CB receptors were evaluated in total homogenates (40 μg) by Western blot analysis with anti-CB1 (1:2000; Abcam, Cat. No. 23703, United Kingdom) or anti-CB2 (1:1000; Cayman Chemical, Cat. No. 101550, United States) primary antibodies, as previously detailed by our group (García-Cabrerizo and García-Fuster, 2016; Bis-Humbert et al., 2021a). Low quantities of total homogenates (15 μg) were loaded to detect β-actin (1:10000; Sigma-Aldrich, clone AC-15, United States), which was used as a negative loading control, since its content was not altered by any of the treatment conditions. Each sample was run at least three times in different gels, and percent changes were calculated for each rat as compared to control-treated samples loaded in the same gels. On the other hand, the left hemisphere was quickly frozen and stored until the entire hippocampus (−1.72 to −6.80 mm from Bregma) was cryostat-cut (30 μm sections) and slide mounted (8 sections/slide, 8 slides/series, and 3 series/animal from the most anterior to the posterior part of the hippocampus) to evaluate the rate of cell proliferation with the anti-Ki-67 antibody (1:40,000; kindly provided by Dr. Huda Akil and Dr. Stanley J. Watson, University of Michigan, United States) by immunohistochemistry as detailed earlier (García-Fuster et al., 2010; García-Cabrerizo et al., 2015; García-Fuster et al., 2017). The number of immunostained Ki-67 + cells was quantified using a Leica DMR light microscope (63× objective lens) in all sections by a blind experimenter to the treatment groups and as previously described in detail (e.g., García-Fuster et al., 2010, 2011, 2017).

Statistics

All data were analyzed with GraphPad Prism, Version 9.3.1 (GraphPad Software, United States). The results are expressed as mean values ± standard error of the mean (SEM), with individual symbols for each rat shown within bar graphs. The changes in body weight were analyzed with two-way repeated-measures ANOVA. Potential overall changes in behavior (s) in the forced-swim test (i.e., immobility, climbing, or swimming) or in the content of brain markers (i.e., CB receptors and Ki-67 + cells) were evaluated by one-way ANOVAs followed by Tukey's multiple comparisons test. The level of significance was set at $p \leq 0.05$.

RESULTS

Cannabidiol Did Not Alter Normal Body Weight (g) in Aged Rats

Although no changes were observed by cannabidiol's treatment ($F_{3,35} = 1.18$, $p = 0.329$), there was a significant effect of day ($F_{6,210} = 68.15$, $p < 0.001$), probably driven by the observed moderate decreases in body weight for all groups during the course of the experimental procedure, and most probably caused by the stress of cannabidiol's treatment (**Figure 1B**).

Dose-Dependent Antidepressant-Like Effects of Cannabidiol in Aged Rats

When evaluating the antidepressant-like potential of cannabidiol (3, 10, and 30 mg/kg; i.p.) in the forced-swim test, although a one-way ANOVA detected a significant difference in the time-aged rats spent immobile ($F_{3,35} = 4.18$, $p = 0.012$; **Figure 1C**), this effect was mainly driven by the dose of 10 mg/kg, which significantly reduced immobility as compared to the other doses tested (−49 ± 16 s, $*p = 0.021$ vs. 3 mg/kg; −44 ± 15 s, $*p = 0.026$ vs. 30 mg/kg; U-shaped dose response; **Figure 1C**). Interestingly, the decrease observed in immobility paralleled an increase in the time rats spent climbing ($F_{3,35} = 3.89$, $p = 0.017$), with significant changes when comparing the dose of 10 mg/kg vs. 3 mg/kg (+49 ± 16 s, $*p = 0.026$) and 30 mg/kg (+44 ± 15 s, $*p = 0.031$; **Figure 1C**).

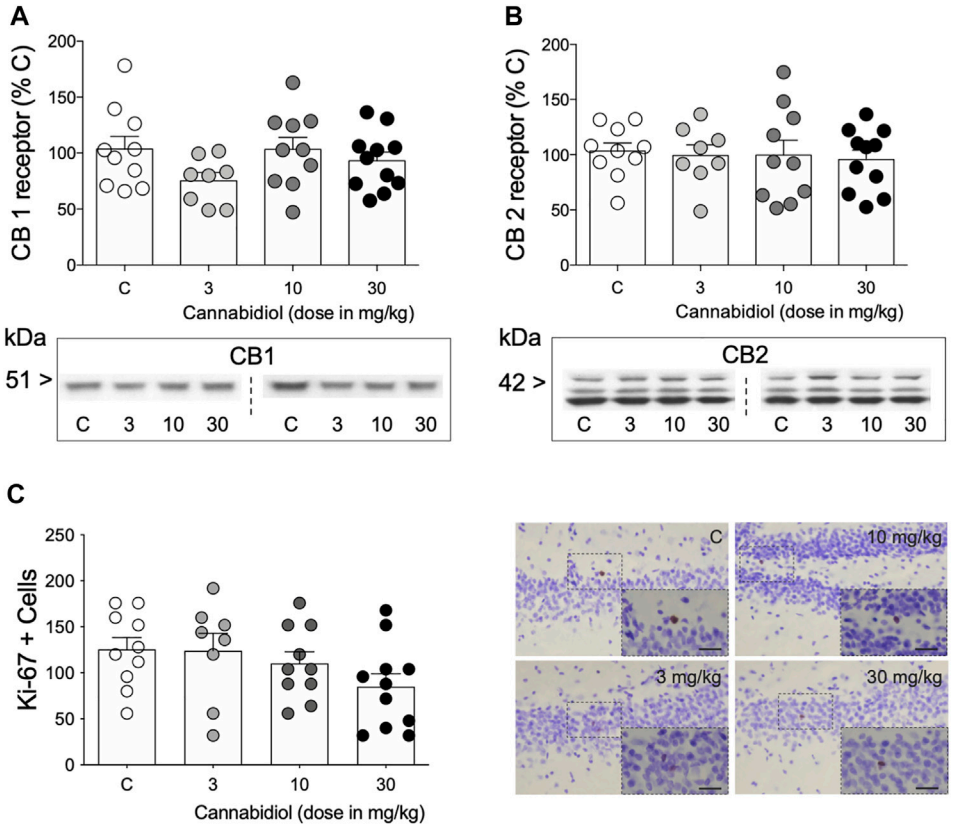

FIGURE 2 | Modulation of hippocampal molecular markers by repeated cannabidiol treatment. **(A)** CB1 and **(B)** CB2 receptors as measured by Western blot analysis. Data represent mean ± SEM of CB1 and CB2 protein contents expressed as % change vs. control-treated rats. Individual values are shown for each rat (symbols). One-way ANOVAs did not detect any significant changes. Representative immunoblots are shown depicting CB1 and CB2 labeling. **(C)** Ki-67 + cells in the dentate gyrus as measured by immunohistochemistry analysis. Data represent mean ± SEM of Ki-67 + cells. Individual values are shown for each rat (symbols). A one-way ANOVA did not detect any significant changes. Representative images of Ki-67 + cells (brown labeling in the blue granular layer) were taken using a light microscope and quantified using a 63× objective lens. Scale bar: 30 μm.

Finally, no changes were observed in swimming behavior ($F_{3,35}$ = 0.33, p = 0.803).

Cannabidiol Did Not Modulate CB1 and CB2 Receptors or the Rate of Early Cell Proliferation in the Hippocampus

When evaluating some of the potential molecular markers regulated by cannabidiol and that could parallel its behavioral actions, the results showed no changes in CB1 ($F_{3,35}$ = 1.68, p = 0.189; **Figure 2A**) and CB2 ($F_{3,35}$ = 0.11, p = 0.105; **Figure 2B**) receptors, nor in the rate of cell proliferation (Ki-67 + cells: $F_{3,35}$ = 1.78, p = 0.168; **Figure 2C**) in the hippocampus of aged rats as measured 3 days post-treatment.

DISCUSSION

The main results of the present study demonstrated that cannabidiol is capable of exerting a dose-dependent antidepressant-like response in aged rats, without inducing changes in body weight. None of the molecular markers analyzed in the hippocampus (CB receptors and cell proliferation) were altered by cannabidiol treatment.

Cannabidiol induced a dose-dependent antidepressant-like effect in aged rats, as observed in the forced-swim test by a decrease in immobility paired with an increase in climbing. Interestingly, these effects were dose-dependent, being efficacious only with the intermediate dose tested (10 mg/kg) and as compared to lower (3 mg/kg) or higher (30 mg/kg) doses. In regards to the effective dose-range for cannabidiol's antidepressant-like efficacy through its ability to reduce immobility scores under the stress of a forced-swim test, prior studies suggested that lower doses were needed for mice (3–30 mg/kg) than rats (30–60 mg/kg) as reviewed in Silote et al. (2019). However, a recent study compared cannabidiol's antidepressant-like potential in adolescent vs. adult rats and demonstrated that while a dose of 30 mg/kg was needed in adulthood to induce changes in the forced-swim test, only the intermediate dose tested (10 mg/kg) rendered efficacious in adolescent rats (Bis-Humbert et al., 2020), demonstrating a similar U-shaped dose–response curve for adolescent and aged rats, and lowering the dose at which cannabidiol could induce an

antidepressant-like effect in older rats. A similar U-shaped pattern has been previously reported for cannabidiol's anxiolytic-like effects, with effective responses at an intermediate dose, but no change with lower or higher doses (García-Gutiérrez et al., 2020 and references within) and for cannabidiol's medicinal usage for cocaine-related behaviors has been reported (Nedelescu et al., 2022). Interestingly, the reduced rate in immobility was paralleled by an increase in climbing behavior, as previously reported for cannabidiol (Bis-Humbert et al., 2020; Ledesma-Corvi and García-Fuster, 2022) and in line with the antidepressants that exert their actions through the modulation of the noradrenergic system (Detke et al., 1995). In conjunction, and to the best of our knowledge, this is the first study to demonstrate that cannabidiol is capable of inducing dose-dependent responses in the forced-swim test indicative of an antidepressant-like response in naïve aged rats, which physiologically show increased negative effect as compared to younger rats (Hernández-Hernández et al., 2018). These data provide a new therapeutical option for late-life depression that deserves further characterization. In this context, the observed lack of effect of cannabidiol on body weight at the doses tested suggested a good safety profile for cannabidiol in aged rats. Although some prior studies reported that repeated cannabidiol treatment could decrease normal body weight gain in adult rats (Ignatowska-Jankowska et al., 2011; Santiago et al., 2019), an effect probably mediated by CB2 receptors (Ignatowska-Jankowska et al., 2011), these effects seemed to be age dependent, since they replicated in a separate study for adult rats, but were not observed when cannabidiol was administered at the same doses during adolescence (Bis-Humbert et al., 2020) or in aged rats (present study). Moreover, one might speculate that the effects observed in the forced-swim test could be driven by changes in locomotor activity; however, several studies with doses up to 60 mg/kg of cannabidiol reported no changes in spontaneous locomotion when administered alone (e.g., Taffe et al., 2015; Anooshe et al., 2021; Ledesma et al., 2021), including our own evaluations when measuring distance traveled in the open field test (e.g., Bis-Humbert et al., 2020; Ledesma-Corvi and García-Fuster, 2022).

In an attempt to study some of the potential molecular targets and/or markers modulated by cannabidiol in aged rats, we explored the regulation of CB receptors (e.g., Fogaça et al., 2018) and a marker of an early stage of hippocampal neurogenesis (i.e., cell proliferation; Luján et al., 2018, 2020; Bis-Humbert et al., 2020). The results showed no changes in any of the markers analyzed. As for CB receptors, cannabidiol did not alter the protein content of CB receptors in the hippocampus at the time rats were sacrificed. Further studies should be carried out to evaluate the dynamics on how cannabidiol modulates CB receptors and include other brain regions. Also, other age-related changes such as the observed decrease in cannabinoid receptor binding and mRNA levels in aged rats (Romero et al., 1998) must be considered. Moreover, regarding cell proliferation, our prior study also showed a lack of regulation by cannabidiol in adolescent or adult rats at the same doses tested here and at the same specific time-points of analysis (Bis-Humbert et al., 2020), reinforcing the idea that the previously described beneficial effects of cannabidiol on improving cell genesis were observed in the context of prior exposure to a given stressor (Luján et al., 2018, 2020). In any case, these results are limited by the fact that brains were analyzed 3 days post-treatment (1 day after the observed antidepressant-like effect), with this timing being a particular photo-finish, and not necessarily correlative of the behavioral effects, and therefore conclusions should be made cautiously and in the context of this limitation. Further studies should collect brains at the specific time when the antidepressant-like effect was observed.

Ideally, we would have included female rats to compare cannabidiol's effects at this age range, since depression is about twice as common in women as in men (e.g., Labaka et al., 2018), and preclinical studies evaluating antidepressant-like responses in females are scarce in general, but even more so for female aged rodents (reviewed in Felice et al., 2015; Fernández-Guasti et al., 2017). Unfortunately, no female rats were available at the time of our experiments, and therefore, the effect of sex as a biological variable could not be included in the present study. In any case, prior studies suggested certain inefficacy for cannabidiol's antidepressant-like potential in female adult rats (e.g., Silote et al., 2021), including our own (Ledesma-Corvi and García-Fuster, 2022), and thus recommending future studies to better characterize the potential of this drug in both sexes and at all age-ranges.

In conclusion, this study increased the age-window at which cannabidiol exerted dose-dependent responses in this behavioral test, to include aged rats (up to 21 months old), at which it could be considered as a potential antidepressant, and in line with other studies suggesting a beneficial role for this drug in age-related behavioral deficits. Further experiments should evaluate other parameters (i.e., a wider range of doses, longer treatment paradigms, and models of induced depression) and include female aged rats to not only characterize the behavioral potential of cannabidiol but also try to better understand the molecular mechanisms underlying its actions.

DATA AVAILABILITY STATEMENT

The orginal contributions presented in this study are included in the article; further inquires can be directed to the corresponding author.

ETHICS STATEMENT

The animal study was reviewed and approved by the Local Bioethical Committee and the Regional Government, Balearic Islands, Spain.

AUTHOR CONTRIBUTIONS

MJG-F conceived the study; MJG-F and EH-H designed the experiments; EH-H performed the experiments, analyzed hte data, and prepared the intiial figures; MJG-F revised all the data and reformatted the figures; EH-H prepared the first draft of the manuscript; MJG-F wrote the final version of the

manuscript. Both authors have read, commented, edited and approved the final version of the manuscript.

FUNDING

This research was partly funded by Grants PID 2020-118582RB-I00 from MCIN/AEI/10.13039/501100011033 (Madrid, Spain), PDR2020/14 from Comunitat Autònoma de les Illes Balears (Direcció General de Política Universitària i Recerca with funds from the Tourist Stay Tax Law ITS 2017-006), and by Fundación Alicia Koplowitz (Madrid, Spain) to MJG-F; a predoctoral scholarship covered the salary of EH-H (FPI/2102/2018; CAIB), who is currently funded by the Margarita Salas Program (Ministerio de Universidades; Plan de Recuperación, Transformación y Resilencia; NextGenerationEU) with the participation of the University of the Balearic Islands.

ACKNOWLEDGMENTS

We would like to thank Professors Huda Akil and Stanley J. Watson (University of Michigan, Ann Arbor, MI, United States) for kindly providing Ki-67 antibody. Open Access was funded by the IV Convocatòria de publicacions en Accés Obert "Liberi" de l'IdISBa.

REFERENCES

Anooshe, M., Nouri, K., Karimi-Haghighi, S., Mousavi, Z., and Haghparast, A. (2021). Cannabidiol Efficiently Suppressed the Acquisition and Expression of Methamphetamine-Induced Conditioned Place Preference in the Rat. *Behav. Brain Res.* 404, 113158. doi:10.1016/j.bbr.2021.113158

Bektas, A., Schurman, S. H., Sen, R., and Ferrucci, L. (2018). Aging, Inflammation and the Environment. *Exp. Gerontol.* 105, 10–18. doi:10.1016/j.exger.2017.12.015

Bis-Humbert, C., García-Cabrerizo, R., and García-Fuster, M. J. (2021a). Antidepressant-like Effects of Cannabidiol in a Rat Model of Early-Life Stress with or without Adolescent Cocaine Exposure. *Pharmacol. Rep.* 73, 1195–1202. doi:10.1007/s43440-021-00285-5

Bis-Humbert, C., García-Cabrerizo, R., and García-Fuster, M. J. (2020). Decreased Sensitivity in Adolescent versus Adult Rats to the Antidepressant-like Effects of Cannabidiol. *Psychopharmacol. Berl.* 237, 1621–1631. doi:10.1007/s00213-020-05481-4

Bis-Humbert, C., García-Cabrerizo, R., and García-Fuster, M. J. (2021b). Dose-dependent Opposite Effects of Nortriptyline on Affective-like Behavior in Adolescent Rats: Comparison with Adult Rats. *Eur. J. Pharmacol.* 910, 174465. doi:10.1016/j.ejphar.2021.174465

Bisogno, T., Hanus, L., De Petrocellis, L., Tchilibon, S., Ponde, D. E., Brandi, I., et al. (2001). Molecular Targets for Cannabidiol and its Synthetic Analogues: Effect on Vanilloid VR1 Receptors and on the Cellular Uptake and Enzymatic Hydrolysis of Anandamide. *Br. J. Pharmacol.* 134, 845–852. doi:10.1038/sj.bjp.0704327

Campos, A. C., Fogaça, M. V., Scarante, F. F., Joca, S. R. L., Sales, A. J., Gomes, F. V., et al. (2017). Plastic and Neuroprotective Mechanisms Involved in the Therapeutic Effects of Cannabidiol in Psychiatric Disorders. *Front. Pharmacol.* 8, 269. doi:10.3389/fphar.2017.00269

Campos, A. C., Fogaça, M. V., Sonego, A. B., and Guimarães, F. S. (2016). Cannabidiol, Neuroprotection and Neuropsychiatric Disorders. *Pharmacol. Res.* 112, 119–127. doi:10.1016/j.phrs.2016.01.033

Campos, A. C., Moreira, F. A., Gomes, F. V., del Bel, E. A., and Guimarães, F. S. (2012). Multiple Mechanisms Involved in the Large-Spectrum Therapeutic Potential of Cannabidiol in Psychiatric Disorders. *Philos. Trans. R. Soc. Lond B Biol. Sci.* 367, 3364–3378. doi:10.1098/rstb.2011.0389

Dash, R., Ali, M. C., Jahan, I., Munni, Y. A., Mitra, S., Hannan, M. A., et al. (2021). Emerging Potential of Cannabidiol in Reversing Proteinopathies. *Ageing Res. Rev.* 65, 101209. doi:10.1016/j.arr.2020.101209

Detke, M. J., Rickels, M., and Lucki, I. (1995). Active Behaviors in the Rat Forced Swimming Test Differentially Produced by Serotonergic and Noradrenergic Antidepressants. *Psychopharmacol. Berl.* 121, 66–72. doi:10.1007/BF02245592

Felice, D., O'Leary, O. F., Cryan, J. F., Dinan, T. G., Gardier, A. M., Sánchez, C., et al. (2015). When Ageing Meets the Blues: Are Current Antidepressants Effective in Depressed Aged Patients? *Neurosci. Biobehav Rev.* 55, 478–497. doi:10.1016/j.neubiorev.2015.06.005

Fernández-Guasti, A., Olivares-Nazario, M., Reyes, R., and Martínez-Mota, L. (2017). Sex and Age Differences in the Antidepressant-like Effect of Fluoxetine in the Forced Swim Test. *Pharmacol. Biochem. Behav.* 152, 81–89. doi:10.1016/j.pbb.2016.01.011

Fogaça, M. V., Campos, A. C., Coelho, L. D., Duman, R. S., and Guimarães, F. S. (2018). The Anxiolytic Effects of Cannabidiol in Chronically Stressed Mice Are Mediated by the Endocannabinoid System: Role of Neurogenesis and Dendritic Remodeling. *Neuropharmacology* 135, 22–33. doi:10.1016/j.neuropharm.2018.03.001

García-Cabrerizo, R., and García-Fuster, M. J. (2016). Opposite Regulation of Cannabinoid CB1 and CB2 Receptors in the Prefrontal Cortex of Rats Treated with Cocaine during Adolescence. *Neurosci. Lett.* 615, 60–65. doi:10.1016/j.neulet.2016.01.018

García-Cabrerizo, R., Keller, B., and García-Fuster, M. J. (2015). Hippocampal Cell Fate Regulation by Chronic Cocaine during Periods of Adolescent Vulnerability: Consequences of Cocaine Exposure during Adolescence on Behavioral Despair in Adulthood. *Neuroscience* 304, 302–315. doi:10.1016/j.neuroscience.2015.07.040

García-Fuster, M. J., Flagel, S. B., Mahmood, S. T., Mayo, L. M., Thompson, R. C., Watson, S. J., et al. (2011). Decreased Proliferation of Adult Hippocampal Stem Cells during Cocaine Withdrawal: Possible Role of the Cell Fate Regulator FADD. *Neuropsychopharmacology* 36, 2303–2317. doi:10.1038/npp.2011.119

García-Fuster, M. J., Parsegian, A., Watson, S. J., Akil, H., and Flagel, S. B. (2017). Adolescent Cocaine Exposure Enhances Goal-Tracking Behavior and Impairs Hippocampal Cell Genesis Selectively in Adult Bred Low-Responder Rats. *Psychopharmacol. Berl.* 234, 1293–1305. doi:10.1007/s00213-017-4566-0

García-Fuster, M. J., Perez, J. A., Clinton, S. M., Watson, S. J., and Akil, H. (2010). Impact of Cocaine on Adult Hippocampal Neurogenesis in an Animal Model of Differential Propensity to Drug Abuse. *Eur. J. Neurosci.* 31, 79–89. doi:10.1111/j.1460-9568.2009.07045.x

García-Gutiérrez, M. S., Navarrete, F., Gasparyan, A., Austrich-Olivares, A., Sala, F., and Manzanares, J. (2020). Cannabidiol: A Potential New Alternative for the Treatment of Anxiety, Depression, and Psychotic Disorders. *Biomolecules* 10, 1575. doi:10.3390/biom10111575

Gonzalez-Cuevas, G., Garcia-Gutierrez, M. S., Navarrete, F., de Guglielmo, G., and Manzanares, J. (2021). Editorial: Cannabidiol Treatment in Neurotherapeutic Interventions. *Front. Pharmacol.* 12, 752292. doi:10.3389/fphar.2021.752292

Haney, M., and Evins, A. E. (2016). Does Cannabis Cause, Exacerbate or Ameliorate Psychiatric Disorders? an Oversimplified Debate Discussed. *Neuropsychopharmacology* 41, 393–401. doi:10.1038/npp.2015.251

Hernández-Hernández, E., and García-Fuster, M. J. (2021). Evaluating the Effects of 2-BFI and Tracizoline, Two Potent I2-Imidazoline Receptor Agonists, on Cognitive Performance and Affect in Middle-Aged Rats. *Naunyn Schmiedeb. Arch. Pharmacol.* 394, 989–996. doi:10.1007/s00210-020-02042-6

Hernández-Hernández, E., Miralles, A., Esteban, S., and García-Fuster, M. J. (2018). Improved Age-Related Deficits in Cognitive Performance and Affective-like Behavior Following Acute, but Not Repeated, 8-OH-DPAT Treatments in Rats: Regulation of Hippocampal FADD. *Neurobiol. Aging* 71, 115–126.

Herrera-Pérez, J. J., Martínez-Mota, L., and Fernández-Guasti, A. (2008). Aging Increases the Susceptibility to Develop Anhedonia in Male Rats. *Prog. Neuropsychopharmacol. Biol. Psychiatry* 32, 1798–1803. doi:10.1016/j.pnpbp.2008.07.020

Ignatowska-Jankowska, B., Jankowski, M. M., and Swiergiel, A. H. (2011). Cannabidiol Decreases Body Weight Gain in Rats: Involvement of CB2 Receptors. *Neurosci. Lett.* 490, 82–84. doi:10.1016/j.neulet.2010.12.031

Labaka, A., Goñi-Balentziaga, O., Lebeña, A., and Pérez-Tejada, J. (2018). Biological Sex Differences in Depression: a Systematic Review. *Biol. Res. Nurs.* 20, 383–392. doi:10.1177/1099800418776082

Laprairie, R. B., Bagher, A. M., Kelly, M. E., and Denovan-Wright, E. M. (2015). Cannabidiol Is a Negative Allosteric Modulator of the Cannabinoid CB1 Receptor. *Br. J. Pharmacol.* 172, 4790–4805. doi:10.1111/bph.13250

Ledesma, J. C., Manzanedo, C., and Aguilar, M. A. (2021). Cannabidiol Prevents Several of the Behavioral Alterations Related to Cocaine Addiction in Mice. *Prog. Neuropsychopharmacol. Biol. Psychiatry* 111, 110390. doi:10.1016/j.pnpbp.2021.110390

Ledesma-Corvi, S., and García-Fuster, M. J. (2022). "Antidepresssant-like Effects of Cannabidiol in a Rat Model of Early-Life Stress: Sex- and Age-dependent Efficacy," in European College of Neuropsychopharmacology Workshop, Nice, France, 17-20 March, 2022.

Luján, M. Á., Castro-Zavala, A., Alegre-Zurano, L., and Valverde, O. (2018). Repeated Cannabidiol Treatment Reduces Cocaine Intake and Modulates Neural Proliferation and CB1R Expression in the Mouse hippocampus. *Neuropharmacology* 143, 163–175. doi:10.1016/j.neuropharm.2018.09.043

Luján, M. A., Cartacorps, L., and Valverde, O. (2020). The Pharmacological Reduction of Hippocampal Neurogenesis Attenuates the Protective Effects of Cannabidiol on Cocaine Voluntary Intake. *Addict. Biol.* 25, e12778. doi:10.1111/adb.12778

Marchalant, Y., Brothers, H. M., Norman, G. J., Karelina, K., DeVries, A. C., and Wenk, G. L. (2009). Cannabinoids Attenuate the Effects of Aging upon Neuroinflammation and Neurogenesis. *Neurobiol. Dis.* 34, 300–307. doi:10.1016/j.nbd.2009.01.014

Marco, E. M., García-Gutiérrez, M. S., Bermúdez-Silva, F. J., Moreira, F. A., Guimarães, F., Manzanares, J., et al. (2011). Endocannabinoid System and Psychiatry: in Search of a Neurobiological Basis for Detrimental and Potential Therapeutic Effects. *Front. Behav. Neurosci.* 5, 63. doi:10.3389/fnbeh.2011.00063

Martín-Sánchez, A., González-Pardo, H., Alegre-Zurano, L., Castro-Zavala, A., López-Taboada, I., Valverde, O., et al. (2022). Early-life Stress Induces Emotional and Molecular Alterations in Female Mice that Are Partially Reversed by Cannabidiol. *Prog. Neuropharmacol. Biol. Psychiatry* 115, 110508. doi:10.1016/j.pnpbp.2021.110508

Martínez-Pinilla, E., Varani, K., Reyes-Resina, I., Angelats, E., Vincenzi, F., Ferreiro-Vera, C., et al. (2017). Binding and Signaling Studies Disclose a Potential Allosteric Site for Cannabidiol in Cannabinoid CB2 Receptors. *Front. Pharmacol.* 8, 744. doi:10.3389/fphar.2017.00744

Mastrodonato, A., Pavlova, I., Kee, N. C., Pham, V. A., McGowan, J. C., Mann, J. J., et al. (2022). Prophylactic (R,S)-ketamine Is Effective against Stress-Induced Behaviors in Adolescent but Not Aged Mice. *Int. J. Neuropsychopharmacol.* 2022, 20. doi:10.1093/ijnp/pyac020

Mattson, M. P., and Magnus, T. (2006). Ageing and Neuronal Vulnerability. *Nat. Rev. Neurosci.* 7, 278–294. doi:10.1038/nrn1886

McKinney, B. C., and Sibille, E. (2013). The Age-By-Disease Interaction Hypothesis of Late-Life Depression. *Am. J. Geriatr. Psychiatry* 21, 418–432. doi:10.1016/j.jagp.2013.01.053

Melas, P. A., Scherma, M., Fratta, W., Cifani, C., and Fadda, P. (2021). Cannabidiol as a Potential Treatment for Anxiety and Mood Disorders: Molecular Targets and Epigenetic Insights from Preclinical Research. *Int. J. Mol. Sci.* 22, 1863. doi:10.3390/ijms22041863

Nedelescu, H., Wagner, G. E., de Ness, G. L., Carroll, A., Kerr, T. M., Wang, J., et al. (2022). Cannabidiol Produces Distinct U-Shaped Dose-Response Effects on Cocaine-Induced Conditioned Place Preference and Associated Recruitment of Prelimbic Neurons in Male Rats. *Biol. Psychiatry Glob. Open Sci.* 2, 70–78. doi:10.1016/j.bpsgos.2021.06.014

Percie du Sert, N., Ahluwalia, A., Alam, S., Avey, M. T., Baker, M., Browne, W. J., et al. (2020). Reporting Animal Research: Explanation and Elaboration for the ARRIVE Guidelines 2.0. *PLoS Biol.* 18, e3000411. doi:10.1371/journal.pbio.3000411

Pertwee, R. G. (2008). The Diverse CB1 and CB2 Receptor Pharmacology of Three Plant Cannabinoids: Delta9-Tetrahydrocannabinol, Cannabidiol and Delta9-Tetrahydrocannabivarin. *Br. J. Pharmacol.* 153, 199–215. doi:10.1038/sj.bjp.0707442

Pisani, S., McGoohan, K., Velayudhan, L., and Bhattacharyya, S. (2021). Safety and Tolerability of Natural and Synthetic Cannabinoids in Older Adults: a Systematic Review and Meta-Analysis of Open-Label Trials and Observational Studies. *Drugs Aging* 38, 887–910. doi:10.1007/s40266-021-00882-2

Romero, J., Berrendero, F., Garcia-Gil, L., de la Cruz, P., Ramos, J. A., and Fernández-Ruiz, J. J. (1998). Loss of Cannabinoid Receptor Binding and Messenger RNA Levels and Cannabinoid Agonist-Stimulated [35S]guanylyl-5'O-(thio)-triphosphate Binding in the Basal Ganglia of Aged Rats. *Neuroscience* 84, 1075–1083. doi:10.1016/s0306-4522(97)00552-6

Rosenzweig, E. S., and Barnes, C. A. (2003). Impact of Aging on Hippocampal Function: Plasticity, Network Dynamics, and Cognition. *Prog. Neurobiol.* 69, 143–179. doi:10.1016/s0301-0082(02)00126-0

Santiago, A. N., Mori, M. A., Guimarães, F. S., Milani, H., and Weffort de Oliveira, R. M. (2019). Effects of Cannabidiol on Diabetes Outcomes and Chronic Cerebral Hypoperfusion Comorbidities in Middle-Aged Rats. *Neurotox. Res.* 35, 463–474. doi:10.1007/s12640-018-9972-5

Shbiro, L., Hen-Shoval, D., Hazut, N., Rapps, K., Dar, S., Zalsman, G., et al. (2019). Effects of Cannabidiol in Males and Females in Two Different Rat Models of Depression. *Physiol. Behav.* 201, 59–63. doi:10.1016/j.physbeh.2018.12.019

Silote, G. P., Gatto, M. C., Eskelund, A., Guimarães, F. S., Wegener, G., and Joca, S. R. L. (2021). Strain-, Sex-, and Time-dependent Antidepressant-like Effects of Cannabidiol. *Pharm. (Basel)* 14, 1269. doi:10.3390/ph14121269

Silote, G. P., Sartim, A., Sales, A., Eskelund, A., Guimarães, F. S., Wegener, G., et al. (2019). Emerging Evidence for the Antidepressant Effect of Cannabidiol and the Underlying Molecular Mechanisms. *J. Chem. Neuroanat.* 98, 104–116. doi:10.1016/j.jchemneu.2019.04.006

Slattery, D. A., and Cryan, J. F. (2012). Using the Rat Forced Swim Test to Assess Antidepressant-like Activity in Rodents. *Nat. Protoc.* 7, 1009–1014. doi:10.1038/nprot.2012.044

Sonnenberg, C. M., Deeg, D. J., Comijs, H. C., van Tilburg, W., and Beekman, A. T. (2008). Trends in Antidepressant Use in the Older Population: Results from the LASA-Study over a Period of 10 Years. *J. Affect Disord.* 111, 299–305. doi:10.1016/j.jad.2008.03.009

Stanciu, C. N., Brunette, M. F., Teja, N., and Budney, A. J. (2021). Evidence for Use of Cannabinoids in Mood Disorders, Anxiety Disorders, and PTSD: A Systematic Review. *Psychiatr. Serv.* 72, 429–436. doi:10.1176/appi.ps.202000189

Stek, M. L., Gussekloo, J., Beekman, A. T., van Tilburg, W., and Westendorp, R. G. (2004). Prevalence, Correlates and Recognition of Depression in the Oldest Old: the Leiden 85-plus Study. *J. Affect Disord.* 78, 193–200. doi:10.1016/S0165-0327(02)00310-5

Taffe, M. A., Creehan, K. M., and Vandewater, S. A. (2015). Cannabidiol Fails to Reverse Hypothermia or Locomotor Suppression Induced by Δ(9)-tetrahydrocannabinol in Sprague-Dawley Rats. *Br. J. Pharmacol.* 172, 1783–1791. doi:10.1111/bph.13024

Tham, M., Yilmaz, O., Alaverdashvili, M., Kelly, M. E. M., Denovan-Wright, E. M., and Laprairie, R. B. (2019). Allosteric and Orthosteric Pharmacology of Cannabidiol and Cannabidiol-Dimethylheptyl at the Type 1 and Type 2 Cannabinoid Receptors. *Br. J. Pharmacol.* 176, 1455–1469. doi:10.1111/bph.14440

Thomas, A., Baillie, G. L., Phillips, A. M., Razdan, R. K., Ross, R. A., and Pertwee, R. G. (2007). Cannabidiol Displays Unexpectedly High Potency as an Antagonist of CB1 and CB2 Receptor Agonists *In Vitro*. *Br. J. Pharmacol.* 150, 613–623. doi:10.1038/sj.bjp.0707133

Conflict of Interest: The authors declare that the research was conducted in the absence of any commercial or financial relationships that could be construed as a potential conflict of interest.

Publisher's Note: All claims expressed in this article are solely those of the authors and do not necessarily represent those of their affiliated organizations, or those of the publisher, the editors, and the reviewers. Any product that may be evaluated in this article, or claim that may be made by its manufacturer, is not guaranteed or endorsed by the publisher.

frontiers | Frontiers in Pharmacology

ORIGINAL RESEARCH
published: 18 July 2022
doi: 10.3389/fphar.2022.925740

Role of 5HT1A Receptors in the Neuroprotective and Behavioral Effects of Cannabidiol in Hypoxic–Ischemic Newborn Piglets

*Lorena Barata[1], María de Hoz-Rivera[2], Angela Romero[2], María Martínez[2], Laura Silva[2], María Villa[2], Leticia Campa[3], Laura Jiménez-Sánchez[4,5] and José Martínez-Orgado[1]**

[1]Servicio de Neonatología, Hospital Clínico San Carlos, IdISSC, Madrid, Spain, [2]Fundación para La Investigación Biomédica del Hospital Clínico San Carlos (IdISSC), Madrid, Spain, [3]Centro de Investigación Biomédica en Red de Salud Mental (CIBERSAM), Spanish National Research Council (CSIC), Institut d'Investigacions Biomèdiques de Barcelona (IIBB), Institut d'Investigacions August Pi i Sunyer (IDIBAPS), ISCIII, Madrid, Spain, [4]Centro de Investigación Biomédica, Instituto de Biotecnoloía, Universidad de Granada, Granada, Spain, [5]Instituto de Investigación Biosanitaria de, Granada, Spain

Background: Hypoxic–ischemic (HI) insults have important deleterious consequences in newborns, including short-term morbidity with neuromotor and cognitive disturbances. Cannabidiol (CBD) has demonstrated robust neuroprotective effects and shows anxiolytic/antidepressant effects as well. These effects are thought to be related to serotonin 5-HT_{1A} receptor ($5HT_{1A}R$) activation. We hereby aimed to study the role of $5HT_{1A}R$ in the neuroprotective and behavioral effects of CBD in HI newborn piglets.

Methods: 1-day-old piglets submitted to 30 min of hypoxia (FiO2 10%) and bilateral carotid occlusion were then treated daily with vehicle, CBD 1 mg/kg, or CBD with the $5HT_{1A}R$ antagonist WAY 100635 1 mg/kg 72 h post-HI piglets were studied using amplitude-integrated EEG to detect seizures and a neurobehavioral test to detect neuromotor impairments. In addition, behavioral performance including social interaction, playful activity, hyperlocomotion, and motionless periods was assessed. Then, brain damage was assessed using histology (Nissl and TUNEL staining) and biochemistry (proton magnetic resonance spectroscopy studies.

Results: HI led to brain damage as assessed by histologic and biochemistry studies, associated with neuromotor impairment and increased seizures. These effects were not observed in HI piglets treated with CBD. These beneficial effects of CBD were not reversed by the $5HT_{1A}R$ antagonist, which is in contrast with previous studies demonstrating that $5HT_{1A}R$ antagonists eliminated CBD neuroprotection as assessed 6 h after HI in piglets. HI led to mood disturbances, with decreased social interaction and playfulness and increased hyperlocomotion. Mood disturbances were not observed in piglets treated with CBD, but in this case, coadministration of the $5HT_{1A}R$ antagonist eliminates the beneficial effects of CBD.

Conclusion: CBD prevented HI-induced mood disturbances in newborn piglets by acting on $5HT_{1A}R$. However, $5HT_{1A}R$ activation seems to be necessary for CBD neuroprotection only in the first hours after HI.

Keywords: hypoxia-ischemia, cannabidiol, serotonin receptors, neuroprotection, mood disorders, piglets

OPEN ACCESS

Edited by:
Jorge Manzanares, Miguel Hernández University of Elche, Spain

Reviewed by:
Claudia Bregonzio, CCT CONICET Córdoba, Argentina
Manuel Narvaez Peláez, University of Malaga, Spain

****Correspondence:***
José Martínez-Orgado
jose.martinezo@salud.madrid.org

Specialty section:
This article was submitted to Neuropharmacology, a section of the journal Frontiers in Pharmacology

Received: *21 April 2022*
Accepted: *30 May 2022*
Published: *18 July 2022*

Citation:
Barata L, de Hoz-Rivera M, Romero A, Martínez M, Silva L, Villa M, Campa L, Jiménez-Sánchez L and Martínez-Orgado J (2022) Role of 5HT1A Receptors in the Neuroprotective and Behavioral Effects of Cannabidiol in Hypoxic–Ischemic Newborn Piglets. Front. Pharmacol. 13:925740. doi: 10.3389/fphar.2022.925740

1 INTRODUCTION

Hypoxic–ischemic (HI) brain damage affects 1–3/1000 live-term newborns, representing one of the leading causes of death and permanent disability in infants (Zhou et al., 2020). The clinical picture of newborns with severe HI encephalopathy is that of deep coma, but newborns with mild-to-moderate HI encephalopathic show a varied neurologic picture that includes increased or decreased muscle tone and reflexes, fluctuating alertness, jitteriness, hyperexcitability, and seizures, depending on the timing and severity of the insult (Sarnat and Sarnat, 1976; Thompson et al., 1997). This situation makes the HI newborn particularly susceptible to the stress inherent in the application of the current standard of care and therapeutic hypothermia (Zhou et al., 2020), which determines that HI newborns under hypothermia very often receive sedatives as opioids (Berube et al., 2020). Since hypothermia affects the metabolism of opiates, opiate treatment during hypothermia easily causes unwanted side effects such as cardiorespiratory instability and neurologic depression (Berube et al., 2020).

Since hypothermia does not benefit a substantial number of HI newborns, additional or alternative neuroprotective strategies are being investigated (Zhou et al., 2020). Cannabidiol, the noneuphoric component of *Cannabis sativa*, has demonstrated robust neuroprotective effects in different models of HI brain damage in newborns, modulating inflammation, excitotoxicity, and oxidative stress, thus protecting neurons and glial cells (Martínez-Orgado et al., 2021). Although the mechanisms of action of CBD are not fully understood, it is known that CBD acts on different signaling pathways by activating different receptors such as the peroxisome proliferator-activated receptor gamma (PPARγ), G protein-coupled receptor 55 (GPR5), transient receptor potential vanilloid subtype 1 (TRPV1), and serotonin (5-hydroxytryptamine, 5-HT) 5-HT_{1A} receptors (de Almeida and Devi, 2020; Silvestro et al., 2020; Martínez-Orgado et al., 2021; Melas et al., 2021). In fact, the main neuroprotective effects of CBD are believed to be related to the activation of the 5-HT_{1A} receptor ($5HT_{1A}R$) (Silvestro et al., 2020). This is interesting since CBD exerts modulatory effects on mood disturbances such as anxiety, panic, or depression mainly through the activation of $5HT_{1A}R$ (De Gregorio et al., 2019; de Almeida and Devi, 2020; Melas et al., 2021). There are no reports on the effects of CBD on mood disturbances in newborn animals. We have reported that $5HT_{1A}R$ blockade abolishes the neuroprotective effects of CBD in HI piglets as assessed 6 h after the insult, but in that study, piglets remained sedated, which together with the short follow-up time made it impossible to assess the effects of CBD and 5HT1AR blockers in the piglet behavior (Pazos et al., 2013).

The aim of this work was to study the involvement of 5HT1AR receptors on CBD neuroprotection and the effects of CBD in HI-induced mood disorders. For this, we used a model with high translational value, in which neuromotor and behavioral evaluations are carried out in HI piglets in addition to histological and biochemical studies (Lafuente et al., 2011; Barata et al., 2019b).

2 METHODS

2.1 Experimental Model

All procedures complied with European Directive (2010/63/EU) and Spanish (RD 53/2013) regulations for the protection of experimental animals and were approved by the Animal Welfare Ethics Committee of Hospital Clinico San Carlos in Madrid, Spain (ProEx 175/14). All experimental procedures were designed and carried out by personnel qualified in Laboratory Animal Science, following FELASA recommendations in categories B and C to reduce animal stress and enhance animal welfare. All surgery was performed under adequate anesthesia and analgesia, and great effort was made to minimize suffering and reduce the number of animals used. Furthermore, all experimental procedures on animal welfare (anesthesia and analgesia; drug and substance administration) and euthanasia of the animals were conducted in compliance with FELASA recommendations. The sample size was calculated accordingly and based on previous results experiments using the same model (Lafuente et al., 2011; Barata et al., 2019b).

2.1.1 Induction of Hypoxia–Ischemia

The protocol was based on the model reported extensively elsewhere (Lafuente et al., 2011; Barata et al., 2019b). In short, one-day-old male Landrace-White large piglets provided by a local certified farm the day the experiment started were intubated and then mechanically ventilated (Babylog8000, Dräger, Germany) under sevoflurane anesthesia (5% induction and 1% maintenance) and received morphine chloride 1 0.1 mg/kg I.M. A right jugular vein indwelling catheter was inserted and kept in place over the entire experimental period for i.v. drug administration. Nontraumatic stainless-steel wires were placed into the piglet head's scalp to continuously monitor brain activity by amplitude-integrated electroencephalography (aEEG; BRM3, BrainZ Instruments, Auckland, New Zealand). Body temperature was maintained at 37.5–38.0°C by an air-warmed blanket. Piglets were then randomly assigned to the experimental group in a blind fashion. In the HI groups, each carotid artery was exposed and surrounded by an elastic band. Then, HI piglets underwent a 20-minute–long cerebral HI insult by interrupting carotid blood flow by pulling out the carotid bands and reducing inspired oxygen fraction (FiO_2) to 10%. The 20-min countdown started when aEEG trace became flat. At the end of the HI period, the carotid flow was restored and FiO_2 increased to 21%. Piglets were similarly managed but without HI insult and were used as reference (sham group, SHM, $n = 6$).

2.1.2 Drug Treatment

Thirty minutes after HI piglets were randomly assigned to receive i.v. vehicle (HV, $n = 16$) or CBD (Abcam, Cambridge, UK) 1 mg/k (HC, $n = 15$), alone or with the antagonist of serotonin $5HT_{1A}R$ WAY100635 (Tocris Bioscience, Abingdon, UK) 1 mg/kg (HCW, $n = 9$). CBD was prepared in a 5 mg/ml formulation of ethanol : colliphor : saline at a ratio of 2 : 1 : 17 and further diluted in saline to administer a total volume of 10 ml by infusion pump over

TABLE 1 | Neurobehavioral score (NBS).

Mental status	Coma	0
	Stupor	1
	Lethargy	3
	Awake	4
Behavior	None	0
	Weak	1
	Aggressive	3
	Normal	4
Pupils	Nonreactive	1
	Slow, asymmetric	2
	Normal	3
Vestibulo–ocular reflex	Absent Nystagmus	1
	Normal	2
		3
Stepping (barrow)	None	1
	Just fore/hind paws	2
	Normal	3
Righting	Absent/present	1
		2
Muscle tone	Atonic/hypertonic	1
	Partially atonic	2
	Partially hypertonic	3
	Normal	4
Standing	No	1
	Paresis	2
	Unsteady	3
	Normal	4
Walking	No	1
	Paresis	2
	Falling	3
	Normal	4
Eating	No suckling reflex	1
	Weak reflex, tube feeding	2
	No appetite	3
	Brief suckling	4
	Normal	5

10 min. WAY 100635 was administered 15 min before CBD and dissolved in the same vehicle. Doses of vehicle, CBD, and WAY 100635 were repeated every 24 h, three doses in total. Doses were selected following previous *in vivo* experiments by our group in HI piglets (Pazos et al., 2013; Barata et al., 2019a).

2.1.3 Follow-Up

Then, after fully regaining consciousness from the experimental procedure and anesthesia, piglets were extubated and transferred to the animal care facility. Piglets were housed in stainless steel cages with 0.5 m^2 per animal in a well-controlled warm-temperature environment. The cage contained a pending rope and a plastic ball for environmental enrichment. From 24 h post-insult, piglets were fed with artificial piglet formula (Nutrilac Milk Replacer for young piglets, Joosten Products B.V. Weert, Netherlands) every 3-4 h by a catheter attached to the examiner's finger to assess suckling. The examiner was blinded to the experimental group. Ceftazidime 15 mg/kg i.v. was administered every 12 h to prevent infections and acetaminophen 15 mg/kg i.v. was administered every 8 h for pain control. Seventy-two hours after the HI insult, piglets were sacrificed by KCl infusion under anesthesia (5% sevoflurane). Both carotid arteries were cannulated to perfuse brains with heparin in cold saline until clean fluid flew from the sectioned jugular arteries. Then, the brains were removed from the skull and sectioned. Brain slices from the left hemisphere were placed into 4% paraformaldehyde for histologic analysis, whereas those from the right hemisphere were snap frozen in isopentane and stored at −80°C for spectroscopy studies.

2.2 Neurobehavioral Assessment

Each morning from 8 to 10 a.m., the piglets were studied in the room where their cage was placed and video-recorded by one examiner. All video recordings were subsequently evaluated and scored when appropriate by three researchers blinded to the experimental group to obtain a mean value of the different items. A neurobehavioral score (NBS: 8–36 pts) (Lafuente et al., 2011; Barata et al., 2019b), based on that by LeBlanc et al. (LeBlanc et al., 1991), was carried out and video-recorded every 24 h, measuring alertness, behavior, muscle tone, standing, walking, and eating (**Table 1**).

Piglets were also video recorded during free wandering for 5 min. According to previous studies (Barata et al., 2019b), time spent interacting with caretakers (following caretaker's movements, pushing, nosing, sniffing, and licking) was considered social interaction time, whereas time spent in playful behavior (pushing, nosing, sniffing, and biting) with some known object (the sheet used for feeding) considered playfulness time. Time spent in unpurposive quick movements was considered hyperactivity time. Time with no activity while standing and lasting more than 5 s was considered motionless time. After the neurobehavioral assessment, piglets were wrapped up with a blanket and held by an examiner who sat in front of the aEEG device, to assess cerebral activity for over 10 min. Test start time and time when the piglet stopped fighting against immobilization (FAI) were recorded. The time of restlessness during slight restraint for aEEG performance was considered an indicator of piglet anxiety.

2.3 Seizures

Raw EEG traces were manually reviewed for electric seizures (periods of rhythmic activity starting with a sudden increase in voltage of at least 2 μV, accompanied by a narrowing of the band of aEEG activity, lasting at least 15 s).

2.4 Histologic Analysis

Histological studies were performed in 4 μm thick coronal sections obtained from fixed brain hemispheres, as reported previously (Lafuente et al., 2011; Pazos et al., 2013; Barata et al., 2019b). Areas of 1 mm^2 in the central three lobes of the parietal cortex and the adjacent CA1 area of the hippocampus were examined by two skilled investigators blinded to the experimental group. Neuronal necrosis was identified by Nissl staining, according to previous studies (Lafuente et al., 2011; Pazos et al., 2013; Barata et al., 2019b). Cell death was further studied in the cortex by TUNEL staining (DeadEnd Colorimetric TUNEL System, Promega, Spain) as reported elsewhere (Lafuente et al., 2011; Pazos et al., 2013; Barata et al., 2019b). Samples were visualized and photographed with a confocal TCS SP5 confocal microscope (Leica Microsystems, Wetzlar, Germany).

2.5 Proton Magnetic Resonance Spectroscopy (^{1}H-NMR)

Ex vivo ^{1}H spectrum was performed on a Bruker Avance 11.7 T spectrometer (Bruker BioSpin, Karlsruhe, Germany) equipped with a 4 mm triple channel 1H/13C/31P HR-MAS (High-Resolution Magic Angle Spinning) resonance probe. HMRS was performed in the MRI Unit of Instituto Investigaciones biomédicas "Alberto Sols" (CSIC-UAM, Madrid, Spain). Frozen cortex samples (5-10 mg weight) were introduced into a 50 µL zirconia rotor (4 mm OD) with 50 µL D2O and spun at 5000 Hz at 4°C to prevent tissue degradation processes. Two types of monodimensional proton spectra were acquired using water suppressed spin echo Carr Purcell Meiboom Gill (CPMG) sequence with 36 and 144 ms echo time and 128 scans. Data were collected into 64k data points using a spectral width of 10 kHz (20ppm) and water presaturation during a relaxation delay of 2 s, total acquisition of 16 min. All spectra were analyzed using the LC Model software; only peak concentrations obtained with a standard deviation lower than 20% were accepted. The content of glutamate (Glu), lactate (Lac), and N-acetylaspartate (NAA) was normalized to the creatine content.

2.6 Brain Neurotransmitter Concentration

Brain concentration of norepinephrine (NE), dopamine (DA), and serotonin (5-HT) was measured in homogenate from frozen brain tissue by high-performance liquid chromatography (Barata et al., 2019b). In short, tissues were ultrasonically homogenized in 0.4 M perchloric acid with 5 mM sodium metabisulfite, 8.3 uM cysteine, and 0.3 mM of EDTA. Samples were then centrifuged at 12,000 g for 30 min at 4°C. The three neurotransmitters were separated using an Ultrasphere 3 µm column (7.5 cm × 0.46 cm, Beckman, San Ramon, CA) and detected with a Hewlett–Packard amperometric detector (Palo Alto, CA). The mobile phase comprised 0.15 M KH2PO4, 0.46 mM octyl sodium sulfate, 0.5 Mm EDTA (pH 2.8 adjusted with phosphoric acid), and 12% methanol and was pumped at a rate of 0.6 ml/min.

2.7 Statistical Analysis

Data were analyzed with a statistical software package (GraphPad Prism 9.1.0; GraphPad Software, San Diego, CA, United States). After assessing the normality of data distribution using the Shapiro–Wilk test, data showing normal distribution were displayed as mean ± SEM and compared using one-way ANOVA with Holm–Šidák's test for multiple comparisons. Data showing a nonnormal distribution were displayed as median (CI 95%) and compared using Kruskall–Wallis with Dunn`s test for multiple comparisons. The distribution of qualitative parameters was studied using the X^2 test. $p < 0.05$ was considered significant.

3 RESULTS

3.1 General Data

Piglets from all groups were similar in weight at the moment of the study (1.70 ± 0.1, 1.73 ± 0.1, 1.69 ± 0.1, and 1.78 ± 0.1 kg for SHM, HV, HC, and HCW, respectively, $p = 0.83$). Four out of 16 HV, three out of 15 HC, and one out of nine HCW piglets died in the first 24 h after HI ($X^2 = 0.69$, $p = 0.7$). This represents a mortality of 27.5%, similar to that reported (Lafuente et al., 2011; Barata et al., 2019b). None of the SHM piglets died during the follow-up.

WAY100635 exerted no demonstrable effects on SHM or vehicle-treated HI animals in all studies. Therefore, those piglets were not included in the final data analysis.

3.2 Assessment of HI-Induced Brain Damage

HI led to a reduction in the density of viable neurons in the cortex and hippocampus, as assessed by Nissl staining and induced a dramatic increase in the number of TUNEL+ cells (**Figure 1A**). Such effects of HI were not observed in CBD-treated piglets, which showed viable neuron and TUNEL+ cell density similar to SHM (**Figure 1B**). Coadministration of the $5HT_{1A}R$ blocker did not modify the protective effects of CBD (**Figures 1A, B**).

HI insult led to brain metabolic derangement, as reflected by the increase in Lac/NAA ratio in the ^{1}H-NMR studies (**Figure 1C**). In addition, HI led to increased excitotoxicity as reflected by the higher Glu/NAA ratio in HI than in SHM animals (**Figure 1C**). Lac/NAA and Glu/NAA increase was not observed in HI piglets treated with CBD (**Figure 1C**). Coadministration of the $5HT_{1A}R$ blocker did not modify the protective effects of CBD (**Figure 1C**).

3.3 Seizures

The aEEG exam revealed electric seizures 72 h after HI in four out of 12 HV piglets but in none of the SHM, HC, or HCW piglets ($X^2 = 8.65$, $p = 0.03$). The seizure burden in those piglets was 17.9 ± 6.8 (1.4–32.5% of the recording time).

3.4 Functional and Behavioral Studies

HI insult led to a decrease in NBS global score 72 h after HI in HV animals (**Table 2**). Such a decrease was because of the decrease in motor and behavioral scores and in eating proficiency (**Table 2**). Such impairments were not observed in HC animals, which showed an NBS global score similar to SHM animals (**Table 2**). HCW animals showed a trend of worse behavioral and eating performance, but this did not reach statistical significance (**Table 2**).

HI led to mood disturbances in piglets as observed in HV piglets 72 h after HI. HV piglets showed increased anxiety as reflected by a nearly twofold increase in the FAI time (**Figure 2A**). In HV piglets there was a reduction in social interaction and playful activity (**Figures 2B, C**). By contrast, HV piglets showed increased hyperactivity time and increased motionless time (**Figures 2D, E**). Mood disturbances were not observed in HI piglets treated with CBD. Thus, playfulness, social interaction, hyperactivity, and motionless time, and FAI time, were similar in HC and SHM animals (**Figures 2A–E**). In this case, coadministration of the $5HT_{1A}R$ antagonist abolished the protective effects of CBD, with HCW showing similar responses to those of HV animals (**Figures 2A–E**)

3.5 Monoamine Brain Concentration

There was an increase in NE, DA, and 5HT concentration in brain samples obtained from HV animals 72 h after HI (**Figures 3A–C**). Such an increase was prevented by CBD administration, with HC animals showing similar monoamine brain

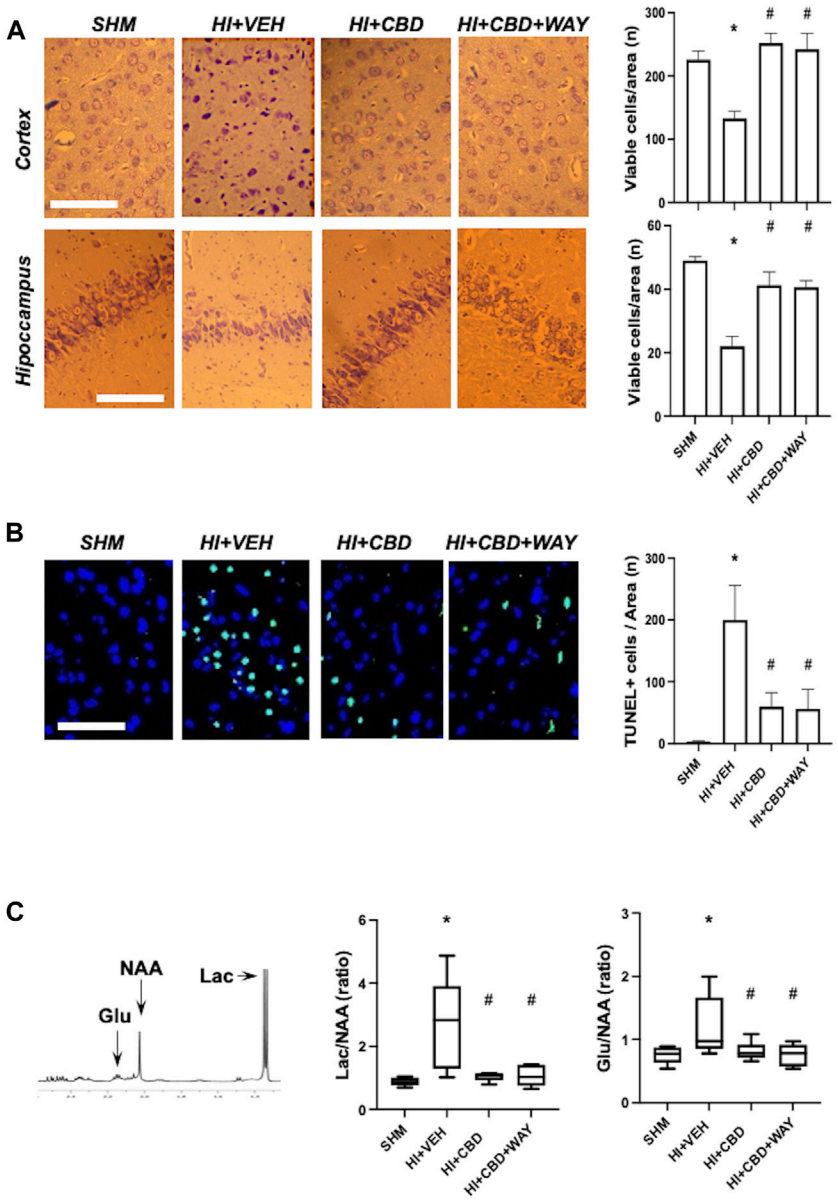

FIGURE 1 | Brain damage assessment 72 h after hypoxic–ischemic insult in brain samples from piglets treated with vehicle (HV), cannabidiol (HC), and WAY 100635 (HCW). Non-hypoxic–ischemic piglets served as controls (SHM). **(A)** Representative microphotographs (*left*) and quantification (*right*) of viable neurons using Nissl staining in the temporoparietal cortex and adjacent CA1 area of the hippocampus. **(B)** Representative microphotographs (*left*) and quantification (*right*) of cell death using TUNEL staining. Bars represent the mean (SEM) of 6–12 experiments. Scale bar: 100 μm. **(C)** Results from proton magnetic resonance spectroscopy. Lac: lactate. Glu: glutamate. NAA: N-acetylaspartate. Boxes represent the median (IQR) and Whiskers' maximum and minimum values. (*) $p < 0.05$ vs. SHM and (#) $p < 0.05$ vs. HV by ANOVA with Holm–Šidack test for multiple comparisons **(A, B)** or Kruskall–Wallis with Dunn's test for multiple comparisons **(C)**.

concentration similar to SHM (**Figures 3A–C**). Coadministration of the $5HT_{1A}R$ blocker did not modify the protective effects of CBD (**Figures 3A–C**).

4 DISCUSSION

HI insult led to brain damage in newborn piglets as assessed 72 h after the insult. HI led to the reduction in the cortex of viable neurons in Nissl-stained preparations and increased TUNEL positive cells, increased Lac/NAA ratio in ^{1}H-NMR studies, increased seizures, and the development of neuromotor deficits, as has been described (Barata et al., 2019b). All these features were not observed in piglets treated with CBD at a daily dose of 1 mg/kg for 3 days. The beneficial histological and neuromotor effects of CBD evaluated 72 h after HI insults in piglets have also been described after administering a single dose of CBD (Lafuente et al., 2011).

TABLE 2 | Neurobehavioral assessment.

	SHM (n = 6)	HI + VEH (*n* = 12)	HI + CBD (*n* = 12)	HI + CBD + WAY (*n* = 8)
Conscience	4.0 (4.0, 4.0)	4.0 (3.6, 4.1)	4.0 (4.0, 4.0)	4.0 (4.0, 4.0)
Behavior	4.0 (3.6, 4.1)	3.0 (1.7, 3,3)*	4.0 (3.3, 4.1)#	3.5 (2.8, 3.9)
Pupils	3.0 (3.0, 3.0)	3.0 (3.0, 3.0)	3.0 (3.0, 3.0)	3.0 (3.0, 3.0)
VOR	3.0 (3.0, 3.0)	3.0 (3.0, 3.0)	3.0 (3.0, 3.0)	3.0 (3.0, 3.0)
Barrow	3.0 (3.0,3 0.0)	3.0 (1.8, 3.1)	3.0 (2.7, 3.0)	3.0 (2.7, 3.0)
Righting	2.0 (2.0, 2.0)	2.0 (1.3, 2.1)	2.0 (2.0, 2.0)	2.0 (2.0, 2.0)
Tone	4.0 (4.0, 4.0)	3.2 (1.9, 3.6)*	4.0 (3.6, 4.0)	4.0 (3.6, 4.0)
Standing	4.0 (4.0, 4.0)	3.7 (2.2, 4.1)	4.0 (3.5, 3.9)	4.0 (3.6, 4.0)
Walking	4.0 (4.0, 4.0)	3.5 (2.2, 4.0)	4.0 (3.6, 4.0)	3.7 (3.5, 3.9)
Eating	5.0 (4.3, 5.3)	4.0 (2.2, 4.4)*	5.0 (4.5, 5.0)#	4.0 (3.4, 4.5)
Total	36.0 (35.1, 36.2)	31.5 (23.6, 34.5)*	35.5 (33.8, 35.8)#	34.0 (32.7, 34.7)

Median (CI, 95%). SHM: sham. HI: hypoxia–ischemia. VEH: vehicle. CBD: cannabidiol. WAY: WAY, 100635. VOR: vestibulo–ocular reflex. (*) $p < 0.05$ *vs. SHM, and (#)* $p < 0.05$ *vs. HV, by ANOVA, with Holm–Šidack test for multiple comparisons.*

4.1 $5HT_{1A}R$ Antagonism Did Not Affect CBD Neuroprotective Effects

In this work, the neuroprotective effects of CBD evaluated 72 h after HI were not affected by the coadministration of $5HT_{1A}R$ antagonist. However, we have reported that coadministration of the same $5HT_{1A}R$ antagonist results in loss of CBD neuroprotection assessed 6 h after a HI insult in piglets (Pazos et al., 2013). CBD is a well-known allosteric agonist of $5HT_{1A}R$ (Russo et al., 2005; de Almeida and Devi, 2020; Silvestro et al., 2020; Melas et al., 2021). It is generally accepted that the main neuroprotective effects of CBD are related to $5HT_{1A}R$ activation (Silvestro et al., 2020). Our results suggest that this is the case for CBD neuroprotection in the brain of newborn piglets in the first hours after HI, but later, CBD could exert neuroprotective actions by mechanisms independent of $5HT_{1A}R$ activation. Although other mechanisms were not studied in this work, it has been widely described that CBD can induce neuroprotective effects by activating other receptors such as PPARγ, GPR55, and TRPV1, increasing brain neurotrophic factor (BDNF) expression, modulating adenosine activity, or exerting antioxidant actions related to its molecular structure (Mori et al., 2017; de Almeida and Devi, 2020; Silvestro et al., 2020; Martínez-Orgado et al., 2021; Melas et al., 2021). $5HT_{1A}R$ agonists are neuroprotective in different preclinical models of HI brain damage in adult animals (Aguiar et al., 2021). It is unlikely that the signaling cascade triggered by $5HT_{1A}R$ activation was operational 6 h but not 72 h after HI insult in piglet brains. Indeed, $5HT_{1A}R$ activation was involved in the neurobehavioral effects of CBD in piglets 72 h after HI, as discussed below, suggesting that $5HT_{1A}R$ were operational at that time. Due to this finding, it is also unlikely that $5HT_{1A}R$ activation was less relevant in CBD neuroprotection due to a dramatic reduction of $5HT_{1A}R$ density. A mild reduction of $5HT_{1A}R$ density in the striatum, related to greater destruction of serotoninergic neurons, is described 7 days after HI insults in P3 rats, which present a brain developmental status similar to that of premature infants (Buller et al., 2012). In contrast, the $5HT_{1A}R$ expression is upregulated in P7 rats, which present a brain developmental status similar to that of term infants, 7 days after HI insult (Franco et al., 2019). In addition, the reduction of $5HT_{1A}R$ in P3 rats is associated with a decrease in the brain concentration of 5HT (Buller et al., 2012), an effect not observed in our experiments. However, since we did not directly study either $5HT_{1A}R$-related signaling pathways or $5HT_{1A}R$ density in the brain, these considerations remain speculative and deserve further study. In a preclinical model of stroke in adult mice, CBD neuroprotection is related to increased regional and intralesional cerebral blood flow, an effect that is dependent on $5HT_{1A}R$ activation (Mishima et al., 2005). It is conceivable that such an effect on cerebral blood flow would be more important in the first few hours after HI, when cerebral blood flow is dramatically reduced (Hassell et al., 2015); however, the relevance of this effect would be much less once brain hypoperfusion evolves into hyperperfusion and then to the normalization of cerebral blood flow (Hassell et al., 2015). More studies are needed, however, to demonstrate that the lack of effect of $5HT_{1A}R$ antagonism on CBD neuroprotection would also be observable in brain areas not explored in our work such as the striatum, cerebellum, or white matter.

4.2 HI Insult Led to Mood Disturbances in Piglets

The HI insult also caused behavioral disturbances in the piglets. Although the NBS includes the item "behavior," its qualitative nature makes it subjective and highly dependent on the examiner's skills. The additional behavioral assessment that we performed, based on some basic behavioral characteristics of piglets such as playfulness, social interaction, and anxiety responses to immobilization, obtains quantitative and objective parameters (Barata et al., 2019b). HI led to mood disturbances in piglets, as evidenced by reduced social interaction and playtime with objects, suggestive of less attention and/or motivation, and by hyperactivity alternating with motionless episodes. This picture was associated with a greater anxious response during restraint. These features, which are related to brain damage in HI piglets (Barata et al., 2019b), mimic some presence in human newborns two-to-three days after mild-to-moderate HI brain insults, such as jitteriness and attention deficits (Sarnat and Sarnat, 1976; Thompson et al., 1997). We found that mood disturbances coincided with increased brain levels of monoamines such as NE, DA, and 5HT.

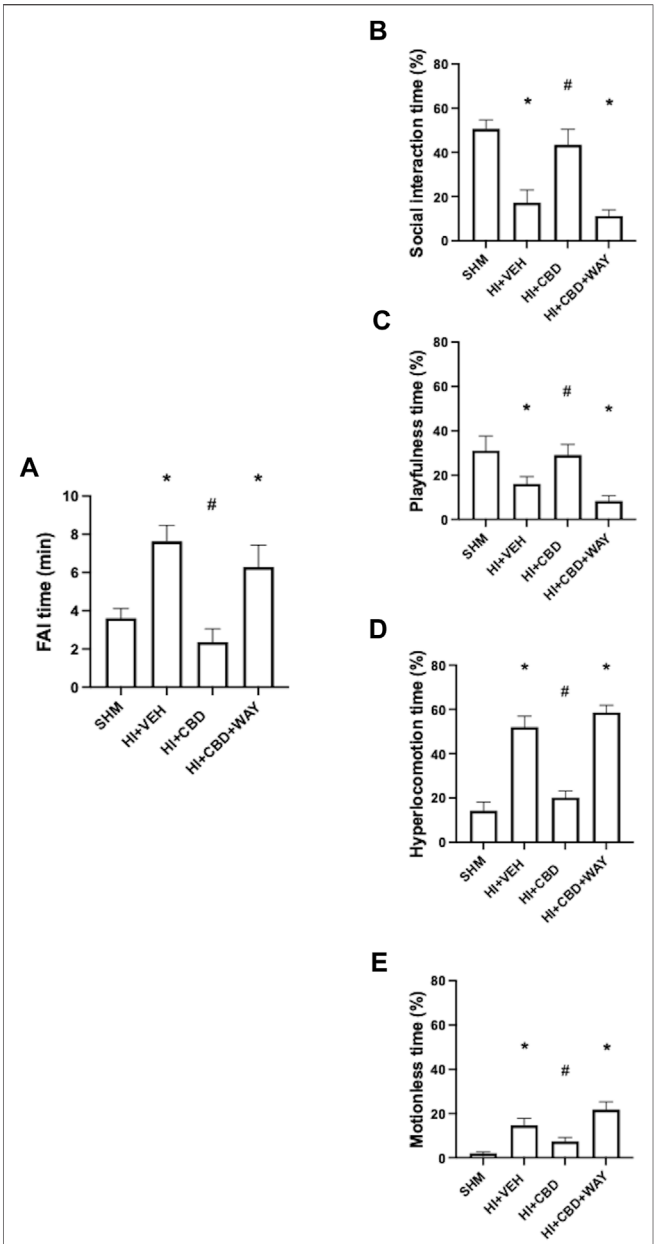

FIGURE 2 | Neurobehavioral assessment 72 h after hypoxic–ischemic insult in piglets treated with vehicle (HV), cannabidiol (HC), and WAY 100635 (HCW). Non-hypoxic–ischemic piglets served as controls (SHM). **(A)** Time spent fighting against immobilization (FAI) (*left*). Relative time (*right*) spent in **(B)** social interaction, **(C)** playfulness, **(D)** hyperlocomotion, and **(E)** motionless periods. Bars represent the mean (SEM) of 6–12 experiments. (*) $p < 0.05$ vs. SHM and (#) $p < 0.05$ vs. HV by ANOVA with Holm–Šidack test for multiple comparisons.

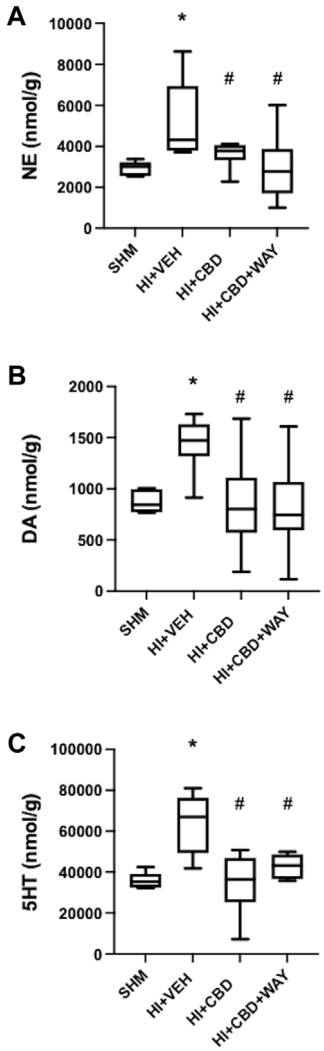

FIGURE 3 | Brain monoamine concentration 72 h after hypoxic–ischemic insult in brain samples from piglets treated with vehicle (HV), cannabidiol (HC), and WAY 100635 (HCW). Non-hypoxic–ischemic piglets served as controls (SHM). Boxes represent the median (IQR) and Whiskers' maximum and minimum values of brain concentration of **(A)** norepinephrine (NE), **(B)** dopamine (A), and **(C)** 5-hydroxytriptamine (5-HT). (*) $p < 0.05$ vs. SHM and (#) $p < 0.05$ vs. HV by Kruskall–Wallis with Dunn's test for multiple comparisons.

Increased brain concentration of NE, DA, and 5HT is observed in the brain of adult Wistar rats that develop hypertonia after transient global brain ischemia and is attributed to increased release due to cell destruction along with reduced reuptake due to energy failure (Globus et al., 1992). In piglets, there is a transient increase in brain concentration of the DA transporter in the first days after HI, which is thought to correspond with increased DA levels, related to the damage of dopaminergic neurons in the striatum (Zhang et al., 2012). In our work, hyperlocomotion and anxious response to stress could be attributed to increased DA concentration in the brain (Liu et al., 2018), but motionless and reduced playfulness are more suggestive of depression-like behavior (Kanitz et al., 2004) that is not an effect of increased monoamine concentration (Liu et al., 2018). These features suggest that mood disturbances observed in HI piglets were due to a dysregulation of monoaminergic networks due to brain damage rather than to a direct effect of increased monoamine concentration in the brain. In addition, depressive behavior is linked to reduced BDNF levels in mice brains after acute ischemic insults (Mori et al., 2017), although this was not explored in our work.

4.3 $5HT_{1A}R$ Antagonism Modified CBD Effects on Mood Disturbances After HI

CBD treatment prevented the development of mood disturbances in piglets after HI. In this case, coadministration of the $5HT_{1A}R$ antagonist eliminated the protective effect of CBD. CBD is a well-known anxiolytic substance (de Almeida and Devi, 2020; Melas et al., 2021) that also shows antidepressant effects (Abame et al., 2021). These effects are mediated by $5HT_{1A}R$ (De Gregorio et al., 2019; de Almeida and Devi, 2020). At 100 mg/kg, CBD can increase 5HT concentration in rat brain (Abame et al., 2021), but at 5 mg/kg, the antipanic effect of CBD is reversed by $5HT_{1A}R$ antagonists, and it is not associated with changes in the concentration of 5HT (Campos et al., 2013). In our case, the CBD dose was even lower than that. Furthermore, the concentration of 5HT in the brain of CBD-treated HI piglets was similar to that of SHM animals, whereas the effects of CBD on mood disturbances disappeared after $5HT_{1A}R$ blockade. The modulatory effects of CBD on brain monoamine concentration after HI were not reversed by $5HT_{1A}R$ blockage. A similar effect on glutamate release was observed, with an increase in Glu/NAA ratio as assessed by ^{1}H-NMR studies in HV but not in HC or HCW animals. These data suggest that the modulatory effects of CBD on neurotransmitter release were not due to a direct effect on $5HT_{1A}R$. CBD is known to reduce the release of neurotransmitter (de Almeida and Devi, 2020; Silvestro et al., 2020; Martínez-Orgado et al., 2021; Melas et al., 2021). But in our case, it could also be the result of the general neuroprotective effects of CBD. Furthermore, CBD normalizes BDNF expression in the mouse brain after hypoxic–ischemic insults, an effect that explains the antidepressant effects of CBD in this condition (Mori et al., 2017).

Taken together, these results support the idea that the effect of CBD on mood disturbances in HI piglets was elicited by direct activation of $5HT_{1A}R$. Interestingly, in our study CBD prevented the appearance of mood disturbances at a dose of 1 mg/kg. In preclinical studies in adult rodents, anxiolytic or antidepressant effects of acute CBD administration are generally obtained at doses of 2.5 mg/kg or higher, although anxiolytic effects as observed in social interaction tests have been reported for CBD 1 mg/kg in mice (Melas et al., 2021). The robust effects we observed with such a low dose of CBD suggest that an immature brain would be particularly sensitive to $5HT_{1A}R$ agonism by CBD. We have described in the brain of immature rats that HI insults lead to increased expression and signaling of $5HT_{1A}R$ in the first days after HI, an effect of greater magnitude in newborns than in adult rats (Franco et al., 2019).

In conclusion, HI insult led to brain damage in newborn piglets, as observed in histological and biochemistry studies 72 h after HI. At that time, brain damage was associated with increased seizures, and neuromotor deficits, and behavioral disorders, including mood disturbances such as reduced social interaction and playfulness and increased anxiety and hyperactivity. Postinsult CBD administration prevented HI-induced brain damage, and neuromotor deficits and behavioral disturbances. Coadministration of the $5HT_{1A}R$ antagonist WAY 100635 did not modify the beneficial effects of CBD on brain damage and neuromotor performance. This is in contrast to previous studies demonstrating that 5HT1AR blockade abolishes CBD neuroprotection assessed 6 h after HI, suggesting that 5HT1AR activation plays a critical role in CBD neuroprotection only in the first moments after HI. Further studies to determine more precisely the time point after which 5HT1AR antagonism no longer reverses the protective effects of CBD are warranted. In contrast, 5HT1AR blockade eliminated the beneficial effects of CBD on HI-induced mood disturbances, suggesting that these effects were related to 5HT1AR activation. These results indicate that, in addition to its robust neuroprotective effects, CBD could be an interesting candidate to be included in the treatment of HI newborns to mitigate the consequences of stress derived from brain damage and hypothermia treatment.

DATA AVAILABILITY STATEMENT

The raw data supporting the conclusion of this article will be made available by the authors, without undue reservation, upon request to the corresponding author.

ETHICS STATEMENT

The animal study was reviewed and approved by the Ethics Committee for Animal Welfare of Hospital Clinico San Carlos-IdISSC. Written informed consent was obtained from the owners for the participation of their animals in this study.

AUTHOR CONTRIBUTIONS

LJ-S and JM-O contributed to the conception and design of the study. LB and JM-O performed the experiments and the neuromotor and neurobehavioral studies and organized the database. MH-R, AR, MM, LS, and MV performed the biochemical and histological studies and interpreted the neuromotor, behavioral, and spectroscopy studies. LJ-S and LC performed de HPL studies. JM-O performed the statistical analysis, wrote the first draft of the manuscript, and edited the final version of the manuscript. All authors contributed to manuscript revision and read and approved the submitted version.

FUNDING

This work was supported by the PI19/00927 project, integrated with the Plan National de I + D + I, AES 2017-2020, funded by the ISCIII and cofunded by the European Regional Development Fund (ERDF) "A way to make Europe".

ACKNOWLEDGMENTS

We are indebted to Carlos Vargas for excellent technical assistance.

SUPPLEMENTARY MATERIAL

The Supplementary Material for this article can be found online at https://www.frontiersin.org/articles/10.3389/fphar.2022.925740/full#supplementary-material

REFERENCES

Abame, M. A., He, Y., Wu, S., Xie, Z., Zhang, J., Gong, X., et al. (2021). Chronic Administration of Synthetic Cannabidiol Induces Antidepressant Effects Involving Modulation of Serotonin and Noradrenaline Levels in the hippocampus. *Neurosci. Lett.* 744, 135594. doi:10.1016/j.neulet.2020.135594

Aguiar, R. P. d., Newman-Tancredi, A., Prickaerts, J., and Oliveira, R. M. W. d. (2021). The 5-HT1A Receptor as a Serotonergic Target for Neuroprotection in Cerebral Ischemia. *Prog. Neuro-Psychopharmacology Biol. Psychiatry* 109, 110210. doi:10.1016/j.pnpbp.2020.110210

Barata, L., Arruza, L., Rodríguez, M. J., Aleo, E., Vierge, E., Criado, E., et al. (2019a). Neuroprotection by Cannabidiol and Hypothermia in a Piglet Model of Newborn Hypoxic-Ischemic Brain Damage. *Neuropharmacology* 146, 1–11. doi:10.1016/j.neuropharm.2018.11.020

Barata, L., Cabañas, A., Lafuente, H., Vargas, C., Ceprián, M., Campa, L., et al. (2019b). aEEG and Neurologic Exam Findings Correlate with Hypoxic-Ischemic Brain Damage Severity in a Piglet Survival Model. *Pediatr. Res.* 85, 539–545. doi:10.1038/s41390-019-0282-2

Berube, M. W., Lemmon, M. E., Pizoli, C. E., Bidegain, M., Tolia, V. N., Cotten, C. M., et al. (2020). Opioid and Benzodiazepine Use during Therapeutic Hypothermia in Encephalopathic Neonates. *J. Perinatol.* 40, 79–88. doi:10.1038/S41372-019-0533-4

Buller, K. M., Wixey, J. A., and Reinebrant, H. E. (2012). Disruption of the Serotonergic System after Neonatal Hypoxia-Ischemia in a Rodent Model. *Neurol. Res. Int.* 2012, 650382. doi:10.1155/2012/650382

Campos, A. C., Ortega, Z., Palazuelos, J., Fogaça, M. V., Aguiar, D. C., Díaz-Alonso, J., et al. (2013). The Anxiolytic Effect of Cannabidiol on Chronically Stressed Mice Depends on Hippocampal Neurogenesis: Involvement of the Endocannabinoid System. *Int. J. Neuropsychopharmacol.* 16, 1407–1419. doi:10.1017/S1461145712001502

de Almeida, D. L., and Devi, L. A. (2020). Diversity of Molecular Targets and Signaling Pathways for CBD. *Pharmacol. Res. Perspect.* 8, e00682. doi:10.1002/prp2.682

De Gregorio, D., McLaughlin, R. J., Posa, L., Ochoa-Sanchez, R., Enns, J., Lopez-Canul, M., et al. (2019). Cannabidiol Modulates Serotonergic Transmission and Reverses Both Allodynia and Anxiety-like Behavior in a Model of Neuropathic Pain. *Pain* 160, 136–150. doi:10.1097/j.pain.0000000000001386

Franco, R., Villa, M., Morales, P., Reyes-Resina, I., Gutiérrez-Rodríguez, A., Jiménez, J., et al. (2019). Increased Expression of Cannabinoid CB2 and Serotonin 5-HT1A Heteroreceptor Complexes in a Model of Newborn Hypoxic-Ischemic Brain Damage. *Neuropharmacology* 152, 58–66. doi:10.1016/j.neuropharm.2019.02.004

Globus, M. Y., Wester, P., Busto, R., and Dietrich, W. D. (1992). Ischemia-induced Extracellular Release of Serotonin Plays a Role in Ca1 Neuronal Cell Death in Rats. *Stroke* 23, 1595–1601. doi:10.1161/01.STR.23.11.1595

Hassell, K. J., Ezzati, M., Alonso-Alconada, D., Hausenloy, D. J., and Robertson, N. J. (2015). New Horizons for Newborn Brain Protection: Enhancing Endogenous Neuroprotection. *Arch. Dis. Child. Fetal Neonatal Ed.* 100, F541–F552. doi:10.1136/archdischild-2014-306284

Kanitz, E., Tuchscherer, M., Puppe, B., Tuchscherer, A., and Stabenow, B. (2004). Consequences of Repeated Early Isolation in Domestic Piglets (*Sus scrofa*) on Their Behavioural, Neuroendocrine, and Immunological Responses. *Brain. Behav. Immun.* 18, 35–45. doi:10.1016/S0889-1591(03)00085-0

Lafuente, H., Alvarez, F. J., Pazos, M. R., Alvarez, A., Rey-Santano, M. C., Mielgo, V., et al. (2011). Cannabidiol Reduces Brain Damage and Improves Functional Recovery after Acute Hypoxia-Ischemia in Newborn Pigs. *Pediatr. Res.* 70, 272–277. doi:10.1203/PDR.0b013e3182276b11

LeBlanc, M. H., Vig, V., Smith, B., Parker, C. C., Evans, O. B., and Smith, E. E. (1991). MK-801 Does Not Protect against Hypoxic-Ischemic Brain Injury in Piglets. *Stroke* 22, 1270–1275. doi:10.1161/01.STR.22.10.1270

Liu, Y., Zhao, J., and Guo, W. (2018). Emotional Roles of Mono-Aminergic Neurotransmitters in Major Depressive Disorder and Anxiety Disorders. *Front. Psychol.* 9, 2201. doi:10.3389/FPSYG.2018.02201

Martínez-Orgado, J., Villa, M., and Del Pozo, A. (2021). Cannabidiol for the Treatment of Neonatal Hypoxic-Ischemic Brain Injury. *Front. Pharmacol.* 11, 584533. doi:10.3389/FPHAR.2020.584533

Melas, P. A., Scherma, M., Fratta, W., Cifani, C., and Fadda, P. (2021). Cannabidiol as a Potential Treatment for Anxiety and Mood Disorders: Molecular Targets and Epigenetic Insights from Preclinical Research. *Int. J. Mol. Sci.* 22, 1–15. doi:10.3390/ijms22041863

Mishima, K., Hayakawa, K., Abe, K., Ikeda, T., Egashira, N., Iwasaki, K., et al. (2005). Cannabidiol Prevents Cerebral Infarction via a Serotonergic 5-hydroxytryptamine1A Receptor-dependent Mechanism. *Stroke* 36, 1077–1082. doi:10.1161/01.STR.0000163083.59201.34

Mori, M. A., Meyer, E., Soares, L. M., Milani, H., Guimarães, F. S., and de Oliveira, R. M. W. (2017). Cannabidiol Reduces Neuroinflammation and Promotes Neuroplasticity and Functional Recovery after Brain Ischemia. *Prog. Neuropsychopharmacol. Biol. Psychiatry* 75, 94–105. doi:10.1016/j.pnpbp.2016.11.005

Pazos, M. R., Mohammed, N., Lafuente, H., Santos, M., Martínez-Pinilla, E., Moreno, E., et al. (2013). Mechanisms of Cannabidiol Neuroprotection in Hypoxic-Ischemic Newborn Pigs: Role of 5HT(1A) and CB2 Receptors. *Neuropharmacology* 71, 282–291. doi:10.1016/j.neuropharm.2013.03.027

Russo, E. B., Burnett, A., Hall, B., and Parker, K. K. (2005). Agonistic Properties of Cannabidiol at 5-HT1a Receptors. *Neurochem. Res.* 30, 1037–1043. doi:10.1007/s11064-005-6978-1

Sarnat, H. B., and Sarnat, M. S. (1976). Neonatal Encephalopathy Following Fetal Distress. A Clinical and Electroencephalographic Study. *Arch. Neurol.* 33, 696–705. Available at: http://www.ncbi.nlm.nih.gov/pubmed/987769 (Accessed April 9, 2018). doi:10.1001/archneur.1976.00500100030012

Silvestro, S., Schepici, G., Bramanti, P., and Mazzon, E. (2020). Molecular Targets of Cannabidiol in Experimental Models of Neurological Disease. *Molecules* 25, 12–15. doi:10.3390/molecules25215186

Thompson, C. M., Puterman, A. S., Linley, L. L., Hann, F. M., Van Der Elst, C. W., Molteno, C. D., et al. (1997). The Value of a Scoring System for Hypoxic Ischaemic Encephalopathy in Predicting Neurodevelopmental Outcome. *Acta Paediatr.* 86, 757–761. doi:10.1111/j.1651-2227.1997.tb08581.x

Zhang, Y. F., Wang, X. Y., Guo, F., Burns, K., Guo, Q. Y., and Wang, X. M. (2012). Simultaneously Changes in Striatum Dopaminergic and Glutamatergic Parameters Following Hypoxic-Ischemic Neuronal Injury in Newborn Piglets. *Eur. J. Paediatr. Neurol.* 16, 271–278. doi:10.1016/j.ejpn.2011.05.010

Zhou, K. Q., Davidson, J. O., Bennet, L., and Gunn, A. J. (2020). Combination Treatments with Therapeutic Hypothermia for Hypoxic-Ischemic Neuroprotection. *Dev. Med. Child. Neurol.* 62, 1131–1137. doi:10.1111/dmcn.14610

Conflict of Interest: The authors declare that the research was conducted in the absence of any commercial or financial relationships that could be construed as a potential conflict of interest.

frontiers | Frontiers in Pharmacology

TYPE Original Research
PUBLISHED 09 August 2022
DOI 10.3389/fphar.2022.945935

OPEN ACCESS

EDITED BY
Gustavo Gonzalez-Cuevas,
Idaho State University, United States

REVIEWED BY
Sun Choi,
Ewha Womans University, South Korea
Jahan Marcu,
University of the Sciences, United States
Franziska Marie Heydenreich,
MRC Laboratory of Molecular Biology, United Kingdom

*CORRESPONDENCE
Jose Manuel Perez-Aguilar,
jmanuel.perez@correo.buap.mx
Brenda L. Sanchez-Gaytan,
brendale.sanchez@correo.buap.mx

SPECIALTY SECTION
This article was submitted to Neuropharmacology, a section of the journal Frontiers in Pharmacology

RECEIVED 17 May 2022
ACCEPTED 12 July 2022
PUBLISHED 09 August 2022

CITATION
Dávila EM, Patricio F, Rebolledo-Bustillo M, Garcia-Gomez D, Hernandez JCG, Sanchez-Gaytan BL, Limón ID and Perez-Aguilar JM (2022), Interacting binding insights and conformational consequences of the differential activity of cannabidiol with two endocannabinoid-activated G-protein-coupled receptors. *Front. Pharmacol.* 13:945935. doi: 10.3389/fphar.2022.945935

Interacting binding insights and conformational consequences of the differential activity of cannabidiol with two endocannabinoid-activated G-protein-coupled receptors

Eliud Morales Dávila[1], Felipe Patricio[2], Mariana Rebolledo-Bustillo[1], David Garcia-Gomez[1], Juan Carlos Garcia Hernandez[1], Brenda L. Sanchez-Gaytan[3]*, Ilhuicamina Daniel Limón[2] and Jose Manuel Perez-Aguilar[1]*

[1]School of Chemical Sciences, Meritorious Autonomous University of Puebla (BUAP), University City, Puebla, Mexico, [2]Neuropharmacology Laboratory, School of Chemical Sciences, Meritorious Autonomous University of Puebla (BUAP), University City, Puebla, Mexico, [3]Chemistry Center, Science Institute, Meritorious Autonomous University of Puebla (BUAP), University City, Puebla, Mexico

Cannabidiol (CBD), the major non-psychoactive phytocannabinoid present in the plant *Cannabis sativa,* has displayed beneficial pharmacological effects in the treatment of several neurological disorders including, epilepsy, Parkinson's disease, and Alzheimer's disease. In particular, CBD is able to modulate different receptors in the endocannabinoid system, some of which belong to the family of G-protein-coupled receptors (GPCRs). Notably, while CBD is able to antagonize some GPCRs in the endocannabinoid system, it also seems to activate others. The details of this dual contrasting functional feature of CBD, that is, displaying antagonistic and (possible) agonistic ligand properties in related receptors, remain unknown. Here, using computational methods, we investigate the interacting determinants of CBD in two closely related endocannabinoid-activated GPCRs, the G-protein-coupled receptor 55 (GPR55) and the cannabinoid type 1 receptor (CB_1). While in the former, CBD has been demonstrated to function as an antagonist, the way by which CBD modulates the CB_1 receptor remains unclear. Namely, CBD has been suggested to directly trigger receptor's activation, stabilize CB_1 inactive conformations or function as an allosteric modulator. From microsecond-length unbiased molecular dynamics simulations, we found that the presence of the CBD ligand in the GPR55 receptor elicit conformational changes associated with antagonist-bound GPCRs. In contrast, when the GPR55 receptor is simulated in complex with the selective agonist ML186, agonist-like conformations are sampled. These results are in agreement with the proposed modulatory function of each ligand, showing that the computational techniques utilized to characterize the GPR55 complexes correctly differentiate the agonist-bound and antagonist-bound systems. Prompted by these results, we investigated the role of the CBD compound

on the CB_1 receptor using similar computational approaches. The all-atom MD simulations reveal that CBD induces conformational changes linked with agonist-bound GPCRs. To contextualize the results we looked into the CB_1 receptor in complex with a well-established antagonist. In contrast to the CBD/CB_1 complex, when the CB_1 receptor is simulated in complex with the ligand antagonist AM251, inactive conformations are explored, showing that the computational techniques utilized to characterize the CB_1 complexes correctly differentiate the agonist-bound and antagonist-bound systems. In addition, our results suggest a previously unknown sodium-binding site located in the extracellular domain of the CB_1 receptor. From our detailed characterization, we found particular interacting loci in the binding sites of the GPR55 and the CB_1 receptors that seem to be responsible for the differential functional features of CBD. Our work will pave the way for understanding the CBD pharmacology at a molecular level and aid in harnessing its potential therapeutic use.

KEYWORDS

cannabidiol, G-protein-coupled receptors, all-atom molecular dynamic simulations, G-protein-coupled receptor 55, cannabinoid type-1 receptor

1 Introduction

The endocannabinoid system is a signaling apparatus that regulates a variety of widespread functions in the central nervous system including, synaptic plasticity, learning, sleep, eating, inflammation, immune responses, and pain and temperature control, to mention a few (Lu and MacKie, 2016). The plethora of cellular functions associated with the endocannabinoid systems makes it an attractive pharmacological target. The endocannabinoid system comprises several cellular entities including the endocannabinoids, which are endogenous cannabinoid compounds that modulate the signaling system, as well as various biomacromolecules, i.e., receptors and enzymes. In addition to the enzymes that synthesize and decompose the endocannabinoids, various receptors constitute the endocannabinoid system including two G-protein-coupled receptors, namely, the cannabinoid type 1 (CB_1) and type 2 (CB_2) receptors. In addition to CB_1 and CB_2, other receptors have been proposed to participate as mediators of the effects of the cannabinoid ligands including the G-protein-coupled receptor 55 (GPR55) (Ryberg et al., 2007; Kapur et al., 2009).

Among the different ligands able to modulate the cannabinoid receptors, those present in the *C. sativa* plant exhibit a significant interest not only because of their role as possible therapeutic agents but also because of their increasing recreational use which may also pose a public health issue (Hall and Lynskey, 2016; Wilkinson et al., 2016). Knowing the details of the stimulation of different cannabinoid receptors by phytocannabinoid compounds may provide pharmacological tools to finely tune the endocannabinoid system. Among the compounds able to modulate the cannabinoid receptors, cannabidiol (CBD), one of the major constituents in the *Cannabis* plant, has attracted significant industrial and medical attention because of its non-psychoactive properties. Yet, the molecular determinants of the CBD interaction with receptors stimulated by endocannabinoids remain poorly understood. In this work and using computational methods, we investigate the interaction of CBD with two endocannabinoid-activated receptors, the GPR55 receptor and the prototypical CB_1 receptor. While in the former, CBD is known to antagonize the receptor, that is, maintain the receptor's inactive conformations, the way by which CBD modulates the latter system remains debatable. That is, CBD has been suggested to directly trigger the activation the CB_1 receptor (Navarro et al., 2020), inactivate the receptor (Grotenhermen, 2004; Batalla et al., 2021; Śmiarowska et al., 2022), or play a role as an allosteric modulator (Shao et al., 2019; Batalla et al., 2021; Austrich-Olivares et al., 2022). First, we looked into the modulation of the CBD ligand on the GPR55 receptor using computational methods. To put our findings in context, we also investigated the GPR55 receptor in complex with a selective agonist. The computational methods utilized are able to capture the ligand-dependent conformational details in the two GPR55 complexes, showing that CBD stabilizes inactive conformations of the receptor while the ML186 agonist favors active-like conformations. Next, we investigated the role of CBD in directly modulating the CB_1 receptor by placing the ligand in the orthosteric binding site based on the chemical homology of CBD to other CB_1 ligands (Hua et al., 2017). Our results suggest that CBD is able to stabilize the receptor's structural changes associated with agonist-bound conformations. Based on these results and similarly to the case of the GPR55, we looked into the CB_1 receptor in complex with a well-established CB_1 antagonist, the AM251 ligand. Furthermore, the computational methods utilized here are able to capture the ligand-dependent

conformational details in the two endocannabinoid-activated GPCRs and provide a view of the main differential interactions involved in the CBD protein complexes.

2 Materials and methods

2.1 Homology modeling of the GPCR structures

We decided to model the receptor's structures of *Rattus norvegicus* to better correlate our findings with the experimental results from our animal models. Additionally, the sequence similarity with *Homo sapiens* is high (around 97% sequence identity in the CB_1 system and around 74% sequence identity in the GPR55). The sequence for both receptors are shown in Supplementary Figure S1.

2.2 GPR55 receptor structures

Thus far, there is no experimentally-determined structural information regarding the GPR55 receptor. Hence, the structure of the rat GPR55 receptor was built using the homology modeling technique (Eswar et al., 2006). To identify possible adequate templates for GPR55, the Swiss-Model server was used (Waterhouse et al., 2018). The selected system was the lysophosphatidic acid receptor 6 (LPA6) which displays a sequence identity with GPR55 of about 30% (PDB ID code 5XSZ). The sequences of the LPA6 template and the rat GPR55 receptors were obtained from UNIPROT (with the codes Q08BG4 and F1MAK4, respectively). The sequences were aligned using BLASTp (Altschul et al., 1990) with subsequent manual adjustments. The pairwise sequence alignment is presented in Supplementary Figure S2. To generate 3D structural models of the rat GPR55 receptor, we used the Modeller 9.23 protocol (Šali and Blundell, 1993). 100 models of the *R. norvegicus* GPR55 receptor were generated and a representative structure was selected based on energetic considerations, that is, using the Modeller's scoring function (see Supplementary Figure S3).

2.3 CB_1 receptor structures

To model the structures for the rat CB_1 receptor we used different templates for each receptor's functional state. In the case of the CB_1 receptor that will form a complex with CBD (an tentative agonist for CB_1), the template utilized was the agonist-bound human CB_1 receptor (PDB ID code 5XRA). In the case of the CB_1 receptor that forms a complex with AM251 (an antagonist for CB_1), two structures of the antagonist-bound human CB_1 receptor were used as templates (PDB ID code 5U09 and code 5TGZ). In both cases, 100 models of the *R. norvegicus* CB_1 structures were modeled *via* homology modeling using the Modeller 9.23 protocol (Šali and Blundell, 1993). The sequences of the human and rat CB_1 receptors were obtained from UNIPROT (with the codes P21554 and P20272, respectively). Based on energetic considerations, a representative structure of the rat CB_1 receptor was selected in each case for further analysis, see Supplementary Figure S4.

2.4 CBD/GPR55 complex structures (inactive-like GPR55 system)

To identify possible molecular poses for the CBD/GPR55 complex, blind docking calculations were performed using the Autodock-Vina software (Trott and Olson, 2009). The selected molecular pose for the CBD/GPR55 complex is shown in Supplementary Figure S3. Chemical structure of the ligands are displayed in Supplementary Figure S5.

2.5 ML186/GPR55 complex structures (active-like GPR55 system)

Similar to the aforementioned case of the CBD/GPR55 complex, molecular poses for the ML186/GPR55 complex were identified via docking calculations using Autodock Vina (Trott and Olson, 2009). The selected molecular pose for the ML186/GPR55 complex is shown in Supplementary Figure S3.

2.6 CBD/CB_1 complex structures (active-like CB_1 system)

To predict possible molecular poses for the CBD ligand in the structural framework of the CB_1 receptor, docking studies were carried out using Autodock Vina (Trott and Olson, 2009). In addition to the energetic considerations (the scoring function of Autodock Vina), we used the structure of the AM11542/CB_1 complex (PDB ID code 5XRA), as a guide to select a representative structure of the CBD/CB_1 complex (see Supplementary Figure S4). The structure of the AM11542/CB_1 complex was selected based on the similarity of the CBD ligand and the AM11542.

2.7 AM251/CB_1 complex structures (inactive CB_1 system)

Similar docking calculations were utilized in the case of the AM251 antagonist. In this case, in addition to Autodock

Vina's scoring function, the structure of the AM6538/CB_1 complex (PDB ID code 5TGZ), was used as a guide due to the similarity between the AM251 ligand and the AM6538 ligand. The selected structure is indicated in Supplementary Figure S4.

2.8 All-atom molecular dynamics simulations

To provide the interacting ligand binding determinants of the protein systems (CBD/GPR55, ML186/GPR55, CBD/CB_1, and AM251/CB_1) and the concomitant conformational consequences, we performed all-atom molecular dynamics (MD) simulations in each of the four protein complexes. Similar general preparation for the systems has been previously used for GPCRs (Perez-Aguilar et al., 2014; Perez-Aguilar et al., 2019; Dror et al., 2011; Lee and Lyman, 2012; Méndez-Luna et al., 2015) and other membrane proteins (Rangel-Galván et al., 2021). Briefly, using the structural information from the docking calculations as the initial complex structure, hydrogen atoms were included representing the most probable protonation states for all the amino acids residues at neutral pH. The protein complexes were embedded in a hydrated symmetric POPC (1-palmitoyl-2-oleoyl-sn-glycero-3-phosphocholine) membrane, where sodium and chlorine ions were included so as to have a physiological salt concentration (0.15 M). Preparation steps that include the imposition of structural force restraints to avoid unrealistic conformation of the system (e.g., water penetration to the lipid membrane) were carried out (Perez-Aguilar et al., 2014; Perez-Aguilar et al., 2019; Rangel-Galván et al., 2021). Next, unbiased MD simulations were carried out for one microsecond (1.0 μs) at a constant temperature and pressure (37°C and 1 atm, respectively).

2.9 Class A GPCR position numbering

To define the position of each residue, we will be using the Ballesteros-Weinstein numbering as superscript. In this nomenclature, the first number indicates the transmembrane helix (from one to seven) whereas the second number indicates the residue position relative to the most conserved residue, which is assigned to the number 50 (Ballesteros and Weinstein, 1995).

2.10 Structural analysis

The analyses herein were performed using the program VMD and in-house TCL scripts (Humphrey et al., 1996).

3 Results

To shed light on the differential activity of CBD in the two endocannabinoid-activated receptors aforementioned, we utilized computational techniques to characterize four protein complexes, CBD/CB_1, ML186/GPR55, CBD/GPR55, and AM251/CB_1.

3.1 Interacting determinants in the CBD/GPR55 and ML186/GPR55 complexes

3.1.1 The CBD/GPR55 system

As described in the Methods section, the initial model of the CBD/GPR55 was obtained from docking approaches using the crystal structure of the lysophosphatidic acid receptor 6 (LPA6, 5XSZ.pdb) to model the structure of the GPR55 receptor. The initial structure of the model is shown in Supplementary Figure S3 and was used as the starting point to investigate the CBD/GPR55 complex by unbiased all-atom MD simulations. Figures 1A,B shows a representative final complex structure after 1 μs simulation, where the interactions that stabilized the CBD molecular pose are displayed.

The molecular pose of CBD in the ligand binding site of GPR55 is located mainly in the vicinity of TM2 and TM3, and close to the conserved disulfide bond formed by $C94^{3.25}$ and $C168^{ECL2}$. In particular, the terpenoid ring moiety of CBD inserts in between TM2 and TM3 as indicated in Figure 1B. In this position, the CBD ligand is flanked by two charged residues, i.e., $K79^{2.60}$ and $E98^{3.29}$. CBD forms polar interaction with the side chain of $E98^{3.29}$ *via* one of the hydroxyl (OH) groups. The time evolution of this distance along the entire MD simulations is shown in Figure 1D. As for residue $K79^{2.60}$, it interacts with CBD using its aliphatic side chain [$(CH_2)_4$]. Residues that delineate the ligand binding site of CBD are indicated in Figure 1B.

3.1.2 The ML186/GPR55 system

To put our findings in context, we also investigate the interactions of the GPR55 selective agonist ML186. A representative structure of the ML186/GPR55 complex at the final stages of the 1 μs simulation is illustrated in Figures 1A,C. In contrast to the location of the CBD ligand in the GPR55 binding site, the ML186 agonist positions in proximity to TM3, TM6 and TM7. The binding site of the selective agonist is partially formed by three bulky aromatic residues, namely $F102^{3.33}$, $Y106^{3.37}$, and $F239^{6.48}$. $F102^{3.33}$ positions along the main axis of the ligand where it established aromatic interactions with the highly delocalized electron (aromatic) region of the molecule, see the right panel in Figure 1D. Residues $Y106^{3.37}$ and $F239^{6.48}$ formed the lowest region of the ligand binding site. In particular, position 6.48 has been denominated "toggle switch" and associated with class A GPCR activation (see below for more details). The sulfonyl functional group (SO_2) group of the agonist forms

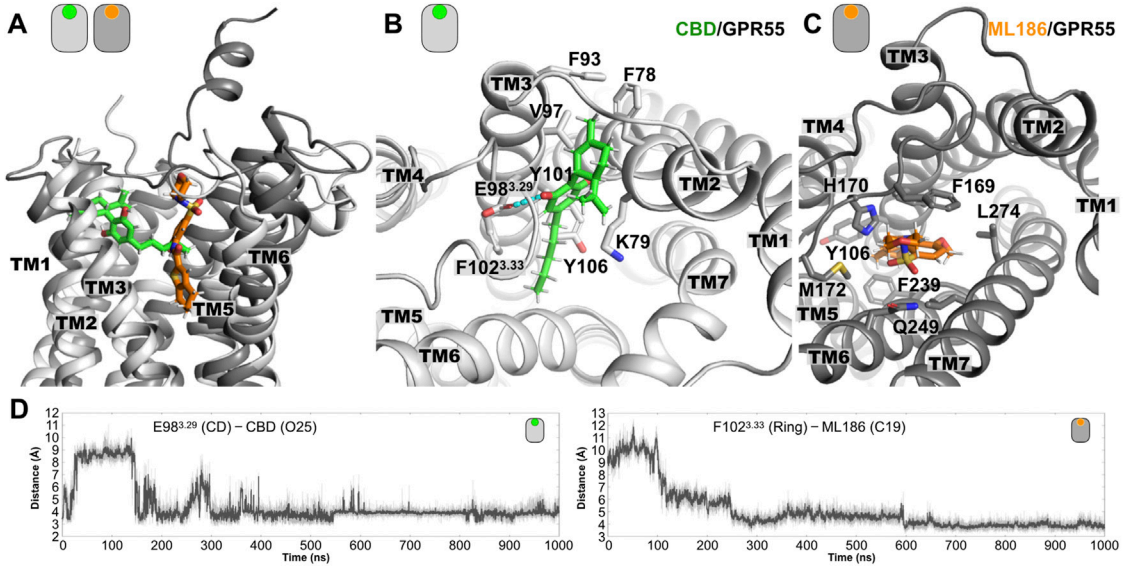

FIGURE 1
Representative poses from the MD simulations of the GPR55 complexes. **(A)** Lateral view of superimposed structures of the CBD/GPR55 and ML186/GPR55 complexes. Relative to the position of the CBD, the position of the ML186 selective ligand is placed deeper into the TM region of the ligand binding site. **(B)** Extracellular view of the CBD/GPR55 complex, where we can see that the two-ring moiety of CBD inserts in between TM2 and TM3. Flanking this part of the ligand, we observed two charged residues, K79$^{2.60}$ and E98$^{3.29}$. While the former interacts via the aliphatic part of its side chain, the latter forms interactions with one of the CBD hydroxyl (OH) groups (see dashed line). Residues forming the CBD binding site in GPR55 are indicated. **(C)** Extracellular view of the ML186/GPR55 complex. Contrary to the location of CBD in the GPR55 binding site, the selective agonist mainly contacts residues located TM3, TM6, and TM7. Three aromatic residues are part of the residues forming the binding site of ML186. F102$^{3.33}$ places along the main axis of the ligands where it established aromatic interactions with the highly delocalized electron (aromatic) region of the ligand. As for residues F239$^{6.48}$ and Y106$^{3.37}$, they formed the lower part of the agonist binding site. Note that position 6.48 has been denominated toggle switch and has been implicated in class A GPCR activation. Lastly, the SO group of the ligands established polar interactions around residue Q249$^{6.58}$. **(D)** Time evolution plots of the distance between acidic residue E98$^{3.29}$ with one of the CBD hydroxyl (OH) groups as well as between the center of the aromatic sidechain of F102$^{3.33}$ and the C19 atom.

polar interactions with residue Q249$^{6.58}$ in the extracellular part of TM6. Finally, in comparison with the relatively shallow position of the CBD, the ML186 agonist places into a deep molecular pose in the GPR55 ligand binding site (Figure 1A).

3.2 Structural consequences observed in the GPR55 receptor by the presence of the ligands

In order to understand the structural consequence of the presence of CBD ligand in the receptor's conformations, we analyze several structural motifs associated with GPCR activation. One particular locus linked with GPCR activation is position 6.48, the so-called toggle switch, which usually bears the aromatic residue tryptophan (W$^{6.48}$). Upon activation, there is a structural rearrangement in the vicinity of this residue, that seems to propagate conformational changes towards the intracellular side (Zhou et al., 2019). At this position, the GPR55 receptor contains another aromatic residue, the F239$^{6.48}$. In this context, we analyzed the conformations of this residue in the CBD-bound and ML186-bound GPR55 systems, particularly the rotameric states explored by the bulky F239$^{6.48}$ residue. As observed by the dihedral angles values of the angle defined by the N-CA-CB-CG atoms, in the case of the CBD/GPR55 complex, the distribution of the values explored by the receptor along the simulated trajectory are mainly distributed around 280°–320° (unimodal distribution, see Figure 2A). In the case of the agonist-bound GPR55 complex, the presence of the ML186 ligand provokes a change in the position of the F239$^{6.48}$ residue, as indicated by the bimodal distribution of the N-CA-CB-CG dihedral angle (Figure 2A). Experimental evidence indicates that a more dynamic and heterogeneous conformational behavior of the receptor is attributed to the binding of an agonist ligand (Manglik et al., 2015; Latorraca et al., 2017). It this case, the bimodal distribution observed in the ML186/GPR55 system at this position may be associated with active-like conformations while the unimodal distribution of this dihedral angles in the CBD/GPR55 complex are attributed to a GPCR's inactive conformations. This behavior may be attributed to the thiophene-containing fused-rings moiety of the ML186 agonist, which directly contacts the side chain of the F239$^{6.48}$ residue (Figure 1A). These results are in good agreement

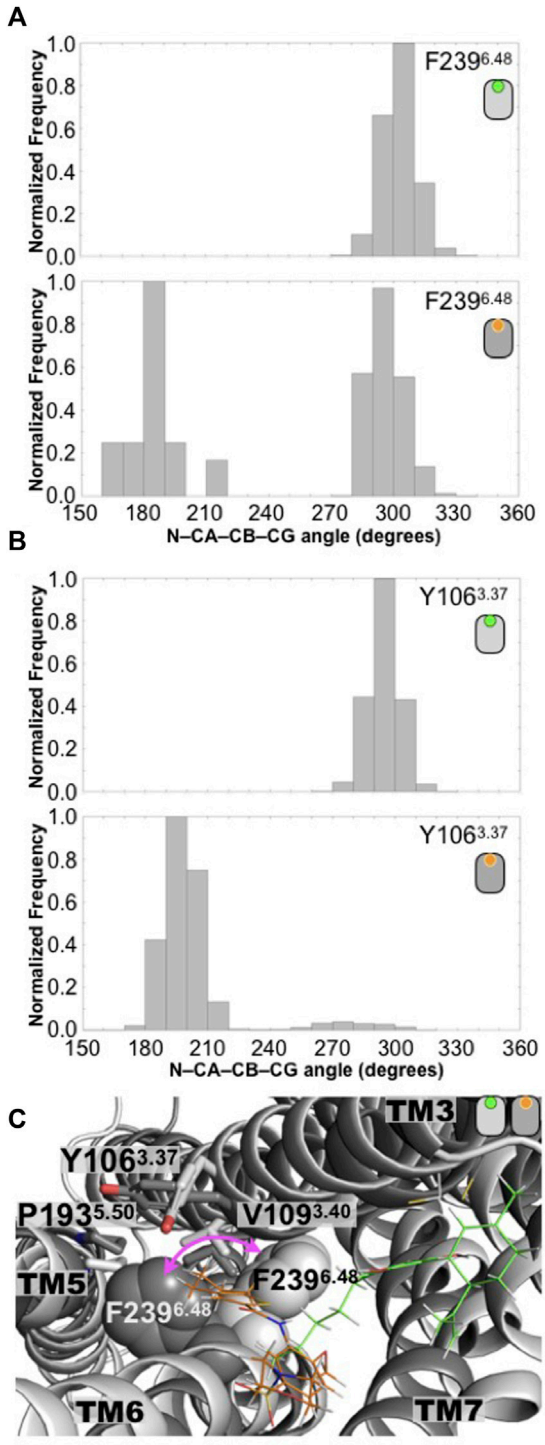

FIGURE 2
Conformation changes in the toggle switch motif distinguished the antagonist-bound versus the agonist-bound GPR55 complexes. **(A)** Distributions of the N-CA-CB-CD dihedral angle of the F239$^{6.48}$ residue in the CBD/GPR55 and ML186/GPR55 complexes. Position 6.48 is known as the toggle switch and has been implicated in GPCR activation. In the case of the GPR55, position 6.48 bears a phenylalanine residue, F239$^{6.48}$. **(B)** Another

(*Continued*)

FIGURE 2
residue that seems to play a role in the changes of F239$^{6.48}$ rotameric state is the Y106$^{3.37}$, which also displays a distinctive dihedral angle distribution. **(C)** Superimposed final structures of the CBD/GPR55 and ML186/GPR55 simulations. The different position of residue F239$^{6.48}$ in the two GPR55 systems is illustrated (magenta arrow). The deeper molecular pose of the selective agonist ML186 (orange) may be responsible for the different position of the F239$^{6.48}$ sidechain.

with the current notion that CBD is an antagonist of the GPR55 receptor while ML186 exhibits agonistic function on the GPR55 (Ryberg et al., 2007; Ross, 2009; Sharir and Abood, 2010).

Additionally, it has been suggested that conformational changes in position 6.48 with residues in TM3 and TM6 occur upon activation (Zhou et al., 2019; Hilger, 2021). Our simulations suggest that the conformational changes of the F239$^{6.48}$ residue are in close relation with those of two other aromatic residues, the bulky aromatic residues Y106$^{3.37}$ and F235$^{6.44}$. Analysis of the equivalent Y106$^{3.37}$ dihedral angle (N-CA-CB-CG atoms) indicates a drastic change in the rotameric states sampled by this residue. While in the CBD/GPR55 system, which displays the unimodal distribution of F239$^{6.48}$, the Y106$^{3.37}$ dihedral angle (N-CA-CB-CG atoms) also indicates that this aromatic residue samples a one-peak distribution conformations (Figure 2A). The more dynamic behavior of F239$^{6.48}$ causes a significant change in the distribution of rotameric states that explores the Y106$^{3.37}$ dresidue (Figure 2B).

Lastly, the changes in the GPR55 toggle switch causes F235$^{6.44}$ to follow similar trend, that is, the CBD/GPR55 displays an unimodal distribution of the dihedral angle define by the N-CA-CB-CG atoms while the ML186/GPR55 complex displays a more heterogenic distribution (Supplementary Figure S6).

The significant conformational response of the GPR55 receptor to the presence of the CBD antagonist and the ML186 agonist on structural motifs known to play a role on activation, seems to be in good agreement with the experimental evidence linked to these two ligands [Ryberg et al., 2007; Ross, 2009; Sharir and Abood, 2010; Kotsikorou et al., 2013; Anderson et al., 2021; Heynen-Genel et al., 2010 September 29 (updated 26 May 2011); Sharir. et al., 2012; Kotsikorou. et al., 2011]. Furthermore and regarding the known modulatory properties of the two ligands, CBD (antagonist) and ML186 (agonist), our computational approaches were able to distinguish the distinct GPR55 conformations elicited by the presence of each ligand (Figure 2C).

In addition to the aforementioned toggle switch residue, another structural feature that is a hallmark of class A GPCR activation is the presence of an charge-charge intracellular interaction, the so-called ionic lock, formed by R$^{3.50}$ and D/E$^{6.30}$ (Zhou et al., 2019). Upon activation, this ionic lock needs to be broken so that an outward shift of TM6 is

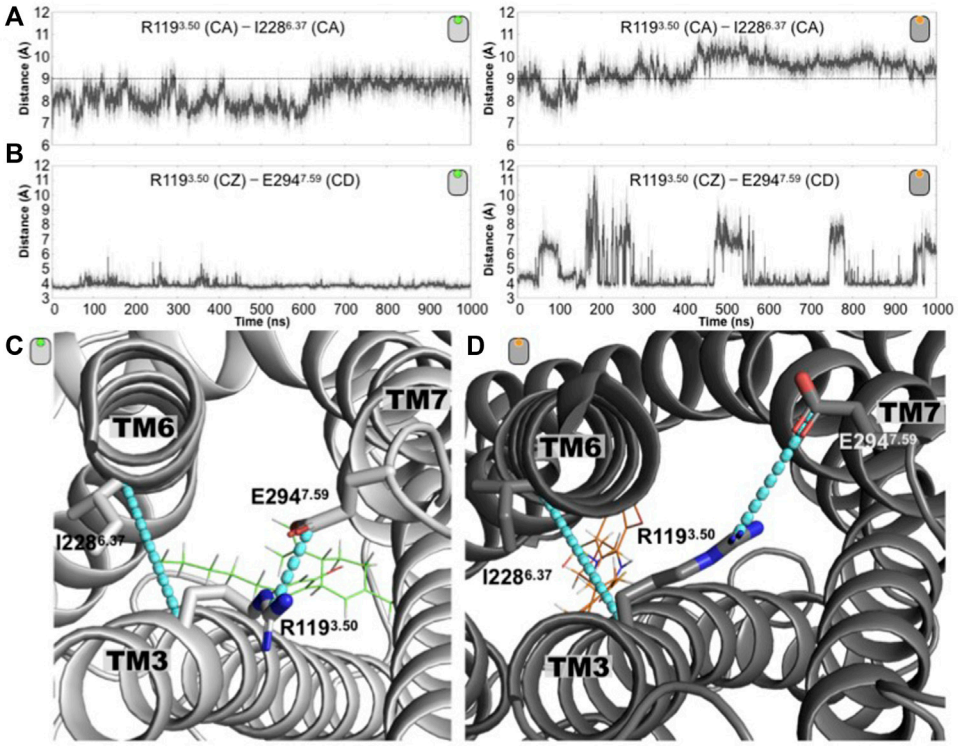

FIGURE 3
Conformation changes around the conserved intracellular residue R3.50 distinguished the antagonist-bound versus the agonist-bound GPR55 complexes. **(A)** Time evolution of the R119$^{3.50}$ (CA)—I228$^{6.37}$ (CA) distance for the antagonist-bound (left) and agonist-bound (right) GPR55 systems. The dashed line at 9 Å is drawn to guide the eye. **(B)** Time evolution of the distance R119$^{3.50}$ (CZ)—E294$^{7.59}$ (CD) distance for the antagonist-bound (left) and agonist-bound (right) GPR55 complexes. This electrostatic interaction remains in the former while in the latter is frequently disrupted. **(C)** Representative structures of the **(C)** CBD/GPR55 and the **(D)** ML186/GPR55 complexes are shown where the two plotted distances are illustrated as cyan lines.

possible (Zhou et al., 2019). Although there is an arginine residue at position 3.50 in GPR55 (R119$^{3.50}$), no acidic residue is present at position 6.30. Nevertheless, to have a sense of the relative displacement of the intracellular segment of TM6 from TM3, we calculate the distance between the CA atoms of R119$^{3.50}$ and I228$^{6.37}$. Position 6.37 was selected since its CA atom is located around the same plane as the CA atom from position 3.50. As indicated in Figure 3A, the R119$^{3.50}$ (CA) and I228$^{6.37}$ (CA) distance in the antagonist-bound receptor barely samples values longer than 9 Å. In contrast, in the agonist-bound receptor, most of the time this distance overpasses the 9 Å value even reaching 11 Å values. Our calculations reveal that R119$^{3.50}$ forms a salt bridge interaction with residue E294$^{7.59}$. Indicative of this interaction, the time evolution of the R119$^{3.50}$ (CZ)—E294$^{7.59}$ (CD) distance is shown in Figure 3B. In the CBD/GPR55 complex, the salt-bridge interaction remains very stable along the entire simulation, however, in the case of the ML186/GPR55 system, the break of this interaction is frequently observed. Again, the computational approaches capture distinctive conformations adopted by the receptor in the presence of different ligands, either antagonist or agonist (Figures 3C,D).

Hence, in the case of the GPR55, the structural consequences of the presence of CBD suggests that the ligand stabilizes the receptor's inactive conformations, which is in good agreement with the suggested antagonistic activity of CBD on the GPR55 (Ryberg et al., 2007; Ross, 2009; Sharir and Abood, 2010). On the other hand, the presence of the selective ML186 agonist favors structural changes linked to GPCR's active-like conformations, again, in good agreement with the functional properties of the ligand [Kotsikorou et al., 2013; Anderson et al., 2021; Heynen-Genel et al., 2010 September 29 (updated 26 May 2011); Sharir et al., 2012; Kotsikorou et al., 2011)

3.3 Interacting determinants of the CBD ligand in the CB_1 receptors

Since our computational approaches were able to distinguish the conformational consequences of each of the ligands, either

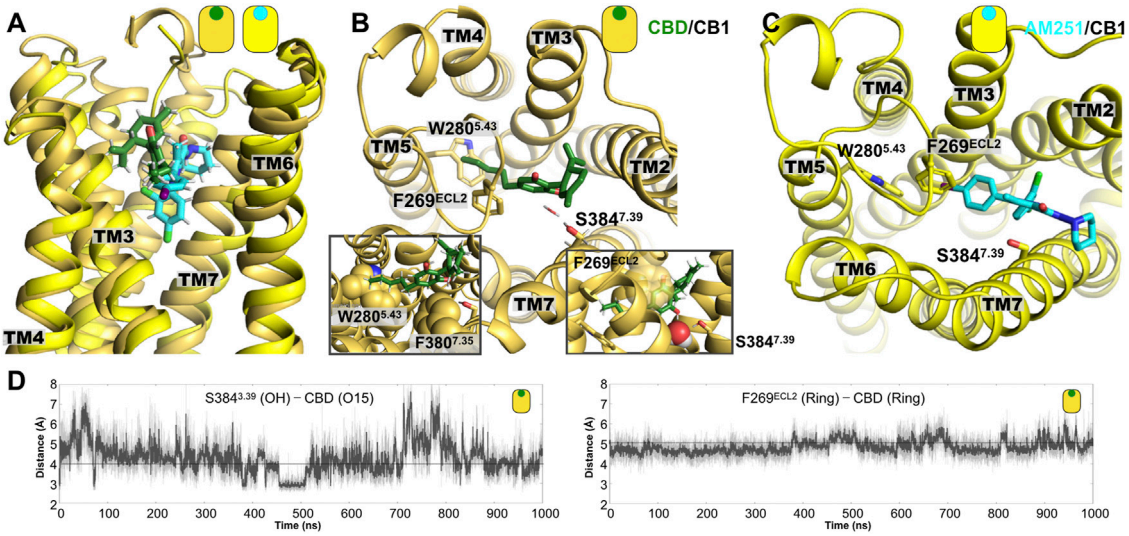

FIGURE 4
Representative poses from the MD simulations of the CB_1 complexes. **(A)** Lateral view of superimposed structures of the CBD/CB_1 and AM251/CB_1 complexes. **(B)** Extracellular view of the CBD/CB_1 complex, where we can see the interaction of the aromatic rings of CBD and the side chain of residue $F269^{ECL2}$. A water-mediated polar interaction of one of the CBD hydroxyl (OH) groups is formed with the side chain of residue $S384^{7.39}$. The left inset shows the aromatic interaction with the side chain of residue $F269^{ECL2}$ and with the side chain of $F380^{7.35}$. The right inset shows in more detail the water molecule that mediates the interaction of CBD with the residue $S384^{7.39}$. Mutation of these two residues in TM7 has been shown to reduce agonist potency of cannabinoid-like ligands. **(C)** Extracellular view of the AM231/CB_1 complex. **(D)** Time evolution plots of the distance between one of the CBD hydroxyl (OH) groups and the hydroxyl group from $S384^{7.39}$ and the ring-ring distance between the aromatic ring of CBD and the side chain of residue $F269^{ECL2}$.

agonist or inverse agonist, for the case of the GPR55 receptor, we decided to apply similar approaches to shed light on the yet-unclear functional activity of CBD on the prototypical CB_1 receptor. Based on the structural similarity of CBD with different cannabinoid ligands (Hua et al., 2017) including the structure of the phytocannabinoid delta-9-tetrahydrocannabinol (Δ^9-THC), which exhibits partial agonism at the CB_1 receptor (Pertwee, 2008; Dutta et al., 2022a), we decided to select molecular poses from our docking calculations that places the CBD compounds in the orthosteric binding site of CB_1.

As described in the Methods section, the initial model of the CBD/CB_1 was obtained from docking approaches. In this case, the information from the crystal structure of the CB_1 receptor in complex with an agonist ligand that shares structural similarities with the CBD ligand (5XRA.pdb accession code), was used as reference to evaluate the ligands poses (Supplementary Figure S5). The CBD/CB_1 system was investigated by unbiased all-atom MD simulations using protocols previously described for transmembrane proteins (see Methods). Figure 4A displays a representative final structure of both CBD complexes at the final stages of the 1 μs simulation. Residues that delineate the CBD binding site are also indicated.

In the case of the CBD/CB_1 complex, the main interactions that stabilized the ligand in the putative orthosteric binding site of CB_1 are indicated. The time evolution of distance representing two of the main interactions are indicated in Figure 4D. As observed, most of the interactions are aliphatic with a particularly relevant aromatic interactions between the aromatic ring of CBD and the side chain of residue $F269^{ECL2}$, which is located in the extracellular loop 2 (right inset Figure 4B) and the side chain of residue $F380^{7.35}$ in TM7 (left inset Figure 4B). The relevance of the latter interaction has been documented for CB_1 agonists, showing the mutation for alanine reduces agonist's potency (Hua et al., 2017). Interestingly, the alkyl tail of CBD directly contacts the bulky side chain of residue $W280^{5.43}$ in TM5. Lastly, one of the OH groups in CBD forms a polar interaction, sometimes mediated by a water molecule, with residue $S384^{7.39}$ (insets Figure 4B). Notably, the presence of this polar residue, $S384^{7.39}$, has been found to be relevant in the interaction of CB_1 with cannabinoid-like agonists, since the removal of the hydroxyl group (mutation for alanine) reduced the potency of this type of ligands (Hua et al., 2017).

3.4 Structural consequence observed by the presence of CBD in the CB_1 receptor

The presence of CBD would elicit conformational changes in the CB_1 that stabilize either active-like or inactive conformations

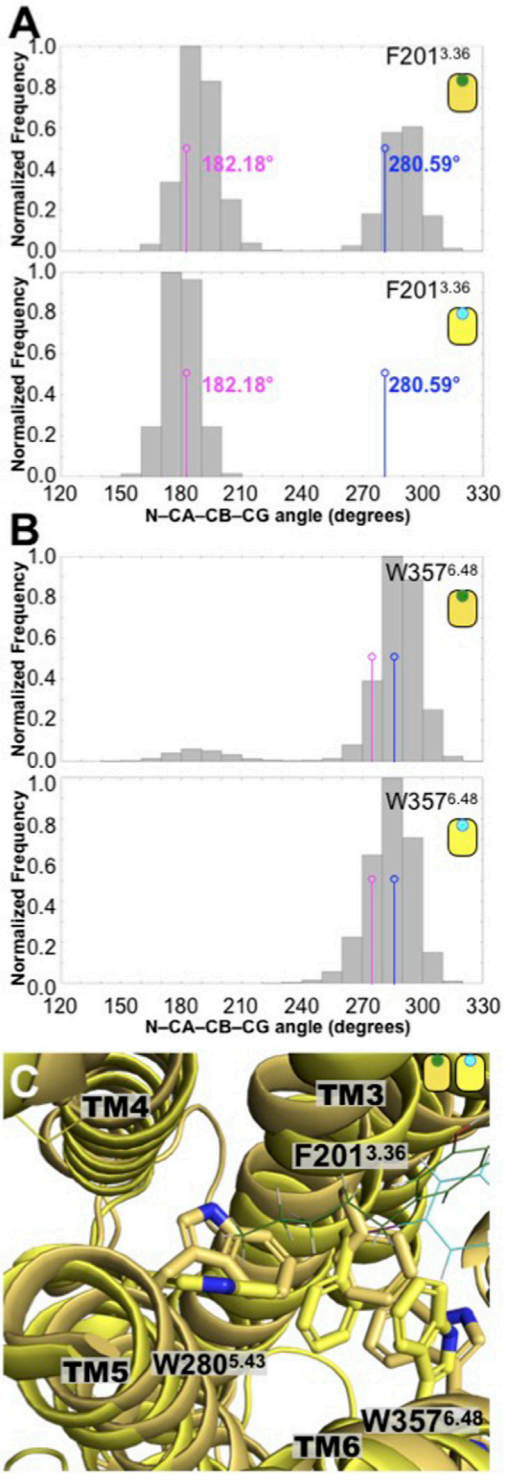

FIGURE 5
Conformation changes in the toggle switch F201$^{3.36}$ and W357$^{6.48}$ residues displayed different distributions in the CBD/CB_1 and AM251/CB_1 complexes. **(A)** Distributions of the N-CA-CB-CD dihedral angle of the F201$^{3.36}$ residue in the CBD/CB_1 and AM231/CB_1 complexes. The values indicated in magenta correspond to the antagonist-bound CB_1 structure (5TGZ.pdb) (*Continued*)

FIGURE 5
while those colored in blue correspond to the agonist-bound CB_1 structure (5XRA.pdb). As seen here, only the CBD complex explored conformations of the twin toggle switch associated with the agonist-bound CB_1 structure. **(B)** Distributions of the N-CA-CB-CD dihedral angle of the W357$^{6.48}$ residue in the CBD/CB_1 and AM231/CB_1 complexes. Together these two residues are known as the twin toggle switch. **(C)** Superimposed final structures of the CBD/CB_1 and AM251/CB_1 complexes. The different rotameric states of the F239$^{3.36}$, W357$^{6.48}$, and W280$^{5.43}$ residues in the two CB_1 complexes are shown. As indicated in the main text and in Figure 6, the alkyl tail of CBD directly contacts the bulky side chain of residue W280$^{5.43}$.

(Navarro et al., 2020; Grotenhermen, 2004; Batalla et al., 2021; Śmiarowska et al., 2022; Pertwee, 2008).

To see the consequences of the presence of CBD on the CB_1, first we analyzed the conformation of two bulky hydrophobic residues, which has been linked to CB_1 activation, that is, the F201$^{3.36}$ and W357$^{6.48}$ residues. These two "bulky" residues are sometimes denominated a "twin toggle switch," since a conformational change in their rotameric state has been proposed to be essential for the receptor activation (Hua et al., 2017). The distribution of the dihedral angle values formed by the (N-CA-CB-CG atoms of each residue are plotted in Figure 5. We can see that, in the presence of CBD, the F201$^{3.36}$ residue explores two distinctive values (bimodal distribution). The first distribution peak overlaps with the value of the antagonist-bound CB_1 receptor [5TGZ.pdb; F$^{3.36}$(N-CA-CB-CG) dihedral angle of 182.18°] (Hua et al., 2016), however, the second distribution peak overlaps with the value observed in the agonist-bound CB_1 receptor [5XRA.pdb; F$^{3.36}$(N-CA-CB-CG) dihedral angle of 280.59°] (Hua et al., 2017). To put our results in context, we investigated the CB_1 receptor in complex with a well-known antagonist, the AM251 ligand using atomistic MD simulations (Figure 4C). In stark contrast with the CBD/CB_1 case, in the presence of the AM251 antagonist, only one conformation was observed (unimodal distribution) that overlaps with the antagonist-bound CB_1 receptor. This particular conformation of the F$^{3.36}$ has been associated with the inactive state of the receptor. Moreover, in the presence of CBD, the W357$^{6.48}$ residue also explores two distinct conformations (bimodal distribution) although the first peak is barely sampled by the system. Once again, in the presence of the AM251 antagonist, only one conformation was observed, which has been associated with the inactive state of the receptor (unimodal distribution). Finally, this conformational difference in the residues that constitute the twin toggle switch are related with the rotameric states explored by the bulky residue W280$^{5.35}$. As observed in Figure 4B, the alkyl tail of CBD contacts the side chain of W280$^{5.35}$ which could facilitate the changes identified in the twin toggle switch. Hence, the presence of CBD causes the receptor to adopt active-like conformations (twin toggle switch) that are associated with agonist-bound systems. In contrast, the

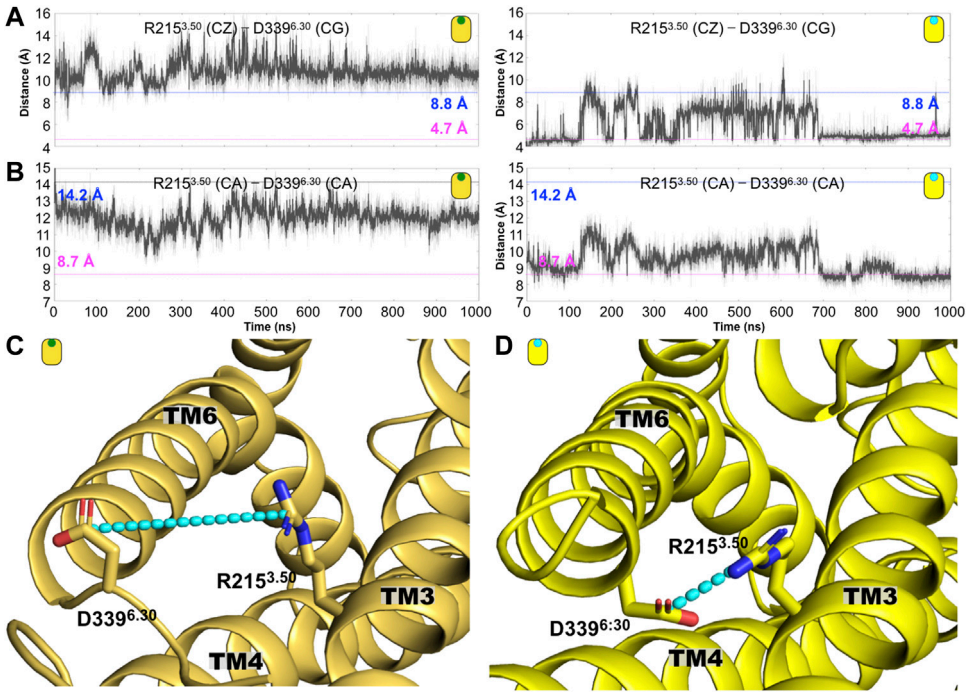

FIGURE 6
Conformation changes around the conserved intracellular residue R3.50 distinguished the antagonist-bound versus the agonist-bound CB_1 complexes. **(A)** Time evolution of the R119$^{3.50}$ (CZ)—D339$^{6.30}$ (CG) distance for the CBD-bound (left) and antagonist-bound (right) CB_1 systems. The dashed line at 4.7 (magenta) and 8.8 Å (blue) indicated corresponding distance in the antagonist-bound (5TGZ.pdb) and agonist-bound (5XRA.pdb) CB_1 structures, respectively. **(B)** Time evolution of the distance R119$^{3.50}$ (CA)-D339$^{6.30}$ (CA) distance for the CBD-bound (left) and antagonist-bound (right) CB_1 complexes. This electrostatic interaction is disrupted in the former while in the latter is frequently formed. **(C)** Representative structures of the **(C)** CBD/CB_1 and the **(D)** AM231/CB_1 complexes are shown where the ionic lock is illustrated as cyan lines.

results for the simulation of the AM251/CB_1 complex indicate that the conformations adopted by the receptor in the presence of the antagonist ligand are linked to inactive conformations of the receptors. Thus, our computational methods correctly differentiate the structural changes in CB_1 elicit by the different ligands, that is, CBD and AM251 (CB_1 antagonist). Moreover, our results suggest that CBD may act as an agonist on the CB_1 receptor.

As mentioned before, one of the hallmarks of GPCR activation is the polar interaction commonly formed by two charged residues located at the intracellular segment of TM3 and TM6. In the case of the CB_1 receptor, this so-called ionic lock is formed by residues R215$^{3.50}$ and D339$^{6.30}$ (see figure Figure 6). As indicated in Figure 6A, along the simulation time, we observed the disruption of the ionic lock, which has been established as a prerequisite for the interaction of the GPCR with its respective G-protein. Indicated by the distance between the R215$^{3.50}$(CZ)-D339$^{6.30}$(CG), our results indicate that the values for this distance remains larger that 8.8 A, which is the distance observed in the case of the agonist-bound CB_1 complex (AM11542/CB_1, PDB ID code 5XRA). This result indicates that in the presence of CBD, the ionic lock displays conformations associated with agonist-bound states. Similarly, we calculate the same distance, R215$^{3.50}$(CZ)-D339$^{6.30}$(CG), for the case of the AM251/CB_1 complex (the antagonist-bound system). As indicated in Figure 6A, the ionic lock remains close, around 4.5/4.7 Å (distances observed in antagonist-bound CB_1 complexes, 5TGZ.pdb/5U09.pdb) and almost never explores distances longer that 8.8 Å. Along the same lines, the R215$^{3.50}$(CA)-D339$^{6.30}$(CA) also indicates the formation of the ionic lock in the antagonist-bound system (AM251/CB_1 complex) but not in the case of the CBD/CB_1 complex, again, suggesting that CBD may act as an agonist on the CB_1 receptor (Figure 6B). Structures illustrating the ionic lock motif for the CBD/CB1 and AM231/CB1 complexes are shown in Figures 6C,D, respectively.

3.5 The unbiased MD simulations suggest a sodium-binding site located in the extracellular domain of the CB_1 receptor

Additionally to the detailed description of the ligand binding determinants and the receptor's structural consequence, our simulations also identified a sodium-binding site located in the

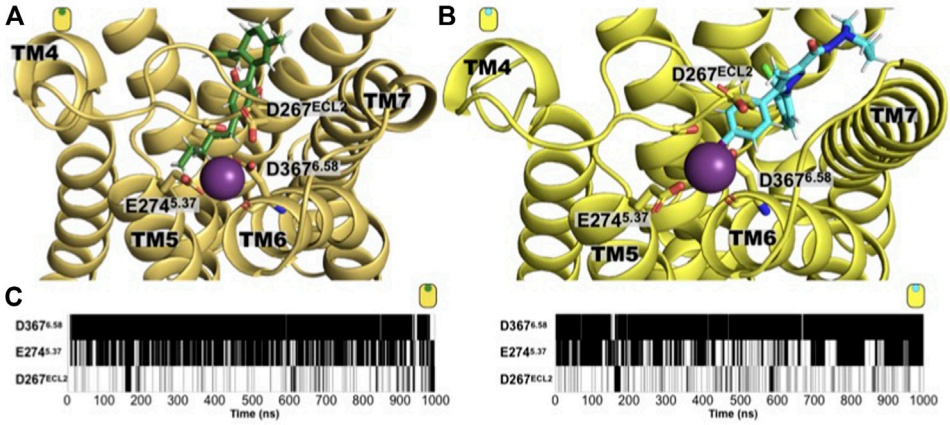

FIGURE 7
An extracellular sodium-binding site is observed in the simulation of both CB_1 complexes. Extracellular view of the sodium-binding site identified by our unbiased simulations in the extracellular side of the **(A)** CBD/CB_1 and **(B)** AM251/CB_1 receptor. The residues that constitute the binding site are: $D367^{6.58}$, $E274^{5.37}$, and $D267^{ECL2}$. **(C)** Time evolution maps of sodium contact by these three residues where black indicated a contact with a sodium ion (define by a distance of 4 Å or less of any residue heavy atom with a sodium atom), while white indicates the absence of such contact. As shown, residue $D367^{6.58}$ is the main responsible for establishing electrostatic interactions with a sodium cation and to do so, it usually utilizes both, its side chain carboxylate group and its backbone carbonyl group. The acidic nature of the residue bore at these positions is conserved in the human CB_1 receptor ($D367^{6.58}$, $E274^{5.37}$, and $D267^{ECL2}$ are the positions in rat with the corresponding human positions, $D366^{6.58}$, $E273^{5.37}$, and $D266^{ECL2}$).

extracellular side. Previously, the location of a binding-site at the TM domain of the CB_1 receptor has been identified (Dutta et al., 2022b; Katritch et al., 2014). From our unbiased MD simulations and in both CB_1 complexes, we observed the formation of this extracellular sodium-binding site formed by residues located in the extracellular segment of TM5 and TM6, and the extracellular loop 2. $D267^{ECL2}$, $E274^{5.37}$, and $D367^{6.58}$. As shown in Figure 7, along the microsecond MD simulations, the residues $D267^{ECL2}$, $E274^{5.37}$, and $D367^{6.58}$ are in contact with a sodium ion forming a sodium-binding site at the receptor's extracellular side, regardless of the characteristics of the ligand. The functional consequences of this site need to be further evaluated for a possible exploitation of this tentative allosteric site. Interestingly, no sodium-binding site at the extracellular site was observed in the case of the GPR55 systems.

4 Discussion

An integral description of the protein's function is fundamental to understand the involvement of these biomacromolecules in different cellular activities. Moreover, discerning how different biochemical entities, including exogenous ligands, ions, peptides, and lipids, to mention a few, regulate the protein's function is needed to finely modulate the cellular response of the proteins.

In this context, computational methods offer tailored tools adapted to investigate at a molecular detail, the function of different biomacromolecules, including proteins. Additionally, computational-based techniques also provide detailed information of the way protein function is modulated by the aforementioned biochemical entities (Almeida et al., 2017; Klepeis et al., 2009; Arinaminpathy et al., 2009; Samish et al., 2011; Hollingsworth and Dror, 2018; Pagadala et al., 2017).

Here we exploit the power of atomistic computer simulations to investigate the role of cannabidiol (CBD), a major cannabinoid compound from the *Cannabis* plant that is closely-related to the well-known delta-9-tetrahydrocannabinol (Δ^9-THC), but lacks its psychoactivity. CBD has attracted great attention in recent years as a possible pharmacological tool to treat different neurological disorders. Additionally, the growing use of CBD as a recreational substance makes it important to understand how this compound interacts with different cellular entities. We applied unbiased all-atom molecular dynamics simulations to investigate the interacting determinants as well as the conformational consequences of CBD in two closely related endocannabinoid-activated GPCRs, the G-protein-coupled receptor 55 (GPR55) and the cannabinoid type 1 receptor (CB_1). Our results in the GPR55 complexes indicate that the computational methods correctly differentiate the structural changes associated with the presence of each ligand, an antagonist (CBD) and an agonist (ML186). That is, the utilized computational methods identified conformational changes in the GPR55 receptors associated with antagonist-bound receptors (the case of the CBD/GPR55 complex) and agonist-bound receptors (the case of the ML186/GPR55); this is in good agreement with the known modulatory function of these ligands in the GPR55 receptor. Prompted by these results, we subsequently applied similar computational methods to shed light into the role of CBD in the CB_1 receptor, one of the most

abundant GPCRs receptors in the CNS. Our results suggest that the presence of CBD causes conformational changes in the CB_1 linked to agonist-bound systems. Currently, the role of CBD in the CB_1 receptor remains debatable, i.e., CBD has been suggested to activate the receptor, to favor CB_1 inactive conformations or to function as an allosteric modulator. From our investigation we propose that CBD triggers activation of the CB_1 receptor, nonetheless, we cannot exclude the possibility that CBD may bias either homo- or hetero-dimerization of the CB_1 receptor and consequently regulate its function in a different way as the agonistic role proposed here. Furthermore, if CBD indirectly modulates the function of the CB_1, it also remains a possibility that our results cannot be excluded. Yet, we are providing strong evidence that CBD is able to trigger changes in the CB_1 receptor associated with agonist-bound GPCRs. The detail of our work aids to suggest an unknown sodium-binding site located at the extracellular side of the receptor and formed mainly by residues located at the extracellular termini of TM5 and TM6.

Our investigation shows that computational-based methods are able to correctly distinguish the conformational changes attributed to either an agonist-bound or antagonist-bound GPCRs.

Data availability statement

The datasets presented in this study can be found in online repositories. The names of the repository/repositories and accession number(s) can be found in the article/ Supplementary Material.

Author contributions

JP-A and BS-G: Project idea and coordination. JP-A: Computational modeling and simulation studies, data analysis, wrote the manuscript, and final approval. ED: Computational modeling and simulation studies, data analysis, wrote the manuscript, and final approval. IL and FP: Project idea, wrote the manuscript, and final approval. MR-B, DG-G, JH, and BS-G: Data analysis, wrote the manuscript, and final approval.

Funding

The work was supported by the PRODEP Academic Group BUAP-CA-263 (SEP, México). ED, FP, MR-B, DG-G, and JH thank CONACYT-México for financial support (Ph.D. fellowship Nos 758730 and 732793, respectively).

Acknowledgments

JP-A acknowledges the computing time granted by the LANCAD on the supercomputer xiuhcoatl at CGSTIC CINVESTAV, members of the CONACyT network of national laboratories. JP-A thanks the Laboratorio Nacional de Supercómputo del Sureste de México (LNS-BUAP) of the CONACyT network of national laboratories for the computer resources and support provided.

Conflict of interest

The authors declare that the research was conducted in the absence of any commercial or financial relationships that could be construed as a potential conflict of

Publisher's note

All claims expressed in this article are solely those of the authors and do not necessarily represent those of their affiliated organizations, or those of the publisher, the editors and the reviewers. Any product that may be evaluated in this article, or claim that may be made by its manufacturer, is not guaranteed or endorsed by the publisher.

Supplementary material

The Supplementary Material for this article can be found online at: https://www.frontiersin.org/articles/10.3389/fphar.2022.945935/full#supplementary-material

References

Almeida, J. G., Preto, A. J., Koukos, P. I., Bonvin, A. M. J. J., and Moreira, I. S. (2017). Membrane proteins structures: A review on computational modeling tools. *Biochim. Biophys. Acta. Biomembr.* 1859, 2021–2039. Elsevier B.V. doi:10.1016/j.bbamem.2017.07.008

Altschul, S. F., Gish, W., Miller, W., Myers, E. W., and Lipman, D. J. (1990). Basic local alignment search tool. *J. Mol. Biol.* 215 (3), 403–410. Academic Press. doi:10.1016/S0022-2836(05)80360-2

Anderson, L. L., Heblinski, M., Absalom, N. L., Hawkins, N. A., Bowen, M. T., Benson, M. J., et al. (2021). Cannabigerolic acid, a major biosynthetic precursor molecule in cannabis, exhibits divergent effects on seizures in mouse models of epilepsy. *Br. J. Pharmacol.* 178 (24), 4826–4841. John Wiley and Sons Inc. doi:10.1111/bph.15661

Arinaminpathy, Y., Khurana, E., Engelman, D. M., and Gerstein, M. B. (2009). Computational analysis of membrane proteins: the largest class of drug targets. *Drug Discov. Today* 14, 1130–1135. Elsevier Current Trends. doi:10.1016/j.drudis.2009.08.006

Austrich-Olivares, A., Garcia-Gutierrez, M. S., Illescas, L., Gasparyan, A., and Manzanares, J. (2022). Cannabinoid CB1 receptor involvement in the actions of CBD on anxiety and coping behaviors in mice. *Pharm. (Basel, Switz.* 15 (4), 473. doi:10.3390/ph15040473

Ballesteros, J. A., and Weinstein, H. (1995). Integrated methods for the construction of three-dimensional models and computational probing of structure-function relations in G protein-coupled receptors. *Methods Neurosci.* 25, 366–428. Academic Press. doi:10.1016/S1043-9471(05)80049-7

Batalla, A., Bos, J., Postma, A., and Bossong, M. G. (2021). The impact of cannabidiol on human brain function: A systematic review. *Front. Pharmacol.* 11, 618184. Frontiers Media S.A. doi:10.3389/fphar.2020.618184

Dror, R. O., Pan, A. C., Arlow, D. H., Borhani, D. W., Maragakis, P., Shan, Y., et al. (2011). Pathway and mechanism of drug binding to G-protein-coupled receptors. *Proc. Natl. Acad. Sci. U. S. A.* 108 (32), 13118–13123. doi:10.1073/pnas.1104614108

Dutta, S., Selvam, B., Das, A., and Shukla, D. (2022a). Mechanistic origin of partial agonism of tetrahydrocannabinol for cannabinoid receptors. *J. Biol. Chem.* 298 (4), 101764. Elsevier BV. doi:10.1016/j.jbc.2022.101764

Dutta, S., Selvam, B., and Shukla, D. (2022b). Distinct binding mechanisms for allosteric sodium ion in cannabinoid receptors', *ACS chemical neuroscience. ACS Chem. Neurosci.* 13 (3), 379–389. doi:10.1021/acschemneuro.1c00760

Eswar, N., Webb, B., Marti-Renom, M. A., Madhusudhan, M. S., Eramian, D., Shen, M. Y., et al. (2006). Comparative protein structure modeling using modeller. *Curr. Protoc. Bioinforma.* 15 (1), 5–6. Wiley. doi:10.1002/0471250953.bi0506s15

Grotenhermen, F. (2004). Pharmacology of cannabinoids. *Neuro Endocrinol. Lett.* 25 (1–2), 14–23.

Hall, W., and Lynskey, M. (2016). Evaluating the public health impacts of legalizing recreational cannabis use in the United States: Impacts of legalizing recreational cannabis use. *Addict. (Abingdon, Engl.* 111 (10), 1764–1773. doi:10.1111/add.13428

Heynen-Genel, S., Dahl, R., Shi, S., Milan, L., Hariharan, S., Yalda, B., et al. (2010). "Screening for selective ligands for GPR55 - agonists," in *Probe reports from the NIH molecular libraries program [internet]* (Bethesda (MD): National Center for Biotechnology Information). PMID: 22091480.

Hilger, D. (2021). The role of structural dynamics in GPCR-mediated signaling. *FEBS J.* 288 (8), 2461–2489. Blackwell Publishing Ltd. doi:10.1111/febs.15841

Hollingsworth, S. A., and Dror, R. O. (2018), Molecular dynamics simulation for all. *Neuron* 99, 1129–1143. Cell Press. doi:10.1016/j.neuron.2018.08.011

Hua, T., Vemuri, K., Nikas, S. P., Laprairie, R. B., Wu, Y., Qu, L., et al. (2017). Crystal structures of agonist-bound human cannabinoid receptor CB 1', *Nature. Nature* 547 (7664), 468–471. doi:10.1038/nature23272

Hua, T., Vemuri, K., Pu, M., Qu, L., Han, G. W., Wu, Y., et al. (2016). Crystal structure of the human cannabinoid receptor CB1. *Cell* 167 (3), 750–762. e14. doi:10.1016/j.cell.2016.10.004

Humphrey, W., Dalke, A., and Schulten, K. (1996). Vmd - visual molecular dynamics. *J. Mol. Graph.* 14, 33–38. doi:10.1016/0263-7855(96)00018-5

Kapur, A., Zhao, P., Sharir, H., Bai, Y., Caron, M. G., Barak, L. S., et al. (2009). Atypical responsiveness of the orphan receptor GPR55 to cannabinoid ligands. *J. Biol. Chem.* 284 (43), 29817–29827. Elsevier. doi:10.1074/jbc.M109.050187

Katritch, V., Fenalti, G., Abola, E. E., Roth, B. L., Cherezov, V., and Stevens, R. C. (2014). Allosteric sodium in class A GPCR signaling. *Trends biochem. Sci.* 39, 233–244. Elsevier Ltd. doi:10.1016/j.tibs.2014.03.002

Klepeis, J. L., Lindorff-Larsen, K., Dror, R. O., and Shaw, D. E. (2009). Long-timescale molecular dynamics simulations of protein structure and function. *Curr. Opin. Struct. Biol.* 19, 120–127. Elsevier Current Trends. doi:10.1016/j.sbi.2009.03.004

Kotsikorou, E., Madrigal, K. E., Hurst, D. P., Sharir, H., Lynch, D. L., Heynen-Genel, S., et al. (2011). Identification of the GPR55 agonist binding site using a novel set of high-potency GPR55 selective ligands', *Biochemistry. Biochemistry* 50 (25), 5633–5647. doi:10.1021/bi200010k

Kotsikorou, E., Sharir, H., Shore, D. M., Hurst, D. P., Lynch, D. L., Madrigal, K. E., et al. (2013). Identification of the GPR55 antagonist binding site using a novel set of high-potency GPR55 selective ligands', *Biochemistry. Biochemistry* 52 (52), 9456–9469. doi:10.1021/bi4008885

Latorraca, N. R., Venkatakrishnan, A. J., and Dror, R. O. (2017). GPCR dynamics: Structures in motion. *Chem. Rev.* 117, 139–155. American Chemical Society. doi:10.1021/acs.chemrev.6b00177

Lee, J. Y., and Lyman, E. (2012). Agonist dynamics and conformational selection during microsecond simulations of the A(2A) adenosine receptor. *Biophys. J.* 102 (9), 2114–2120. doi:10.1016/j.bpj.2012.03.061

Lu, H. C., and MacKie, K. (2016). An introduction to the endogenous cannabinoid system. *Biol. Psychiatry* 79, 516–525. Elsevier USA. doi:10.1016/j.biopsych.2015.07.028"

Manglik, A., Kim, T. H., Masureel, M., Altenbach, C., Yang, Z., Hilger, D., et al. (2015). Structural insights into the dynamic process of β2-adrenergic receptor signaling. *Cell* 161 (5), 1101–1111. doi:10.1016/j.cell.2015.04.043

Méndez-Luna, D., Martinez-ArchundiaM.Maroun, R. C., Ceballos-Reyes, G., Fragoso-Vazquez, M. J., Gonzalez-Juarez, D. E., et al. (2015). Deciphering the GPER/GPR30-agonist and antagonists interactions using molecular modeling studies, molecular dynamics, and docking simulations. *J. Biomol. Struct. Dyn.* 33 (10), 2161–2172. doi:10.1080/07391102.2014.994102

Navarro, G., Varani, K., Lillo, A., Vincenzi, F., Rivas-Santisteban, R., Raich, I., et al. (2020). Pharmacological data of cannabidiol- and cannabigerol-type phytocannabinoids acting on cannabinoid CB1, CB2 and CB1/CB2 heteromer receptors. *Pharmacol. Res.* 159, 104940. Academic Press. doi:10.1016/j.phrs.2020.104940

Pagadala, N. S., Syed, K., and Tuszynski, J. (2017). Software for molecular docking: a review. *Biophys. Rev.* 9, 91–102. Springer Verlag. doi:10.1007/s12551-016-0247-1"

Perez-Aguilar, J. M., Shan, J., LeVine, M. V., Khelashvili, G., and Weinstein, H. (2014). A functional selectivity mechanism at the serotonin-2A GPCR involves ligand-dependent conformations of intracellular loop 2', *Journal of the American Chemical Society. Am. Chem. Soc.* 136 (45), 16044–16054. doi:10.1021/ja508394x

Perez-Aguilar, J. M., Kang, S.-g, Zhang, L., and Zhou, R. (2019). Modeling and structural characterization of the sweet taste receptor heterodimer', *ACS chemical neuroscience. Am. Chem. Soc.* 10 (11), 4579–4592. doi:10.1021/acschemneuro.9b00438

Pertwee, R. G. (2008). The diverse CB_1 and CB_2 receptor pharmacology of three plant cannabinoids: Δ^9 -tetrahydrocannabinol, cannabidiol and Δ^9 -tetrahydrocannabivarin. *Br. J. Pharmacol.* 153 (2), 199–215. John Wiley & Sons, Ltd. doi:10.1038/sj.bjp.0707442

Rangel-Galván, M., Rangel, A., Romero-Méndez, C., Dávila, E. M., Castro, M. E., Caballero, N. A., et al. (2021). Inhibitory mechanism of the isoflavone derivative genistein in the human CaV3.3 channel', *ACS chemical neuroscience. Am. Chem. Soc.* 12 (4), 651–659. doi:10.1021/acschemneuro.0c00684

Ross, R. A. (2009). The enigmatic pharmacology of GPR55. *Trends Pharmacol. Sci.* 36, 156–163. Elsevier Current Trends. doi:10.1016/j.tips.2008.12.004

Ryberg, E., LarssoNN.Sjogren, S., Hjorth, S., Hermansson, N. O., Leonova, J., et al. (2007). The orphan receptor GPR55 is a novel cannabinoid receptor. *Br. J. Pharmacol.* 152 (7), 1092–1101. John Wiley & Sons, Ltd. doi:10.1038/sj.bjp.0707460

Šali, A., Blundell, T. L., and SAli, A. (1993). Comparative protein modelling by satisfaction of spatial restraints. *J. Mol. Biol.* 234 (3), 779–815. Academic Press. doi:10.1006/jmbi.1993.1626

Samish, I., MacDermaid, C. M., Perez-Aguilar, J. M., and Saven, J. G. (2011). Theoretical and computational protein design', *annual Review of physical chemistry. Annu. Rev. Phys. Chem.* 62 (1), 129–149. doi:10.1146/annurev-physchem-032210-103509

Shao, Z., Yan, W., Chapman, K., Ramesh, K., Ferrell, A. J., Yin, J., et al. (2019)., Structure of an allosteric modulator bound to the CB1 cannabinoid receptor. *Nat. Chem. Biol.* 15, 1199–1205. doi:10.1038/s41589-019-0387-2

Sharir, H., and Abood, M. E. (2010). Pharmacological characterization of GPR55, a putative cannabinoid receptor. *Pharmacol. Ther.* 126, 301–313. Pergamon. doi:10.1016/j.pharmthera.2010.02.004"

Sharir, H., Console-Bram, L., Mundy, C., Popoff, S. N., Kapur, A., and Abood, M. E. (2012). The endocannabinoids anandamide and virodhamine modulate the activity of the candidate cannabinoid receptor GPR55. *J. Neuroimmune Pharmacol.* 7 (4), 856–865. Springer. doi:10.1007/s11481-012-9351-6

Śmiarowska, M., Białecka, M., and Machoy-Mokrzyńska, A. (2022). Cannabis and cannabinoids: pharmacology and therapeutic potential. *Neurol. Neurochir. Pol.* 56, 4–13. doi:10.5603/PJNNS.A2022.0015

Trott, O., and Olson, A. J. (2009). AutoDock Vina: Improving the speed and accuracy of docking with a new scoring function, efficient optimization, and multithreading. *J. Comput. Chem.* 31 (2), 455–461. Wiley. doi:10.1002/jcc.21334

Waterhouse, A., Bertoni, M., Bienert, S., Studer, G., Tauriello, G., Gumienny, R., et al. (2018). SWISS-MODEL: Homology modelling of protein structures and complexes. *Nucleic Acids Res.* 46 (1), W296–W303. Oxford University Press. doi:10.1093/nar/gky427

Wilkinson, S. T., Yarnell, S., Radhakrishnan, R., Ball, S. A., and D'Souza, D. C. (2016). Marijuana legalization: Impact on physicians and public health. *Annu. Rev. Med.* 67 (1), 453–466. doi:10.1146/annurev-med-050214-013454

Zhou, Q., Yang, D., Wu, M., Guo, Y., Guo, W., Zhong, L., et al. (2019), Common activation mechanism of class a GPCRs. eLife 8, e50279. eLife Sciences Publications Ltd. doi:10.7554/eLife.50279*Elife*

frontiers | Frontiers in Pharmacology

TYPE Original Research
PUBLISHED 02 September 2022
DOI 10.3389/fphar.2022.945836

OPEN ACCESS

EDITED BY
Gustavo Gonzalez-Cuevas,
Idaho State University, United States

REVIEWED BY
Andreas Wree,
University of Rostock, Germany
Catalina Requejo,
Spanish National Research Council (CSIC), Spain

*CORRESPONDENCE
Ilhuicamina Daniel Limón,
ilhlimon@yahoo.com.mx,
daniel.limon@correo.buap.mx

SPECIALTY SECTION
This article was submitted to Neuropharmacology, a section of the journal Frontiers in Pharmacology

RECEIVED 17 May 2022
ACCEPTED 09 August 2022
PUBLISHED 02 September 2022

CITATION
Patricio F, Morales Dávila E, Patricio-Martínez A, Arana Del Carmen N, Martínez I, Aguilera J, Perez-Aguilar JM and Limón ID (2022), Intrapallidal injection of cannabidiol or a selective GPR55 antagonist decreases motor asymmetry and improves fine motor skills in hemiparkinsonian rats. *Front. Pharmacol.* 13:945836. doi: 10.3389/fphar.2022.945836

Intrapallidal injection of cannabidiol or a selective GPR55 antagonist decreases motor asymmetry and improves fine motor skills in hemiparkinsonian rats

Felipe Patricio[1], Eliud Morales Dávila[2], Aleidy Patricio-Martínez[1,3], Nayeli Arana Del Carmen[1], Isabel Martínez[4], José Aguilera[5,6], Jose Manuel Perez-Aguilar[2] and Ilhuicamina Daniel Limón[1]*

[1]Laboratorio de Neurofarmacología, Facultad de Ciencias Químicas, Benemérita Universidad Autónoma de Puebla, Puebla, Mexico, [2]Facultad de Ciencias Químicas, Benemérita Universidad Autónoma de Puebla, Puebla, Mexico, [3]Facultad de Ciencias Biológicas, Benemérita Universidad Autónoma de Puebla, Puebla, Mexico, [4]Laboratorio de Neuroquímica, Facultad de Ciencias Químicas, Benemérita Universidad Autónoma de Puebla, Puebla, Mexico, [5]Departament de Bioquímica i de Biologia Molecular, Facultad de Medicina, Institut de Neurociències, Universitat Autònoma de Barcelona, Barcelona, Spain, [6]Centro de Investigación Biomédica en Red sobre Enfermedades Neurodegenerativas (CIBERNED), Barcelona, Spain

Cannabidiol (CBD) presents antiparkinsonian properties and neuromodulatory effects, possibly due to the pleiotropic activity caused at multiple molecular targets. Recently, the GPR55 receptor has emerged as a molecular target of CBD. Interestingly, GPR55 mRNA is expressed in the *external globus pallidus* (GPe) and striatum, hence, it has been suggested that its activity is linked to motor dysfunction in Parkinson's disease (PD). The present study aimed to evaluate the effect of the intrapallidal injection of both CBD and a selective GPR55 antagonist (CID16020046) on motor asymmetry, fine motor skills, and GAD-67 expression in hemiparkinsonian rats. The hemiparkinsonian animal model applied involved the induction of a lesion in male Wistar rats *via* the infusion of the neurotoxin 6-hydroxydopamine (6-OHDA) into the medial forebrain bundle *via* stereotaxic surgery. After a period of twenty days, a second surgical procedure was performed to implant a guide cannula into the GPe. Seven days later, lysophosphatidylinositol (LPI), CBD, or

Abbreviations: AMPH, Amphetamine; BG, Basal ganglia; CB_1, Cannabinoid receptor type 1; CBD, Cannabidiol; CNS, Central nervous system; DMSO, Dimethyl sulfoxide; ER, Endoplasmic reticulum; FAAH, Fatty acid amide hydrolase; GAD-67, Glutamic acid decarboxylase 67; GPe, external globus pallidus; GPR55, G-protein coupled receptor 55; H_2O_2, Hydrogen peroxide; 6-OHDA, 6-hydroxydopamine; LPI, Lysophosphatidylinositol; MPP+, 1-methyl-4-phenylpyridinium; MPTP, 1-methyl-4-phenyl-1,2,3,6-tetrahydropyridine; PD, Parkinson's disease; PLC, Phospholipase C; ROCK, Rho-associated protein kinase; SNpc, substantia nigra pars compacta; SNpr, substantia nigra pars reticulata; STN, Subthalamic nucleus; TH, Tyrosine hydroxylase; THC, Δ^9-tetrahydrocannabinol.

CID16020046 were injected once a day for three consecutive days (from the 28th to the 30th day post-lesion). Amphetamine-induced turning behavior was evaluated on the 14th and 30th days post-injury. The staircase test and fine motor skills were evaluated as follows: the rats were subject to a ten-day training period prior to the 6-OHDA injury; from the 15th to the 19th days post-lesion, the motor skills alterations were evaluated under basal conditions; and, from the 28th to the 30th day post-lesion, the pharmacological effects of the drugs administered were evaluated. The results obtained show that the administration of LPI or CBD generated lower levels of motor asymmetry in the turning behavior of hemiparkinsonian rats. It was also found that the injection of CBD or CID16020046, but not LPI, in the hemiparkinsonian rats generated significantly superior performance in the staircase test, in terms of the use of the forelimb contralateral to the 6-OHDA-induced lesion, when evaluated from the 28th to the 30th day post-lesion. Similar results were also observed for superior fine motor skills performance for pronation, grasp, and supination. Finally, the immunoreactivity levels were found to decrease for the GAD-67 enzyme in the striatum and the ipsilateral GPe of the rats injected with CBD and CID16020046, in contrast with those lesioned with 6-OHDA. The results obtained suggest that the inhibitory effects of CBD and CID16020046 on GPR55 in the GPe could be related to GABAergic overactivation in hemiparkinsonism, thus opening new perspectives to explain, at a cellular level, the reversal of the motor impairment observed in PD models.

KEYWORDS

cannabidiol, CID16020046, GPR55 receptor, behavioral test, motor asymmetry, fine motor skills, hemiparkinsonian rats, Parkinson's disease

1 Introduction

Cannabidiol (CBD) is the second most abundant component of *Cannabis sativa* L., after Δ^9-tetrahydrocannabinol (THC), which is responsible for the psychoactive properties of plant (Pertwee, 2008; Ibeas Bih et al., 2015; Pellati et al., 2018). As CBD does not directly activate the cannabinoid receptor type 1 (CB_1), it is, thus, devoid of the psychoactive side effects exhibited by THC and is also considered a safe drug (Pisanti et al., 2017). Given its action as a pleiotropic molecule and its targeting of various proteins of the cannabinoid system, CBD can be described as a neuromodulator, with an increasing amount of data evidencing its neuromodulatory properties in different neurological and neuropsychiatric disorders (Fernández-Ruiz et al., 2013; Campos et al., 2017; Patricio et al., 2020; Xiong and Lim, 2021). Moreover, cannabinoid-related receptors, such as the G-protein coupled receptor 55 (GPR55), may play an important role in the effects exerted by CBD in the central nervous system (CNS) (Ryberg et al., 2007; Ligresti et al., 2016; Kaplan et al., 2017).

It has been shown that GPR55 is coupled to the proteins $G\alpha_{12/13}$ and $G\alpha_q$, which are activated by cannabinoids and the endogenous ligand of the GPR55, lysophosphatidylinositol (LPI); therefore, it promotes both the Rho-associated protein kinase (ROCK) and phospholipase C (PLC) pathways (Henstridge et al., 2011; Alhouayek et al., 2018). The cellular effects of the activation of GPR55 are the release of intracellular calcium from the endoplasmic reticulum (ER), the phosphorylation of the protein ERK1/2, and the activation of ROCK (Oka et al., 2007; Ryberg et al., 2007; Lauckner et al., 2008). Interestingly, data shows that CBD acts as an inverse agonist of GPR55 and, therefore, inhibits the LPI-induced stimulation of ERK1/2 phosphorylation (Anavi-Goffer et al., 2012) and the stimulation of [^{35}S]GTPγS binding by LPI (Ford et al., 2010). Research has revealed the structure-activity relationship of GPR55 with the selective antagonist CID16020046, while the antagonism of GPR55 has been proposed as an efficacious treatment for several neurological diseases (Brown et al., 2018). CID16020046 has been used to study the physiological role of GPR55 in nociception (Okine et al., 2020), cognitive processes (Marichal-Cancino et al., 2016; Hurst et al., 2017; Marichal-Cancino et al., 2018), and the neuroprotective effects observed in neuroinflammation and Dravet syndrome animal models (Kaplan et al., 2017; Shen et al., 2022).

Early reports have demonstrated a high level of GPR55 mRNA expression in different areas of the CNS in both humans (Sawzdargo et al., 1999; Wu et al., 2013; García-Gutiérrez et al., 2018; Hill et al., 2018) and rodents (Ryberg et al., 2007; Sylantyev et al., 2013; Wu et al., 2013). As the main regions in which this expression has been observed are the striatum, hippocampus, cortex, and brainstem, it has been related to various behavioral processes, such as learning, memory, food

intake, the emotions, and movement control (Marichal-Cancino et al., 2017). Moreover, impaired movement coordination in GPR55 knockout mice has been observed, thus suggesting that the receptor plays a role in motor control, given the relationship between its presence in the striatum and its potential link to the dopaminergic system (Wu et al., 2013). Indeed, PD is a neurodegenerative disorder characterized by dopamine deprivation in various nuclei of the basal ganglia (BG) due to dopaminergic neuron loss in the *substantia nigra pars compacta* (SNpc) (Smith and Villalba, 2008; Rommelfanger and Wichmann, 2010; Benazzouz et al., 2014).

The BG is an interconnected group of subcortical nuclei, in the deep encephalon, which, in a healthy state, are responsible for movement planning and modulation (Lanciego et al., 2012). The functional disruption of the BG causes the manifestation of motor symptoms such as akinesia, muscle rigidity, and tremor at rest (Rommelfanger and Wichmann, 2010; Galvan et al., 2015; Neumann et al., 2018). According to the classic BG model (Albin et al., 1989), the *external globus pallidus* (GPe) has been considered a relevant factor in PD, as it is highly over-inhibited in parkinsonism due to the loss of striatal dopaminergic activity leading to the disinhibition of the D_2-striatal projection neurons. These processes are attributed to the hypokinetic states observed in the PD, in both in animal models and human patients (Berardelli et al., 2001; Galvan and Wichmann, 2008; Dong et al., 2021). Interestingly, the GPR55 mRNA transcript has been identified, *via in situ* hybridization, in the GPe and striatum of mice, as well as other nuclei of the BG circuit that are associated with movement control (Celorrio et al., 2017).

Recent studies have reported that GPR55 may serve as a therapeutic agent in the treatment of PD. Celorrio et al. (2017) studied the effect of the peripheral administration of abnormal cannabidiol (a synthetic isomer of CBD), to explore its agonist effects on the GPR55 receptor. They observed a beneficial neuroprotective effect on dopaminergic neurons injured by 1-methyl-4-phenyl-1,2,3,6-tetrahydropyridine (MPTP) and an anti-inflammatory and anti-cataleptic effect as a result of GPR55 activation in parkinsonian mice models. Burgaz et al. (2021) found similar results in two PD models, which revealed the neuroprotective effect of VCE-006.1, which is a chromenopyrazole derivative with biased orthosteric and positive allosteric modulator effects on GPR55. They found that the drug reversed motor dysfunction, the loss of tyrosine hydroxylase-containing neurons, and the elevated glial reactivity detected in the SNpc of parkinsonian mice. Another study found that neurons expressing heteromers (CB_1/GPR55) are more resistant to 1-methyl-4-phenylpyridinium-induced (MPP^+) cell death (Martínez-Pinilla et al., 2019). These findings suggest the use of GPR55 as a potential neuroprotective agent and a therapeutic target for the treatment of PD. The role played by GPR55 in the striatum of hemiparkinsonian rats has been subject to recent research, which reported similar effects on locomotor activity, in terms of both agonism and antagonism of GPR55. It may be, therefore, that this receptor has a modulatory effect on motor behavior (Fatemi et al., 2021). The foregoing evidence suggests that GPR55 may play a role in the modulation occurring in several nuclei of the BG circuit and may have an impact on movement control in an animal model of PD.

The study of the hemiparkinsonian model in rodents has frequently used the neurotoxin 6-hydroxydopamine (6-OHDA) to induce dopaminergic neuronal death in the SNpc (Deumens et al., 2002; Francardo et al., 2017; Hernandez-Baltazar et al., 2017; Segura-Aguilar, 2018). Lesions induced *via* 6-OHDA in the medial forebrain bundle show generalized degeneration and, thus, dopaminergic denervation in both the striatum and GPe (Mallet et al., 2008; Kita and Kita, 2011; Fernández-Suárez et al., 2012; Mallet et al., 2012; Abedi et al., 2013; Dong et al., 2021). This model enables the assessment of quantifiable turning behavior, which can be correlated to the extent of the lesion, while it has also been shown that the 6-OHDA lesion model impairs both gross and fine motor skills (Galvan et al., 2001; Klein et al., 2007; Rattka et al., 2016). To date, the effects of either the administration of CBD or the selective antagonism of GPR55 in the GPe on the asymmetrical motor and fine motor skills of hemiparkinsonian rats are unknown. Therefore, the present study aimed to examine the effect of the intrapallidal injection of LPI, CBD, or CID16020046 and its repercussions on the motor behavior of animal models of PD unilaterally induced *via* 6-OHDA lesion.

2 Material and methods

2.1 Animals

Eighty-seven male Wistar rats, weighing 250–300 g at the start of the study, were obtained from the Claude Bernard Vivarium at the Benemérita Universidad Autónoma de Puebla (BUAP or Meritorious Autonomous University of Puebla) and individually housed in groups of five to six with water and food *ad libitum* in a temperature-controlled room (22 ± 2°C) under controlled light conditions (12:12-h light-dark cycle). All the procedures described in the present study were conducted in accordance with the *Guide for Care and Use of Laboratory Animals* of the Mexican Council for Animal Care (Official Mexican Standard NOM-062-ZOO-1999) and were approved by the BUAP's Use of Laboratory Animals and Ethics Committee, under protocol number VIEP.buap/#2122/2017.

2.2 Stereotaxic surgery

2.2.1 Unilateral dopaminergic lesion

The rats were anesthetized, *via* intraperitoneal injection, with a mixture of ketamine (70 mg/kg) and xylazine (10 mg/kg), and placed in a Stoelting stereotaxic apparatus (ITEM: 51,600, Wood

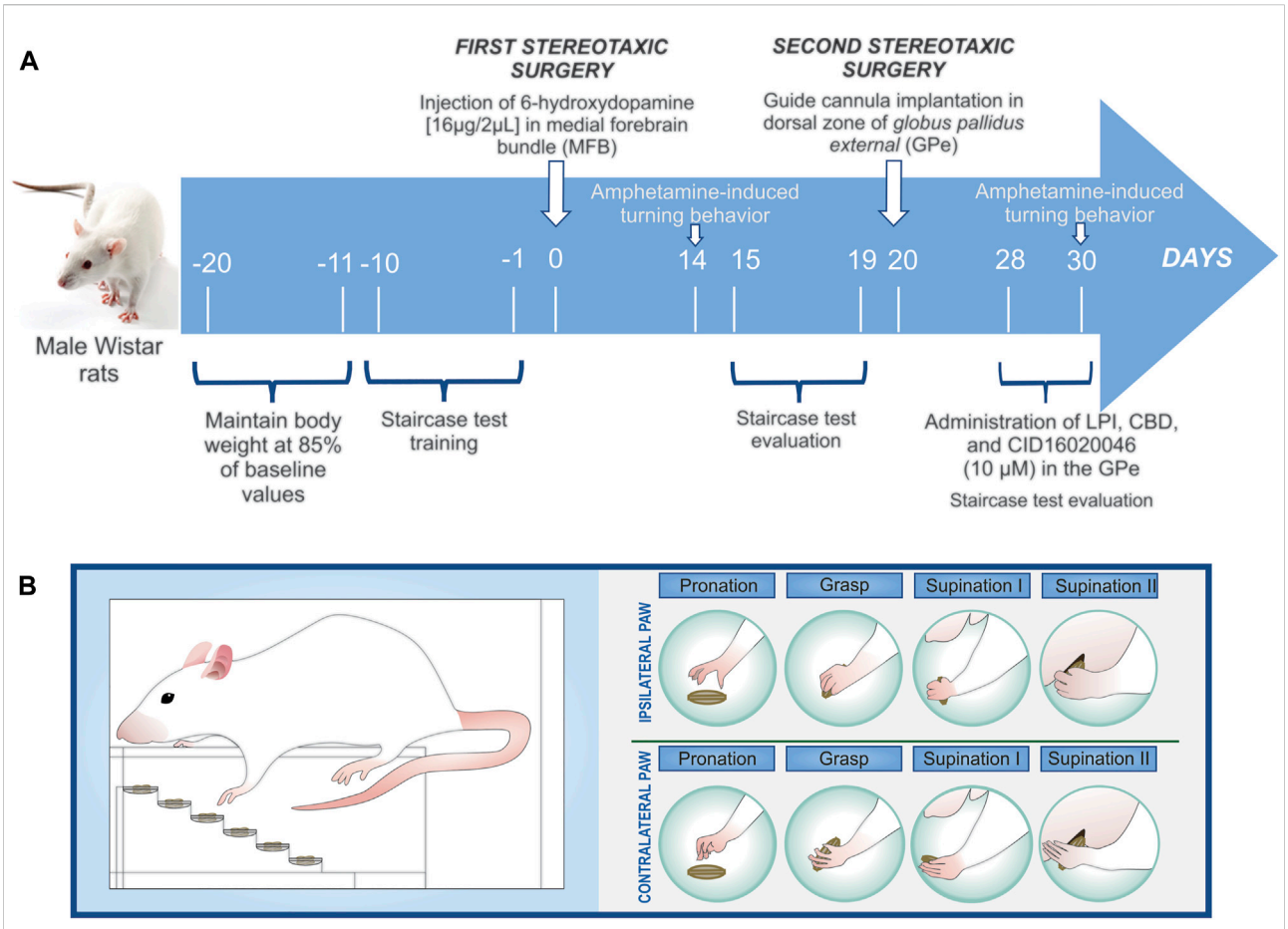

FIGURE 1
(A) Schematic of the experimental design. Day Zero is considered the beginning of the 6-OHDA-induced denervation of the dopaminergic neurons (the first stereotaxic surgery). Amphetamine-induced turning behavior was evaluated twice, on the 14th and 30th days post-lesion. Once the guide cannula had been implanted on the 15th day post-lesion (the second stereotaxic surgery), eight groups were obtained: vehicle + DMSO 0.01%; vehicle + LPI 10 µM; vehicle + CBD 10 µM; vehicle + CID160 10 µM; 6-OHDA + DMSO 0.01%; 6-OHDA + LPI 10 µM; 6-OHDA + CBD 10 µM; and, 6-OHDA + CID160 10 µM. The staircase test training was conducted ten days prior to the first stereotaxic surgery, with the motor alterations presenting in 6-OHDA-induced hemiparkinsonism then evaluated from the 15th to the 19th days post-lesion and the pharmacological effects of the drugs of interest then analyzed from the 28th to 30th days post-lesion. **(B)** The fine motor skills evaluated in the forelimbs ipsilateral and contralateral to lesion were pronation, grasp, supination I, and supination II.

Dale, IL, EE. UU.). The rat's skull was then exposed and trepanned, with a microsyringe then introduced into the medial forebrain bundle (MFB) in order to administer a unilateral injection of 6-hydroxydopamine (6-OHDA) solution (16 µg/2 µL of saline containing 0.1% ascorbic acid), while the control group was administered 2 µL of vehicle without 6-OHDA. The stereotaxic coordinates used were: AP, -2.1 mm from the Bregma; ML, +2.5 mm from the midline; and, DV, -7.4 below the dura (Paxinos and Watson, 1998). Each solution was injected using a 10 µL Hamilton syringe coupled with a motorized injector (Nanomite Syringe Pump, Harvard Apparatus), at an infusion rate of 0.2 µL/min. For this part of the study, all animals were randomly divided into two groups: 6-OHDA (n = 47); and, vehicle (ascorbic acid) (n = 40).

2.2.2 Guide cannula placement

Twenty days after the first surgical procedure (the 6-OHDA lesion administered in the MFB), a second procedure was undertaken to implant a guide cannula in the GPe, ipsilateral to the lesion (Figure 1). The cannula was used to locally administer the LPI [10 µM], CBD [10 µM], and CID16020046 [10 µM]. Once the rat's skull had been exposed in the stereotaxic apparatus, it was trepanned and a 15-mm length of 22-gauge stainless steel tubing was then implanted in the top of the left GPe using the following coordinates: AP, -1.0 mm from the Bregma; ML, +2.9 mm from the midline; and, DV, -4.8 below the dura. Subsequently, the cannula was anchored to the skull with two stainless steel screws and secured with dental acrylic cement, with wire stylets then inserted into the guide

cannula to prevent clogging. For all surgical procedures, postoperative care was applied, with an anti-inflammatory (12.5 mg/kg tramadol, s.c.) and antibiotic (10 mg/kg enrofloxacin, i.m.) administered, both on the day of surgery and the following two days, with the surgical wound checked every day until the animal made a full recovery.

2.3 Drugs

The following drugs were used in the present study: 4-[4,6-Dihydro-4-(3-hydroxyphenyl)-3-(4-methylphenyl)-6-oxopyrrolo [3,4-c] pyrazol-5(1H)-yl]-benzoic acid (CID16020046, Sigma-Aldrich, #SML0805); 6-hydroxydopamine (6-OHDA, Sigma-Aldrich, #H4381); ascorbic acid (Sigma-Aldrich, #A92902); D-Amphetamine (AMPH); dimethyl sulfoxide (DMSO, Sigma-Aldrich, #34869); L-α-lysophosphatidylinositol (LPI, Sigma-Aldrich, #L7635); and, cannabidiol (CBD), kindly provided by the company HempMeds® México.

2.3.1 Drug treatments

The GPR55 agonist LPI [10 μM], the GPR55 inverse agonist CBD [10 μM], the selective GPR55 antagonist CID16020046 [10 μM], and the vehicle dimethyl sulfoxide (DMSO) (0.01%) were injected using a 10 μL microsyringe (Hamilton digital syringe, Harvard Apparatus) and a 30-gauge, 16-mm-long stainless-steel internal cannula inserted into the guide cannula. The drugs were administered, *via* infusion at a volume of 1 μL for five minutes, for three consecutive days, namely the 28th to the 30th day post-6-OHDA-induced injury, in order to study the acute effect of the drugs on the GPe of rats subject freedom of movement. After a further five minutes, the animals were subjected to behavioral tests, which lasted a total of 10 min, thus allowing the drug to be distributed around the GPe.

2.4 Motor behavior tests

2.4.1 Amphetamine-induced turning behavior

The experimental groups participating in the turning behavior test from the 28th day post-lesion onwards were as follows: Vehicle + DMSO 0.01% (n = 6); Vehicle + LPI 10 μM (n = 6); Vehicle + CBD 10 μM (n = 6); 6-OHDA + DMSO 0.01% (n = 6); 6-OHDA + LPI 10 μM (n = 6); and, 6-OHDA + CBD 10 μM (n = 8).

All experimental subjects were evaluated for amphetamine-induced turning behavior, in order to determine the degree of 6-OHDA-induced dopaminergic denervation in the MFB. Fourteen days post-6-OHDA injury or vehicle administration, each rat was administered with amphetamine (AMPH) (5 mg/kg s.c.) and then placed in a plastic box that was 50 cm in diameter and 40 cm long (Ramírez-García et al., 2015). The turning behavior exhibited by all the rats was monitored for up to 100 min and their turns quantified at 10-min intervals. Only those rats that presented 14 turns per minute were selected for the administration of the drugs of interest into the GPe. Subsequently, the intrapallidal administration of 1 μL of LPI [10 μM] and CBD [10 μM] was performed on the 28th, 29th, and 30th days post-dopaminergic injury, ten minutes after which, the AMPH (5 mg/kg s.c.) was administered, to enable the evaluation of turning behavior (Figure 1).

2.4.2 Staircase test

The experimental groups participating in the staircase test from the 28th day post-lesion onwards were as follows: Vehicle + DMSO 0.01% (n = 6); Vehicle + LPI 10 μM (n = 5); Vehicle + CBD 10 μM (n = 5); Vehicle + CID160 10 μM (n = 5); 6-OHDA + DMSO 0.01% (n = 7); 6-OHDA + LPI 10 μM (n = 7); 6-OHDA + CBD 10 μM (n = 7); and, 6-OHDA + CID160 10 μM (n = 7).

2.4.2.1 Apparatus

The staircase test, as proposed by Montoya et al. (1991), was used to measure the reaching and grasping abilities of the rats' independent forelimb. This test can be used to evaluate motor asymmetry, in order to individually determine the grasping performance of both the unaffected (ipsilateral) and impaired (contralateral) paw of the hemiparkinsonian rats (Barnéoud et al., 2000; Klein et al., 2007; Cordeiro et al., 2010; Rattka et al., 2016). The apparatus used was in accordance with that described in previous studies (Mendieta et al., 2009) and consisting of a clear acrylic box (200 mm long, 100 mm wide, and 100 mm high) which channeled the rats to a narrower compartment (170 mm long, 65 mm wide, and 100 mm high) with a central platform running along its length. A removable double staircase comprising six steps of increasing distance from the top of the platform was placed in such a way that in ran from the front of the box into the troughs on both sides.

2.4.2.2 Testing procedure

Two 45-mg pellets (Dustless Precision Pellets, #F0165, Bio-Serv Inc., United States) were placed on each step, which was 3 mm in height (Figure 1B), meaning that 12 pellets were placed on each of the six steps comprising the right and left staircases, giving a total of 24 pellets for both staircases. Measures were taken to control the animals' body weight for the twenty days prior to the first stereotaxic surgery, from which point on and after each training session, the rats were provided a measured and decreasing (from 20 to 14 g) ration of food per day, in order to ensure that they presented 85% of their original weight until the surgery was carried out. Feeding was only resumed, on an *ad libitum* basis, after the surgeries were performed, in order to assist in the post-operative recovery, with the body weight control measures then implemented again six days prior to the procedures conducted on the 15th and 28th days post-injury

to assess motor performance (Figure 1). The animals were familiarized with the pellets by being presented with them on two consecutive days prior to the beginning of training. Ten days prior to the first stereotaxic surgery, each rat was trained in the staircase test, with one trial conducted per day. The rats remained on the staircase for ten minutes, with the total number of pellets eaten then recorded. The objective of the training was to habituate the rats to consuming the pellets placed on the steps of the staircase. The same test was used to evaluate both the hemiparkinsonian rats' motor asymmetry, from the 15th to the 19th day post-injury, and the effect of the drugs administered on motor asymmetry, from the 28th to the 30th day post-injury.

2.4.2.3 Motor asymmetry evaluation

The present study used a modified version of the model reported by Nikkhah et al. (Nikkhah et al., 1998) and Klein et al. (2007) for examining the behavior of rats in the staircase test. After each daily 10-min evaluation period had been completed and the rats' performance in the staircase test had been recorded, the number of pellets eaten, the number of remaining pellets, and the number of dislodged pellets were also recorded, with the latter two parameters described as follows: 1) the number of remaining pellets, refers to those left on the step on which they had originally been placed; and, 2) the number of dislodged pellets refers to those dropped onto other steps or beyond the staircases and into other areas of the box. The first parameter can be more precisely described as follows, along with two more parameters calculated based on the data obtained for the foregoing three parameters: 1) The number of pellets eaten (12 - [number of remaining pellets + number of dislodged pellets]) expresses the ratio of the number of pellets eaten to the total number of pellets placed; 2) The number of pellets taken (12 - number of remaining pellets) is considered to be a good measure of general reaching activity and motivation; and, 3) Grasping success in % ([number of pellets eaten/number of pellets taken] × 100) shows the level of success of all attempts to grasp a pellet. All trials were videotaped with a Sony DCR-SR85 video camera.

2.4.2.4 Fine motor skills evaluation

The hemiparkinsonian rats' grasping ability was qualitatively evaluated in the staircase test, as were their fine motor skills by analyzing the individual components of reaching and grasping patterns observed in high-speed video recordings. The evaluation was scored according to the scale described by Metz and Whishaw (2000), with some modifications. Each reaching movement was divided into four movement components: pronation; grasp; supination I; and, supination II. The four components were subdivided into ten subcomponents, with each subcomponent scored as a normal movement (1 point), an abnormal movement (0.5 points), or no movement (0 points), with a higher score indicating superior reaching movement performance and a lower score indicating inferior performance.

2.5 Histological examination

Thirty days after the administration of the 6-OHDA lesion and on the third day of the intrapallidal administration of the drugs of interest, the rats were euthanized by means of pentobarbital overdose and transcardially perfused with 4% paraformaldehyde in 0.1 M phosphate-buffered saline (PBS, pH 7.4). The brains were post-fixed in the same solution for 24 h. Coronal sections of 50 µm-thickness were cut, using a vibratome (VT1000S, Leica, Germany).

2.5.1 Nissl staining

In order to study the cytoarchitecture of the GPe and verify the correct placement of the cannula, Nissl staining was performed, wherein brain sections were rinsed with 0.1 M PBS, pH 7.4, mounted on gelatinized slides, and stained with a 0.1% cresyl violet solution for 10 min. The sections were rinsed in distilled water and dehydrated with ascending grades of alcohol, cleared with xylene, and coverslipped with Entellan Mounting Medium.

2.5.2 Tyrosine hydroxylase and glutamic acid decarboxylase (GAD-67) immunohistochemistry

Bright-field immunohistochemistry for TH and GAD-67 was carried out on tissue sections taken from the striatum, Gpe and SNpc *via* the application of the previously-described free-floating, protocol (Apóstol Del Rosal et al., 2021; Patricio et al., 2022). The sections were washed three times in PBS-Triton X-100 at 0.2% for 10 min and then treated with 3% hydrogen peroxide (H_2O_2) and 10% methanol to quench endogenous peroxidase activity. Subsequently, the sections were incubated for 1 h in a blocking buffer (IgG-free 2% bovine serum albumin in PBS-Triton X-100 at 0.2%) and incubated for two nights at 4°C with the primary antibody anti-TH (Merck Millipore, #MAB5280, 1:1000) or anti-GAD-67 (Santa Cruz Biothecnology, # SC-390383, 1:50). The sections were rinsed and incubated with biotinylated goat anti-mouse secondary antibody (Vector Laboratories, #BA-9200, 1:200) for two hours, followed by incubation in streptavidin horseradish peroxidase conjugate (Thermo Fisher, #43–4323, 1:500) for 1.5 h at room temperature. Finally, the sections were rinsed in 0.1 M PBS, pH 7.4, and incubated in 0.05% of 3,3-diaminobenzidine (DAB) and 0.03% H_2O_2 to visualize the immunocomplexes. Finally, the tissue sections were mounted onto gelatinized-coated slides, dehydrated in an ascending series of alcohols, cleared in xylene, and coverslipped with Entellan Mounting Medium. Images of the slides were captured using a Leica ICC50 camera with a Leica DM750 optical microscope, which was set at 4 × objective and the same level of contrast and sharpness for each slide, while the images analysis was performed with the ImageJ free software. The color intensities were converted into grayscale in order to graph the percentage of the area that had been stained, while the measurements were

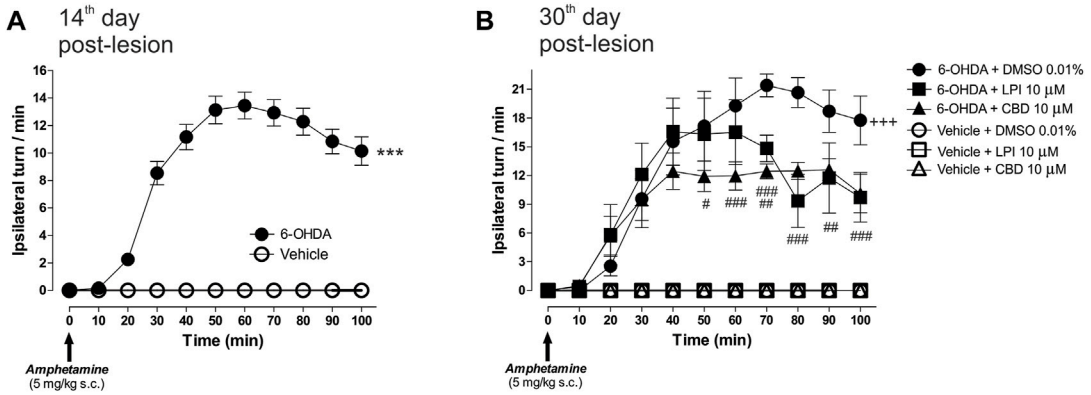

FIGURE 2
The administration of LPI and CBD in the GPe generated lower levels of 6-OHDA-induced motor asymmetry. **(A)** Amphetamine-induced turning behavior (5 mg/kg) was evaluated 14 days after the 6-OHDA injection into the MFB, with all animals placed into two groups–vehicle and 6-OHDA. The 6-OHDA group showed an increase in the number of ipsilateral turns per minute, in contrast to the vehicle group, which did not show any ipsilateral turns. **(B)** Six experimental groups were formed in order to evaluate the amphetamine-induced turning behavior presented by the animals after the intrapallidal administration of 1 µL [LPI 10 µM], [CBD 10 µM], or vehicle (DMSO 0.01%) on the 30th day post-lesion. Lower levels of 6-OHDA-induced motor asymmetry in 6-OHDA + LPI and 6-OHDA + CBD groups, a finding which contrasts with the 6-OHDA + DMSO. Data are represented as the mean ± SEM of ipsilateral turns per minute (10 periods of 10 min). ***$p < 0.001$ *vs.* vehicle; $^{+++}p < 0.001$ *vs.* vehicle + DMSO 0.01%; $^{\#}p < 0.05$, $^{\#\#}p < 0.01$ and $^{\#\#\#}p < 0.001$ *vs.* 6-OHDA + DMSO 0.01%; a two-way ANOVA followed by a Bonferroni *post-hoc* test, (n = 6–8/group).

conducted on four animals per group, with three slices taken per animal.

2.6 Statistical analysis

The data are presented as mean ± standard error of the mean (SEM), wherein the results for amphetamine-induced turning behavior and fine motor skills were analyzed using a two-way analysis of variance (ANOVA) followed by a Bonferroni post-test. The motor asymmetry assessed in the staircase test was analyzed by means of a one-way ANOVA followed by a Tukey post-test. Results $p < 0.05$ were considered statistically significant for both analyses conducted. The software GraphPad Prism version 5.0 (GraphPad Software, La Jolla, CA, United States) was used for all statistical analyses.

3 Results

3.1 Effect of LPI and CBD administration in the external globus pallidus on amphetamine-Induced turning behavior in hemiparkinsonian rats

The amphetamine-induced turning behavior was assessed on the 14th day post-injury, in order to examine the dopaminergic denervation in rats injected with 6-OHDA into the MFB. Figure 2A shows a higher number of ipsilateral turns in the 6-OHDA-lesioned group, with a maximum peak observed at Minute 60 (13.4 ± 0.9 turns/min) and a decrease by Minute 100 (10.1 ± 1.0 ipsilateral turns/min), which corresponds to a significant difference ($p < 0.001$) compared to the vehicle (ascorbic acid) group. Once the cannula had been implanted in the GPe, the rats were subdivided into six groups for the administration of the LPI [10 µM] and CBD [10 µM] on the 28th, 29th, and 30th days post-lesion, with the behavioral evaluation performed again on the 30th day. Figure 2B shows the turning behavior evaluated on the 30th day post-injury and the effect of the intrapallidal injection of both LPI and CBD. A significantly higher number of ipsilateral turns can be observed in the 6-OHDA + DMSO 0.01% group from Minute 30 onwards (9.5 ± 3.0 turns/min), reaching a maximum point at Minute 70 (21.4 ± 1.1 turns/min), and slightly decreasing by Minute 100 (17.7 ± 2.5 ipsilateral turns/min). Both the 6-OHDA + 10 µM LPI group and the 6-OHDA + 10 µM CBD group show an evident decrease in ipsilateral turns at the 70th and 80th minute intervals (14.8 ± 1.3 and 12.4 ± 0.7 ipsilateral turns/min; 9.3 ± 2.7 and 12.4 ± 0.8 ipsilateral turns/min), respectively ($p < 0.01$).

3.2 The administration of LPI in the external globus pallidus does not modify the motor asymmetry of hemiparkinsonian rats evaluated in the staircase test

The hemiparkinsonian model involved the unilateral injection of 6-OHDA into the MFB, thus impairing the BG circuit and inducing motor asymmetry (Taylor et al., 1992;

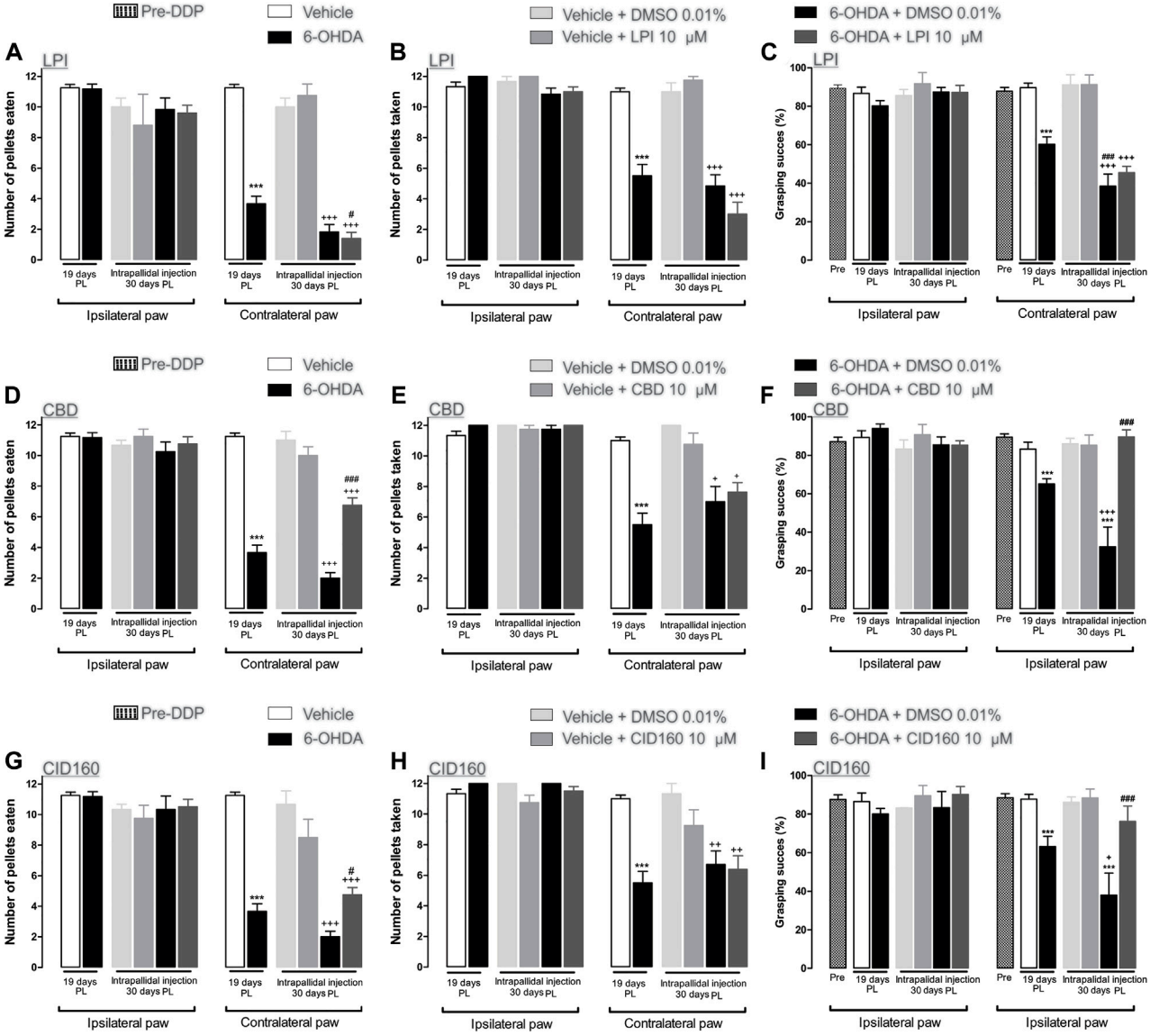

FIGURE 3
The CBD and CID160 administered in the GPe generated superior forelimb performance in the staircase test. The number of pellets eaten, the number of pellets taken, and the percentage of grasping success were recorded on the 19th day post-lesion. The GPR55r agonist LPI (10 µM) **(A–C)**, the inverse agonist CBD (10 µM) **(D–F)**, and the selective antagonist CID160 10 µM **(G–I)** were administered via intrapallidal injection on the 30th day. It is shown that the 6-OHDA + CBD and 6-OHDA + CID160 groups increase the indices of motor performance in contrast with the 6-OHDA + LPI and 6-OHDA + DMSO groups. Data are represented as group mean ± SEM. $^{***}p < 0.001$ *vs.* vehicle; $^{+}p < 0.05$, $^{++}p < 0.01$, $^{+++}p < 0.001$ *vs.* vehicle + DMSO 0.01%; $^{\#}p < 0.05$, $^{\#\#\#}p < 0.001$ *vs.* 6-OHDA + DMSO 0.01%; a one-way ANOVA followed by a Tukey *post-hoc* test, (n = 5–7/group).

Meredith et al., 2008; Glajch et al., 2012). Therefore, GPR55 was activated *via* the injection of the agonist LPI at a dose of [10 µM] *via* the guide cannula. On the 19th day post-lesion, the effect of the dopaminergic lesion on motor behavior was evaluated in the staircase model, with the results obtained showing a motor deficit in the limb contralateral to the lesion in the 6-OHDA group. This deficit is indicated by the number of pellets both eaten (3.6 ± 1.7) and taken (5.5 ± 0.74) and the percentage of grasping success (60.1 ± 3.9), when compared to the corresponding results obtained for the vehicle group (pellets eaten: 11.25 ± 0.21, pellets taken: 11.0 ± 0.23, and percentage of grasping success: 89.3 ± 2.6) ($p < 0.001$). On the 30th day post-lesion, the effect of each pharmacological treatment was evaluated. The 6-OHDA + DMSO and 6-OHDA + LPI groups presented a lower number of pellets eaten (1.8 ± 0.47; 1.4 ± 0.4) (Figure 3A) and taken (4.8 ± 0.73; 3.0 ± 0.77) (Figure 3B) and a lower percentage of grasping success (38.4 ± 6.2; 45.4 ± 3.3) (Figure 3C) than the vehicle + DMSO group (pellets eaten: 10.0 ± 0.57, pellets taken: 11.0 ± 0.57,

percentage of grasping success: 91.1 ± 5.2). It should be noted that a statistically-significant difference was found between the percentage of grasping success observed for the 6-OHDA group on the 19th day post-lesion and that observed on the 30th day post-lesion ($p < 0.001$). Finally, the number of pellets eaten by the 6-OHDA + LPI group presented a statistically-significant difference to the 6-OHDA group on the 19th day post-injury. No significant changes were observed among the ipsilateral paw control groups (Figures 3A–C).

3.3 The administration of CBD and CID16020046 in the external globus pallidus decreases motor asymmetry in hemiparkinsonian rats evaluated in the staircase test

Cannabidiol was used to evaluate motor behavior in the staircase test. On the 19th day post-lesion, the effects of the dopaminergic injury were evaluated in the staircase model. The results obtained showed a motor deficit in the contralateral limb of the 6-OHDA group, as indicated by the lower number of pellets eaten (3.6 ± 0.4) and taken (5.5 ± 0.74) and the lower percentage of grasping success (83.1 ± 3.6) than those observed in the results obtained for the vehicle group (pellets eaten: 11.2 ± 0.75, pellets taken: 11.0 ± 0.70, percentage of grasping success: 89.3 ± 1.7). On the 30th day post-injury, the effect of each pharmacological treatment was evaluated. The 6-OHDA + DMSO groups showed a lower number of number of pellets eaten (2.0 ± 0.36) (Figure 3D) and taken (7.0 ± 1.0) (Figure 3E) and a lower percentage of grasping success (32.4 ± 10.1) (Figure 3F) than those observed for the vehicle + DMSO group (pellets eaten: 11.0 ± 0.57, pellets taken: 12.0 ± 0.01, percentage of grasping success: 86.0 ± 2.8). A statistically-significant difference was observed between the percentage of grasping success for the 6-OHDA group on the 19th day post-lesion and that observed for the 6-OHDA group by the 30th day post-lesion ($p < 0.001$). Unlike the 6-OHDA + DMSO control group, the 6-OHDA + CBD group presented a lower number of pellets eaten (6.7 ± 0.56) (Figure 3D) and taken (7.6 ± 0.62) (Figure 3E) than the vehicle + DMSO group ($p < 0.001$). Finally, the number of pellets eaten by the 6-OHDA + CBD group (6.7 ± 0.47) and the percentage of grasping success (89.5 ± 3.7) observed presented a significant difference to that observed for the 6-OHDA + DMSO group ($p < 0.05$ and $p < 0.001$, respectively) (Figure 3F). No significant changes were observed for the ipsilateral paw control groups.

The selective GPR55 antagonist was used to evaluate motor behavior in the staircase test. Figures 3G–I show the evaluation of the dopaminergic lesion in the staircase test on the 19th day after it was induced. The results obtained show a motor deficit for the contralateral limb of the 6-OHDA group, given that the number of pellets eaten (3.6 ± 1.7) and taken (12 ± 0.7) and the percentage of grasping success (63.1 ± 5.3) were lower than the corresponding results obtained for the vehicle group (pellets eaten: 11.2 ± 0.21, pellets taken: 11.0 ± 0.23, percentage of grasping success: 87.7 ± 2.5) ($p < 0.001$). The pharmacological effect of CID16020046 was evaluated on the 30th day post-lesion. The 6-OHDA + DMSO groups showed a lower number of pellets eaten (2.0 ± 0.36) (Figure 3G) and taken (6.7 ± 0.9) (Figure 3H) and a lower percentage of grasping success (37.9 ± 11.34) (Figure 3I) than the vehicle + DMSO group (pellets eaten: 10.6 ± 0.88, pellets taken: 11.3 ± 0.66, percentage of grasping success: 86.1 ± 2.8). A statistically-significant difference was found for the 6-OHDA group between the percentage of grasping success observed the 19th day post-lesion and that observed on the 30th day post-lesion ($p < 0.001$). Unlike the results observed for the 6-OHDA + DMSO control group, the 6-OHDA + CID16020046 group presented a lower number of pellets eaten (4.7 ± 0.47) (Figure 3G) and taken (6.3 ± 0.89) (Figure 3H) than the vehicle + DMSO group ($p < 0.001$). Finally, the number of pellets eaten by the 6-OHDA + CID16020046 group (4.7 ± 0.47) and the percentage of grasping success (76.1 ± 8.0) for the same group presented a significant difference to the results observed for the 6-OHDA + DMSO group ($p < 0.05$ and $p < 0.001$, respectively) (Figure 3I). No significant changes were observed for the ipsilateral paw control groups.

3.4 The intrapallidal injection of LPI dies not modify the fine motor skills of hemiparkinsonian rats

The performance of all the experimental groups evaluated in the staircase test was videotaped in order to later evaluate the rats' fine motor skills. The video analysis conducted showed significantly lower scores for the pronation, grasp, supination I, and supination II movement components for the 6-OHDA group than those recorded for the control group ($p < 0.001$), as observed from the 15th to 19th day post-injury. After the intrapallidal administration of LPI, it was observed that the 6-OHDA + DMSO groups presented lower pronation scores, on the 28th, 29th, and 30th days post-injury, than the vehicle + DMSO group (0.3 ± 0.04; 0.3 ± 0.06; and, 0.2 ± 0.06, respectively). The 6-OHDA + LPI groups presented the following lower scores for the four movement components than the 6-OHDA + DMSO group ($p < 0.001$) on the 28th, 29th, and 30th days post-injury: pronation (Figure 4A) (0.2 ± 0.07; 0.3 ± 0.05; and, 0.3 ± 0.06, respectively); grasp (Figure 4B) (0.4 ± 0.07; 0.4 ± 0.04; and, 0.3 ± 0.08, respectively); supination I (Figure 4C) (0.1 ± 0.02; 0.2 ± 0.02; and, 0.3 ± 0.04, respectively); and, supination II (Figure 4D) (0.1 ± 0.02; 0.2 ± 0.02; and, 0.3 ± 0.04, respectively). The evaluation of the limb ipsilateral to the injury did not show statistically-significant changes for any of the movements evaluated during the course of the test.

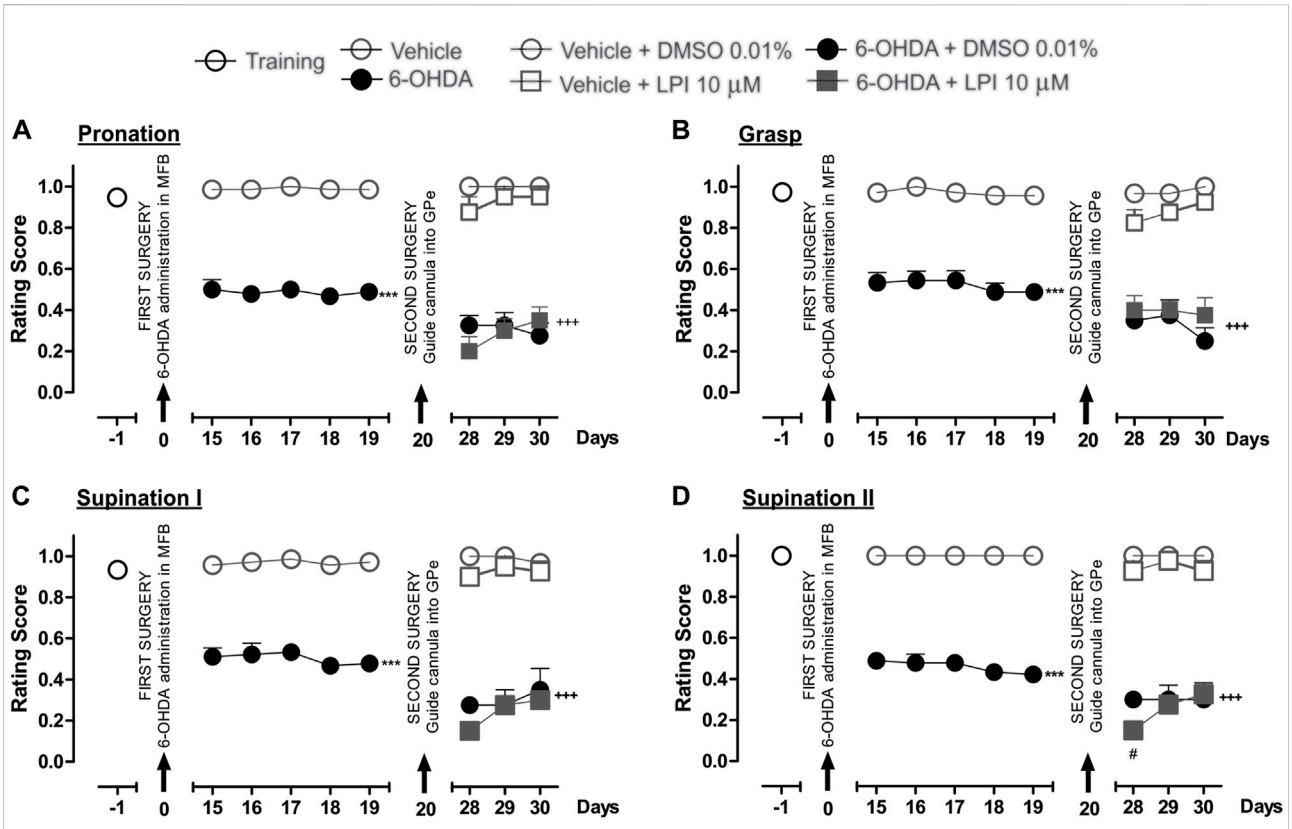

FIGURE 4
The administration of LPI in the GPe did not affect the fine motor skills of the hemiparkinsonian rats evaluated in the staircase test. The four movement components selected to evaluate the contralateral forelimb performance for fine motor skills were as follows: **(A)** Pronation; **(B)** Grasp; **(C)** Supination I; and, **(D)** Supination II. The effect of the intrapallidal administration of LPI (10 µM) on the movement components was evaluated one day prior to the first stereotaxic surgery (from the 15th to the 19th days post-lesion) and from the 28th to the 30th days post-lesion. It is shown that the 6-OHDA + LPI group performed worse in terms of fine motor skills than the control groups. Data are represented as the mean ± SEM of the fine motor skills scores obtained. ***$p < 0.001$ *vs.* vehicle; $^{+++}p < 0.001$ *vs.* vehicle + DMSO 0.01%; $^{\#}p < 0.05$ *vs.* 6-OHDA + DMSO 0.01%; a two-way ANOVA followed by a Bonferroni *post-hoc* test, (n = 5–7/group).

3.5 The administration of CBD and CID16020046 in the external globus pallidus improves the fine motor skills of hemiparkinsonian rats

Figure 5 shows the effect of the intrapallidal injection of CBD on 6-OHDA-induced impaired fine motor skills. The hemiparkinsonian model showed significantly lower scores for the pronation, grasp, supination I, and supination II movement components for the 6-OHDA group than those observed for the control group ($p < 0.001$), from the 15th to the 19th day post-injury. After the intrapallidal administration of LPI, it was observed that the 6-OHDA + DMSO group presented lower scores than the vehicle + DMSO group for the 28th, 29th, and 30th days post-injury, for the following movement components: pronation (0.3 ± 0.04; 0.3 ± 0.06; and, 0.2 ± 0.05, respectively); grasp (0.3 ± 0.04; 0.2 ± 0.07; and, 0.2 ± 0.06, respectively); supination I (0.2 ± 0.02; 0.2 ± 0.07; and, 0.3 ± 0.1, respectively); and, supination II (0.3 ± 0.03; 0.3 ± 0.07; and, 0.3 ± 0.8, respectively). The 6-OHDA + CBD groups presented the following lower scores for the four fine movement components than the 6-OHDA + DMSO group ($p < 0.001$), for the 28th, 29th, and 30th days post-injury: pronation (Figure 5A) (0.6 ± 0.02; 0.7 ± 0.04; and, 0.6 ± 0.05, respectively); grasp (Figure 5B) (0.6 ± 0.04; 0.6 ± 0.02; and, 0.7 ± 0.06, respectively); supination I (Figure 5C) (0.6 ± 0.02; 0.6 ± 0.04; and, 0.7 ± 0.06, respectively); and, supination II (Figure 5D) (0.6 ± 0.06; 0.7 ± 0.07; and, 0.7 ± 0.04, respectively). The evaluation of the limb ipsilateral to the injury did not show statistically-significant changes for any of the movements evaluated during the course of the test.

Finally, Figure 6 shows the effect of the intrapallidal injection of CID16020046 on 6-OHDA-induced impaired fine motor skills. The hemiparkinsonian model showed significantly lower scores for the pronation, grasp, supination I, and supination II movement components for the 6-OHDA group than those observed for the control group ($p < 0.001$), from the 15th to the 19th day post-injury. After the intrapallidal administration of

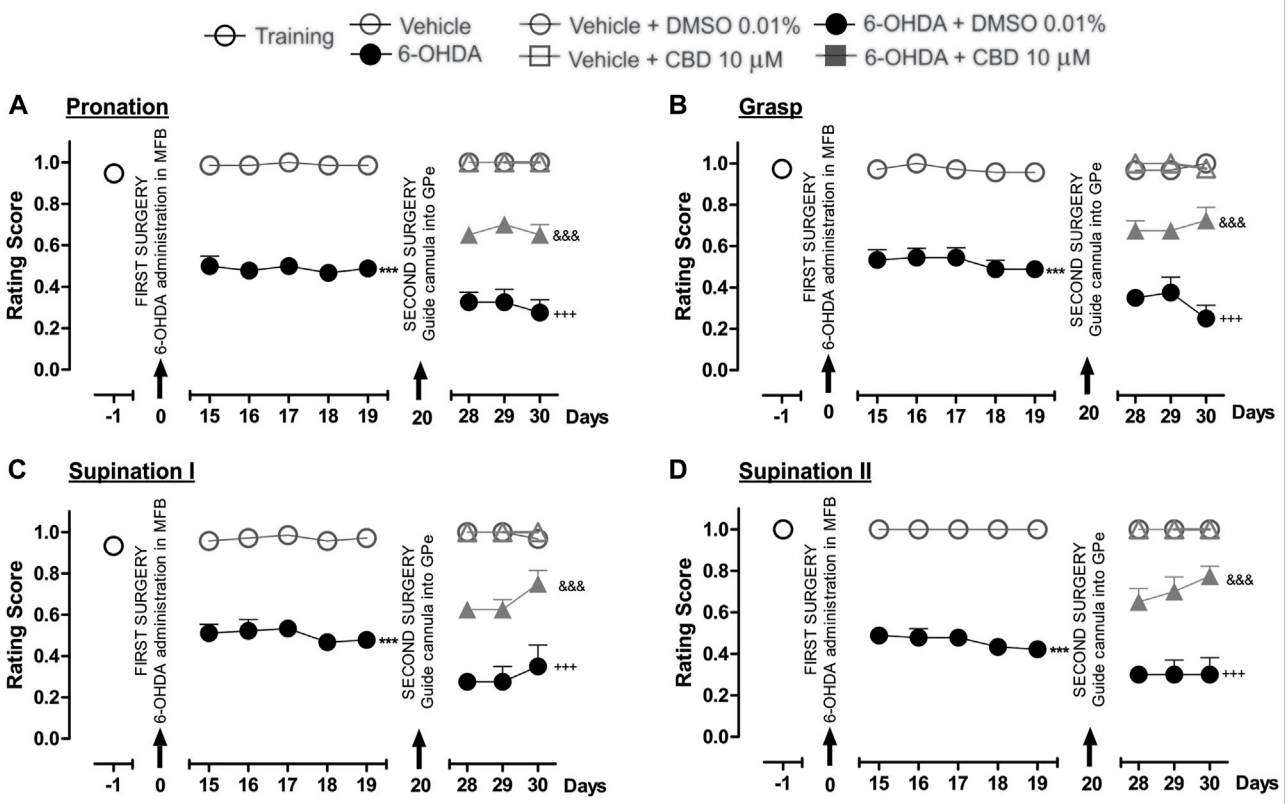

FIGURE 5
The administration of CBD in the GPe generated superior fine motor skills performance in the hemiparkinsonian rats analyzed in the staircase test. The four movement components selected to evaluate the contralateral forelimb performance for fine motor skills were as follows: **(A)** Pronation; **(B)** Grasp; **(C)** Supination I; and, **(D)** Supination II. The effect of the intrapallidal administration of CBD (10 μM) on the movement components were evaluated one day prior to the first stereotaxic surgery (from the 15th to the 19th days post-lesion) and from the 28th to the 30th days post-lesion. It is shown that 6-OHDA + CBD group performed better in terms of fine motor skills than the 6-OHDA + DMSO group. Data are represented as the mean ± SEM of the fine motors skills scores obtained. $^{***}p < 0.001$ *vs.* vehicle; $^{+++}p < 0.001$ *vs.* vehicle + DMSO 0.01%; $^{\&\&\&}p < 0.001$ *vs.* 6-OHDA + DMSO 0.01%; a two-way ANOVA followed by a Bonferroni *post-hoc* test (n = 5–7/group).

CID16020046, it was observed that the 6-OHDA + DMSO groups presented lower scores for the 28th, 29th, and 30th days post-injury than the vehicle + DMSO group for the following movement components: pronation (0.3 ± 0.04; 0.3 ± 0.04; and, 0.2 ± 0.06, respectively); grasp (0.3 ± 0.02; 0.3 ± 0.05; and, 0.2 ± 0.06, respectively); supination I (0.2 ± 0.02; 0.2 ± 0.07; and, 0.2 ± 0.06, respectively); and, supination II (0.3 ± 0.04; 0.2 ± 0.04; and, 0.2 ± 0.04, respectively). The 6-OHDA + CID16020046 groups presented lower scores for the following four fine movement components than the 6-OHDA + DMSO group ($p < 0.001$) for the 28th, 29th, and 30th days post-injury: pronation (Figure 6A) (0.4 ± 0.06; 0.4 ± 0.06; and, 0.5 ± 0.02, respectively); grasp (Figure 6B) (0.5 ± 0.02; 0.6 ± 0.04; and, 0.5 ± 0.04, respectively); supination I (Figure 6C) (0.6 ± 0.02; 0.6 ± 0.04; and, 0.5 ± 0.04, respectively); and, supination II (Figure 6D) (0.6 ± 0.06; 0.6 ± 0.06; and, 0.7 ± 0.07, respectively). The evaluation of the limb ipsilateral to the injury did not show statistically significant changes for any of the movement components evaluated during the course of the test.

3.6 The administration of LPI, CBD, and CID16020046 does not modify the expression of tyrosine hydroxylase in the striatum and substantia nigra pars compacta or the cell morphology in the external globus pallidus of hemiparkinsonian rats

In order to corroborate the success of the 6-OHDA-induced dopaminergic injury, TH immunoreactivity was performed in both the striatum and the SNpc (Figure 7). The graphs presented in Figures 7B,C show that the 6-OHDA + DMSO group presented a lower percentage area in the striatum stained for the TH enzyme (11.6 ± 2.6 percentage stained area) and a lower number of TH positive cells in the SNpc (13.2 ± 5.0 number of TH positive cells) (Figure 7C) than the control group (72.6 ± 5.0 percentage stained area) (167.6 ± 12.1 number of TH positive cells), with a significance of $p < 0.001$. No significant differences were found among the 6-OHDA + LPI, 6-OHDA + CBD, 6-OHDA + CID16020046 experimental

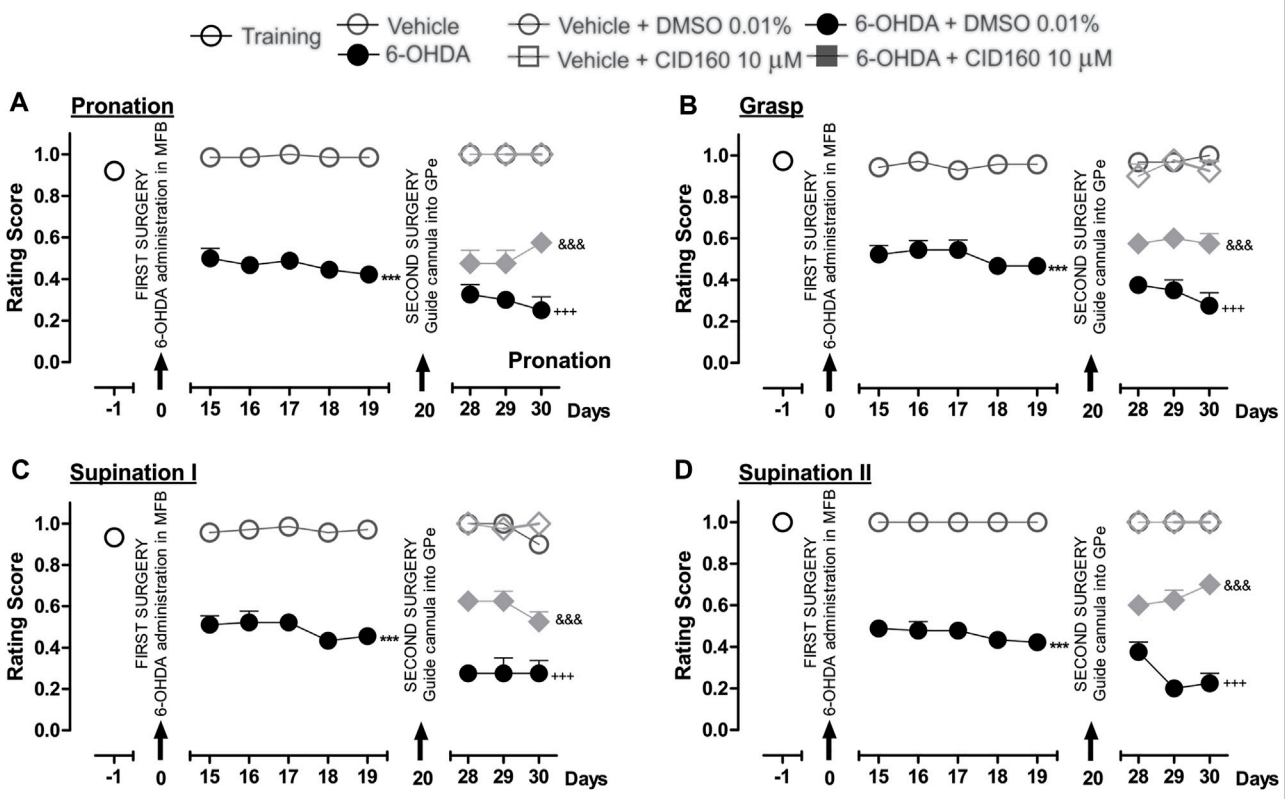

FIGURE 6
The administration of CID16020046 in the GPe generated superior fine motor skills performance in the hemiparkinsonian rats analyzed in the staircase test. The four movement components selected to evaluate the contralateral forelimb performance for fine motor skills were as follows: **(A)** Pronation; **(B)** Grasp; **(C)** Supination I; and, **(D)** Supination II. The effect of the intrapallidal administration of CID160 (10 µM) on the movement components were evaluated one day prior to the first stereotaxic surgery (from the 15th to the 19th days post-lesion) and from the 28th to the 30th days post-lesion. It is shown that 6-OHDA + CID160 group performed better in terms of fine motor skills than the 6-OHDA + DMSO group. Data are represented as the mean ± SEM of the fine motor skills scores obtained. $^{***}p < 0.001$ *vs.* vehicle; $^{+++}p < 0.001$ *vs.* vehicle + DMSO 0.01%; $^{\&\&\&}p < 0.001$ *vs.* 6-OHDA + DMSO 0.01%; a two-way ANOVA followed by a Bonferroni *post-hoc* test (n = 5–7/group).

groups for both the percentage area in the striatum stained for the TH enzyme (15.3 ± 2.4; 14.7 ± 1.4; 13.5 ± 2.8, respectively) and the number of TH positive cells in the SNpc (16.2 ± 6.0; 14.4 ± 5.4; 13.2 ± 4.7, respectively). The foregoing findings similarity with the results obtained for the 6-OHDA + DMSO group. Nissl staining was undertaken to reveal the cytoarchitecture and verify the correct placement of the cannula in the nucleus of the GPe. Figure 8 shows the placement of the cannula in the dorsal area of the GPe.

3.7 The intrapallidal injection of CBD or CID16020046 decreases GAD67 expression in the external globus pallidus and striatum of hemiparkinsonian rats

In order to explore the effect of the intrapallidal administration of LPI, CBD, or CID16020046 on 6-OHDA-induced alterations of GAD-67 expression, GAD-67 immunoreactivity in the GPe, striatum, and SNpr was measured (Figure 9A). The results obtained show that GAD-67 expression, in the striatum ipsilateral to the lesion (presented in Figure 9B) and the ipsilateral GPe, (presented in Figure 9C), increased significantly ($p < 0.01$ and $p < 0.001$, respectively) for the 6-OHDA + DMSO group (82.3 ± 2.9, 57.3 ± 1.7 percentage stained area) compared to the control group (69.2 ± 2.7, 42.8 ± 1.4 percentage stained area). Moreover, a lower level of GAD-67 immunoreactivity was observed for the groups treated with 6-OHDA + CBD and 6-OHDA + CID16020046 in the striatum (67.6 ± 2.2, 68.7 ± 3.3 percentage stained area) and GPe (37.7 ± 3.3, 42.7 ± 2.5 percentage stained area), with a significance of $p < 0.01$ and $p < 0.001$, respectively. The 6-OHDA + LPI group did not show differences to the 6-OHDA + DMSO group, in both the striatum (75.9 ± 2.3 percentage stained area) and GPe (51.8 ± 2.0 percentage stained area).

The GAD-67 expression observed in the SNpr was higher for the 6-OHDA + DMSO group (37.1 ± 1.7 percentage stained area) than the control group (26.8 ± 2.1 percentage stained

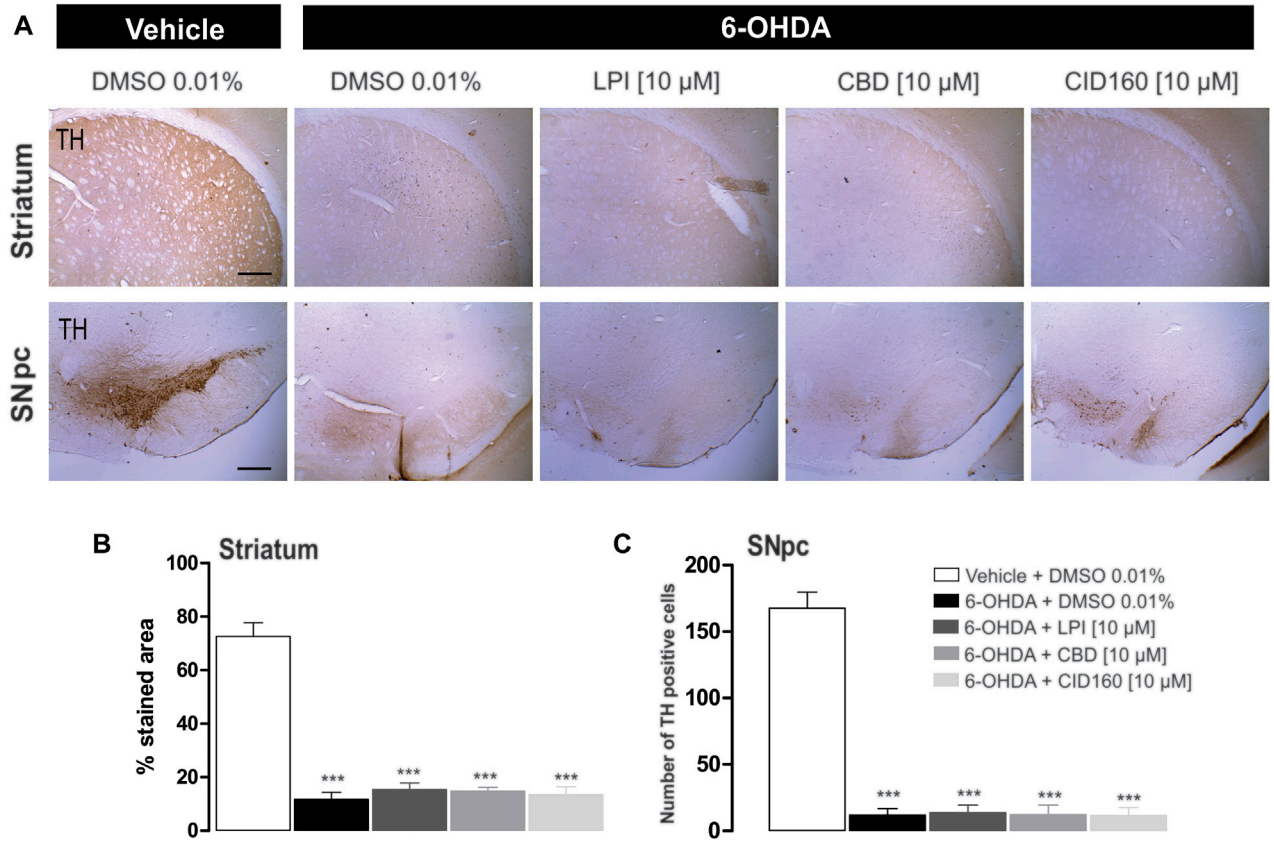

FIGURE 7
The administration of LPI, CBD, and CID16020046 does not modify the expression of TH in the striatum and SNpc. The photomicrography in **(A)** shows the representative images for TH expression in the striatum ipsilateral to the 6-OHDA lesion induced in the MFB. Photomicrographs were taken at 40x, while the scale bar represents 500 μm. Graph **(B)** shows the proportion of the area stained for TH in the striatum and Graph **(C)** shows the number of TH-positive cells in the SNpc. All groups show decreased immunoreactivity to the TH enzyme. The values show mean ± SEM (*n* = 4 per group). The statistics were determined *via* a one-way ANOVA and a Tukey *post-hoc* test. ***$p < 0.001$ *vs.* vehicle group.

area) (Figure 9D). No differences were observed among the 6-OHDA + LPI, 6-OHDA + CBD, 6-OHDA + CID16020046 experimental groups for the percentage area stained for the GAD-67 enzyme in the SNpr (33.5 ± 1.3; 27.4 ± 2.9; 30.0 ± 2.8, respectively), findings which contrast with the 6-OHDA + DMSO group.

4 Discussion

The present study evaluated the effect, on motor asymmetry and fine motor skills, of the intrapallidal administration of LPI, CBD, and CID16020046, which acted as an agonist, inverse agonist, and selective antagonist of GPR55, respectively, in a 6-OHDA-induced hemiparkinsonian model. Motor asymmetry was evaluated in amphetamine-induced turning behavior, while fine motor skills were evaluated in the staircase test. Immunoreactivity to the TH and GAD-67 enzymes in the nuclei of the striatum, GPe, and SNpc ipsilateral to the 6-OHDA-induced injury was also evaluated.

The results obtained show that the intrapallidal administration of LPI [10 μM] in hemiparkinsonian rats caused motor deficits in the staircase test and a deficit in fine motor skills, while a lower level of amphetamine-induced turning behavior was also observed (Figure 2B). The latter finding is of particular interest due to reported alterations in the BG circuit in parkinsonian states, especially those that presented increased GABAergic activity in the GPe (Galvan and Wichmann, 2008). Said reports show the expression of GPR55 mRNA in the BG (mainly in the GPe), the subthalamic nucleus (STN), and the striatum (Henstridge et al., 2011; Celorrio et al., 2017), proposing that the receptor plays an important role in GABA release. Therefore, the agonism of GPR55 to LPI would increase the release of GABA, as has been observed with other agonists such as palmitoylethanolamine (Musella et al., 2017). It is likely that the effects observed in terms of a lower incidence of turning

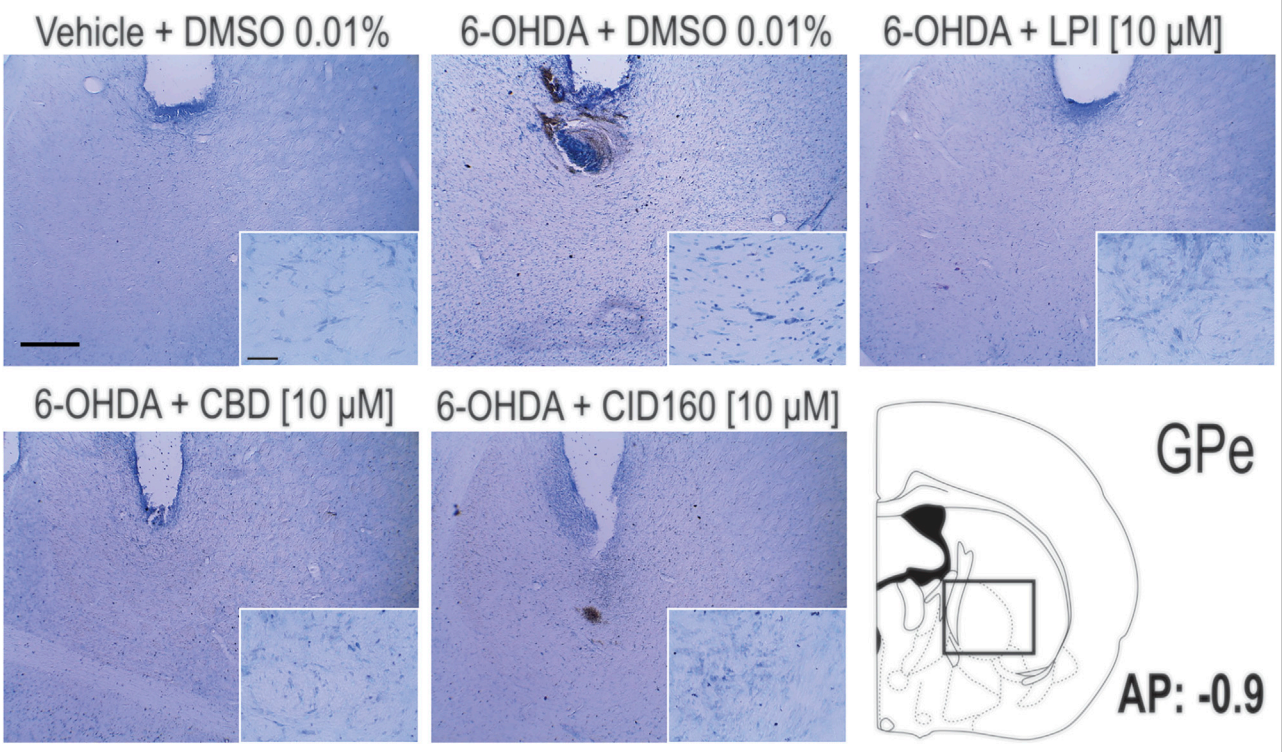

FIGURE 8
Pallidal cell morphology and verification of the correct placement of the cannula in the nucleus of the GPe. The photomicrographs show the images obtained *via* the Nissl staining of the GPe and the placement of the cannula in the dorsal area of the GPe. Photomicrographs were taken at 4x and 40x and the scale bar represents 500 and 50 μm, respectively.

behavior due to the intrapallidal administration of LPI are attributed to the activation of GPR55 in the afferents of other neuronal populations, such as the STN (Celorrio et al., 2017), which can be attributed to the findings reported for the nerve impulses received by the GPe from the striatum, STN, and SNpc (Eid and Parent, 2016). Furthermore, it has been shown that the STN presents efferents to the GPe (Kita and Kitai, 1987) and that the modulation occurring in both nuclei is strongly correlated in parkinsonian models (Kovaleski et al., 2020). The dopaminergic system does affect the GPe through the activation of the D1 receptor in the presynapse of the STN and the consequent release of glutamate (Hernández et al., 2007). Therefore, both the intrapallidal administration of LPI and the subcutaneous administration of amphetamine in hemiparkinsonian rats could modulate the GABAergic tone of the GPe as a function of the time period for which turning behavior is evaluated.

The intrapallidal administration of CBD [10 μM] conducted in the present study showed a more consistent and beneficial effect in terms of decreasing turning behavior in hemiparkinsonian rats. Cannabidiol is known to have different molecular targets, such as the CB1 receptor, the CB2 receptor, the fatty acid amide hydrolase (FAAH), the PPARγ receptor, the A2A receptor, the 5-HT1A receptor, and GPR55 (Peres et al., 2018). The effect of CBD as an inverse agonist of GPR55 has been widely accepted, as has its probable neuromodulatory role (Patricio et al., 2020). The negative effects of CBD on GPR55 in terms of glutamatergic, adenosinergic, and dopaminergic neurotransmission have been demonstrated *in vitro* (Ryberg et al., 2007; Sharir and Abood, 2010; Pandolfo et al., 2011). Therefore, the effect, as observed in the present study, exerted by CBD in reducing amphetamine-induced turning behavior should not only be interpreted in terms of its interaction with GPR55. In addition, the expression and activity of the A2A (Diao et al., 2017), 5-HT (Parent et al., 2011), and CB1 receptors have been demonstrated in the GPe (Chaves-Kirsten et al., 2013).

The evaluation of motor asymmetry in the staircase model was performed in the present study using the following parameters: number of pellets eaten; number of pellets taken; and, the percentage of grasping success. The staircase model enables the grasp capacity of the limb contralateral to the injury to be analyzed. Therefore, the results can be interpreted in terms of these three parameters: 1) The motivation and action required to attain a goal (number of pellets taken); 2) The ability to reach and grasp (number of pellets eaten); and, 3) The success of the attempts to grasp a pellet (grasping success percentage) (Klein et al., 2007). It was observed that the injection of LPI into the GPe of hemiparkinsonian rats

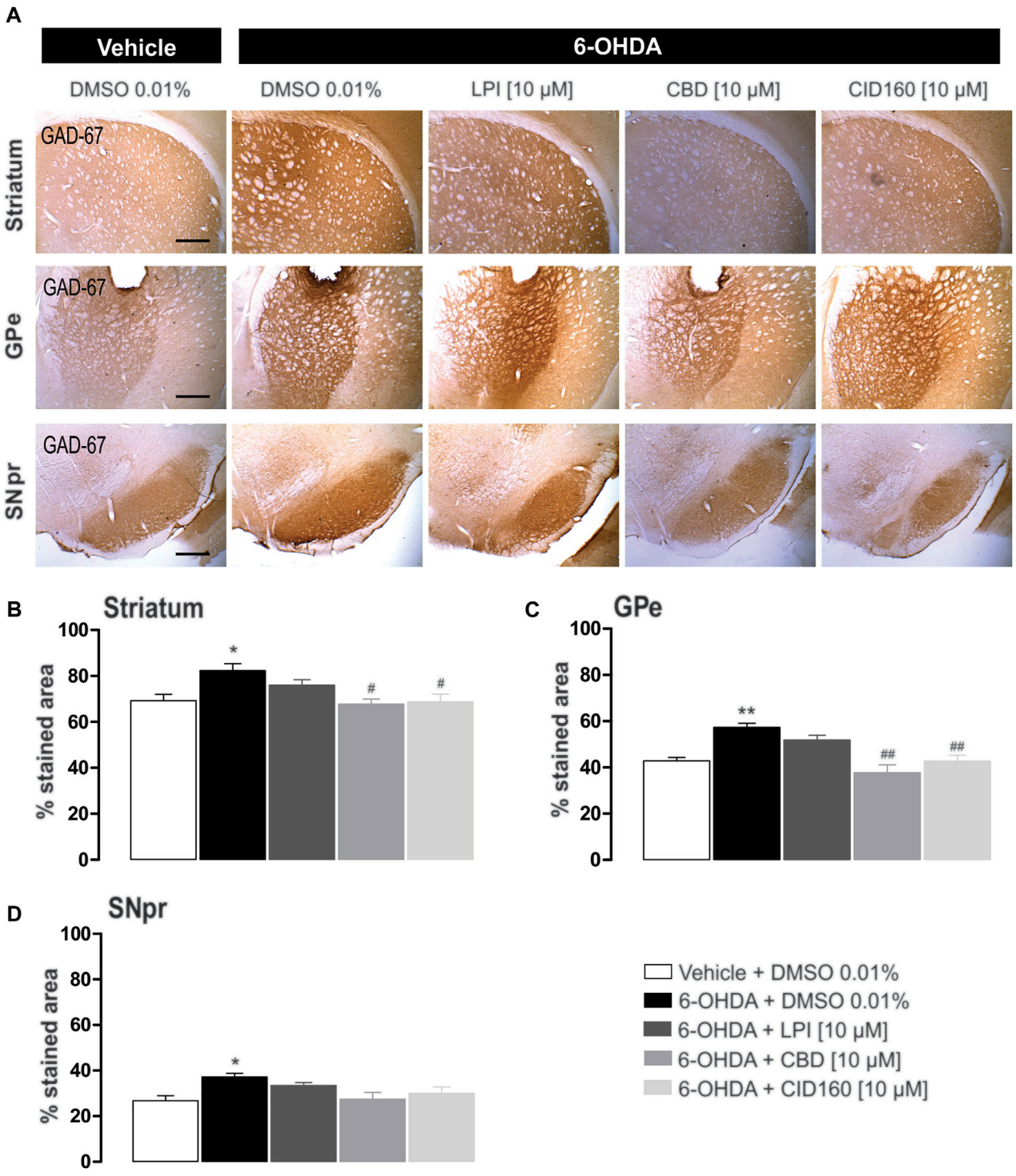

FIGURE 9
The intrapallidal injection of CBD or CID16020046 decreases the immunoreactivity of GAD-67 in the GPe and striatum of rats with 6-OHDA-induced injury. **(A)** shows the immunoreactivity of GAD-67 in the striatum, GPe, and SNpr. Photomicrographs were taken at 40x, while the scale bar represents 500 μm. Graph **(B)** shows the proportion of the area stained for TH in the striatum, while **(C,D)** show the percentage area stained for TH in the GPe and SNpr, respectively. The results obtained show that GAD-67 expression increased in the ipsilateral striatum, GPe, and SNpr of the 6-OHDA + DMSO group in contrast with the control group. However, a decreased level of GAD-67 immunoreactivity was only observed in the nuclei of the striatum and GPe ipsilateral to the lesion in 6-OHDA + CBD and 6-OHDA + CID160 groups. The values show mean ± SEM (n = 4 per group). Statistics were determined with a one-way ANOVA and a Tukey *post-hoc* test. *$p < 0.05$, **$p < 0.01$ *vs*. vehicle group. $^{\#}p < 0.05$, $^{\#\#}p < 0.01$ *vs*. 6-OHDA + DMSO group.

caused a motor deficit in the limb contralateral to the injury, as observed in the staircase test (Figure 3), while motivation, grasping ability, and grasping success decreased. This finding is contrary to that observed in the tests conducted on turning behavior, due to the way in which the agonism of GPR55 to LPI in the GPe decreased the number of turns ipsilalateral to the lesion, a difference in behavior that is likely due to the dopamine released with the administration of amphetamine. The present study has also shown that the lower scores for fine motor skills presented by the groups injured with 6-OHDA and those in receipt of the intrapallidal administration of LPI on the 28th, 29th, and 30th days post-lesion (Figures 5, 6) are likely due to the low concentrations of bioavailable dopamine in the nigrostriatal and nigropallidal pathways (Rajput et al., 2008). Therefore, the absence of dopamine would cause a decrease in D2 receptor signaling and would also lead to an increase in striatopallidal and nigropallidal GABAergic tone. This absence could lead to the neuronal repolarization of the pallidosubthalamic pathway and may be translated into the over activation of glutamatergic neurons moving towards the BG output nuclei, thus promoting hypokinesia (Galvan and Wichmann, 2008; Lanciego et al., 2012).

The GPR55 receptor can activate the ROCK and/or PLC signaling pathway and induce the intracellular release of Ca^{2+} in the GABAergic neurons of the GPe. As this mechanism has only been reported in the hippocampal (Sylantyev et al., 2013) and dorsal root ganglia neurons (Lauckner et al., 2008), it is proposed that it also occurs in the hippocampal GABAergic neurons *via* the activation of GPR55 (Musella et al., 2017). The consequent release of intracellular Ca^{2+} in GABAergic neurons would trigger neuronal depolarization, which could result in an inhibition of GABA release and a decrease in hypokinesia. Our findings at the pharmacological level suggest that the activation of GPR55 in the GPe does not generate a change in the motor deficit observed in hemiparkinsonian rats, with both an increase in motor asymmetry and a decrease in fine motor skills observed. It is probable that this process is related to increased levels of GABA in the striatopallidal pathway (Galvan et al., 2005) which, acting alongside the antagonism, may reverse the overactivation. Thus, it is proposed that the indirect pathway of the GB circuit participates in the inhibition of movements corresponding to fine motor skills.

The intrapallidal injection of both CBD and CID16020046 led to a reduction in the motor asymmetry of hemiparkinsonian rats and an improvement in the fine motor skills of the contralateral limb, in contrast to the results obtained for the 6-OHDA + DMSO group. Interestingly, while there were no differences in the number of pellets taken, a parameter related to general reaching activity and motivation, the number of pellets eaten did increase, as did the grasping success percentage, which is a parameter related to the balance between motivation and grasping ability. These data provide evidence to support the proposal that GPR55 antagonism improves grip quality in hemiparkinsonian rats and may be related to neurotransmitter release (Marichal-Cancino et al., 2017). The results obtained reveal that CBD increased the grasping success percentage to a similar degree to that observed for the control groups. This finding may implicate the modulatory mechanism of CBD, as, after 30 days of 6-OHDA-induced injury, a higher percentage of dopaminergic neurons in the nigrostriatal pathway have degenerated and the neuroprotective role of CBD has been reduced to nil (García-Arencibia et al., 2007). The findings of the present study regarding motor asymmetry and fine motor skills provide evidence of the probable effect exerted on fine motor skills by GPR55 in the GPe of hemiparkinsonian rats.

5 Conclusion

In conclusion, these results provide findings pointing to the possible role played by CBD in the GPe of hemiparkinsonian rats, in terms of both gross and fine motor skills. Moreover, the effect on motor behavior of the selective GPR55 antagonist CID16020046 is similar to that obtained *via* CBD, thus opening new perspectives for explaining, at a cellular level, the role played by GPR55 in the GABAergic system and the reversal of the motor impairment observed in PD models.

Data availability statement

The original contributions presented in the study are included in the article/Supplementary Material, further inquiries can be directed to the corresponding author.

Ethics statement

The animal study was reviewed and approved by Use of Laboratory Animals and Ethics Committee of Benemérita Universidad Autónoma de Puebla.

Author contributions

FP, AP-M, and IDL designed the experiments, generated the statistics, interpreted the data, and wrote the first draft of the manuscript. FP, EMD, and NA carried out the surgical procedures and behavioral motor tests. FP, EMD, AP-M, IM, JA, JP-A, and IDL contributed to the scientific discussion and critically reviewed the content. All authors approved the final version of the manuscript.

Funding

This study was supported by the 2021–2022 grants awarded by the BUAP Vicerrectoría de Investigación y Estudios de Posgrado (Vice-rectory for Research and Postgraduate Studies) to I.D. Limón. F. Patricio was

awarded support *via* CONACYT-Mexico grant 732793. E. Morales Dávila was awarded support *via* CONACYT-Mexico grant 758730.

Acknowledgments

Thanks to Benjamin Stewart (native English speaker and academic proofreader) for editing the English language text.

Conflict of interest

The authors declare that the research was conducted in the absence of any commercial or financial relationships that could be construed as a potential conflict of interest.

Publisher's note

All claims expressed in this article are solely those of the authors and do not necessarily represent those of their affiliated organizations, or those of the publisher, the editors and the reviewers. Any product that may be evaluated in this article, or claim that may be made by its manufacturer, is not guaranteed or endorsed by the publisher.

Supplementary Material

The Supplementary Material for this article can be found online at: https://www.frontiersin.org/articles/10.3389/fphar.2022.945836/full#supplementary-material

References

Abedi, P. M., Delaville, C., De Deurwaerdère, P., Benjelloun, W., and Benazzouz, A. (2013). Intrapallidal administration of 6-hydroxydopamine mimics in large part the electrophysiological and behavioral consequences of major dopamine depletion in the rat. *Neuroscience* 236, 289–297. doi:10.1016/j.neuroscience.2013.01.043

Albin, R. L., Young, A. B., and Penney, J. B. (1989). The functional anatomy of basal ganglia disorders. *Trends Neurosci.* 12 (10), 366–375. doi:10.1016/0166-2236(89)90074-x

Alhouayek, M., Masquelier, J., and Muccioli, G. G. (2018). Lysophosphatidylinositols, from cell membrane constituents to GPR55 ligands. *Trends Pharmacol. Sci.* 39 (6), 586–604. doi:10.1016/j.tips.2018.02.011

Anavi-Goffer, S., Baillie, G., Irving, A. J., Gertsch, J., Greig, I. R., Pertwee, R. G., et al. (2012). Modulation of L-α-lysophosphatidylinositol/GPR55 mitogen-activated protein kinase (MAPK) signaling by cannabinoids. *J. Biol. Chem.* 287 (1), 91–104. doi:10.1074/jbc.M111.296020

Apóstol del Rosal, G. D., Limón, I. D., Martínez, I., and Patricio-Martínez, A. (2021). The chronic oral administration of clobenzorex or amphetamine decreases motor behavior and induces glial activation in the striatum without dopaminergic degeneration. *Neurotox. Res.* 39 (5), 1405–1417. doi:10.1007/s12640-021-00395-1

Barnéoud, P., Descombris, E., Aubin, N., and Abrous, D. N. (2000). Evaluation of simple and complex sensorimotor behaviours in rats with a partial lesion of the dopaminergic nigrostriatal system. *Eur. J. Neurosci.* 12 (1), 322–336. doi:10.1046/j.1460-9568.2000.00896.x

Benazzouz, A., Mamad, O., Abedi, P., Bouali-Benazzouz, R., and Chetrit, J. (2014). Involvement of dopamine loss in extrastriatal basal ganglia nuclei in the pathophysiology of Parkinson's disease. *Front. Aging Neurosci.* 6, 87. doi:10.3389/fnagi.2014.00087

Berardelli, A., Rothwell, J. C., Thompson, P. D., and Hallett, M. (2001). Pathophysiology of bradykinesia in Parkinson's disease. *Brain* 124 (11), 2131–2146. doi:10.1093/brain/124.11.2131

Brown, A. J., Castellano-Pellicena, I., Haslam, C. P., Nichols, P. L., and Dowell, S. J. (2018). Structure-activity relationship of the GPR55 antagonist, CID16020046. *Pharmacology* 102 (5-6), 324–331. doi:10.1159/000493490

Burgaz, S., García, C., Gonzalo-Consuegra, C., Gómez-Almería, M., Ruiz-Pino, F., Unciti, J. D., et al. (2021). Preclinical investigation in neuroprotective effects of the GPR55 ligand VCE-006.1 in experimental models of Parkinson's disease and amyotrophic lateral sclerosis. *Molecules* 26 (24), 7643. doi:10.3390/molecules26247643

Campos, A. C., Fogaça, M. V., Scarante, F. F., Joca, S. R. L., Sales, A. J., Gomes, F. V., et al. (2017). Plastic and neuroprotective mechanisms involved in the therapeutic effects of cannabidiol in psychiatric disorders. *Front. Pharmacol.* 8, 269. doi:10.3389/fphar.2017.00269

Celorrio, M., Rojo-Bustamante, E., Fernández-Suárez, D., Sáez, E., Estella-Hermoso de Mendoza, A., Müller, C. E., et al. (2017). GPR55: A therapeutic target for Parkinson's disease? *Neuropharmacology* 125, 319–332. doi:10.1016/j.neuropharm.2017.08.017

Chaves-Kirsten, G. P., Mazucanti, C. H., Real, C. C., Souza, B. M., Britto, L. R., and Torrão, A. S. (2013). Temporal changes of CB1 cannabinoid receptor in the basal ganglia as a possible structure-specific plasticity process in 6-OHDA lesioned rats. *PLoS One* 8 (10), e76874. doi:10.1371/journal.pone.0076874

Cordeiro, K. K., Jiang, W., Papazoglou, A., Tenório, S. B., Döbrössy, M., and Nikkhah, G. (2010). Graft-mediated functional recovery on a skilled forelimb use paradigm in a rodent model of Parkinson's disease is dependent on reward contingency. *Behav. Brain Res.* 212 (2), 187–195. doi:10.1016/j.bbr.2010.04.012

Deumens, R., Blokland, A., and Prickaerts, J. (2002). Modeling Parkinson's disease in rats: An evaluation of 6-OHDA lesions of the nigrostriatal pathway. *Exp. Neurol.* 175 (2), 303–317. doi:10.1006/exnr.2002.7891

Diao, H. L., Xue, Y., Han, X. H., Wang, S. Y., Liu, C., Chen, W. F., et al. (2017). Adenosine A2A receptor modulates the activity of globus pallidus neurons in rats. *Front. Physiol.* 8, 897. doi:10.3389/fphys.2017.00897

Dong, J., Hawes, S., Wu, J., Le, W., and Cai, H. (2021). Connectivity and functionality of the globus pallidus externa under normal conditions and Parkinson's disease. *Front. Neural Circuits* 15, 645287. doi:10.3389/fncir.2021.645287

Eid, L., and Parent, M. (2016). Chemical anatomy of pallidal afferents in primates. *Brain Struct. Funct.* 221 (9), 4291–4317. doi:10.1007/s00429-016-1216-y

Fatemi, I., Abdollahi, A., Shamsizadeh, A., Allahtavakoli, M., and Roohbakhsh, A. (2021). The effect of intra-striatal administration of GPR55 agonist (LPI) and antagonist (ML193) on sensorimotor and motor functions in a Parkinson's disease rat model. *Acta Neuropsychiatr.* 33 (1), 15–21. doi:10.1017/neu.2020.30

Fernández-Ruiz, J., Sagredo, O., Pazos, M. R., García, C., Pertwee, R., Mechoulam, R., et al. (2013). Cannabidiol for neurodegenerative disorders: Important new clinical applications for this phytocannabinoid? *Br. J. Clin. Pharmacol.* 75 (2), 323–333. doi:10.1111/j.1365-2125.2012.04341.x

Fernández-Suárez, D., Celorrio, M., Lanciego, J. L., Franco, R., and Aymerich, M. S. (2012). Loss of parvalbumin-positive neurons from the globus pallidus in animal models of Parkinson disease. *J. Neuropathol. Exp. Neurol.* 71 (11), 973–982. doi:10.1097/NEN.0b013e3182717cba

Ford, L. A., Roelofs, A. J., Anavi-Goffer, S., Mowat, L., Simpson, D. G., Irving, A. J., et al. (2010). A role for L-alpha-lysophosphatidylinositol and GPR55 in the modulation of migration, orientation and polarization of human breast cancer cells. *Br. J. Pharmacol.* 160 (3), 762–771. doi:10.1111/j.1476-5381.2010.00743.x

Francardo, V., Schmitz, Y., Sulzer, D., and Cenci, M. A. (2017). Neuroprotection and neurorestoration as experimental therapeutics for Parkinson's disease. *Exp. Neurol.* 298 (1), 137–147. doi:10.1016/j.expneurol.2017.10.001

Galvan, A., Devergnas, A., and Wichmann, T. (2015). Alterations in neuronal activity in basal ganglia-thalamocortical circuits in the parkinsonian state. *Front. Neuroanat.* 9, 5. doi:10.3389/fnana.2015.00005

Galvan, A., Floran, B., Erlij, D., and Aceves, J. (2001). Intrapallidal dopamine restores motor deficits induced by 6-hydroxydopamine in the rat. *J. Neural Transm. (Vienna)* 108 (2), 153–166. doi:10.1007/s007020170085

Galvan, A., Villalba, R. M., West, S. M., Maidment, N. T., Ackerson, L. C., Smith, Y., et al. (2005). GABAergic modulation of the activity of globus pallidus neurons in primates: *In vivo* analysis of the functions of GABA receptors and GABA transporters. *J. Neurophysiol.* 94 (2), 990–1000. doi:10.1152/jn.00068.2005

Galvan, A., and Wichmann, T. (2008). Pathophysiology of parkinsonism. *Clin. Neurophysiol.* 119 (7), 1459–1474. doi:10.1016/j.clinph.2008.03.017

García-Arencibia, M., González, S., de Lago, E., Ramos, J. A., Mechoulam, R., and Fernández-Ruiz, J. (2007). Evaluation of the neuroprotective effect of cannabinoids in a rat model of Parkinson's disease: Importance of antioxidant and cannabinoid receptor-independent properties. *Brain Res.* 1134 (1), 162–170. doi:10.1016/j.brainres.2006.11.063

García-Gutiérrez, M. S., Navarrete, F., Navarro, G., Reyes-Resina, I., Franco, R., Lanciego, J. L., et al. (2018). Alterations in gene and protein expression of cannabinoid CB2 and GPR55 receptors in the dorsolateral prefrontal cortex of suicide victims. *Neurotherapeutics* 15 (3), 796–806. doi:10.1007/s13311-018-0610-y

Glajch, K. E., Fleming, S. M., Surmeier, D. J., and Osten, P. (2012). Sensorimotor assessment of the unilateral 6-hydroxydopamine mouse model of Parkinson's disease. *Behav. Brain Res.* 230 (2), 309–316. doi:10.1016/j.bbr.2011.12.007

Henstridge, C. M., Balenga, N. A., Kargl, J., Andradas, C., Brown, A. J., Irving, A., et al. (2011). Minireview: Recent developments in the physiology and pathology of the lysophosphatidylinositol-sensitive receptor GPR55. *Mol. Endocrinol.* 25 (11), 1835–1848. doi:10.1210/me.2011-1197

Hernández, A., Sierra, A., Valdiosera, R., Florán, B., Erlij, D., and Aceves, J. (2007). Presynaptic D1 dopamine receptors facilitate glutamatergic neurotransmission in the rat globus pallidus. *Neurosci. Lett.* 425 (3), 188–191. doi:10.1016/j.neulet.2007.08.026

Hernandez-Baltazar, D., Zavala-Flores, L. M., and Villanueva-Olivo, A. (2017). The 6-hydroxydopamine model and parkinsonian pathophysiology: Novel findings in an older model. *Neurologia* 32 (8), 533–539. doi:10.1016/j.nrl.2015.06.011

Hill, J. D., Zuluaga-Ramirez, V., Gajghate, S., Winfield, M., and Persidsky, Y. (2018). Activation of GPR55 increases neural stem cell proliferation and promotes early adult hippocampal neurogenesis. *Br. J. Pharmacol.* 175 (16), 3407–3421. doi:10.1111/bph.14387

Hurst, K., Badgley, C., Ellsworth, T., Bell, S., Friend, L., Prince, B., et al. (2017). A putative lysophosphatidylinositol receptor GPR55 modulates hippocampal synaptic plasticity. *Hippocampus* 27 (9), 985–998. doi:10.1002/hipo.22747

Ibeas Bih, C., Chen, T., Nunn, A. V., Bazelot, M., Dallas, M., and Whalley, B. J. (2015). Molecular targets of cannabidiol in neurological disorders. *Neurotherapeutics* 12 (4), 699–730. doi:10.1007/s13311-015-0377-3

Kaplan, J. S., Stella, N., Catterall, W. A., and Westenbroek, R. E. (2017). Cannabidiol attenuates seizures and social deficits in a mouse model of Dravet syndrome. *Proc. Natl. Acad. Sci. U. S. A.* 114 (42), 11229–11234. doi:10.1073/pnas.1711351114

Kita, H., and Kita, T. (2011). Role of striatum in the pause and burst generation in the globus pallidus of 6-OHDA-treated rats. *Front. Syst. Neurosci.* 5, 42. doi:10.3389/fnsys.2011.00042

Kita, H., and Kitai, S. T. (1987). Efferent projections of the subthalamic nucleus in the rat: Light and electron microscopic analysis with the PHA-L method. *J. Comp. Neurol.* 260 (3), 435–452. doi:10.1002/cne.902600309

Klein, A., Metz, G. A., Papazoglou, A., and Nikkhah, G. (2007). Differential effects on forelimb grasping behavior induced by fetal dopaminergic grafts in hemiparkinsonian rats. *Neurobiol. Dis.* 27 (1), 24–35. doi:10.1016/j.nbd.2007.03.010

Kovaleski, R. F., Callahan, J. W., Chazalon, M., Wokosin, D. L., Baufreton, J., and Bevan, M. D. (2020). Dysregulation of external globus pallidus-subthalamic nucleus network dynamics in parkinsonian mice during cortical slow-wave activity and activation. *J. Physiol.* 598 (10), 1897–1927. doi:10.1113/JP279232

Lanciego, J. L., Luquin, N., and Obeso, J. A. (2012). Functional neuroanatomy of the basal ganglia. *Cold Spring Harb. Perspect. Med.* 2 (12), a009621. doi:10.1101/cshperspect.a009621

Lauckner, J. E., Jensen, J. B., Chen, H. Y., Lu, H. C., Hille, B., and Mackie, K. (2008). GPR55 is a cannabinoid receptor that increases intracellular calcium and inhibits M current. *Proc. Natl. Acad. Sci. U. S. A.* 105 (7), 2699–2704. doi:10.1073/pnas.0711278105

Ligresti, A., De Petrocellis, L., and Di Marzo, V. (2016). From phytocannabinoids to cannabinoid receptors and endocannabinoids: Pleiotropic physiological and pathological roles through complex pharmacology. *Physiol. Rev.* 96 (4), 1593–1659. doi:10.1152/physrev.00002.2016

Mallet, N., Micklem, B. R., Henny, P., Brown, M. T., Williams, C., Bolam, J. P., et al. (2012). Dichotomous organization of the external globus pallidus. *Neuron* 74 (6), 1075–1086. doi:10.1016/j.neuron.2012.04.027

Mallet, N., Pogosyan, A., Márton, L. F., Bolam, J. P., Brown, P., and Magill, P. J. (2008). Parkinsonian beta oscillations in the external globus pallidus and their relationship with subthalamic nucleus activity. *J. Neurosci.* 28 (52), 14245–14258. doi:10.1523/JNEUROSCI.4199-08.2008

Marichal-Cancino, B. A., Fajardo-Valdez, A., Ruiz-Contreras, A. E., Mendez-Díaz, M., and Prospero-García, O. (2017). Advances in the physiology of GPR55 in the central nervous system. *Curr. Neuropharmacol.* 15 (5), 771–778. doi:10.2174/1570159X14666160729155441

Marichal-Cancino, B. A., Fajardo-Valdez, A., Ruiz-Contreras, A. E., Méndez-Díaz, M., and Prospéro-García, O. (2018). Possible role of hippocampal GPR55 in spatial learning and memory in rats. *Acta Neurobiol. Exp. (Wars)* 78 (1), 41–50. doi:10.21307/ane-2018-001

Marichal-Cancino, B. A., Sánchez-Fuentes, A., Méndez-Díaz, M., Ruiz-Contreras, A. E., and Prospéro-García, O. (2016). Blockade of GPR55 in the dorsolateral striatum impairs performance of rats in a T-maze paradigm. *Behav. Pharmacol.* 27 (4), 393–396. doi:10.1097/FBP.0000000000000185

Martínez-Pinilla, E., Aguinaga, D., Navarro, G., Rico, A. J., Oyarzábal, J., Sánchez-Arias, J. A., et al. (2019). Targeting CB1 and GPR55 endocannabinoid receptors as a potential neuroprotective approach for Parkinson's disease. *Mol. Neurobiol.* 56 (8), 5900–5910. doi:10.1007/s12035-019-1495-4

Mendieta, L., Venegas, B., Moreno, N., Patricio, A., Martínez, I., Aguilera, J., et al. (2009). The carboxyl-terminal domain of the heavy chain of tetanus toxin prevents dopaminergic degeneration and improves motor behavior in rats with striatal MPP(+)-lesions. *Neurosci. Res.* 65 (1), 98–106. doi:10.1016/j.neures.2009.06.001

Meredith, G. E., Sonsalla, P. K., and Chesselet, M. F. (2008). Animal models of Parkinson's disease progression. *Acta Neuropathol.* 115 (4), 385–398. doi:10.1007/s00401-008-0350-x

Metz, G. A., and Whishaw, I. Q. (2000). Skilled reaching an action pattern: Stability in rat (*Rattus norvegicus*) grasping movements as a function of changing food pellet size. *Behav. Brain Res.* 116 (2), 111–122. doi:10.1016/s0166-4328(00)00245-x

Montoya, C. P., Campbell-Hope, L. J., Pemberton, K. D., and Dunnett, S. B. (1991). The "staircase test": A measure of independent forelimb reaching and grasping abilities in rats. *J. Neurosci. Methods* 36 (2-3), 219–228. doi:10.1016/0165-0270(91)90048-5

Musella, A., Fresegna, D., Rizzo, F. R., Gentile, A., Bullitta, S., De Vito, F., et al. (2017). A novel crosstalk within the endocannabinoid system controls GABA transmission in the striatum. *Sci. Rep.* 7 (1), 7363. doi:10.1038/s41598-017-07519-8

Neumann, W. J., Schroll, H., de Almeida Marcelino, A. L., Horn, A., Ewert, S., Irmen, F., et al. (2018). Functional segregation of basal ganglia pathways in Parkinson's disease. *Brain* 141 (9), 2655–2669. doi:10.1093/brain/awy206

Nikkhah, G., Rosenthal, C., Hedrich, H. J., and Samii, M. (1998). Differences in acquisition and full performance in skilled forelimb use as measured by the 'staircase test' in five rat strains. *Behav. Brain Res.* 92 (1), 85–95. doi:10.1016/s0166-4328(97)00128-9

Oka, S., Nakajima, K., Yamashita, A., Kishimoto, S., and Sugiura, T. (2007). Identification of GPR55 as a lysophosphatidylinositol receptor. *Biochem. Biophys. Res. Commun.* 362 (4), 928–934. doi:10.1016/j.bbrc.2007.08.078

Okine, B. N., Mc Laughlin, G., Gaspar, J. C., Harhen, B., Roche, M., and Finn, D. P. (2020). Antinociceptive effects of the GPR55 antagonist CID16020046 injected into the rat anterior cingulate cortex. *Neuroscience* 443, 19–29. doi:10.1016/j.neuroscience.2020.07.013

Pandolfo, P., Silveirinha, V., dos Santos-Rodrigues, A., Venance, L., Ledent, C., Takahashi, R. N., et al. (2011). Cannabinoids inhibit the synaptic uptake of adenosine and dopamine in the rat and mouse striatum. *Eur. J. Pharmacol.* 655 (1-3), 38–45. doi:10.1016/j.ejphar.2011.01.013

Parent, M., Wallman, M. J., Gagnon, D., and Parent, A. (2011). Serotonin innervation of basal ganglia in monkeys and humans. *J. Chem. Neuroanat.* 41 (4), 256–265. doi:10.1016/j.jchemneu.2011.04.005

Patricio, F., Juárez-Torres, D., Patricio-Martínez, A., Mendieta, L., Pérez-Severiano, F., Montes, S., et al. (2022). The C-terminal domain of the heavy chain of tetanus toxin prevents the oxidative and nitrosative stress induced by acute toxicity of 1-methyl-4-phenylpyridinium, a rat model of Parkinson's disease. *Neurosci. Res.* 174, 36–45. doi:10.1016/j.neures.2021.08.005

Patricio, F., Morales-Andrade, A. A., Patricio-Martínez, A., and Limón, I. D. (2020). Cannabidiol as a therapeutic target: Evidence of its neuroprotective and neuromodulatory function in Parkinson's disease. *Front. Pharmacol.* 11, 595635. doi:10.3389/fphar.2020.595635

Paxinos, G., and Watson, C. (1998). *The rat brain in stereotactic coordinates*. London: Academic Press.

Pellati, F., Brighenti, V., Sperlea, J., Marchetti, L., Bertelli, D., and Benvenuti, S. (2018). New methods for the comprehensive analysis of bioactive compounds in *Cannabis sativa* L. (hemp). *Molecules* 23 (10), 2639. doi:10.3390/molecules23102639

Peres, F. F., Lima, A. C., Hallak, J. E. C., Crippa, J. A., Silva, R. H., and Abílio, V. C. (2018). Cannabidiol as a promising strategy to treat and prevent movement disorders? *Front. Pharmacol.* 9, 482. doi:10.3389/fphar.2018.00482

Pertwee, R. G. (2008). The diverse CB1 and CB2 receptor pharmacology of three plant cannabinoids: delta9-tetrahydrocannabinol, cannabidiol and delta9-tetrahydrocannabivarin. *Br. J. Pharmacol.* 153 (2), 199–215. doi:10.1038/sj.bjp.0707442

Pisanti, S., Malfitano, A. M., Ciaglia, E., Lamberti, A., Ranieri, R., Cuomo, G., et al. (2017). Cannabidiol: State of the art and new challenges for therapeutic applications. *Pharmacol. Ther.* 175, 133–150. doi:10.1016/j.pharmthera.2017.02.041

Rajput, A. H., Sitte, H. H., Rajput, A., Fenton, M. E., Pifl, C., and Hornykiewicz, O. (2008). Globus pallidus dopamine and Parkinson motor subtypes: Clinical and brain biochemical correlation. *Neurology* 70 (2), 1403–1410. doi:10.1212/01.wnl.0000285082.18969.3a

Ramírez-García, G., Palafox-Sánchez, V., and Limón, I. D. (2015). Nitrosative and cognitive effects of chronic L-DOPA administration in rats with intra-nigral 6-OHDA lesion. *Neuroscience* 290, 492–508. doi:10.1016/j.neuroscience.2015.01.047

Rattka, M., Fluri, F., Krstić, M., Asan, E., and Volkmann, J. (2016). A novel approach to assess motor outcome of deep brain stimulation effects in the hemiparkinsonian rat: Staircase and cylinder test. *J. Vis. Exp.* 111. doi:10.3791/53951

Rommelfanger, K. S., and Wichmann, T. (2010). Extrastriatal dopaminergic circuits of the basal ganglia. *Front. Neuroanat.* 4, 139. doi:10.3389/fnana.2010.00139

Ryberg, E., Larsson, N., Sjögren, S., Hjorth, S., Hermansson, N. O., Leonova, J., et al. (2007). The orphan receptor GPR55 is a novel cannabinoid receptor. *Br. J. Pharmacol.* 152 (7), 1092–1101. doi:10.1038/sj.bjp.0707460

Sawzdargo, M., Nguyen, T., Lee, D. K., Lynch, K. R., Cheng, R., Heng, H. H., et al. (1999). Identification and cloning of three novel human G protein-coupled receptor genes GPR52, PsiGPR53 and GPR55: GPR55 is extensively expressed in human brain. *Brain Res. Mol. Brain Res.* 64 (2), 193–198. doi:10.1016/s0169-328x(98)00277-0

Segura-Aguilar, J. (2018). Neurotoxins as preclinical models for Parkinson's disease. *Neurotox. Res.* 34 (4), 870–877. doi:10.1007/s12640-017-9856-0

Sharir, H., and Abood, M. E. (2010). Pharmacological characterization of GPR55, a putative cannabinoid receptor. *Pharmacol. Ther.* 126 (3), 301–313. doi:10.1016/j.pharmthera.2010.02.004

Shen, S. Y., Yu, R., Li, W., Liang, L. F., Han, Q. Q., Huang, H. J., et al. (2022). The neuroprotective effects of GPR55 against hippocampal neuroinflammation and impaired adult neurogenesis in CSDS mice. *Neurobiol. Dis.* 169, 105743. doi:10.1016/j.nbd.2022.105743

Smith, Y., and Villalba, R. (2008). Striatal and extrastriatal dopamine in the basal ganglia: An overview of its anatomical organization in normal and parkinsonian brains. *Mov. Disord.* 23 Suppl 3 (3), S534–S547. doi:10.1002/mds.22027

Sylantyev, S., Jensen, T. P., Ross, R. A., and Rusakov, D. A. (2013). Cannabinoid- and lysophosphatidylinositol-sensitive receptor GPR55 boosts neurotransmitter release at central synapses. *Proc. Natl. Acad. Sci. U. S. A.* 110 (13), 5193–5198. doi:10.1073/pnas.1211204110

Taylor, M. D., De Ceballos, M. L., Rose, S., Jenner, P., and Marsden, C. D. (1992). Effects of a unilateral 6-hydroxydopamine lesion and prolonged L-3,4-dihydroxyphenylalanine treatment on peptidergic systems in rat basal ganglia. *Eur. J. Pharmacol.* 219 (2), 183–192. doi:10.1016/0014-2999(92)90295-f

Wu, C. S., Chen, H., Sun, H., Zhu, J., Jew, C. P., Wager-Miller, J., et al. (2013). GPR55, a G-protein coupled receptor for lysophosphatidylinositol, plays a role in motor coordination. *PLoS One* 8 (4), e60314. doi:10.1371/journal.pone.0060314

Xiong, Y., and Lim, C. S. (2021). Understanding the modulatory effects of cannabidiol on alzheimer's disease. *Brain Sci.* 11 (9), 1211. doi:10.3390/brainsci11091211

frontiers | Frontiers in Pharmacology

TYPE Original Research
PUBLISHED 27 September 2022
DOI 10.3389/fphar.2022.931384

OPEN ACCESS

EDITED BY
Huazheng Liang,
Translational Research Institute of Brain and Brain-Like Intelligence affiliated to Tongji University School of Medicine, China

REVIEWED BY
Oliver Wirths,
University Medical Center Göttingen, Germany
Andres Ozaita,
Pompeu Fabra University, Spain
Marta Valenza,
Sapienza University of Rome, Italy
Sarah Beggiato,
University of Studies G. d'Annunzio Chieti and Pescara, Italy

*CORRESPONDENCE
Tim Karl,
t.karl@westernsydney.edu.au

†These authors have contributed equally to this work

SPECIALTY SECTION
This article was submitted to Neuropharmacology, a section of the journal Frontiers in Pharmacology

RECEIVED 28 April 2022
ACCEPTED 05 September 2022
PUBLISHED 27 September 2022

CITATION
Chesworth R, Cheng D, Staub C and Karl T (2022), Effect of long-term cannabidiol on learning and anxiety in a female Alzheimer's disease mouse model.
Front. Pharmacol. 13:931384.
doi: 10.3389/fphar.2022.931384

Effect of long-term cannabidiol on learning and anxiety in a female Alzheimer's disease mouse model

Rose Chesworth[1†], David Cheng[2†], Chloe Staub[1] and Tim Karl[1,2*]

[1]School of Medicine, Western Sydney University, Campbelltown, NSW, Australia, [2]Neuroscience Research Australia, Randwick, NSW, Australia

Cannabidiol is a promising potential therapeutic for neurodegenerative diseases, including Alzheimer's disease (AD). Our laboratory has shown that oral CBD treatment prevents cognitive impairment in a male genetic mouse model of AD, the *amyloid precursor protein 1 x presenilin 1* hemizygous (*APPxPS1*) mouse. However, as sex differences are evident in clinical populations and in AD mouse models, we tested the preventive potential of CBD therapy in female *APPxPS1* mice. In this study, 2.5-month-old female wildtype-like (WT) and *APPxPS1* mice were fed 20 mg/kg CBD or a vehicle *via* gel pellets daily for 8 months and tested at 10.5 months in behavioural paradigms relevant to cognition (fear conditioning, FC; cheeseboard, CB; and novel object recognition test, NORT) and anxiety-like behaviours (elevated plus maze, EPM). In the CB, CBD reduced latencies to find a food reward in *APPxPS1* mice, compared to vehicle-treated *APPxPS1* controls, and this treatment effect was not evident in WT mice. In addition, CBD also increased speed early in the acquisition of the CB task in *APPxPS1* mice. In the EPM, CBD increased locomotion in *APPxPS1* mice but not in WT mice, with no effects of CBD on anxiety-like behaviour. CBD had limited effects on the expression of fear memory. These results indicate preventive CBD treatment can have a moderate spatial learning-enhancing effect in a female amyloid-β-based AD mouse model. This suggests CBD may have some preventive therapeutic potential in female familial AD patients.

KEYWORDS

Alzheimer's disease, behaviour, cannabidiol (CBD), spatial memory, female, amyloid precursor protein, presenilin 1

1 Introduction

Recently, there has been increasing interest in cannabidiol (CBD), a non-intoxicating phytocannabinoid compound in the *Cannabis sativa L.* [Cannabaceae] plant, for the treatment of several neurodegenerative and psychiatric disorders. CBD possesses antioxidant, anti-apoptotic, neuroprotective, and anti-inflammatory properties [reviews: (Scuderi et al., 2009; Campos et al., 2016)]. This is particularly relevant for brain disorders characterised by neuroinflammation and cell death including

neurodegenerative disorders such as Alzheimer's disease (AD), which has no cure. Dementia affects over 55 million people globally, of which AD is the most common form (Wimo et al., 2015). AD is characterised by the presence of extracellular amyloid-beta (Aβ) plaques and intracellular neurofibrillary tangles consisting of hyperphosphorylated tau (Bloom, 2014); these are found in the neocortex (Aβ) and the transentorhinal cortex (tau) in early disease stages but spread throughout the brain as the disease progresses (Braak and Braak, 1991; Thal et al., 2002). Inflammatory markers [e.g., interleukin (IL)-1, IL-6, tumour necrosis factor (TNF)-α, and activated microglia] and markers for oxidative stress [e.g. oxidised proteins and oxidative modifications in nuclear and mitochondrial DNA (Gella and Durany, 2009; Chen and Zhong, 2014)] are also commonly found in AD postmortem brain tissue (McGeer et al., 2016) and are hypothesised to precede the development of Aβ and tau pathology (Holmes, 2013). Targeting inflammation is of increasing interest as an AD treatment approach (McGeer et al., 2016). The failure of anti-inflammatory therapies to date may be due to missing the therapeutic window (Rivers-Auty et al., 2020) or requiring multimodal drug strategies to target a complex disease (Karl et al., 2017). Considering the anti-inflammatory, anti-apoptotic, and neuroprotective properties of CBD, there is growing interest in its potential for the treatment of AD (Karl et al., 2017).

In vitro data indicate CBD can reduce AD-relevant pathology [reviews: (Karl et al., 2017; Watt and Karl, 2017)]. CBD inhibits tau hyperphosphorylation (Esposito et al., 2006a; Vallee et al., 2017), reduces full-length APP expression, and reduces Aβ peptide expression (Scuderi et al., 2014), suggesting CBD can reduce AD pathology in cell culture. CBD also improves cell survival and reduces the production of reactive oxygen species and nitric oxide production (Iuvone et al., 2004; Esposito et al., 2006b; Amini and Abdolmaleki, 2022), suggesting CBD can reduce Aβ-induced toxicity. CBD can also protect against cell viability loss induced by $A\beta_{42}$ (Janefjord et al., 2014), which is a major component of amyloid plaques (Gu and Guo, 2013). CBD reduces microglial function and cytokine gene and protein expression after intracerebroventricular (i.c.v.) or hippocampal Aβ administration to mice (Esposito et al., 2007; Martin-Moreno et al., 2011) and can upregulate the immune system function and increase autophagy in AD models (Hao and Feng, 2021), which may be another mechanism by which CBD improves AD pathology. CBD may also have therapeutic effects in AD by acting on hippocampal long-term potentiation (LTP); pretreatment with CBD prevents the $A\beta_{1\text{-}42}$ oligomer-induced reduction in hippocampal CA1 LTP in mice (Hughes and Herron, 2019), thereby reversing effects of AD pathology on synaptic plasticity.

Preclinical *in vivo* data suggest remedial CBD treatment *via* i.p. administration reverses cognitive impairment in pharmacological and genetic mouse models for Alzheimer's disease [reviews: (Karl et al., 2017; Watt and Karl, 2017)]. For example, chronic CBD prevents learning and memory impairments in mice injected with Aβ intraventricularly (Martin-Moreno et al., 2011). Also, in a mouse model of familial AD (Cheng et al., 2014a; Aso et al., 2015; Coles et al., 2020; Watt et al., 2020a), i.e., mice hemizygous for *amyloid precursor protein* (*APP*) and *presenilin 1* (*PS1*) genes (i.e. *APPxPS1* mice), they are characterised by increased Aβ accumulation and accelerated plaque pathology from 4 months of age (Wang et al., 2003) and spatial learning and memory deficits from 7 to 8 months of age (Cao et al., 2007; Reiserer et al., 2007). Therapeutic effects of CBD in APPxPS1 mice have been found at different CBD doses [range of 5–50 mg/kg (Cheng et al., 2014a; Coles et al., 2020; Watt et al., 2020a)] and also when using CBD-enriched extracts (Aso et al., 2015). The mechanisms involved are not entirely clear. Chronic CBD has moderate effects on Aβ levels in the hippocampus (Watt et al., 2020a) and reduces the astrocytic response and cell surface adhesion molecule CCL4 mRNA expression in *APPxPS1* mice (Aso et al., 2015). However, to date, remedial CBD treatment has not been shown to strongly affect other AD-relevant receptors and molecules in *APPxPS1* mice, including brain-derived neurotrophic factor (BDNF), proliferator-activated receptor γ (PPARγ), ionised calcium-binding adaptor molecule 1 (IBA1) and various cytokines (Watt et al., 2020a).

In addition to the remedial effects (i.e., CBD administered when behavioural impairment is present), CBD has been found to prevent the development of AD-relevant behavioural impairments. When CBD is administered orally for 8 months from 2.5 months of age, CBD prevents the development of social recognition impairment in male *APPxPS1* mice (Cheng et al., 2014c). In this study, there were also subtle effects of CBD on neuroinflammation and cholesterol in the cortex and dietary phytosterol retention in the cortex and hippocampus (Cheng et al., 2014c). This suggests CBD has potential preventive and pro-cognitive effects on AD in male animals.

Despite this, the potential preventive effects of CBD treatment on cognition in female *APPxPS1* mice are unknown. This is a critical question as sex differences are evident in AD: there is a higher prevalence of AD in women, and women suffer greater cognitive deterioration than men at the same disease stage (Laws et al., 2018; Medeiros and Silva, 2019). Importantly, sex differences are also found in the *APPxPS1* mouse model, e.g., social novelty recognition impairment is evident in male *APPxPS1* mice but not in female mice, while spatial memory impairment is evident in female *APPxPS1* mice but not in male *APPxPS1* mice (Cheng et al., 2013; Cheng et al., 2014b). Female *APPxPS1* mice also show greater amyloid burden and higher plaque number (Wang et al., 2003), as well as higher levels of phosphorylated tau and proinflammatory cytokines, more severe astrocytosis and microgliosis, and greater neuronal and synaptic degeneration than male mice at the same age (Jiao et al., 2016). These sex differences make the *APPxPS1* mice an

appropriate model to investigate potential sex differences in CBD's efficacy for treating cognitive impairment in AD. Furthermore, remedial CBD treatment (i.e., after the development of cognitive deficits) affects different domains in male and female *APPxPS1* mice: CBD improves social recognition, object recognition, and spatial reversal learning in male *APPxPS1* mice (Cheng et al., 2014a; Watt et al., 2020a) but only object recognition deficits in female *APPxPS1* mice (Coles et al., 2020). Indeed, there has been limited investigation of sex differences in CBD's effects on anxiety-like behaviour and cognition, e.g., (Osborne et al., 2017; Osborne et al., 2019; Garcia-Baos et al., 2021), highlighting the importance of examining female and male animals. Thus, we sought to determine if *preventive* CBD affects different behavioural domains in male and female *APPxPS1* mice. Finally, we assessed a preventative approach because treatment after symptom onset may be too late to limit ongoing neurodegenerative processes in AD (Lee et al., 2022), and thus, treatments with preventative potential could have significant clinical impact by limiting disease progression and symptom onset.

Thus, the present study was designed to complement earlier behavioural research in our laboratory (Cheng et al., 2014c), to determine if 20 mg/kg CBD treatment given orally *via* gel pellets for 8 months prevents the development of the AD-relevant behavioural phenotype in *APPxPS1* female mice.

2 Materials and methods

2.1 Animals

APPxPS1 hemizygous mice on a congenic C57BL/6JxC3H/HeJ background were generated, as described previously (Cheng et al., 2013; Cheng et al., 2014a; Cheng et al., 2014b; Cheng et al., 2014c). These mice were originally described by Borchelt et al. (1997). They express the "humanized" mouse amyloid beta precursor protein gene modified at three amino acids to reflect the human residues and further modified to contain the K595N/M596L (also called K670N/M671L) mutations linked to familial Alzheimer's. They also express a mutant human presenilin 1 carrying the exon-9-deleted variant (PSEN1dE9) associated with familial Alzheimer's disease. These gene mutations are controlled by mouse prion protein promoter elements, directing transgene expression predominantly to CNS neurons.

Mice were bred at Australian BioResources (ABR: Moss Vale, NSW, Australia), where they were group housed in individually ventilated cages (Type Mouse Version 1: Airlaw, Smithfield, Australia) under a 12/12 h light/dark cycle with a dawn/dusk simulation. Mice were transported to the Neuroscience Research Australia animal facility (Randwick, Australia) at ~10 weeks of age, where littermates were group housed (two to three mice per cage) in polysulfone cages (1144B: Techniplast, Rydalmere, Australia) with corn cob bedding (PuraCob Premium: Able Scientific, Perth, Australia) and tissues for nesting. Mice were kept under a 12:12 h light:dark schedule [light phase: white light (illumination: 210 lx); lights on 0700–1900 h]. Environmental temperature was automatically regulated at 21 ± 1°C, and relative humidity was 40–60%. Food (Gordon's Rat and Mouse Maintenance Pellets: Gordon's Specialty Stockfeeds, Yanderra, Australia) and water were provided *ad libitum*, except where specified.

Research and animal care procedures were approved by the University of New South Wales Animal Care and Ethics Committee in accordance with the Australian Code of Practice for the Care and Use of Animals for Scientific Purposes. *APPxPS1* mice and their non-transgenic wild type-like littermates (WT) were approximately 2.4 months of age at the onset of the study. The number of animals per group was as follows: 14 WT-vehicle, 16 *APPxPS1*-vehicle, 14 WT-CBD, and 12 *APPxPS1*-CBD.

2.2 Drugs

Powdered CBD (CAS: 13956-29-1, THC Pharm GmbH, Frankfurt/Main, Germany) was used at a dose of 20 mg/kg body weight, based on previous work in our laboratory (Cheng et al., 2014a; Cheng et al., 2014c). CBD was administered in gel pellets to prevent the stress of chronic injections on behavioural and cognitive results; methods were identical to those published previously (Cheng et al., 2014c). Briefly, CBD or the vehicle were dissolved in a highly palatable, sweetened, and chocolate-flavoured gel pellet and administered at a volume of 8 ml/kg body weight. CBD was dissolved in gel pellets with a final composition of 2.0% ethanol, 2.0% Tween 80, 15.2% Splenda (Splenda Low Calorie Sweetener: Johnson & Johnson Pacific Pty, Broadway, Australia), 8.7% gelatine (Davis Gelatine: GELITA Australia Pty, Josephville, Australia), 20.1% chocolate flavouring (Queen Flavouring Essence Imitation Chocolate: Queen Fine Foods Pty, Alderley, Australia), and 52.0% water for irrigation. Vehicle gel pellets were identical but contained no CBD.

2.3 Treatment schedule

Mice were initially habituated to vehicle gel pellets in their home cages for 7 days prior to the start of treatment. Following this, mice were isolated within their home cages during treatment by placing a plastic divider in the home cage. Then, animals were given either a vehicle or a CBD gel pellet (treatments were quasi-randomized), which they consumed within 2–5 min. Mice did not need to be food-deprived to ensure they ate the gel pellet. A trained experimenter watched all the animals consume the gel

pellets daily to ensure the correct dose was administered each day. The plastic divider was removed once the mice had consumed the gel pellets. Mice were treated daily for 8 months (i.e., from 2.5 to 10.5 months of age) late in the afternoon, to avoid potential effects of acute CBD on test outcomes.

2.4 Behavioural testing

Starting at 10 months of age, mice were tested with an inter-test interval of at least 48 h (Cheng et al., 2014c). We chose paradigms based on the baseline behavioural phenotype previously reported in these mice in our laboratory (Cheng et al., 2014b). This strategy was chosen rather than directly replicating the test biography of CBD-treated *APPxPS1* male mice (Cheng et al., 2014c)] as female AD transgenic mice exhibit a different cognitive profile to males, i.e., only females exhibit impaired spatial memory (Cheng et al., 2014b), whereas only transgenic males show impaired social recognition memory (Cheng et al., 2013). All tests were conducted during the first 5 h of the light phase to minimize the effects of the circadian rhythm. All test apparatus was cleaned with 70% v/v ethanol in between test animals. Behavioural tests were conducted in the following order: fear conditioning, cheeseboard, elevated plus maze, and novel object recognition.

2.4.1 Fear conditioning (FC)

FC assesses hippocampal- and amygdala-dependent associative learning, and methods were identical to those published previously (Cheng et al., 2013; Cheng et al., 2014a; Cheng et al., 2014c). During conditioning, mice were placed into the test chamber (Model H10-11R-TC, Coulbourn Instruments, United States) for 2 min. An 80 dB conditioned stimulus (CS) was presented twice for 30 s with a co-terminating 0.4-mA 2-s foot shock (unconditioned stimulus; US) with an inter-pairing interval of 2 min. The test concluded 2 min later. The next day (context test), mice were returned to the apparatus for 7 min. On day 3 (cue test), animals were placed in an altered context for 9 min. After 2 min (pre-CS/baseline), the CS was presented continuously for 5 min. The test concluded after another 2 min, without the CS. Time spent *freezing* was measured by Any-Maze™ software.

2.4.2 Cheeseboard (CB)

Spatial memory was assessed in the CB using established methods (Cheng et al., 2014b; Coles et al., 2020; Watt et al., 2020a). Sweetened condensed milk, 1:4 in water, was used as a food reward, and mice were food-restricted during CB training and testing (access to food for 1–2 h, following completion of daily testing, mice kept at 85-90% of free feeding body weight). There were three trials per day, except at the probe, where there was one trial. All trials were 2 min, unless the food reward was located in <2 min, with a 20-min intertrial interval (ITI).

Mice were habituated to the blank side of the board for 2 days. Next, mice were trained for 7 days to locate a well containing a food reward. The latency of the mice to find the target well was recorded, and if the food reward was not located within 2 min, the mouse was gently guided to the well by the experimenter. Mice were considered to have learnt the task if the average latency of all three trials in 1 day was <20 s. After 7 days, our control group (WT VEH) met acquisition criteria. The next day, a probe trial was conducted to assess spatial reference memory. No wells were baited, and mice were given 2 min to explore the apparatus freely. To assess if animals could update their spatial learning contingencies, we conducted reversal learning, whereby the location of the food reward was changed. Mice completed 4 days of reversal training before the reversal probe trial (WT VEH mice met reversal criteria in 4 days), which was conducted 24 h after reversal training. During the reversal probe, no wells were baited and mice were given 2 min to explore the apparatus freely. Mice were returned to free feeding, following completion of the CB, and subsequent behavioural tests were conducted, and only once mice had returned to free feeding weight.

The average latency to find the reward was analysed as a general indication of learning, and this was used to determine when mice acquired the task (Cheng et al., 2014b; Coles et al., 2020). The first trial per day across training was also analysed to assess long-term reference memory (retention of ≥24 h), and the average of trials 2 and 3 each day across training was analysed to assess intermediate-term memory [retention falling between short-term (<2 min) and long-term (>24 h) memory] (Taglialatela et al., 2009; Coles et al., 2020). The average speed and distance were analysed throughout acquisition and reversal learning. At probe tests, the time spent in the different CB zones (i.e., board was separated into 8 equal zones, corresponding with the lines of wells) and the average speed and distance travelled were measured by Any-Maze™ software.

2.4.3 Elevated plus maze (EPM)

The EPM assesses the natural conflict between the tendency of mice to explore a novel environment and their avoidance of a brightly lit, elevated, and open area (Montgomery, 1955). Methods have been described previously (Cheng et al., 2013; Cheng et al., 2014b). The '+' apparatus consisted of two alternate open arms (35 cm × 6 cm; without side walls) and two alternate enclosed arms (35 cm × 6 cm; height of enclosing walls 28 cm) connected by a central platform (6 cm × 6 cm), elevated 70 cm above the floor. Mice were placed at the centre of the '+' of the grey PVC plus maze, facing an enclosed arm, and were allowed to explore the maze for 5 min. The time spent on open arms, entries into the open arms, and the distance travelled on the open and enclosed arms were recorded by AnyMaze™ tracking software.

2.4.4 Novel object recognition test

The innate preference of a mouse for novelty and its ability to distinguish a novel object from a familiar object (Dere et al., 2007) are utilised in the NORT. The NORT was conducted over 3 days [methods: (Cheng et al., 2014a)]. Two 10-min trials were conducted per day, with a 1 h ITI. On day 1, mice were habituated to the empty arena during both trials. On day 2, mice were habituated to the empty arena during trial 1 and to two identical objects during trial 2. On the test day (day 3), mice were exposed to two identical objects in the training trial (objects distinct from day 2) and then one familiar and one novel object in the test trial. The objects used were a mini Rubik's cube and a plastic garden hose nozzle. The objects and their locations were counterbalanced across genotypes and treatment groups. Time spent *nosing* and *rearing* on the objects was recorded by AnyMaze™ tracking software and confirmed by manual scoring. The percentage of time spent *nosing* the novel object indicated short-term object recognition memory (% novel object recognition) and was calculated using [(novel object *nosing* time/ novel + familiar object *nosing* time) × 100]. The percentage of time spent *nosing* and *rearing* was combined to create an "*exploration*" score, and the percentage of novel object *exploration* was calculated in the same way as % *nosing*.

2.5 Statistical analysis

Data were analysed using SPSS Statistics 25 (IBM, NY, United States). Three- and two-way repeated measures (RM) analysis of variance (ANOVA) with within factors "minutes" (FC) or "cue" (FC) and between factors "genotype" (WT vs. *APPxPS1*) and "treatment" (VEH vs. CBD 20 mg/kg) was conducted. Where interactions were found, we conducted subsequent two- and one-way ANOVA split by the corresponding factor, as published previously (Long et al., 2012; Cheng et al., 2014a; Cheng et al., 2014c; Coles et al., 2020; Watt et al., 2020a). *Post hoc* effects are shown in figures only. Data from fear conditioning and cheeseboard were analysed with three-way ANOVA but are presented in separate graphs for visual clarity.

Data for the FC cue test were also analysed as total *freezing* in the 2 min prior to tone presentation, the 5 min during tone presentation, and the 2 min post-tone. Data for NORT, CB probe, and CB reversal probe tests were analysed using single-sample t-tests comparing data to the chance level for each test (Cheng et al., 2013; Cheng et al., 2014b; Coles et al., 2020). The chance level for NORT is 50% (1/2 objects), and for CB, it is 12.5% (1/8 zones). Data were presented as mean ± SEMs, and differences were regarded as statistically significant if $p < 0.05$.

Exclusions: FC: one WT CBD-treated mouse was excluded due to high baseline *freezing* (>2.5 SDs above the mean for that group). CB: three mice (1x WT VEH, 2x *APPxPS1* CBD) were excluded from the CB analysis as their latency to find the food reward did not decrease across days (i.e., stayed at 120 s for the 7 days of training), so they did not engage with the paradigm.

3 Results

3.1 Fear conditioning

There were no "genotype" or "treatment" differences in baseline *freezing* during conditioning (i.e., the first 2 min of the test), indicating baseline genotype or treatment differences did not confound the interpretation of subsequent analyses (all "treatment" and "genotype" p-values > 0.05; Table 1). During acquisition of fear conditioning, all mice increased their *freezing* behaviour as the test progressed, indicating acquisition of the tone-shock association ["minutes" $F(6,306) = 40.3$, $p < 0.0001$]. Although there was no overall effect of "treatment" on *freezing* [$F(1,52) = 1.0$, $p = 0.3$; no "treatment" interactions, all p-values > 0.05], a "minutes" by "genotype" interaction was detected [$F(6,306) = 2.5$, $p = 0.02$]. However, when split by "genotype", both genotypes increased their *freezing* as the test progressed, irrespective of CBD treatment (all "time" p-values < 0.0001, no main "treatment" main effects, or interactions with 'treatment') (Figures 1A,B).

In the context test, there were no effects of "genotype" [$F(1,51) = 0.7$, $p = 0.4$] or "treatment" [$F(1,51) = 2.3$, $p = 0.1$] on *freezing* in the shock-associated environment, and no interactions were detected (all p-values > 0.05) (Figures 1C,D). All mice, regardless of treatment or genotype, showed higher levels of *freezing* earlier in the test, which decreased as the test progressed ["minutes" $F(6,306) = 6.8$, $p < 0.0001$; no interactions] (Figures 1C,D).

During the cue test, there were no overall effects of "genotype" [$F(1,51) = 0.1$, $p = 0.9$] or "treatment" [$F(1,51) = 0.1$, $p = 0.8$]. There was an interaction between "minutes" × "treatment" [$F(8,408) = 2.2$, $p = 0.02$], suggesting CBD-treated animals *froze* less than VEH-treated animals, particularly in the 2nd half of the test, although follow-up analyses splitting by corresponding factors revealed no further significant differences (all p-values > 0.1) (Figures 1E,F). When data were analysed according to total time spent *freezing* pre-cue, during cue presentation, and post-cue, there were no effects of "genotype" or "treatment" and no interactions (all p-values > 0.05, Table 2).

3.2 Cheeseboard

3.2.1 Acquisition

Averaging latency to find the food reward from all three trials on each day, we found that all experimental groups reduced their latency during acquisition, indicating they learnt the location of the food reward ["days" $F(6,294) = 102.1$, $p < 0.0001$]. Generally,

TABLE 1 Freezing during fear conditioning. Percentage of *freezing* within each time block [%] during the first 2 min on conditioning day and during the cue test.

Measure	WT VEH	WT CBD	*APPxPS1* VEH	*APPxPS1* CBD
Baseline *freezing* (first 2 min of conditioning)	1.00 ± 0.42	1.25 ± 0.50	0.58 ± 0.25	1.83 ± 1.08
Cue test: *freezing* pre-cue	17.92 ± 2.33	25.25 ± 4.92	17.25 ± 3.08	19.25 ± 4.83
Cue test: *freezing* during cue	22.37 ± 3.87	27.53 ± 4.13	29.40 ± 4.13	22.30 ± 3.73
Cue test: *freezing* post-cue	16.5 ± 4.00	24.58 ± 4.75	24.58 ± 4.75	13.92 ± 2.42

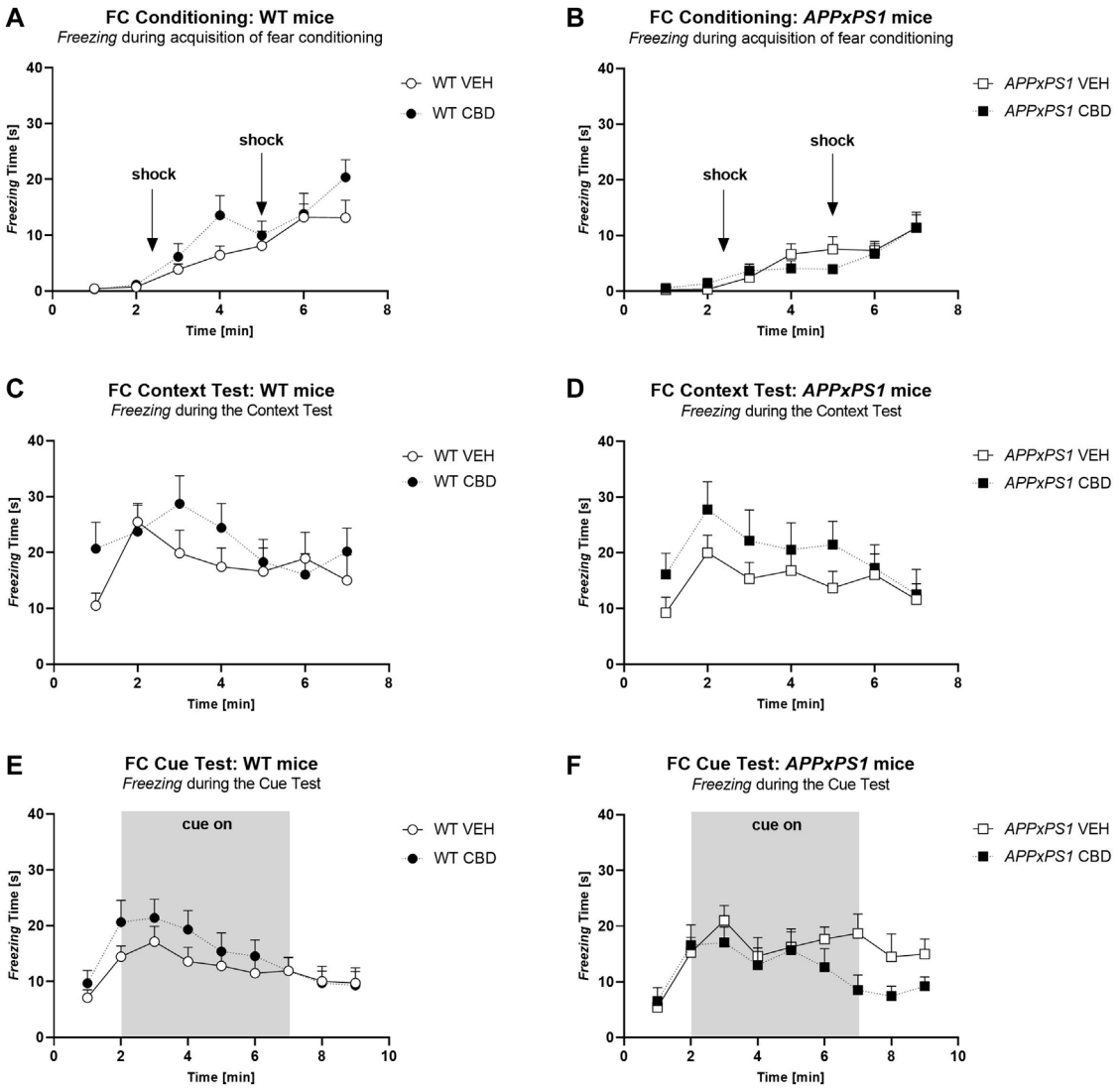

FIGURE 1
Freezing time [s] during **(A,B)** acquisition of fear conditioning, **(C,D)** context test, and **(E,F)** cue test in *APPxPS1* and WT female mice treated daily with 20 mg/kg CBD or VEH for 8 months. Interactions were present in (A, B) between "minutes" × "genotype" (p = 0.02) and in **(E,F)** between "minutes" × "treatment" (p = 0.02). Data were analysed using three-way RM ANOVA and presented as mean ± SEM in separate graphs for visual clarity. N = 14 WT VEH, 16 *APPxPS1* VEH, 14 WT CBD, and 13 *APPxPS1* CBD. Abbreviations: *APPxPS1*: *amyloid precursor protein x presenilin 1*; CBD: cannabidiol; VEH: vehicle; WT: wildtype-like.

TABLE 2 Open arm measures in the elevated plus maze test. Open arm entries [n] and the open arm distance ratio [%] in WT and *APPxPS1* mice, following chronic treatment with a vehicle or 20 mg/kg CBD. Data presented as mean ± SEM.

Measure	WT VEH	WT CBD	*APPxPS1* VEH	*APPxPS1* CBD
Open arm entries [n]	4.57 ± 1.48	3.93 ± 1.19	2.47 ± 0.67	2.08 ± 0.79
Open arm distance ratio [%]	5.25 ± 2.02	9.73 ± 3.1	8 ± 4.31	5.66 ± 3.15

APPxPS1 mice had longer latencies than WT mice ["genotype" F (1,49) = 5.7, $p = 0.02$]. The latency improved across days to match control levels by the last 2 days of training ["days" × "genotype" F (6,294) = 2.5, $p = 0.02$]. CBD treatment did not influence the average latency to find the food reward during acquisition ["treatment" F (1,49) = 3.1, $p = 0.09$; no "treatment" interactions]. We explored these data further with two-way ANOVA split by "genotype", which showed longer latencies in VEH-treated *APPxPS1* mice than CBD-treated *APPxPS1* mice ["treatment" F (1,24) = 5.1, $p = 0.03$] but not in WT mice [F (1,25) = 0.1, $p = 0.9$] (Figures 2A,B). Follow-up analyses split by "treatment" in WT mice revealed no further significant differences (all p-values > 0.1).

Similarly, examination of intermediate-term memory revealed that *APPxPS1* mice had longer latencies than WT mice ["genotype" F (1,49) = 8.0, $p = 0.007$], which was more prominent earlier in acquisition ["days" × "genotype" F (6,294) = 3.2, $p = 0.004$]. Overall, CBD had no effect on intermediate-term memory ["treatment" [F (1,49) = 2.8, $p = 0.1$; no "treatment" interactions]. Split by "genotype," CBD reduced intermediate-term memory latencies specifically in *APPxPS1* mice ["treatment" F (1,24) = 4.6, $p = 0.04$] but not in WT mice [F (1,25) = 0.1, $p = 0.9$] (Figures 2C,D). Follow-up ANOVA split by "days" revealed no further significant differences (all p-values > 0.1). Long-term memory was not different between the genotypes or treatment groups (all "genotype" or "treatment" main effects and interaction p-values > 0.05, Supplementary Figures S1A,B).

The speed of mice was also assessed. *APPxPS1* mice were slower than WT controls across days ["days" × "genotype" F (6,294) = 2.6, $p = 0.02$], and CBD treatment affected speed as well ["days" × "treatment" F (6,294) = 3.2, $p = 0.005$] (Figures 2E,F). Split by "genotype," in *APPxPS1* mice, there was a "days" × "treatment" interaction [F (6,144) = 3.4, $p = 0.003$], suggesting *APPxPS1* VEH mice were slower than CBD-treated *APPxPS1* mice in the first half of acquisition, but *APPxPS1* VEH mice were faster than *APPxPS1* CBD mice by the end of training (Figure 2F). We split by "day" and confirmed "treatment" effects on day 1 only ($p = 0.02$). Similarly, split by "treatment", VEH-treated *APPxPS1* mice were initially slower than VEH-treated WT mice, but this reached WT levels by mid-training ["genotype" F (1,27) = 5.6, $p = 0.03$; "days" × "genotype" F (6,162) = 2.6, $p = 0.02$]. Splitting by "day" confirmed "genotype" differences on days 1–3 (p-values < 0.02). This speed difference was not evident in CBD-treated *APPxPS1* mice (no "genotype" or "days" × "genotype" interaction, all p-values > 0.2). *APPxPS1* VEH mice were slower than WT VEH or *APPxPS1* CBD mice only on days 1–3 of acquisition (Figures 2E,F). No other significant differences were detected.

The distance travelled during acquisition is presented in the Supplementary Results section (see also Supplementary Figure S1).

3.2.2 Probe

At probe, all groups spent more time in the target zone than by chance [WT VEH: t = 2.7, df = 12, $p = 0.03$; *APPxPS1* VEH: t = 3.8, df = 15, $p = 0.002$; WT CBD: t = 2.4, df = 13, $p = 0.03$; *APPxPS1* CBD: t = 2.4, df = 9, $p = 0.04$] (Figure 3A).

Data for reversal learning and reversal probe are presented in the Supplementary Results section (see also Supplementary Figures S2–S4).

3.3 EPM

APPxPS1 mice showed more anxiety-like behaviour in the EPM, evidenced by a reduced percentage of time spent in the open arms ["genotype" F (1,51) = 4.3, $p = 0.04$] (Figure 4A). "CBD treatment" did not affect the percentage of open arm time ["treatment" F (1,51) = 0.09, $p = 0.8$; no interaction]. Open arm entries and open arm distance ratios were unaffected by the "genotype" or "treatment" (all main effect and interaction p-values > 0.05; Table 2). Although there was no overall effect of the "genotype" or "treatment" on the total distance travelled in the EPM, a "genotype" x "treatment" interaction [F (1,51) = 9.2, $p = 0.004$] indicates chronic CBD increased locomotion in *APPxPS1* mice but not in WT mice (Figure 4B). This was confirmed when data were split by the "genotype": CBD increased locomotion in *APPxPS1* mice ["treatment" F (1,25) = 7.9, $p = 0.009$] but not WT mice ["treatment" F (1.26) = 2.4, $p = 0.1$]. Also, when data were split by "treatment," there was a main effect of the "genotype" in CBD-treated mice [F (1,24) = 6.1, $p = 0.02$] but not VEH-treated mice [F (1,27) = 3.4, $p = 0.08$], suggesting greater distance travelled in CBD-treated *APPxPS1* mice than CBD-treated WT mice (Figure 4B).

3.4 NORT

The NORT data are presented in Supplementary Figure S5 as WT VEH-treated mice did not

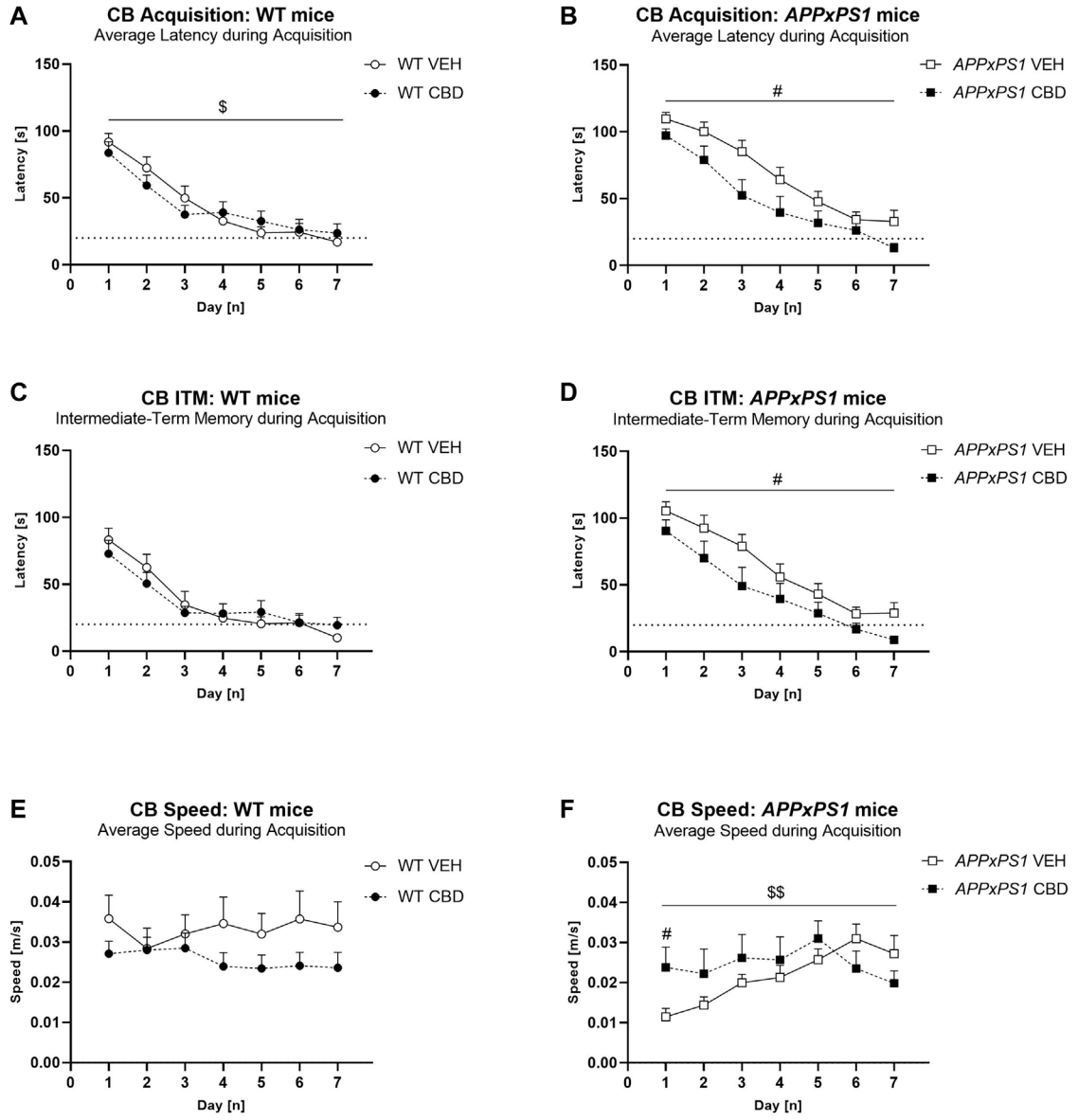

FIGURE 2
Long-term CBD improves average latency, intermediate-term memory latency, and speed during cheeseboard acquisition in APPxPS1 female mice. Latency [s] and speed [m/s] when finding the food reward in the cheeseboard in *APPxPS1* and WT mice treated daily with 20 mg/kg CBD for 8 months. **(A,B)** Average latency [s] to find the food reward (averaged across 3 trials per day) during acquisition of the cheeseboard task. **(C,D)** Intermediate-term memory latency [s] (i.e., average latency for trials 2 and 3 of each day) during acquisition. **(E,F)** Average speed [m/s] (averaged across three trials per day) during cheeseboard acquisition. The dotted line in **(A–D)** indicates the 20-s cut-off threshold for acquisition. In **(A,B),** a "days" × "genotype" interaction ($p = 0.02$) was detected, and in **(C,D),** a "days" × "genotype" interaction ($p = 0.004$) was detected. In (**E,F**), a "days" × "treatment" interaction was detected; when split by "treatment," there was a "days" × "genotype" interaction ($p = 0.02$) in VEH-treated mice. Splitting by "day" confirmed "genotype" differences on days 1–3 (p-values < 0.02). Data analysed using three-way RM ANOVA and presented as mean ± SEM in separate graphs for visual clarity. When data were split by the corresponding factor, significant "treatment" effects in *APPxPS1* mice are indicated by hash symbols ($^{\#}p < 0.05$); interactions between "treatment" and "days" are indicated by '$' ($^{\$}p < 0.05$; $^{\$\$}p < 0.01$). N = 13 WT VEH, 16 *APPxPS1* VEH, 14 WT CBD, and 10 *APPxPS1* CBD. Abbreviations: *APPxPS1*: *amyloid precursor protein x presenilin 1*; CB: cheeseboard; CBD: cannabidiol; ITM: intermediate-term memory; VEH: vehicle; WT: wildtype-like.

demonstrate novel object recognition (i.e. > 50% time *nosing* the novel object) [see a similar lack of object preference: (Kreilaus et al., 2019)] despite this protocol producing significant object novelty recognition in female *APPxPS1* mice previously in our laboratory (Cheng et al., 2014b).

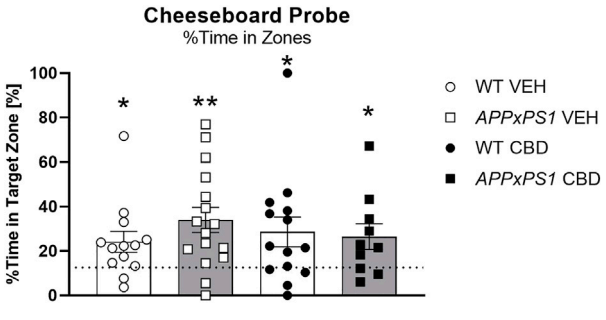

FIGURE 3
No effect of long-term CBD on recall of spatial memory. Percentage [%] of time spent in the target zone at A probe test in *APPxPS1* and WT mice treated daily with 20 mg/kg CBD for 8 months. Data were analysed using a single sample t-test against chance levels, i.e., 12.5%, corresponding to 1/8 zones. Data presented as mean ± SEM. Significant t-tests against chance are indicated by asterisks (*$p < 0.05$; **$p < 0.01$). N = 13 WT VEH, 16 *APPxPS1* VEH, 14 WT CBD, and 10 *APPxPS1* CBD. Abbreviations: *APPxPS1*: *amyloid precursor protein x presenilin 1*; CBD: cannabidiol; VEH: vehicle; WT: wildtype-like.

4 Discussion

In the current study, we found that long-term preventative oral CBD improved spatial memory acquisition, which was accompanied by changes to speed and locomotion in female *APPxPS1* mice. No effects of CBD treatment were detected on reversal learning or the recall of previously rewarded locations in AD transgenic mice. CBD reduced *freezing*, following the presentation of a discrete cue associated with footshock in both genotypes. Long-term CBD increased the distance travelled in the EPM in *APPxPS1* females but did not affect anxiety-like behaviours in either genotype.

In the CB task, CBD improved the spatial learning of AD transgenic females. *APPxPS1* VEH mice had longer average and intermediate-term memory latencies to find the reward location than *APPxPS1* CBD mice. This effect was not evident in WT mice, suggesting CBD improved spatial learning specifically in AD-affected *APPxPS1* mice but not at baseline (i.e., WT mice), potentially aligning with its low side effect profile (Gaston and Szaflarski, 2018). Interestingly, CBD increased speed and distance travelled by *APPxPS1* mice in the early phases of CB learning (i.e., days 1–3), suggesting effects of CBD on spatial task acquisition may be linked to improved motor function. However, improved locomotion cannot account for all the spatial learning effects observed, as by the end of acquisition *APPxPS1* VEH mice had similar speed yet still slower latencies than *APPxPS1* CBD mice, suggesting *APPxPS1* CBD mice moved more directly to the rewarded location rather than simply moving faster. Strengthening this argument, slower reversal latencies in *APPxPS1* mice also did not correspond with slower speed.

The effects of CBD on motor function require further clarification as the CB and EPM are not traditionally utilised as primary measures for locomotor ability. There are currently no reports of improved locomotor activity by chronic CBD in mouse models of dementia (Cheng et al., 2014a, Cheng et al., 2014c, Coles et al., 2020, de Paula Faria et al., 2022; Khodadadi et al., 2021; Kreilaus et al., 2022; Watt et al., 2020b), and indeed, inconsistent effects of acute and chronic CBD on locomotor activity across a variety of neurological models have been found (reviewed in Calapai et al., 2022). Interestingly, locomotor impairment can occur in some individuals with AD (Scarmeas et al., 2004) and may be linked to *PS1* mutations (Ryan et al.,

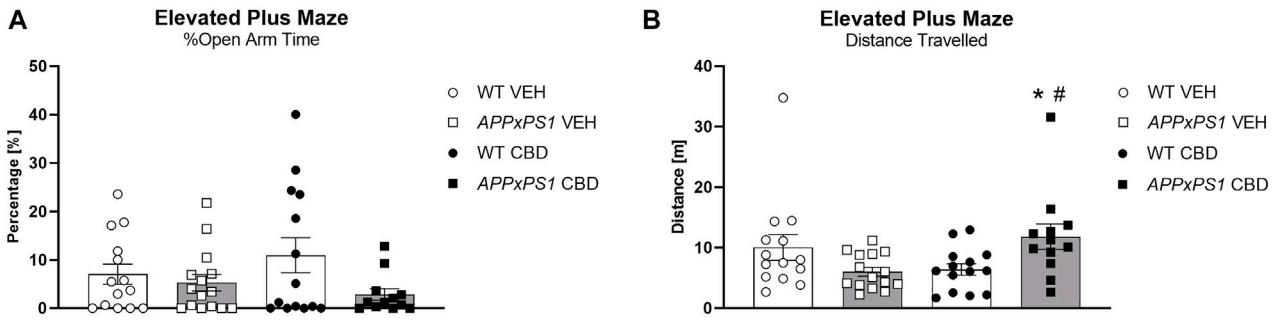

FIGURE 4
Increased locomotion but unaltered anxiety-like behaviour in *APPxPS1* mice in the elevated plus maze test, following long-term CBD. **(A)** Distance travelled [m] and **(B)** percentage of open arm time [%] in the elevated plus maze test in *APPxPS1* and WT mice treated daily with 20 mg/kg CBD for 8 months. A main effect of "genotype" ($p = 0.04$) was detected in **(A)**. A "genotype" x "treatment" interaction ($p = 0.004$) was detected in **(B)**. Data were analysed using two-way RM ANOVA and presented as mean ± SEM. When data were split by the corresponding factor, significant "genotype" effects in CBD-treated mice are indicated by asterisks (*$p < 0.05$, vs. WT CBD), and significant "treatment" effects in *APPxPS1* mice are indicated by hash symbols ($^{\#}p < 0.05$, vs. *APPxPS1* VEH). N = 14 WT VEH, 15 *APPxPS1* VEH, 14 WT CBD, and 12 *APPxPS1* CBD. Abbreviations: *APPxPS1*: *amyloid precursor protein x presenilin 1*; CBD: cannabidiol; VEH: vehicle; WT: wildtype-like.

2016), which may explain some of the locomotor changes observed here in *APPxPS1* mice.

Despite improvements in spatial learning, CBD had no effect on the recall of spatial learning at probe or reversal probe. This reflects previous reports where chronic CBD did not affect spatial memory recall in the CB (Coles et al., 2020; Watt et al., 2020a). We also found no effect of CBD on reversal learning, suggesting oral preventive CBD may not improve performance once the task has been learnt and suggesting only specific cognitive domains may be ameliorated by preventative oral CBD.

The finding of improved spatial learning by CBD is similar to other reports investigating remedial CBD treatment in AD mouse models (i.e., treatment started after spatial learning deficits were present; Amini and Abdolmaleki, 2022; Coles et al., 2020; Martin-Moreno et al., 2011; Watt et al., 2020a). Importantly, ours is the first study to show that long-term CBD can *prevent* the development of some spatial learning deficits in female AD transgenic mice, suggesting CBD may have the potential to *prevent* cognitive impairment in both men (Cheng et al., 2014c) and women. Considering a preventative approach may limit the development or severity of AD pathology and symptoms, our results demonstrate some utility of preventive CBD, although the moderate nature of our findings suggests that preventive CBD may not be as effective as remedial CBD (see Amini and Abdolmaleki, 2022; Coles et al., 2020; Cheng et al., 2014a; Martin-Moreno et al., 2011; Watt et al., 2020a). It is also possible that a higher preventive oral CBD dose may have resulted in more pronounced effects on spatial learning. Nonetheless, by using an oral route of CBD administration in this study and previous work (Cheng et al., 2014c), we provide data which are highly clinically relevant as oral administration is clinically preferable to intravenous or intramuscular injections, and using an oral route significantly boosts the translational power of our findings.

Long-term oral CBD treatment reduced *freezing* in the cue test of all females, regardless of the genotype. Although it is well established that acute systemic CBD can impair fear memory consolidation (Han et al., 2022; Shallcross et al., 2019; review: Stern et al., 2018), including in female mice (Montoya et al., 2020), effects of chronic CBD on fear memory have had limited investigation, and chronic CBD does not affect fear memory acquisition (Cheng et al., 2014a; 2014c). Considering CBD-induced differences in *freezing* were very limited in this study, future research should consider evaluating the effects of long-term CBD on fear learning in female mice.

Chronic CBD had no effect on anxiety-like behaviours in the EPM, and this corresponds with previous reports. Although the anxiolytic-like effects of acute systemic CBD are well established [reviews: (Blessing et al., 2015; Wright et al., 2020)], the anxiolytic-like effects of chronic CBD are less clear. Chronic low-dose CBD (up to 30 mg/kg) does not affect anxiety-like behaviour in the EPM in *APPxPS1* male mice (Cheng et al., 2014a; Cheng et al., 2014c) or in outbred rats and mice (Schiavon et al., 2016; Murphy et al., 2017; Gall et al., 2020). However, high-dose chronic CBD (30-100 mg/kg i. p. or subcutaneous, s. c.) can decrease anxiety-like behaviour in the EPM in mice (Long et al., 2012; Fogaca et al., 2018; Patra et al., 2020). It is possible that higher doses of CBD are necessary for anxiolytic-like effects, following long-term administration. Also, most studies use systemic injections (i.p. or s.c.) to evaluate the anxiolytic effects of CBD (Long et al., 2012; Schiavon et al., 2016; Murphy et al., 2017; Fogaca et al., 2018; Gall et al., 2020; Patra et al., 2020), and it is unknown if the oral route may alter CBD's effects on anxiety-like behaviour.

The mechanisms by which CBD exerts pro-cognitive effects are poorly understood, but recent reports suggest potential mechanisms. Chronic CBD can enhance the immune response and increase hippocampal autophagy in *APPxPS1* mice (Hao and Feng, 2021). An enhanced immune response by CBD may also drive increased microglial migration and reduced nitrite generation (Martin-Moreno et al., 2011), which can facilitate Aβ phagocytosis and decrease hippocampal Aβ plaque load, thus improving cognition in *APPxPS1* mice (Watt et al., 2020a; Hao and Feng, 2021). Alternatively, it is possible that CBD ameliorates hippocampal synaptic plasticity deficits to improve spatial learning as CBD pretreatment prevents $A\beta_{1-42}$-mediated LTP deficits in mouse hippocampal slices (Hughes and Herron, 2019). Examining the brain pathology in these mice to determine the mechanism/s of CBD in this instance would be a valuable focus for future research studies.

It is possible there are sex differences in the effects of CBD on cognition in *APPxPS1* mice. In the present study, long-term CBD reversed spatial learning impairment in female *APPxPS1* mice, while in male *APPxPS1* mice, long-term CBD reversed social recognition impairment (Cheng et al., 2014c). It should be noted that male and female *APPxPS1* mice show deficits in different cognitive behavioural domains (Cheng et al., 2013; Cheng et al., 2014b; Richetin et al., 2017), and this is why the behavioural tests conducted in the present study were not identical to those conducted in male *APPxPS1* mice treated with long-term oral CBD (Cheng et al., 2014c). Nonetheless, it is possible that CBD could have sex-specific effects on cognition, and this may be related to sex-specific differences in hippocampal dendritic spine density. Hippocampal dendritic spine density is reduced in female *APPxPS1* mice compared to WT female mice, where this effect is not as pronounced in male *APPxPS1* mice (Richetin et al., 2017). Dendritic spine density is associated with spatial memory function (Mahmmoud et al., 2015), and CBD can ameliorate stress-induced reductions in the hippocampal spine density in mice (Fogaca et al., 2018). Thus, in female *APPxPS1* mice, CBD may increase the hippocampal dendritic spine density to improve spatial memory.

A final consideration for the current study is that of the administration route. This study and others (Cheng et al., 2014c) gave 20 mg/kg CBD orally, whereas other work has administered 20 mg/kg CBD i. p. (Cheng et al., 2014a). In mice, i.

p. administration leads to a faster peak brain concentration of CBD than oral administration (Deiana et al., 2012), and the plasma concentration of i. v. CBD is consistently higher than oral CBD for up to 24 h post-administration (Xu et al., 2019). The bioavailability of i. v. or i. p. CBD is close to 100% (Zgair et al., 2016; Xu et al., 2019), whereas oral CBD is 8.6% (Xu et al., 2019). This suggests a faster and more potent effect of i. p. CBD than oral CBD even at the same CBD dose, which may explain why the effects of oral CBD are not as pronounced as for i. p. CBD, e.g., i. p. CBD reversed both object and social memory impairment in male *APPxPS1* mice (Cheng et al., 2014a), but oral CBD only reversed social memory impairment in male mice (Cheng et al., 2014c).

In conclusion, we found moderate effects of long-term oral CBD treatment on the acquisition of spatial learning by CBD in a female mouse model of familial AD. This suggests that *preventive* CBD may help limit some cognitive impairment in women with AD.

Data availability statement

The original contributions presented in the study are included in the article/Supplementary Material; further inquiries can be directed to the corresponding author.

Ethics statement

The animal study was reviewed and approved by the University of New South Wales Animal Care and Ethics Committee.

Author contributions

DC and TK designed the research. DC ran all the experiments. DC, RC, and CS conducted the data analysis. RC wrote the manuscript. RC and TK edited the manuscript.

Funding

TK was supported by two project grants from the National Health and Medical Research Council (NHMRC: #1102012 and #1141789) and the NHMRC dementia research team initiative (#1095215). RC and TK were supported by the Ainsworth Medical Research Innovation Fund. In addition, RC was supported by the Rebecca Cooper Medical Research Foundation (Project Grant PG2020883). DC received an Australian Postgraduate Award scholarship from the University of New South Wales and a supplementary scholarship provided by Neuroscience Research Australia.

Acknowledgments

We thank JacKee Low and Warren Logge (Neuroscience Research Australia, Randwick, Australia) for assisting in the treatment of our test mice and the staff of Australian BioResources and Adam Bryan at Neuroscience Research Australia for taking care of our test mice. We thank Jerry Tanda for critical comments on the manuscript.

Conflict of interest

The authors declare that the research was conducted in the absence of any commercial or financial relationships that could be construed as a potential conflict of interest.

The handling editor HL declared a past collaboration with the author TK.

Publisher's note

Supplementary material

The Supplementary Material for this article can be found online at: https://www.frontiersin.org/articles/10.3389/fphar.2022.931384/full#supplementary-material.

References

Amini, M., and Abdolmaleki, Z. (2022). The effect of cannabidiol coated by nano-chitosan on learning and memory, hippocampal CB1 and CB2 levels, and amyloid plaques in an Alzheimer's disease rat model. *Neuropsychobiology* 81 (3), 171–183. doi:10.1159/000519534

Aso, E., Sanchez-Pla, A., Vegas-Lozano, E., Maldonado, R., and Ferrer, I. (2015). Cannabis-based medicine reduces multiple pathological processes in AβPP/PS1 mice. *J. Alzheimers Dis.* 43, 977–991. doi:10.3233/JAD-141014

Blessing, E. M., Steenkamp, M. M., Manzanares, J., and Marmar, C. R. (2015). Cannabidiol as a potential treatment for anxiety disorders. *Neurotherapeutics* 12, 825–836. doi:10.1007/s13311-015-0387-1

Bloom, G. S. (2014). Amyloid-beta and tau: The trigger and bullet in alzheimer disease pathogenesis. *JAMA Neurol.* 71, 505–508. doi:10.1001/jamaneurol.2013.5847

Borchelt, D. R., Ratovitski, T., van Lare, J., Lee, M. K., Gonzales, V., Jenkins, N. A., et al. (1997). Accelerated amyloid deposition in the brains of transgenic mice coexpressing mutant presenilin 1 and amyloid precursor proteins. *Neuron* 19 (4), 939–945. doi:10.1016/s0896-6273(00)80974-5

Braak, H., and Braak, E. (1991). Neuropathological stageing of Alzheimer-related changes. *Acta Neuropathol.* 82, 239–259. doi:10.1007/BF00308809

Calapai, F., Cardia, L., Calapai, G., Di Mauro, D., Trimarchi, F., Ammendolia, I., et al. (2022). Effects of cannabidiol on locomotor activity. *Life (Basel)* 12 (5), 652. doi:10.3390/life12050652

Campos, A. C., Fogaca, M. V., Sonego, A. B., and Guimaraes, F. S. (2016). Cannabidiol, neuroprotection and neuropsychiatric disorders. *Pharmacol. Res.* 112, 119–127. doi:10.1016/j.phrs.2016.01.033

Cao, D., Lu, H., Lewis, T. L., and Li, L. (2007). Intake of sucrose-sweetened water induces insulin resistance and exacerbates memory deficits and amyloidosis in a transgenic mouse model of Alzheimer disease. *J. Biol. Chem.* 282 (50), 36275–36282. doi:10.1074/jbc.M703561200

Chen, Z., and Zhong, C. (2014). Oxidative stress in Alzheimer's disease. *Neurosci. Bull.* 30, 271–281. doi:10.1007/s12264-013-1423-y

Cheng, D., Logge, W., Low, J. K., Garner, B., and Karl, T. (2013). Novel behavioural characteristics of the APP(Swe)/PS1ΔE9 transgenic mouse model of Alzheimer's disease. *Behav. Brain Res.* 245, 120–127. doi:10.1016/j.bbr.2013.02.008

Cheng, D., Low, J. K., Logge, W., Garner, B., and Karl, T. (2014a). Chronic cannabidiol treatment improves social and object recognition in double transgenic APPswe/PS1E9 mice. *Psychopharmacol. Berl.* 231, 3009–3017. doi:10.1007/s00213-014-3478-5

Cheng, D., Low, J. K., Logge, W., Garner, B., and Karl, T. (2014b). Novel behavioural characteristics of female APPSwe/PS1ΔE9 double transgenic mice. *Behav. Brain Res.* 260, 111–118. doi:10.1016/j.bbr.2013.11.046

Cheng, D., Spiro, A. S., Jenner, A. M., Garner, B., and Karl, T. (2014c). Long-term cannabidiol treatment prevents the development of social recognition memory deficits in Alzheimer's disease transgenic mice. *J. Alzheimers Dis.* 42, 1383–1396. doi:10.3233/JAD-140921

Coles, M., Watt, G., Kreilaus, F., and Karl, T. (2020). Medium-dose chronic cannabidiol treatment reverses object recognition memory deficits of *APP_{Swe}/PS1ΔE9* transgenic female mice. *Front. Pharmacol.* 11, 587604. doi:10.3389/fphar.2020.587604

de Paula Faria, D., Estessi de Souza, L., Duran, F. L. S., Buchpiguel, C. A., Britto, L. R., Crippa, J. A. S., et al. (2022). Cannabidiol treatment improves glucose metabolism and memory in streptozotocin-induced Alzheimer's disease rat model: A proof-of-concept study. *Int. J. Mol. Sci.* 23 (3), 1076. doi:10.3390/ijms23031076

Deiana, S., Watanabe, A., Yamasaki, Y., Amada, N., Arthur, M., Fleming, S., et al. (2012). Plasma and brain pharmacokinetic profile of cannabidiol (CBD), cannabidivarine (CBDV), Δ^9-tetrahydrocannabivarin (THCV) and cannabigerol (CBG) in rats and mice following oral and intraperitoneal administration and CBD action on obsessive-compulsive behaviour. *Psychopharmacol. Berl.* 219, 859–873. doi:10.1007/s00213-011-2415-0

Dere, E., Huston, J. P., and De Souza Silva, M. A. (2007). The pharmacology, neuroanatomy and neurogenetics of one-trial object recognition in rodents. *Neurosci. Biobehav. Rev.* 31, 673–704. doi:10.1016/j.neubiorev.2007.01.005

Esposito, G., De Filippis, D., Carnuccio, R., Izzo, A. A., and Iuvone, T. (2006a). The marijuana component cannabidiol inhibits beta-amyloid-induced tau protein hyperphosphorylation through Wnt/beta-catenin pathway rescue in PC12 cells. *J. Mol. Med.* 84, 253–258. doi:10.1007/s00109-005-0025-1

Esposito, G., De Filippis, D., Maiuri, M. C., De Stefano, D., Carnuccio, R., and Iuvone, T. (2006b). Cannabidiol inhibits inducible nitric oxide synthase protein expression and nitric oxide production in beta-amyloid stimulated PC12 neurons through p38 MAP kinase and NF-kappaB involvement. *Neurosci. Lett.* 399, 91–95. doi:10.1016/j.neulet.2006.01.047

Esposito, G., Scuderi, C., Savani, C., Steardo, L., Jr., De Filippis, D., Cottone, P., et al. (2007). Cannabidiol *in vivo* blunts beta-amyloid induced neuroinflammation by suppressing IL-1beta and iNOS expression. *Br. J. Pharmacol.* 151, 1272–1279. doi:10.1038/sj.bjp.0707337

Fogaca, M. V., Campos, A. C., Coelho, L. D., Duman, R. S., and Guimaraes, F. S. (2018). The anxiolytic effects of cannabidiol in chronically stressed mice are mediated by the endocannabinoid system: Role of neurogenesis and dendritic remodeling. *Neuropharmacology* 135, 22–33. doi:10.1016/j.neuropharm.2018.03.001

Gall, Z., Farkas, S., Albert, A., Ferencz, E., Vancea, S., Urkon, M., et al. (2020). Effects of chronic cannabidiol treatment in the rat chronic unpredictable mild stress model of depression. *Biomolecules* 10, E801. doi:10.3390/biom10050801

Garcia-Baos, A., Puig-Reyne, X., Garcia-Algar, O., and Valverde, O. (2021). Cannabidiol attenuates cognitive deficits and neuroinflammation induced by early alcohol exposure in a mice model. *Biomed. Pharmacother.* 141, 111813. doi:10.1016/j.biopha.2021.111813

Gaston, T. E., and Szaflarski, J. P. (2018). Cannabis for the treatment of epilepsy: An update. *Curr. Neurol. Neurosci. Rep.* 18 (11), 73. doi:10.1007/s11910-018-0882-y

Gella, A., and Durany, N. (2009). Oxidative stress in Alzheimer disease. *Cell adh. Migr.* 3, 88–93. doi:10.4161/cam.3.1.7402

Gu, L., and Guo, Z. (2013). Alzheimer's Aβ42 and Aβ40 peptides form interlaced amyloid fibrils. *J. Neurochem.* 126, 305–311. doi:10.1111/jnc.12202

Han, X., Song, X., Song, D., Xie, G., Guo, H., Wu, N., et al. (2022). Comparison between cannabidiol and sertraline for the modulation of post-traumatic stress disorder-like behaviors and fear memory in mice. *Psychopharmacol. Berl.* 239 (5), 1605–1620. doi:10.1007/s00213-022-06132-6

Hao, F., and Feng, Y. (2021). Cannabidiol (CBD) enhanced the hippocampal immune response and autophagy of APP/PS1 Alzheimer's mice uncovered by RNA-seq. *Life Sci.* 264, 118624. doi:10.1016/j.lfs.2020.118624

Holmes, C. (2013). Review: Systemic inflammation and Alzheimer's disease. *Neuropathol. Appl. Neurobiol.* 39, 51–68. doi:10.1111/j.1365-2990.2012.01307.x

Hughes, B., and Herron, C. E. (2019). Cannabidiol reverses deficits in hippocampal LTP in a model of Alzheimer's disease. *Neurochem. Res.* 44, 703–713. doi:10.1007/s11064-018-2513-z

Iuvone, T., Esposito, G., Esposito, R., Santamaria, R., Di Rosa, M., and Izzo, A. A. (2004). Neuroprotective effect of cannabidiol, a non-psychoactive component from Cannabis sativa, on beta-amyloid-induced toxicity in PC12 cells. *J. Neurochem.* 89, 134–141. doi:10.1111/j.1471-4159.2003.02327.x

Janefjord, E., Maag, J. L., Harvey, B. S., and Smid, S. D. (2014). Cannabinoid effects on beta amyloid fibril and aggregate formation, neuronal and microglial-activated neurotoxicity *in vitro*. *Cell. Mol. Neurobiol.* 34, 31–42. doi:10.1007/s10571-013-9984-x

Jiao, S. S., Bu, X. L., Liu, Y. H., Zhu, C., Wang, Q. H., Shen, L. L., et al. (2016). Sex dimorphism profile of Alzheimer's disease-type pathologies in an APP/PS1 mouse model. *Neurotox. Res.* 29, 256–266. doi:10.1007/s12640-015-9589-x

Karl, T., Garner, B., and Cheng, D. (2017). The therapeutic potential of the phytocannabinoid cannabidiol for Alzheimer's disease. *Behav. Pharmacol.* 28, 142–160. doi:10.1097/FBP.0000000000000247

Khodadadi, H., Salles, E. L., Jarrahi, A., Costigliola, V., Khan, M. B., and Yu, J. C. (2021). Cannabidiol ameliorates cognitive function *via* regulation of IL-33 and TREM2 upregulation in a murine model of Alzheimer's disease. *J. Alzheimers Dis.* 80 (3), 973–977. doi:10.3233/JAD-210026

Kreilaus, F., Chesworth, R., Eapen, V., Clarke, R., and Karl, T. (2019). First behavioural assessment of a novel Immp2l knockdown mouse model with relevance for Gilles de la Tourette syndrome and Autism spectrum disorder. *Behav. Brain Res.* 374, 112057. doi:10.1016/j.bbr.2019.112057

Kreilaus, F., Przybyla, M., Ittner, L., and Karl, T. (2022). Cannabidiol (CBD) treatment improves spatial memory in 14-month-old female TAU58/2 transgenic mice. *Behav. Brain Res.* 425, 113812. doi:10.1016/j.bbr.2022.113812

Laws, K. R., Irvine, K., and Gale, T. M. (2018). Sex differences in Alzheimer's disease. *Curr. Opin. Psychiatry* 31, 133–139. doi:10.1097/YCO.0000000000000401

Lee, J., Howard, R. S., and Schneider, L. S. (2022). The current landscape of prevention trials in dementia. *Neurotherapeutics* 19 (1), 228–247. doi:10.1007/s13311-022-01236-5

Long, L. E., Chesworth, R., Huang, X. F., Wong, A., Spiro, A., Mcgregor, I. S., et al. (2012). Distinct neurobehavioural effects of cannabidiol in transmembrane domain neuregulin 1 mutant mice. *PLoS One* 7, e34129. doi:10.1371/journal.pone.0034129

Mahmmoud, R. R., Sase, S., Aher, Y. D., Sase, A., Groger, M., Mokhtar, M., et al. (2015). Spatial and working memory is linked to spine density and mushroom spines. *PLoS One* 10, e0139739. doi:10.1371/journal.pone.0139739

Martin-Moreno, A. M., Reigada, D., Ramirez, B. G., Mechoulam, R., Innamorato, N., Cuadrado, A., et al. (2011). Cannabidiol and other cannabinoids reduce microglial activation *in vitro* and *in vivo*: Relevance to Alzheimer's disease. *Mol. Pharmacol.* 79, 964–973. doi:10.1124/mol.111.071290

McGeer, P. L., Rogers, J., and Mcgeer, E. G. (2016). Inflammation, antiinflammatory agents, and Alzheimer's disease: The last 22 years. *J. Alzheimers Dis.* 54, 853–857. doi:10.3233/JAD-160488

Medeiros, A. M., and Silva, R. H. (2019). Sex differences in Alzheimer's disease: Where do we stand? *J. Alzheimers Dis.* 67, 35–60. doi:10.3233/JAD-180213

Montgomery, K. C. (1955). The relation between fear induced by novel stimulation and exploratory behavior. *J. Comp. Physiol. Psychol.* 48, 254–260. doi:10.1037/h0043788

Montoya, Z. T., Uhernik, A. L., and Smith, J. P. (2020). Comparison of cannabidiol to citalopram in targeting fear memory in female mice. *J. Cannabis Res.* 2 (1), 48. doi:10.1186/s42238-020-00055-9

Murphy, M., Mills, S., Winstone, J., Leishman, E., Wager-Miller, J., Bradshaw, H., et al. (2017). Chronic adolescent d9-tetrahydrocannabinol treatment of male mice leads to long-term cognitive and behavioral dysfunction, which are prevented by concurrent cannabidiol treatment. *Cannabis Cannabinoid Res.* 2, 235–246. doi:10.1089/can.2017.0034

Osborne, A. L., Solowij, N., Babic, I., Huang, X. F., and Weston-Green, K. (2017). Improved social interaction, recognition and working memory with cannabidiol treatment in a prenatal infection (poly I:C) rat model. *Neuropsychopharmacology* 42 (7), 1447–1457. doi:10.1038/npp.2017.40

Osborne, A. L., Solowij, N., Babic, I., Lum, J. S., Huang, X. F., Newell, K. A., et al. (2019). Cannabidiol improves behavioural and neurochemical deficits in adult female offspring of the maternal immune activation (poly I:C) model of neurodevelopmental disorders. *Brain Behav. Immun.* 81, 574–587. doi:10.1016/j.bbi.2019.07.018

Patra, P. H., Serafeimidou-Pouliou, E., Bazelot, M., Whalley, B. J., Williams, C. M., and Mcneish, A. J. (2020). Cannabidiol improves survival and behavioural co-morbidities of Dravet syndrome in mice. *Br. J. Pharmacol.* 177, 2779–2792. doi:10.1111/bph.15003

Reiserer, R. S., Harrison, F. E., Syverud, D. C., and McDonald, M. P. (2007). Impaired spatial learning in the APPSwe + PSEN1DeltaE9 bigenic mouse model of Alzheimer's disease. *Genes Brain Behav.* 6 (1), 54–65. doi:10.1111/j.1601-183X.2006.00221.x

Richetin, K., Petsophonsakul, P., Roybon, L., Guiard, B. P., and Rampon, C. (2017). Differential alteration of hippocampal function and plasticity in females and males of the APPxPS1 mouse model of Alzheimer's disease. *Neurobiol. Aging* 57, 220–231. doi:10.1016/j.neurobiolaging.2017.05.025

Rivers-Auty, J., Mather, A. E., Peters, R., Lawrence, C. B., and Brough, D. (2020). Anti-inflammatories in Alzheimer's disease-potential therapy or spurious correlate? *Brain Commun.* 2, fcaa109. doi:10.1093/braincomms/fcaa109

Ryan, N. S., Nicholas, J. M., Weston, P. S. J., Liang, Y., Lashley, T., Guerreiro, R., et al. (2016). Clinical phenotype and genetic associations in autosomal dominant familial Alzheimer's disease: A case series. *Lancet. Neurol.* 15 (13), 1326–1335. doi:10.1016/S1474-4422(16)30193-4

Scarmeas, N., Hadjigeorgiou, G. M., Papadimitriou, A., Dubois, B., Sarazin, M., Brandt, J., et al. (2004). Motor signs during the course of Alzheimer disease. *Neurology* 63 (6), 975–982. doi:10.1212/01.wnl.0000138440.39918.0c

Schiavon, A. P., Bonato, J. M., Milani, H., Guimaraes, F. S., and Weffort De Oliveira, R. M. (2016). Influence of single and repeated cannabidiol administration on emotional behavior and markers of cell proliferation and neurogenesis in non-stressed mice. *Prog. Neuropsychopharmacol. Biol. Psychiatry* 64, 27–34. doi:10.1016/j.pnpbp.2015.06.017

Scuderi, C., Filippis, D. D., Iuvone, T., Blasio, A., Steardo, A., and Esposito, G. (2009). Cannabidiol in medicine: A review of its therapeutic potential in CNS disorders. *Phytother. Res.* 23, 597–602. doi:10.1002/ptr.2625

Scuderi, C., Steardo, L., and Esposito, G. (2014). Cannabidiol promotes amyloid precursor protein ubiquitination and reduction of beta amyloid expression in SHSY5YAPP+ cells through PPARγ involvement. *Phytother. Res.* 28, 1007–1013. doi:10.1002/ptr.5095

Shallcross, J., Hamor, P., Bechard, A. R., Romano, M., Knackstedt, L., and Schwendt, M. (2019). The divergent effects of CDPPB and cannabidiol on fear extinction and anxiety in a predator scent stress model of PTSD in rats. *Front. Behav. Neurosci.* 13, 91. doi:10.3389/fnbeh.2019.00091

Stern, C. A. J., de Carvalho, C. R., Bertoglio, L. J., and Takahashi, R. N. (2018). Effects of cannabinoid drugs on aversive or rewarding drug-associated memory extinction and reconsolidation. *Neuroscience* 370, 62–80. doi:10.1016/j.neuroscience.2017.07.018

Taglialatela, G., Hogan, D., Zhang, W. R., and Dineley, K. T. (2009). Intermediate- and long-term recognition memory deficits in Tg2576 mice are reversed with acute calcineurin inhibition. *Behav. Brain Res.* 200, 95–99. doi:10.1016/j.bbr.2008.12.034

Thal, D. R., Rub, U., Orantes, M., and Braak, H. (2002). Phases of A beta-deposition in the human brain and its relevance for the development of AD. *Neurology* 58, 1791–1800. doi:10.1212/wnl.58.12.1791

Vallee, A., Lecarpentier, Y., Guillevin, R., and Vallee, J. N. (2017). Effects of cannabidiol interactions with Wnt/β-catenin pathway and PPARγ on oxidative stress and neuroinflammation in Alzheimer's disease. *Acta Biochim. Biophys. Sin.* 49, 853–866. doi:10.1093/abbs/gmx073

Wang, J., Tanila, H., Puolivali, J., Kadish, I., and Van Groen, T. (2003). Gender differences in the amount and deposition of amyloidbeta in APPswe and PS1 double transgenic mice. *Neurobiol. Dis.* 14, 318–327. doi:10.1016/j.nbd.2003.08.009

Watt, G., Chesworth, R., Przybyla, M., Ittner, A., Garner, B., Ittner, L. M., et al. (2020b). Chronic cannabidiol (CBD) treatment did not exhibit beneficial effects in 4-month-old male TAU58/2 transgenic mice. *Pharmacol. Biochem. Behav.* 196, 172970. doi:10.1016/j.pbb.2020.172970

Watt, G., and Karl, T. (2017). *In vivo* evidence for therapeutic properties of cannabidiol (CBD) for Alzheimer's disease. *Front. Pharmacol.* 8, 20. doi:10.3389/fphar.2017.00020

Watt, G., Shang, K., Zieba, J., Olaya, J., Li, H., Garner, B., et al. (2020a). Chronic treatment with 50 mg/kg cannabidiol improves cognition and moderately reduces Aβ40 levels in 12-month-old male AβPPswe/PS1ΔE9 transgenic mice. *J. Alzheimers Dis.* 74, 937–950. doi:10.3233/JAD-191242

Wimo, A., Ali, G.-C., Guerchet, M., Prince, M., Prina, M., and Wu, Y.-T. (2015). *World alzheimer report 2015. The global impact of dementia*. London, UK: Alzheimer's Disease International.

Wright, M., Di Ciano, P., and Brands, B. (2020). Use of cannabidiol for the treatment of anxiety: A short synthesis of pre-clinical and clinical evidence. *Cannabis Cannabinoid Res.* 5, 191–196. doi:10.1089/can.2019.0052

Xu, C., Chang, T., Du, Y., Yu, C., Tan, X., and Li, X. (2019). Pharmacokinetics of oral and intravenous cannabidiol and its antidepressant-like effects in chronic mild stress mouse model. *Environ. Toxicol. Pharmacol.* 70, 103202. doi:10.1016/j.etap.2019.103202

Zgair, A., Wong, J. C., Lee, J. B., Mistry, J., Sivak, O., Wasan, K. M., et al. (2016). Dietary fats and pharmaceutical lipid excipients increase systemic exposure to orally administered cannabis and cannabis-based medicines. *Am. J. Transl. Res.* 8, 3448–3459.

frontiers | Frontiers in Pharmacology

TYPE Brief Research Report
PUBLISHED 03 October 2022
DOI 10.3389/fphar.2022.856846

OPEN ACCESS

EDITED BY
Francisco Navarrete,
Miguel Hernández University of Elche, Spain

REVIEWED BY
Marta Marin,
University Hospital October 12, Spain
Elena Martín-García,
Pompeu Fabra University, Spain

*CORRESPONDENCE
José Diogo S. Souza,
jose.diogo.souza@usp.br

SPECIALTY SECTION
This article was submitted to Neuropharmacology, a section of the journal Frontiers in Pharmacology

RECEIVED 17 January 2022
ACCEPTED 10 August 2022
PUBLISHED 03 October 2022

CITATION
Souza JDS, Zuardi AW, Guimarães FS, Osório FdL, Loureiro SR, Campos AC, Hallak JEC, Dos Santos RG, Machado Silveira IL, Pereira-Lima K, Pacheco JC, Ushirohira JM, Ferreira RR, Costa KCM, Scomparin DS, Scarante FF, Pires-Dos-Santos I, Mechoulam R, Kapczinski F, Fonseca BAL, Esposito DLA, Andraus MH and Crippa JAS (2022), Maintained anxiolytic effects of cannabidiol after treatment discontinuation in healthcare workers during the COVID-19 pandemic. *Front. Pharmacol.* 13:856846. doi: 10.3389/fphar.2022.856846

Maintained anxiolytic effects of cannabidiol after treatment discontinuation in healthcare workers during the COVID-19 pandemic

José Diogo S. Souza[1]*, Antonio W. Zuardi[1,2], Francisco S. Guimarães[2,3], Flávia de Lima Osório[1,2], Sonia Regina Loureiro[1], Alline Cristina Campos[3], Jaime E. C. Hallak[1,2], Rafael G. Dos Santos[1,2], Isabella Lara Machado Silveira[1], Karina Pereira-Lima[4,5], Julia Cozar Pacheco[1], Juliana Mayumi Ushirohira[1], Rafael Rinaldi Ferreira[3], Karla Cristinne Mancini Costa[3], Davi Silveira Scomparin[3], Franciele Franco Scarante[3], Isabela Pires-Dos-Santos[3], Raphael Mechoulam[6], Flávio Kapczinski[2,7,8], Benedito A. L. Fonseca[9], Danillo L. A. Esposito[9], Maristela Haddad Andraus[10] and José Alexandre S. Crippa[1,2]

[1]Department of Neuroscience and Behavior, Ribeirão Preto Medical School, University of São Paulo, Ribeirão Preto, Brazil, [2]National Institute for Science and Technology—Translational Medicine, Ribeirão Preto, Brazil, [3]Department of Pharmacology, Ribeirão Preto Medical School, University of São Paulo, Ribeirão Preto, Brazil, [4]University of Michigan Medical School, Ann Arbor, IN, United States, [5]Department of Psychiatry, Federal University of São Paulo, São Paulo, São Paulo, Brazil, [6]The Institute for Drug Research, School of Pharmacy, The Hebrew University of Jerusalem, Jerusalem, Israel, [7]Department of Psychiatry and Behavioural Neurosciences, McMaster University and St. Joseph's Healthcare Hamilton, Hamilton, ON, Canada, [8]Department of Psychiatry, Faculty of Medicine, Graduate Program in Psychiatry and Behavioral Sciences, Universidade Federal do Rio Grande do Sul, Porto Alegre, Brazil, [9]Department of Internal Medicine, Ribeirão Preto Medical School, University of São Paulo, Ribeirão Preto, Brazil, [10]Chromatox Laboratory Ltd São Paulo, Brazil

Objective: To assess whether the effects of oral administration of 300 mg of Cannabidiol (CBD) for 28 days on mental health are maintained for a period after the medication discontinuation.

Methods: This is a 3-month follow-up observational and clinical trial study. The data were obtained from two studies performed simultaneously by the same team in the same period and region with Brazilian frontline healthcare workers during the COVID-19 pandemic. Scales to assess emotional symptoms were applied weekly, in the first month, and at weeks eight and 12.

Results: The primary outcome was that, compared to the control group, a significant reduction in General Anxiety Disorder-7 Questionnaire (GAD-7) from baseline values was observed in the CBD group on weeks two, four, and eight (Within-Subjects Contrasts, time-group interactions: $F_{1\text{-}125}$

= 7.67; $p = 0.006$; $\eta_p^2 = 0.06$; $F_{1\text{-}125} = 6.58$; $p = 0.01$; $\eta_p^2 = 0.05$; $F_{1\text{-}125} = 4.28$; $p = 0.04$; $\eta_p^2 = 0.03$, respectively) after the end of the treatment.

Conclusions: The anxiolytic effects of CBD in frontline health care professionals during the COVID-19 pandemic were maintained up to 1 month after the treatment discontinuation, suggesting a persistent decrease in anxiety in this group in the real world. Future double-blind placebo-controlled clinical trials are needed to confirm the present findings and weigh the benefits of CBD therapy against potential undesired or adverse effects.

KEYWORDS

Cannabidiol, CBD, Anxiety, emotional exhausion, burnout, depression, healthcare worker (HCW), follow-up

Introduction

Anxiety disorders are the most prevalent mental illnesses globally, causing high social and economic costs (Stein et al., 2017). The usual pharmacological treatments for these conditions (anxiolytic and antidepressant medications) often have adverse effects and low efficacy (40%–60% of patients), with most patients failing to achieve complete remission (Bandelow et al., 2012). Thus, it is essential to develop novel treatment approaches for anxiety disorders.

Cannabidiol (CBD) is a nonpsychotomimetic constituent of the *Cannabis* plant, which has potential therapeutic properties across many neuropsychiatric disorders, such as anxiety, depression, psychotic disorder, epilepsy, cognitive disorder, addiction, and other indications like chronic pain, (Crippa et al., 2018) with a favorable safety and tolerability profile (Bergamaschi et al., 2011a). Several preclinical studies using different animal models have shown the potential anxiolytic properties of CBD (Guimarães et al., 1990; Moreira et al., 2006; Campos and Guimaraes, 2009; Soares et al., 2010; Campos et al., 2012). These properties have been found in humans after experimentally induced anxiety in healthy volunteers (Zuardi et al., 1993; Zuardi et al., 2017; Linares et al., 2018) and social phobia patients (Bergamaschi et al., 2011b; Crippa et al., 2011). A recent small clinical trial with Japanese teenagers also showed beneficial effects of CBD in this later disorder (Masataka, 2019). However, the number of clinical studies investigating the anxiolytic effects of CBD after repeated treatment is still limited.

Moreover, considering the increase in the medicinal use of CBD in recent years, the importance of extensive real-world studies in this area has been recently highlighted 16 (Schlag et al., 2021). We recently showed that CBD decreased emotional exhaustion/burnout and anxiety symptoms in healthcare workers (HCWs) in a 28-days intervention (Crippa et al., 2021) during the COVID-19 pandemic. This population is recognized as being at exceptionally high risk of developing anxiety symptoms (Sahebi et al., 2021). In a series of prospective cases of non-frontline health workers treated with CBD during the COVID-19 pandemic, we observed that the improvement of anxiety symptoms was sustained for more than 4 weeks after the treatment discontinuation (Pacheco et al., 2021). To verify in a controlled study if the anxiolytic effect of CBD persists for at least 4 weeks after its discontinuation, in the present paper, we conducted a 3-month follow-up of the clinical trial with frontline HCWs (Crippa et al., 2021) and compare this group with similar demographic and professional characteristics control group from another study conducted in parallel at the same period (Osório et al., 2021).

Materials and methods

Design

The data of this study were obtained from two studies with frontline HCWs involved with COVID-19 treatment performed simultaneously by the same team in the same period and region. Partial results of these studies have been published (Crippa et al., 2021) (Osório et al., 2021). One study was a clinical trial, two-arm, parallel-group, unblinded with evaluator blinded, to test the efficacy of oral CBD to prevent or reduce emotional distress in HCWs dealing with COVID-19 patients (Crippa et al., 2021). The other was an observational study to assess and monitor emotional distress among health workers providing care to patients with COVID-19 (Osório et al., 2021). The two studies were approved by the Institutional Review Board (Process Nº 4.190.338 and 4.032.190).

Summary of the reference studies

The participants of the two studies were recruited between May to November 2020, during the first wave of COVID-19 in Brazil, *via* institutional advertising, email, and social media. The inclusion criteria were being healthcare workers (nurses, physicians, physical therapists, occupational therapists, speech therapists, psychologists, social workers, and nutritionists) of

both sexes involved in the treatment of COVID-19 patients and providing their informed consent. The exclusion criteria in the clinical trial were the use of any medication with potential interactions with CBD, a history of undesirable reactions to CBD or other cannabinoids, pregnancy, and belonging to COVID-19 risk groups.

Participants of the two studies completed an online survey with scales applied weekly, in the first month, and at weeks 8–12. The primary outcome measure includes the Generalized Anxiety Disorder Questionnaire—[GAD-7] (Moreno et al., 2016), a 7-item self-report instrument that screens anxiety-associated symptoms rated on a three-point scale ranging from 0 (never) to 3 (almost every day). The secondary outcome measures include the Patient Health Questionnaire-9 [PHQ-9] (de Lima Osório et al., 2009), a 9-item self-report instrument intended to assess depression indicators, rated from 0 ("never") to 3 ("almost every day"); the Abbreviated Maslach Burnout Inventory-subscale emotional exhaustion [aMBI]) (Carlotto and Camara, 2007), a four items that evaluate emotional depletion due to job demand on a seven-point Likert scale, ranging from 0 ("never") to 6 ("every day"); the Posttraumatic Stress Disorder Checklist – 5 (PCL-5) (Osório et al., 2017), a self-report instrument used to assess symptoms of posttraumatic stress disorder using the criteria established by the DSM-5; and a questionnaire about their demographic and professional characteristics, and personal clinical variables associated with mental health. These data were automatically stored in the RedCap platform.

In the clinical trial, in addition to the follow-up with the rankings, one group received oral CBD (99.6% purity: PurMed Global, Delray Beach, Florida, United States) dissolved in medium-chain triglyceride oil for the first 4 weeks (150 mg twice a day). The dose of CBD was defined based on previous evidence showing that 300–400 mg/d doses promote anxiolytic effects within good safety and tolerability standards (Zuardi et al., 2017; Crippa et al., 2018; Linares et al., 2018). The treatment safety of CBD was assessed with a modified version of the UKU side effect rating scale of the Scandinavian Society of Psychopharmacology (Lingjaerde, 1987), highlighting the most common adverse effects of CBD, the "CBD Adverse Effects Scale" (CARE Scale). In these participants, we evaluated the plasma levels of CBD and general laboratory exams in samples collected at baseline and on days 7, 14, 21, and 28.

Procedure of the present study

We compared two groups with data extracted from participants of the referred studies (Crippa et al., 2021; Osório et al., 2021). The healthcare workers from the clinical trial (Crippa et al., 2021), who received CBD during the first month of follow-up, formed one group (CBD group). The other group consisted of healthcare workers from the observational study (Osório et al., 2021), who did not receive a pharmacological intervention (Control group-CG). All healthcare workers worked in institutions located in the northeast region of the state of São Paulo, Brazil (100 km around the city of Ribeirão Preto).

Participants were paired allocated into the two groups by a researcher blinded to the individual results of the rating scales. Considering that the dropouts were around twice as prominent in the study without CBD (Osório et al., 2021), the participants were randomized in a 1:2 (CBD:CG) ratio concerning sex, age, and profession (Nursing or other). Assuming an effect size (Cohen's d) of 0.1, level of significance of 0.05, and a statistical power of 0.8, we estimated that 142 participants (around 71 per group) who completed the 3 months were adequate for detecting a small effect. To obtain this number of participants at the end of 12 weeks, we selected at baseline 100 and 200 subjects in the CBD group (30% of dropouts) and Control group (65% dropouts), respectively.

Statistical analysis

Clinical and demographic data comparing CBD and Control groups at baseline, and after 12 weeks, from subjects that completed or not completed the 12-weeks observational period, were analyzed using the t-test for continuous data and the Fisher's Exact test for nominal data. Data from the rating scales were analyzed with a repeated-measures analysis of variance (repeated-measures ANOVA) with factors time, group, and time × group interaction. The degrees of freedom of the repeated factor were corrected with Huynh-Feldt epsilon when sphericity conditions were not met. Within-subjects contrasts with a significant time × group interaction assessed the differences between groups in each measured compared to the baseline.

In the group treated with CBD during the first 4 weeks, we compared the percentage of participants that showed a reduction in clinical anxiety (cutoff score of 10 points or greater on GAD-7) in the four quartiles of the CBD plasma level. To assess whether the decrease in clinical anxiety was associated with plasma levels of CBD, we used the bipolar logistic regression (fourth quartile compared with the other quartiles). The significance level was set at $p < 05$.

Results

Participants

At baseline and after 12 weeks of follow-up, there was no significant difference between the CBD and Control groups concerning sex, age, occupation, psychiatric diagnosis, psychological treatment, and psychiatric medication. In addition, the same characteristics did not differ significantly

TABLE 1 Demographic and Clinical Characteristics of Participants.

Characteristic	Baseline			Completed 3 months			Comparison of whether they completed 3 months		
	CBD	Control	p	CBD	Control	p	Yes	No	p
	N = 100	N = 200		N = 71	N = 79		N = 150	N = 150	
Sex N (%)									
Female	79 (79)	153 (76.5)	0.626	56 (78.9)	63 (79.7)	0,895	119 (79.3)	113 (75.3)	0.408
Male	21(21)	47 (23.5)		15 (21.1)	16 (20.3)		31 (20.7)	37 (24.7)	
Age (years) Mean (SD)									
	34.45 (7.30)	34.75 (9.56)	0.783	34.51 (7.36)	35.6 (10.16)	0.458	35.08 (8.93)	34.22 (8.79)	0.401
Occupation – No. (%)									
Nurse	44 (44)	105 (52.5)	0.165	30 (42.3)	36 (45.6)	0,136	73 (48.7)	76 (50.7)	0.729
Other	56 (56)	95 (47.5)		41 (57.7)	43 (54.4)		77 (51.3)	74(49.3)	
Psychiatric diagnosis No. (%)									
Yes	22(22)	52 (26)	0.397	16 (22.5)	26 (32.9)	0,158	42 (28)	32 (21.1)	0.16
No	78 (78)	148 (74)		55(77.5)	53 (67.1)		108 (72)	120 (78.9)	
Psychological treatment – No. (%)									
Yes	43 (43)	86 (43)	1.0	27 (38)	39 (49.4)	0,162	66 (44)	63 (42)	0.726
No	57 (57)	114 (57)		44 (62)	40 (50.6)		84 (56)	87 (58)	
Psychiatric medication No. (%)									
Yes	20 (20)	44 (22)	0.630	16 (22.5)	26 (32.9))	0,158	36 (24)	28 (18.67)	0.236
No	80(80)	156 (78)		55 (75.5)	53 (67.1)		114 (76)	122 (81.33)	

between those who completed or not the 12 weeks of follow-up. Demographic and clinical characteristics are summarized in Table 1.

Primary outcome

The ANOVA repeated measures of GAD-7 scores showed a significant effect of time ($F_{3.28\text{-}410.18} = 8.18$; $p < 0.001$; $\eta_p^2 = 0.06$), group ($F_{1\text{-}125} = 4.69$; $p = 0.03$; $\eta_p^2 = 0.04$), and time-group interaction ($F_{3.28\text{-}410.18} = 3.51$; $p = 0.01$; $\eta_p^2 = 0.03$). Compared to Control group, a significant reduction in delta score concerning baseline values was observed in the CBD group on weeks two, four, and eight (Within-Subjects Contrasts, time-group interactions: $F_{1\text{-}125} = 7.67$; $p = 0.006$; $\eta_p^2 = 0.06$; $F_{1\text{-}125} = 6.58$; $p = 0.01$; $\eta_p^2 = 0.05$; $F_{1\text{-}125} = 4.28$; $p = 0.04$; $\eta_p^2 = 0.03$, respectively). Figure 1A showed the delta score, concerning baseline values in weeks 2,4,8, and 12. The repeated measures ANOVA of the GAD-7 scores showed a significant effect of time only for the CBD group ($F_{3.46\text{-}235.05} = 10.56$; $p < 0.001$; $\eta_p^2 = 0.13$). The differences between the basal and the other time points are shown in Figure 1A.

In the group treated with CBD during the first 4 weeks, the percentage of participants that showed a reduction in clinical anxiety in the four quartiles of the CBD plasma level was shown in Figure 2. CBD plasma levels were significantly associated with the reduction in clinical anxiety (Odd ratio = 8.854; Confidence interval = 1.146-68.386; $p = 0.037$).

Secondary outcome

The delta score concerning baseline values of the scales PHQ-9, aMBI, and PCL-5 was shown in Figure 1 as well.

There were significant effects of time ($F_{3.31\text{-}443.49} = 5.37$; $p < 0.001$; $\eta_p^2 = 0.04$), group ($F_{1\text{-}134} = 4.85$; $p = 0.03$; $\eta_p^2 = 0.04$), and tendency to significant effect of time × group interaction ($F_{3.31\text{-}443.49} = 2.09$; $p = 0.08$; $\eta_p^2 = 0.02$), on PHQ-9 scores. The Within-Subjects Contrasts showed a significant effect of time × group interaction on weeks two ($F_{1\text{-}134} = 4.02$; $p = 0.04$; $\eta_p^2 = 0.03$), four ($F_{1\text{-}134} = 4.23$; $p = 0.04$; $\eta_p^2 = 0.03$), and eight ($F_{1\text{-}134} = 5.32$; $p = 0.02$; $\eta_p^2 = 0.04$), with a lower value in CBD group (Figure 1B). The repeated measures ANOVA of the PHQ-9 scores showed a significant effect of time only for the CBD group [$F_{3.36\text{-}228.23} = 5.62$; $p = 0.001$; $\eta_p^2 = 0.08$]. The differences between the basal and the other time points are shown in Figure 1B.

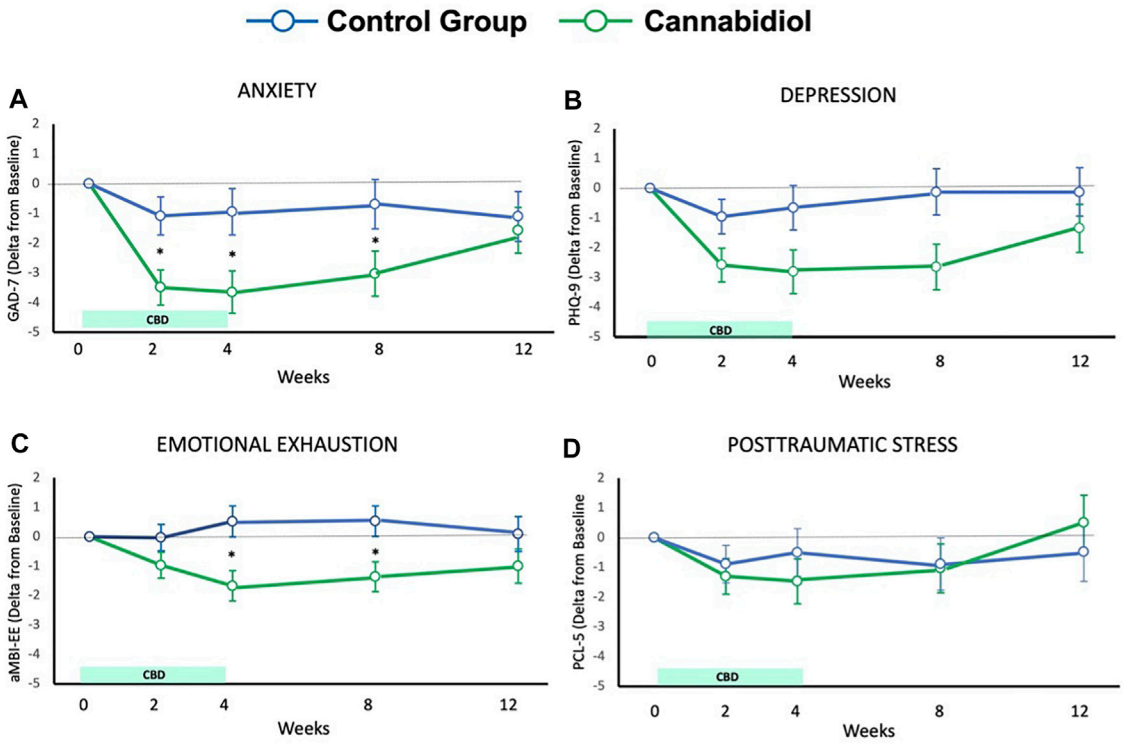

FIGURE 1
Results for Anxiety **(A)**, depression **(B)**, emotional exhaustion **(C)**, and posttraumatic stress **(D)**.

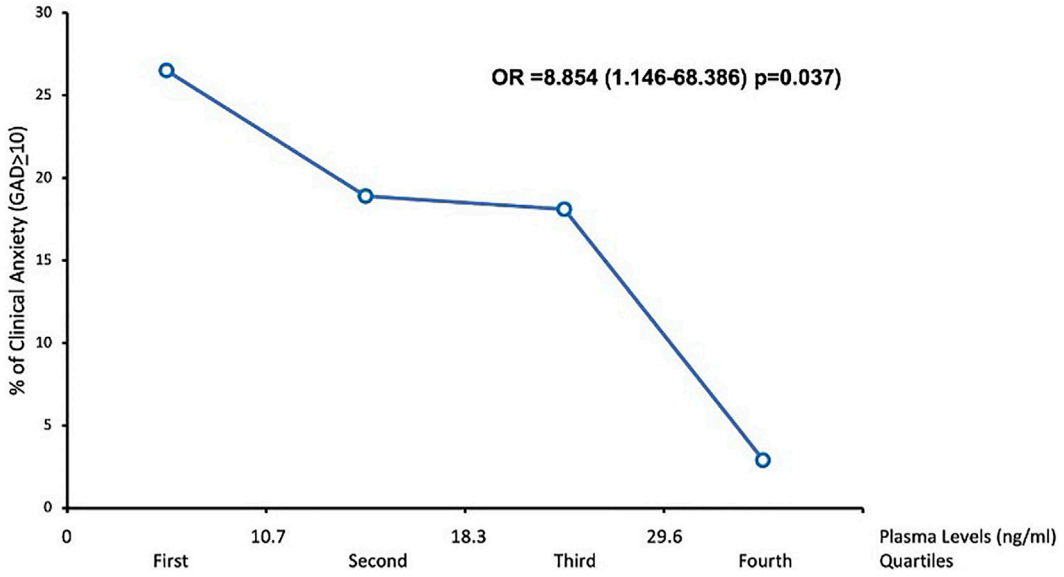

FIGURE 2
Association between CBD plasma levels and anxiety symptoms.

Concerning aMBI scores, there were significant effects of group ($F_{1\text{-}133}$ = 6.04; p = 0.02; η_p^2 = 0.04), and time × group interaction ($F_{3.57\text{-}474.03}$ = 3.19; p = 0.02; η_p^2 = 0.02), but no significant effect of time ($F_{3.57\text{-}474.03}$ = 3.19; p = 0.02; η_p^2 = 0.02). The Within-Subjects Contrasts showed a significant effect of time × group interaction on weeks four ($F_{1\text{-}133}$ = 8.73; p = 0.004; η_p^2 = 0.06), and eight ($F_{1\text{-}133}$ = 6.66; p = 0.01; η_p^2 = 0.05), with a lower value in CBD group. (Figure 1C). The repeated measures ANOVA of the aMBI scores showed a significant effect of time only for the CBD group ($F_{3.18\text{-}216.23}$ = 3.57; p = 0.007; η_p^2 = 0.05). The differences between the basal and the other time points can be seen in Figure 1C.

The repeated measures ANOVA of the PCL scores did not show a significant effect of time ($F_{3.19\text{-}414.59}$ = 2.08; p = 0.1; η_p^2 = 0.02), group ($F_{1\text{-}130}$ = 0.02; p = 0.89; η_p^2<0.001), and time-group interactions ($F_{3.19\text{-}414.59}$ = 0.85; p = 0.47; η_p^2 = 0.006). The repeated measures ANOVA of the PCL scores showed a significant effect of times only for the CBD group ($F_{3.41\text{-}235.10}$ = 2.61; p = 0.036; η_p^2 = 0.04). The differences between the basal and the other time points are shown in Figure 1D.

Safety of cannabidiol treatment

The serious adverse events observed during the 4 weeks of CBD treatment were increased hepatic enzymes greater than three times the upper limit (4%), none with total serum bilirubin levels greater than two-fold, and reports of skin erythema diagnosed as pharmacodermia (4%) (Souza et al., 2022). All cases fully recovered after CBD discontinuation. The most common adverse effects were somnolence (19%), diarrhea (15%), increased appetite (11%), and fatigue (10%).

Discussion

This observational and clinical trial study combination follow-up showed that CBD's beneficial effects on mental health were maintained after 1 month of its discontinuation in frontline HCWs during the COVID-19 pandemic. Compared to the control group, these effects included a reduction in anxiety, depressive, and emotional exhaustion/burnout symptoms measured by the GAD-7, PHQ-9, and aMBI scores, respectively. Furthermore, there was a statistically significant association between the higher CBD plasma level and the lower number of participants with scores indicative of anxiety (GAD-7 score >9 points. Overall, existing preclinical and clinical evidence support a potential role for CBD as a novel treatment for anxiety disorders (Crippa et al., 2018). The clinical evidence to date is mostly based on acute single-dose studies. Therefore, the present research contributes by showing not only the beneficial effects of daily CBD administration for 28 days but also that these effects are maintained over a similar period. Since the half-life of CBD after chronic oral administration is between two and 5 days (Millar et al., 2018), the maintenance of the anxiety and emotional exhaustion attenuation could not be attributed to the plasma level of the drug. Instead, one possible explanation is that a period of less anxiety at work induced by CBD would transiently change their aversive memory concerning the work by their effects of enhancing the extinction (Das et al., 2013) or interfering with the reconsolidation of traumatic memories (Bolsoni et al., 2022). However, these effects did not occur in depression and post-traumatic stress disorder. The discontinuation of CBD after 4 weeks did not induce withdrawal signs.

Cannabis products are widely employed worldwide, and their use has been illegalized in several countries (Bonomo et al., 2018). After legalizing medicinal and recreational cannabis in some countries, its use highly increased (Wen et al., 2015; Martins et al., 2016; Hasin et al., 2017). CBD has gained special attention for its therapeutic potency for several physical and mental health conditions (Sholler et al., 2020). Anxiety is regularly one of the most frequent conditions for which patients use cannabis (Schlag et al., 2021), particularly pure CBD products (Leas et al., 2020) There are other anxiolytic drugs; however, these can have some adverse effects that are even more harmful to healthcare professionals on the front lines of caring for COVID-19 patients. Among these, we can mention sedation, cognitive dysfunction, decreased performance of benzodiazepines (Lader, 2014) and latency to onset of anxiolytic effects with a possible increase in anxiety, at the beginning of treatment, with antidepressants (Moreno et al., 1999). Therefore, considering the increase in the medicinal use of CBD in recent years, extensive real-world studies on this area are urgently needed.

Treatment with cannabidiol was associated with few reported cases of serious AEs, which resolved after drug discontinuation. Still, their presence highlights the need for close clinical monitoring (especially liver function testing) of patients receiving CBD therapy (Sholler et al., 2020). To our knowledge, this is the first study to assess the effects of CBD even after the medication discontinuation. Thus, the present work results could significantly impact the medicinal cannabinoids used worldwide. However, more clinical trials are needed to assess the long-term effects of Cannabidiol.

Limitations

The main limitation is that the samples compared, although with similar demographic and professional characteristics, are from different studies. An ideal protocol would include a placebo-controlled treatment to discard a putative placebo effect in the CBD group. However, the main objective of this study was to evaluate the duration of the effects observed after the treatment discontinuation, and in the 2 months after CBD treatment, the two groups had the same protocol, only the monitoring with self-evaluated scales. In addition, the much lower dropout rate in the control (65%) compared to the CBD-treated group (30%) could reflect a more significant

beneficial effect observed in this group. Since the survey was online, no urine tests were made to rule out substance use.

Conclusion

This observational and clinical trial study combination follow-up showed that the beneficial effects on anxiety, emotional exhaustion/burnout, and depressive symptoms observed among frontline health care professionals working with patients with COVID-19 after 28 days of daily CBD administration were maintained for up to a month after the treatment discontinuation. This study meets the recently highlighted need for extensive real-world studies on CBD's potential medicinal use. Future double-blind placebo-controlled clinical trials are needed to assess the CBD long-term effects and confirm the present findings.

Data availability statement

The original contributions presented in the study are included in the article, further inquiries can be directed to the corresponding author.

Ethics Statement

The studies involving human participants were reviewed and approved by the Institutional Review Board (Process No 4.190.338 and 4.032.190). The participants provided their written informed consent to participate in this study.

Author contributions

JS, AZ, JP, FG, FO, and SL: Conception and design or analysis and interpretation of data and final approval of the present study. All other authors are related to the two substudies that provided the samples for this present study: Conception and design or analysis and interpretation of data. All authors contributed to the article and approved the submitted version.

Funding

This work was supported by grants from The São Paulo Research Foundation (2014/50891-1; 2020/12110-9); Grant 2008/09009-2 from the National Institute of Translational Science and Technology in Medicine; National Council for Scientific and Technological Development (401058/2020-4; 465458/2014-9); Productivity Research Fellows: No. 302601/2019-8 (FO); 307945/2018-9 (SL); in-kind donations of cannabidiol from PurMed Global; and donated services (dosing plasma levels of cannabidiol) from Laboratório Chromatox. The funding organizations had no role in the design and conduct of the study; collection, management, analysis, and interpretation of the data; preparation, review, or approval of the manuscript; and decision to submit the manuscript for publication.

Conflict of interest

AZ reported receiving grants from the National Institute of Translational Science and Technology in Medicine and personal fees from the National Council for Scientific and Technological Development during the conduct of the study, being a co-owner of a patent for fluorinated cannabidiol compounds (licensed to Phytecs), and having a patent pending for a cannabinoid-containing oral pharmaceutical composition outside the submitted work. FG reported receiving grants from Prati-Donaduzzi, being a co-owner of a patent for fluorinated cannabidiol compounds (licensed to Phytecs), and having a patent pending for a cannabinoid-containing oral pharmaceutical composition outside the submitted work. AC reported having a patent pending for a cannabinoid-containing oral pharmaceutical composition outside the submitted work. JH reported receiving grants from Prati-Donaduzzi, travel support and personal fees from BioSynthesis Pharma Group, being a co-owner of a patent for fluorinated cannabidiol compounds (licensed to Phytecs), and having a patent pending for a cannabinoid-containing oral pharmaceutical composition outside the submitted work. RD Santos reported receiving grants from the National Council for Scientific and Technological Development during the conduct of the study. RM reported being a co-owner of a patent for fluorinated cannabidiol compounds (licensed to Phytecs) outside the submitted work. FK reported receiving grants from the Canada Foundation for Innovation, the National Council for Scientific and Technological Development, Mitacs, and the Stanley Medical Research Institute; personal fees from Aché Laboratorios Farmaceuticos, Daiichi Sankyo, and Janssen-Cilag; and being a co-owner of a patent for fluorinated cannabidiol compounds (licensed to Phytecs) outside the submitted work. MA reported receiving technical support from Salomao Zoppi Serviços Médicos e Participações during the conduct of the study and personal fees from Laboratório Chromatox outside the submitted work. JC reported receiving grants from the São Paulo Research Foundation and the National Institute of Translational Science and Technology in Medicine and personal fees from the National Council for Scientific and Technological Development and Salomão e Zoppi Serviços Médicos e Participações during the conduct of the study and receiving travel support and personal fees from BioSynthesis

Pharma Group; serving as a member of the international advisory board of the Australian Centre for Cannabinoid Clinical and Research Excellence, National Health and Medical Research Council; being a co-owner of a patent for fluorinated cannabidiol compounds (licensed to Phytecs); and having a patent pending for a cannabinoid-containing oral pharmaceutical composition outside the submitted work. No other disclosures were reported.

Publisher's note

References

Bandelow, B., Sher, L., Bunevicius, R., Hollander, E., Kasper, S., Zohar, J., et al. (2012). Guidelines for the pharmacological treatment of anxiety disorders, obsessive-compulsive disorder and posttraumatic stress disorder in primary care. *Int. J. Psychiatry Clin. Pract.* 16, 77–84. doi:10.3109/13651501.2012.667114

Bergamaschi, M. M., Queiroz, R. H., Chagas, M. H. N., de Oliveira, D. C. G., De Martinis, B. S., Kapczinski, F., et al. (2011). Cannabidiol reduces the anxiety induced by simulated public speaking in treatment naïve social phobia patients. *Neuropsychopharmacology* 36 (6), 1219–1226. doi:10.1038/npp.2011.6

Bergamaschi, M. M., Queiroz, R. H., Zuardi, A. W., and Crippa, J. A. (2011). Safety and side effects of cannabidiol, a Cannabis sativa constituent. *Curr. Drug Saf.* 6, 237–249. doi:10.2174/157488611798280924

Bolsoni, L. M., Crippa, J. A. S., Hallak, J. E. C., Guimarães, F. S., and Zuardi, A. W. (2022). Effects of cannabidiol on symptoms induced by the recall of traumatic events in patients with posttraumatic stress disorder. *Psychopharmacology* 239, 1499–1507. doi:10.1007/s00213-021-06043-y

Bonomo, Y., Souza, J. D. S., Jackson, A., Crippa, J. A. S., and Solowij, N. (2018). Clinical issues in cannabis use. *Br. J. Clin. Pharmacol.* 84, 2495–2498. doi:10.1111/bcp.13703

Campos, A. C., Ferreira, F. R., and Guimarães, F. S. (2012). Cannabidiol blocks long lasting behavioral consequences of predator threat stress: Possible involvement of 5HT1A receptors. *J. Psychiatr. Res.* 46, 1501–1510. doi:10.1016/j.jpsychires.2012.08.012

Campos, A. C., and Guimaraes, F. S. (2009). Evidence for a potential role for TRPV1 receptors in the dorsolateral periaqueductal gray in the attenuation of the anxiolytic effects of cannabinoids. *Prog. Neuropsychopharmacol. Biol. Psychiatry* 33 (8), 1517–1521. doi:10.1016/j.pnpbp.2009.08.017

Carlotto, M. S., and Camara, S. G. (2007). Artigo parcialmente retratado: Propriedades psicométricas do Maslach burnout inventory em uma amostra multifuncional. *Estud. Psicol.* 24 (3), 325–332. doi:10.1590/S0103-166X2007000300004

Crippa, J. A., Derenusson, G. N., Ferrari, T. B., Wichert-Ana, L., Duran, F. L., Martin-Santos, R., et al. (2011). Neural basis of anxiolytic effects of cannabidiol (CBD) in generalized social anxiety disorder: A preliminary report. *J. Psychopharmacol.* 25, 121–130. doi:10.1177/0269881110379283

Crippa, J. A., Guimarães, F. S., Campos, A. C., and Zuardi, A. W. (2018). Translational investigation of the therapeutic potential of cannabidiol (CBD): Toward a new age. *Front. Immunol.* 21, 2009. doi:10.3389/fimmu.2018.02009

Crippa, J. A. S., Zuardi, A. W., Guimarães, F. S., Campos, A. C., de Lima Osório, F., Loureiro, S. R., et al. (2021). Efficacy and safety of cannabidiol plus standard care vs standard care alone for the treatment of emotional exhaustion and burnout among frontline health care workers during the COVID-19 pandemic: A randomized clinical trial. *JAMA Netw. Open* 4, e2120603. doi:10.1001/jamanetworkopen.2021.20603

Das, R. K., Kamboj, S. K., Ramadas, M., Yogan, K., Gupta, V., Redman, E., et al. (2013). Cannabidiol enhances consolidation of explicit fear extinction in humans. *Psychopharmacology* 226 (4), 781–792. doi:10.1007/s00213-012-2955-y

de Lima Osório, F., Mendes, A. V., Crippa, J. A., and Loureiro, S. R. (2009). Study of the discriminative validity of the PHQ-9 and PHQ-2 in a sample of Brazilian women in the context of primary health care. *Perspect. Psychiatric Care* 45, 216–227. doi:10.1111/j.1744-6163.2009.00224.x

Guimarães, F. S., Chiaretti, T. M., Graeff, F. G., and Zuardi, A. W. (1990). Antianxiety effect of cannabidiol in the elevated plus-maze. *Psychopharmacology* 100, 558–559. doi:10.1007/BF02244012

Hasin, D. S., Sarvet, A. L., Cerdá, M., Keyes, K. M., Stohl, M., Galea, S., et al. (2017). US adult illicit cannabis use, cannabis use disorder, and medical marijuana laws: 1991-1992 to 2012-2013. *JAMA Psychiatry* 74, 579–588. doi:10.1001/jamapsychiatry.2017.0724

Lader, M. (2014). Benzodiazepine harm: How can it be reduced? *Br. J. Clin. Pharmacol.* 77 (2), 295–301. doi:10.1111/j.1365-2125.2012.04418.x

Leas, E. C., Hendrickson, E. M., Nobles, A. L., Todd, R., Smith, D. M., Dredze, M., et al. (2020). Self-reported cannabidiol (CBD) use for conditions with proven therapies. *JAMA Netw. Open* 3, e2020977. doi:10.1001/jamanetworkopen.2020.20977

Linares, I., Zuardi, A. W., Pereira, L. C., Hallak, J. E. C., Queiroz, R. H. C., Guimarães, F. S., et al. (2018). Cannabidiol presents an inverted U-shaped dose-response curve in the simulated public speaking test. *Eur. Neuropsychopharmacol.* 26, S617. doi:10.1016/S0924-977X(16)31702-3

Lingjaerde, O. (1987). The UKU side effect rating scale: A new comprehensive rating scale for psychotropic drugs and a cross-sectional study of side effects in neuroleptic-treated patients. *Acta Psychiatr. Scand. Suppl.* 334, 1–100. doi:10.1111/j.1600-0447.1987.tb10566.x

Martins, S. S., Mauro, C. M., Santaella-Tenorio, J., Kim, J. H., Cerda, M., Keyes, K. M., et al. (2016). State-level medical marijuana laws, marijuana use and perceived availability of marijuana among the general U.S. population. *Drug Alcohol Depend.* 169, 26–32. doi:10.1016/j.drugalcdep.2016.10.004

Masataka, N. (2019). Anxiolytic effects of repeated cannabidiol treatment in teenagers with social anxiety disorders. *Front. Psychol.* 10, 2466. doi:10.3389/fpsyg.2019.02466

Millar, S. A., Stone, N. L., Yates, A. S., and O'Sullivan, S. E. (2018). A systematic review on the Pharmacokinetics of cannabidiol in Humans. *Front. Pharmacol.* 9, 1365. doi:10.3389/fphar.2018.01365

Moreira, F. A., Aguiar, D. C., and Guimarães, F. S. (2006). Anxiolytic-like effect of cannabidiol in the rat Vogel conflict test. *Prog. Neuropsychopharmacol. Biol. Psychiatry* 30, 1466–1471. doi:10.1016/j.pnpbp.2006.06.004

Moreno, A. L., DeSousa, D. A., Souza, A. M. F. L., Manfro, G. G., Salum, G. A., Koller, S. H., et al. (2016). Factor structure, reliability, and item parameters of the Brazilian-Portuguese version of the GAD-7 questionnaire. *Temas Psicol.* 24, 367–376. doi:10.9788/tp2016.1-25

Moreno, A. R., Moreno, D. H., and Soares, M. B. M. (1999). Psicofarmacologia de antidepressivos. *Braz. J. Psychiatry.* 21 (1), 24–40. doi:10.1590/S1516-44461999000500006

Osório, F. L., da Silva, T. D. A., Dos Santos, R. G., Chagas, M. H. N., Chagas, N. M. S., Sanches, R. F., et al. (2017). Posttraumatic stress disorder checklist for DSM-5 (PCL-5): Transcultural adaptation of the Brazilian version. *Archives Clin. Psychiatry* 44, 10–19. doi:10.1590/0101-60830000000107

Osório, F. L., Silveira, I. L. M., Pereira-Lima, K., Crippa, J. A. de S., Hallak, J. E. C., Zuardi, A. W., et al. (2021). Risk and protective factors for the mental health of Brazilian healthcare workers in the frontline of COVID-19 pandemic. *Front. Psychiatry* 12, 662742. doi:10.3389/fpsyt.2021.662742

Pacheco, J. C., Souza, J. D., Hallak, J. E. C., Osório, F. L., Campos, A., Guimarães, F. S., et al. (2021). Cannabidiol as a treatment for mental health OutcomesAmong health care workers during the coronavirus disease pandemic. *J. Clin. Psychopharmacol.* 41 (3), 327–329. doi:10.1097/JCP.0000000000001405

Sahebi, A., Nejati-Zarnaqi, B., Moayedi, S., Yousefi, K., Torres, M., and Golitaleb, M. (2021). The prevalence of anxiety and depression among healthcare workers during the COVID-19 pandemic: An umbrella review of meta-analyses. *Prog. Neuropsychopharmacol. Biol. Psychiatry* 107, 110247. doi:10.1016/j.pnpbp.2021.110247

Schlag, A. K., O'Sullivan, S. E., Zafar, R. R., and Nutt, D. J. (2021). Current controversies in medical cannabis: Recent developments in human clinical applications and potential therapeutics. *Neuropharmacology* 191, 108586. doi:10.1016/j.neuropharm.2021.108586

Sholler, D. J., Schoene, L., and Spindle, T. R. (2020). Therapeutic efficacy of cannabidiol (CBD): A review of the evidence from clinical trials and human laboratory studies. *Curr. Addict. Rep.* 7, 405–412. doi:10.1007/s40429-020-00326-8

Soares, V. P., Campos, A. C., Bortoli, V. C., Zangrossi, H., and Guimarães, F. S. (2010). Intra-dorsal periaqueductal gray administration of cannabidiol blocks panic-like response by activating 5-HT1A receptors. *Behav. Brain Res.* 213 (2), 225–229. doi:10.1016/j.bbr.2010.05.004

Souza, J. D. S., Fassoni-Ribeiro, M., Batista, R. M., Ushirohira, J. M., Zuardi, A. W., Guimarães, F. S., et al. (2022). Case report: Cannabidiol-induced skin rash: A case series and key recommendations. *Front. Pharmacol.* 13, 881617. doi:10.3389/fphar.2022.881617

Stein, D. J., Scott, K. M., de Jonge, P., and Kessler, R. C. (2017). Epidemiology of anxiety disorders: From surveys to nosology and back. *Dialogues Clin. Neurosci.* 19, 127–136. doi:10.31887/DCNS.2017.19.2/dstein

Wen, H., Hockenberry, J. M., and Cummings, J. R. (2015). The effect of medical marijuana laws on adolescent and adult use of marijuana, alcohol, and other substances. *J. Health Econ.* 42, 64–80. doi:10.1016/j.jhealeco.2015.03.007

Zuardi, A. W., Cosme, R. A., Graeff, F. G., and Guimarães, F. S. (1993). Effects of ipsapirone and cannabidiol on human experimental anxiety. *J. Psychopharmacol.* 7 (1), 82–88. doi:10.1177/026988119300700112

Zuardi, A. W., Rodrigues, N. P., Silva, A. L., Bernardo, S. A., Hallak, J. E. C., Guimarãe, F. S., et al. (2017). Inverted U-shaped dose-response curve of the anxiolytic effect of cannabidiol during public speaking in real life. *Front. Pharmacol.* 8, 259. doi:10.3389/fphar.2017.00259

frontiers | Frontiers in Pharmacology

TYPE Original Research
PUBLISHED 05 October 2022
DOI 10.3389/fphar.2022.907579

OPEN ACCESS

EDITED BY
Jorge Manzanares,
Miguel Hernández University of Elche, Spain

REVIEWED BY
Robert B. Laprairie,
University of Saskatchewan, Canada
Luzia Sampaio,
Federal University of Rio de Janeiro, Brazil
Trevor James Hamilton,
MacEwan University, Canada
Meng Jin,
Qilu University of Technology (Shandong Academy of Sciences), China

*CORRESPONDENCE
Lee D. Ellis,
lee.ellis@nrc-cnrc.gc.ca

SPECIALTY SECTION
This article was submitted to Neuropharmacology, a section of the journal Frontiers in Pharmacology

RECEIVED 29 March 2022
ACCEPTED 15 August 2022
PUBLISHED 05 October 2022

CITATION
Morash MG, Nixon J, Shimoda LMN, Turner H, Stokes AJ, Small-Howard AL and Ellis LD (2022), Identification of minimum essential therapeutic mixtures from cannabis plant extracts by screening in cell and animal models of Parkinson's disease.
Front. Pharmacol. 13:907579.
doi: 10.3389/fphar.2022.907579

Identification of minimum essential therapeutic mixtures from cannabis plant extracts by screening in cell and animal models of Parkinson's disease

Michael G. Morash[1], Jessica Nixon[1], Lori M. N. Shimoda[2], Helen Turner[2], Alexander J. Stokes[3], Andrea L. Small-Howard[4] and Lee D. Ellis[1]*

[1]National Research Council of Canada, Halifax, NS, Canada, [2]Laboratory of Immunology and Signal Transduction, School of Natural Sciences and Mathematics, Chaminade University, Honolulu, HI, United States, [3]Laboratory of Experimental Medicine, John A Burns School of Medicine, University of Hawaii, Honolulu, HI, United States, [4]GBS Global Biopharma, Inc., Ottawa, ON, Canada

Medicinal cannabis has shown promise for the symptomatic treatment of Parkinson's disease (PD), but patient exposure to whole plant mixtures may be undesirable due to concerns around safety, consistency, regulatory issues, and psychoactivity. Identification of a subset of components responsible for the potential therapeutic effects within cannabis represents a direct path forward for the generation of anti-PD drugs. Using an *in silico* database, literature reviews, and cell based assays, GB Sciences previously identified and patented a subset of five cannabinoids and five terpenes that could potentially recapitulate the anti-PD attributes of cannabis. While this work represents a critical step towards harnessing the anti-PD capabilities of cannabis, polypharmaceutical drugs of this complexity may not be feasible as therapeutics. In this paper, we utilize a reductionist approach to identify minimal essential mixtures (MEMs) of these components that are amenable to pharmacological formulation. In the first phase, cell-based models revealed that the cannabinoids had the most significant positive effects on neuroprotection and dopamine secretion. We then evaluated the ability of combinations of these cannabinoids to ameliorate a 6-hydroxydopmamine (OHDA)-induced change in locomotion in larval zebrafish, which has become a well-established PD disease model. Equimolar mixtures that each contained three cannabinoids were able to significantly reverse the OHDA mediated changes in locomotion and other advanced metrics of behavior. Additional screening of sixty-three variations of the original cannabinoid mixtures identified five highly efficacious mixtures that outperformed the original equimolar cannabinoid MEMs and represent the most attractive candidates for therapeutic development. This work highlights the strength of the reductionist approach for the development of ratio-controlled, cannabis mixture-based therapeutics for the treatment of Parkinson's disease.

KEYWORDS

Parkinson's disease, cannabinoids, zebrafish, dopamine, neuroprotection, movement disorder, cannabis, cannabidiol

Introduction

Neurodegeneration in Parkinson's disease (PD), Alzheimer's disease, Lewy Body Dementia, and Huntington's disease is a growing health burden. Among these, the pathophysiology of PD has been intensively studied, but its underlying cause remains enigmatic (Gan-Or et al., 2015; Bandres-Ciga et al., 2020; Mani et al., 2021). Mechanistically, motor symptoms of PD are linked to the death of dopamine (DA)-producing neurons in the substantia nigra (Surmeier, 2018; Gonzalez-Rodriguez et al., 2020) and to the deposition of misfolded alpha-synuclein protein aggregates in Lewy bodies (Greenamyre and Hastings, 2004; Lin et al., 2019). Desensitization of the DA response system has also been documented, suggesting that both DA production and efficacy are compromised in PD (More and Choi, 2015). Most of the agents currently approved for treating PD address symptoms of DA depletion, such as bradykinesia, and do not modify disease progression. Levodopa remains the most common symptomatic treatment for PD; however, 30–35% of patients develop Levodopa Induced Dyskinesia (LID) after as little as 24 months of Levodopa usage (Utsumi et al., 2013; More and Choi, 2015). Given these significant side effects, there remains a need for non-Levodopa based symptomatic therapies for PD.

The potential for cannabis-derived compounds to provide symptom improvement in PD patients is suggested by anecdotal and patient reported outcomes (PRO) data (Venderova et al., 2004; Feeney et al., 2021; Yenilmez et al., 2021). Unfortunately, with native cannabis or cannabis extracts, there are unnecessary and unwanted psychoactive side effects from delta-9 tetrahydrocannabinol (THC) (Oultram et al., 2021), along with plant material contamination and complexities in the accurate delivery of therapeutic extracts (Couch et al., 2020; Wiseman et al., 2021) that may compromise patient safety. Additionally, single cannabinoid therapeutics composed of THC or cannabidiol (CBD) do not fully recapitulate the PRO effectiveness of the native plant (Turner et al., 2017) or it's extracts (Blasco-Benito et al., 2018; Russo, 2018; Ferber et al., 2020). This suggests that cannabis plant extracts, which contain hundreds of compounds, include components other than these major cannabinoids that contribute significantly to their effectiveness. The pharmacodynamic properties of the cannabinoid and terpene active ingredients from cannabis plant extracts have been described in detail (Maayah et al., 2020; Patricio et al., 2020). In the cannabinoid research field, the ability of cannabis-derived ingredients to act synergistically by enhancing or diminishing the net effectiveness of a therapy has been identified and is referred to as the 'entourage effect' (Ben-Shabat et al., 1998; Russo, 2011). While the entourage effect is typically expected to be modulated pharmacodynamically through the interactions of multiple ligands with one or more receptors, pharmacokinetic effects such as metabolism have also been demonstrated (Cogan, 2020). This makes assessing their activity more complicated, but also makes them potentially more effective therapeutics than single target drugs due to positive co-operative interactions. The cannabinoids and terpenes from cannabis plant extracts are ligands of multiple receptors including metabotropic cannabinoid receptors, ionotropic cannabinoid receptors, serotonin receptors, and orphan G-protein coupled receptors, making it likely that they would individually act as multi-target drugs (Stasilowicz et al., 2021), and indeed cannabis extracts demonstrate more potency than CBD alone in cell based assays (Milligan et al., 2022). A number of minor cannabinoids have been shown to bind to CB1 and CB2 receptors, although with varying affinities (Zagzoog et al., 2020). While some terpenes have shown an additive effect with cannabinoid agonists in rodents (LaVigne et al., 2021), the direct interaction of terpenes with the CB receptors (Santiago et al., 2019; Finlay et al., 2020) and TRP channels (Heblinski et al., 2020) is contested. Developing a model to study these complex interactions is a critical step to the rational design of multi-component, efficacious, cannabis-inspired therapeutics for PD.

Based on the complexity, side effects, and off target interactions that may be inevitable using whole plant extracts, it is essential to identify the core components of cannabis that are required for the treatment of PD. To this end in 2016, using a combination of *in silico* (Reimann-Philipp et al., 2020) and cell based assays, GB Sciences identified and patented a mixture of 8 essential cannabis components that when combined with CBD or cannabinol (CBN) recapitulated the anti-Parkinsonian activity anecdotally ascribed to whole plant cannabis (U.S. Patent Number 10,653,640). These compounds include the three minor cannabinoids cannabigerol (CBG), cannabichromene (CBC), and cannabidivarin (CBDV) (<5% of the original cannabis extracts), and five terpenes (α-pinene, trans-nerolidol, limonene, linalool, and phytol). While the identification of 8 compounds from a pool of >100,000 represents a tremendous reduction in complexity, unfortunately these mixtures remain difficult to formulate into therapeutics owing to the diversity of the chemical structures and the differences in pharmacokinetics of each component. Aside from the practical difficulties in creating therapeutics containing multiple drugs, known as Fixed-dose Drug Combinations (FDCs), these polypharmaceuticals also present challenges with respect to patient interactions (Gautam and Saha, 2008). FDCs can pose a challenge with dosage adjustments of individual drugs, drug interactions, and off-target effects, with each additional ingredient creating more opportunities for adverse

reactions. Thus, the identification of the minimal set of cannabis ingredients that can recapitulate the effects of whole plant is crucial in the creation of a multicomponent therapeutic.

Therefore in this study we sought to further reduce the number of compounds in the patented formulation to a minimal essential mixture (MEM) that could recapitulate as many of the effects of the original combination as possible with the goal of generating a mixture that would be more amenable to pharmacological production. Two cell assays were initially used to evaluate the potential therapeutic efficacy of the mixtures by using both an *in vitro* neuroprotection assay and a dopamine secretion assay in dopaminergic neuronal cell models. From these cell assays, we identified the cannabinoids as being largely responsible for the activity seen in the patented mixture with a nominal effect of the terpenes. We then assayed multiple drug combinations that contained three individual cannabinoids for their ability to ameliorate a 6-hydroxydopmamine (OHDA)-induced model of PD in zebrafish larvae. The results have allowed us to move sequentially from the remarkable chemical complexity of the cannabis plant, to moderately complex mixtures with potential PD-therapeutic activity as evaluated in cell models, to refined minimal essential mixtures of cannabinoids that demonstrate therapeutic effects on OHDA treated zebrafish. The sequentially reductionist process used in this study preserves some of the entourage-like effects of whole plant extracts, while achieving 'relative' simplicity within MEM that is a requirement for obtaining the manufacturing and quality control advantages of single ingredient drugs.

Materials and methods

Chemicals and cell lines

All cannabinoids used in this study were purchased as 1 mg/ml standards in methanol (Sigma, Ontario, Canada): Cannabidiol (CBD), Cannabichromene (CBC), Cannabidivarin (CBDV), Cannabigerol (CBG), and Cannabinol (CBN). The α-pinene (98% purity), trans-nerolidol (>85% purity), and Methanol (99.9% purity) were also purchased from Sigma (Sigma, Ontario, Canada). D-Limonene (96.9% purity) was purchased from MPBIO (MP Biomedicals LLC, Ohio, USA), Linalool (>96% purity) was purchased from TCI (TCI, Oregon, USA) and Phytol was from Agilent Technologies (Agilent Technologies, Inc., Rhode Island, USA). All terpenes were diluted in methanol. 6-hydroxydopamine (OHDA) (Sigma, Ontario, Canada) was diluted in saline buffer (0.9% NaCl) supplemented with 0.02% Ascorbic acid. Mixtures produced for cell line experiments used equimolar components as follows: MIX-1 = minor cannabinoids (CBC, CBG and CBDV) + Terpenes (Linalool, α-pinene, limonene, t-nerolidol and phytol), MIX-2 = terpenes only, and MIX-3 = Minor cannabinoids only. Individual major cannabinoids, CBD and CBN, were added at the same equimolar amount. Please refer to legends in Figures 3, 6 for specifics regarding mixture compositions.

Cell lines used were from ATCC (Manassas, Virginia, United States). Cath.a cells (sp. = mouse, cat# CRL-11179), a CNS catecholaminergic cell line, were cultured according to ATCC instructions and were induced to CAD differentiated status by serum deprivation (0.5% FBS culture for 36 h) prior to experiments as described (Qi et al., 1997). PC12 cells (sp. = rat, ATCC #CRL-1721) were cultured in RPMI 10% FBS. PC12 differentiation used Minimal Essential Medium containing 1% HS and 0.5% FBS, then the cells were treated with 100 ng/ml NGF, 100 ng/ml basic fibroblast growth factor (bFGF), and serum-starved media containing 2 mg/ml BSA for 2 days (Jeon et al., 2010). Schematic representations of exposure paradigms available in Supplementary Figure S2.

In vitro neuroprotection assays

Neuroprotective effects were assessed based on the ability of both individual compounds and mixtures of compounds to protect against neuronal cell death induced by 1-methyl-4-phenylpyridinium (MPP^+) in the 1-methyl-4-phenyl-1,2,3,6-tetrahydropyridine (MPTP)-based selective cytotoxicity assay (Arshad et al., 2014). MPP^+ is an active metabolite of MPTP that is known to cause human Parkinsonism after injection (Langston and Palfreman, 2014). As in Arshad et al. (2014), MPTP/MPP^+ assays were performed *in vitro* on Cath. a cells by applying each compound or mixture of compounds to the cell cultures 18 h after application of MPP^+ (Arshad et al., 2014). Cell viability assessments were performed using a standard MTT cell viability assay (MTT Cell Proliferation Assay Kit, Cayman Chemicals, Ann Arbor, Michigan, Item No. 10009365). Cell viability was assessed 24 h after exposure to MPP^+, which is 6 h after exposure to the tested compound or compound mixture. Percent protection was normalized to MPTP control alone (100% cell death). To establish an effective dose range across the compounds in this assay system, the neuroprotective effects of each individual compound were tested at 5 different concentrations (Supplementary Figure S1). Based on these results the individual and equimolar mixtures were tested in the cell assays at 10 μM each (Figure 1). Equimolar mixtures contained 10 μM of each compound. In all cases vehicle controls contained methanol at equal concentrations to those found in test compounds/mixtures, ≤ 5%.

In vitro dopamine-release assay

In parallel with the neuroprotection assays, cannabinoid and terpene compounds were tested alone and in mixtures to

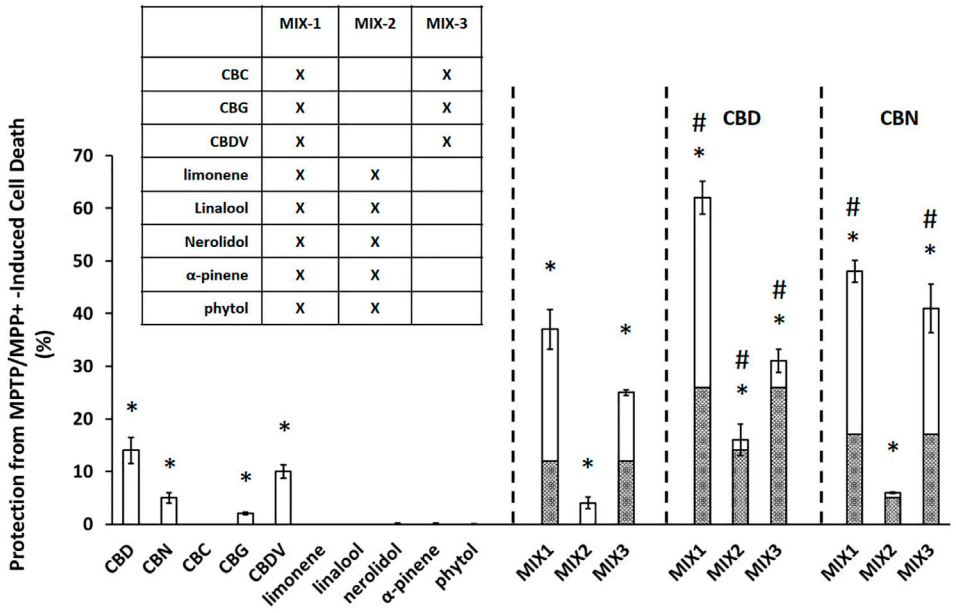

FIGURE 1
Cannabinoids produce significant neuroprotection in MPTP/MPP⁺ assay. Data are presented as the percent protection from MPTP/MPP⁺ cell death evaluated based on the MTT cell viability assay, where the experimental value is normalized relative to the vehicle control. An asterisk * indicates a p-value <0.05 for the replicates relative to their respective vehicle control replicates. MIX-1, MIX-2, and MIX-3 tested without or with the addition of a major cannabinoid (CBD or CBN) a hashtag # represents $p < 0.05$ major cannabinoid vs. native mixture. Calculated (hashed shading) prediction of efficacy based on the sum of the efficacy of each ingredient measured separately and Measured (open shading) efficacy are shown. Each data point in the figure represents the mean ± the standard deviation of twenty-four experimental results obtained at 10 μM of each major or minor cannabinoid and terpene (alone or in equimolar mixtures as described in the inset table in Panel). Twenty-four experimental results were obtained by repeating eight independent experiments three times on three different days ("8 × 3").

determine their effects on dopamine release from differentiated PC12 cells (Greene and Tischler, 1976). PC12 cells were differentiated as described (Jeon et al., 2010; Hu et al., 2018). Supernatant samples were collected from 3 replicate wells 30 min after application of PMA/Ionomycin (positive control) or the indicated compounds, and dopamine was measured in the medium using the Dopamine ELISA Kit #KA1887 from Abnova (Abnova, California, US) according to manufacturer's instructions. For dopamine secretion, dopamine release was normalized to PMA/ionomycin control (0% baseline).

Zebrafish

The fish used in this study were wild-type AB/Tubingen hybrids. Age-matched embryos were reared in Pentair Aquatic Ecosystem (Apopka, Florida, USA) nursery baskets (200 embryos per basket) on a ZebTec Recirculation Water Treatment System (Tecniplast, Buguggiate, Varese, Italy) at 28.5 ± 0.5°C, on a 14-h day–10-h night light cycle. All adult zebrafish husbandry and breeding was in accordance with the Canadian Council of Animal Care guidelines.

Behavioral testing in zebrafish

All compounds were diluted in 100% methanol (MeOH) and experiments were performed in a HEPES buffered E3 (HE3) medium (5 mM NaCl, 0.17 mM KCl, 0.33 mM CaCl2-2H2O, 0.33 mM MgSO4-7H2O, 10 mM HEPES, pH 7.2). Individual 120 h post fertilization (hpf) larval zebrafish were transferred to a 48-well microtiter plate in 500 μL of HE3 media. Larvae were acclimated for at least 1 hour in a lighted 28.5°C incubator (photon flux: 3–5 μmol s−1 m^2) prior to experimentation and larval behavior was analyzed using DanioVision larval tracking systems with EthoVisionXT14/15 software (Noldus Information Technology Inc., Virginia, USA). Distance traveled was measured using dynamic subtraction at 28.5°C over 120 min with the first 90 min under lighted conditions (15 μmol m-2 s-1), followed by alternating 5-min dark/light cycles. Each larvae represents an independent measurement. Any larvae that were dead or displayed phenotypic abnormalities were removed from analysis. 12 larvae were used in each experimental condition, and at least 2 replicates of each concentration were performed.

6-Hydroxydopamine Parkinson's model development and advanced behavioral analysis

Larvae were exposed to varying concentrations of 6-hydroxydopamine (OHDA) from 48 to 120 h post fertilization (hpf). 15 dechorionated larvae were transferred in 5 ml of HE3 to each well of a six-well plate. The 5 ml exposure media was replaced daily, and ascorbic acid/saline buffer (used to resuspend OHDA) was used as a vehicle control. Larvae were then loaded into 48-well microtiter plate in 500 µL of HE3 media as described above. Schematic representations of exposure paradigms available in Supplementary Figure S2.

In addition to distance travelled, activity was measured as a percentage change in pixel density during data acquisition. The integrated visualization feature in EthoVision software (Noldus Information Technology Inc., Virginia, USA) was used to detect larval activity during three distinct activity types: high (greater than 0.5% pixel change per sampling), moderate (between 0.03 and 0.5%), and inactive (less than 0.03%) states. The frequency with which larvae switched between activity states and the cumulative duration of time spent in each activity state was then measured. Metrics were captured in 1 min bins, and the average over 90 min was used to calculate each metric in each activity state. For frequency calculations, the number of times larvae switched between activity states (high, moderate, and low) was calculated (termed Total Frequency). The cumulative amount of time spent in the high and moderate activity states combined (termed Cumulative Duration) was averaged over 90 min and measured as a percentage.

Equimolar minimum essential mixture and defined cannabinoid-ratio MEM testing using OHDA PD model

Acute behavioral assays were performed on the cannabinoids selected for the study as described above except larvae were loaded into the well plates with 450 µL HE3. Immediately prior to recording 50 µL of 10 × test compound solution was added to each well. For the OHDA challenge experiments 150 µM OHDA was used for all challenge experiments. During media replacements at 72 and 96 hpf, 25 µL of 200X stock solutions of the respective cannabinoid or E-MEM was added to the exposure media. At 120 hpf larvae were washed with HE3 and transferred in 500 µL to 48-well plates. Behavioral analysis was then performed as described above. All experiments were performed at least in duplicate. The E-MEM selected for further study (above) were combined in non-equimolar ratios (defined cannabinoid-ratios DCR-MEM) and subjected to both the total distance and activity analysis metrics, as described above. This procedure was done in 3 steps, reducing a single component by 50% (a 1:2 ratio relative to their original equimolar concentrations) or 90% (a 1:10 ratio relative to their original equimolar concentrations), reducing 2 components by 50% (1:2) or 90% (1:10), or a defined cannabinoid-ratio (DCR)-MEM reducing 2 components by different cannabinoid-ratios (1:2 or 1:10 relative to their original equimolar concentrations).

Analysis and statistical methods

The mean ± the standard deviations were calculated for all samples in the cell assays. A two-tailed student's t-test was used to evaluate the statistical differences between sample types. Calculation of statistical significance for total distance traveled over 90 min was performed by one-way ANOVA using a Dunnett's multiple comparison test using GraphPad Prism 7.04 software (La Jolla, California, United States). Comparisons of either OHDA + Drug vs. OHDA, or Drug vs. MeOH were performed as an unpaired Student's t-test. An asterisk is used to represent a p-value less than 0.05 or lower, unless otherwise defined.

Results

Neuroprotective effects of cannabis-compounds alone and in combination

At 10 µM, all of the individual cannabinoids except CBC displayed some neuroprotective effects while none of the terpenes were able to prevent MPTP/MPP^+ induced apoptosis (Figure 1). A mixture of the minor cannabinoids and the terpenes (MIX-1) showed a substantial neuroprotective effect with an increase in cell survival of 37 ± 3.8%. Mixtures of either the terpenes alone (MIX-2) or the minor cannabinoids (MIX-3) were then created to assess their contribution to the overall activity of MIX-1. MIX-2 (terpenes) showed a limited overall protection (4 ± 1.1%) while MIX-3 (minor cannabinoids) demonstrated similar activity to MIX-1 (25 ± 0.5%). The effects of the major cannabinoids were then assessed by adding each individually to the mixtures. CBD increased cell survival in all three mixtures (62 ± 3.1% vs. 37 ± 3.8% (MIX1), 16 ± 3% vs. 4 ± 1.1% (MIX-2) and 31 ± 2.2% vs. 25 ± 0.5% (MIX-3). The effects of the second major cannabinoid (CBN) were similar but less pronounced than those seen for CBD. Importantly, in all cases the mixtures were more neuroprotective than would have been estimated from the sum (hashed shading area of bars) of their individual effects.

Effects of cannabis-compounds in mixtures on dopamine-release responses

In parallel with the MPTP testing described in the previous section, we tested the effects of the same individual compounds

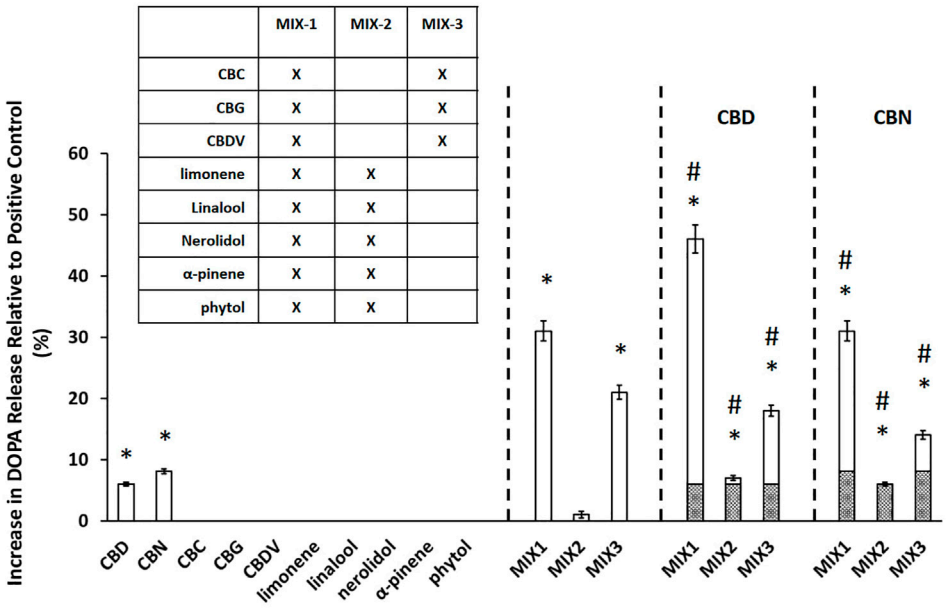

FIGURE 2
Cannabinoids mixtures elicit significant dopamine secretion. The experimental value is presented as the normalized value, which is a percent of the positive control value (secretion achieved with PMA/Ionomycin application). An asterisk * indicates a p-value <0.05 for the replicates relative to their respective vehicle control replicates. MIX-1, MIX-2, and MIX-3 were tested without or with the addition of a major cannabinoid (CBD or CBN). A hashtag # represents $p < 0.05$ major cannabinoid vs. native mixture. Calculated (hashed shading) prediction of efficacy based on the sum of the efficacy of each ingredient measured separately and Measured (open shading) efficacy were shown. Each data point in the figure represents the mean ± the standard deviation of twenty-four experimental results obtained at 10 μM of each major or minor cannabinoid and terpene (alone or in equimolar mixtures as described in the inset table in Panel B). Twenty-four experimental results were obtained by repeating eight independent experiments three times on three different days ("8 × 3").

and mixtures on dopamine release from PC12 cells (Figure 2). The major cannabinoids, CBD (6.0 ± 0.3% DOPA release) and CBN (8.1 ± 0.4% DOPA release), were the only individual compounds tested that produced a statistically significant ($p < 0.05$) increase in dopamine release. The relative performance of the mixtures in the dopamine assay was similar to the trend observed in the MPTP/MPP^+ assay. MIX-1 led to the largest increase in DOPA release of 31 ± 1.6%, followed by MIX-3 (21 ± 1.1%), while the DOPA release for MIX-2 was not significant. Again, we also evaluated the effectiveness of adding the major cannabinoids (CBD or CBN) to each MIX relative to the effectiveness of each MIX alone. When CBD was added to MIX-1, the effectiveness was increased leading to a DOPA release of 46 ± 2.3% for MIX-1 + CBD, while adding CBN to MIX-1 did not significantly increase the DOPA release. The addition of CBD or CBN to MIX-2 were able to produce modest but significant increases in dopamine secretion up to 7.0 ± 0.4% DOPA release for MIX-2 + CBD and 6.0 ± 0.3% DOPA release for MIX-2 + CBN. Similarly, the addition of CBD to MIX-3 produced an increase in DOPA release relative to MIX-3 alone (MIX-3 + CBD produced 18 ± 0.9% DOPA release), while the addition of CBN to MIX-3 produced a significant reduction in the DOPA release compared to MIX-3 alone (MIX-3 + CBD produced 14 ± 0.7% DOPA release). As in the neuroprotection assays, mixtures of the components were able to elicit significantly more robust responses than the individual components.

Taken together, these results demonstrate that the effects of the mixtures cannot be attributed to a single ingredient. On the contrary, it suggests that interactions between the components in the mixtures are critical for the maximal efficacy of the mixture. In addition, it appears from the cell assay data that the terpene components of the mixtures have a minimal contribution on their efficacy and that the cannabinoid components are sufficient to use as a potential therapeutic.

Assessment of cannabinoid effects in a zebrafish OHDA Parkinson's model

In order to test whether the cannabinoids and cannabinoid-based mixtures identified by the cell screening assays would potentially alleviate symptomatic effects in an animal model of Parkinson's disease, we applied a previously developed zebrafish larval model of dopamine cell loss caused by exposure to 6-hydroxydopamine (OHDA) (Feng et al., 2014; Cronin and Grealy, 2017; Benvenutti et al., 2018) and refined it based on a

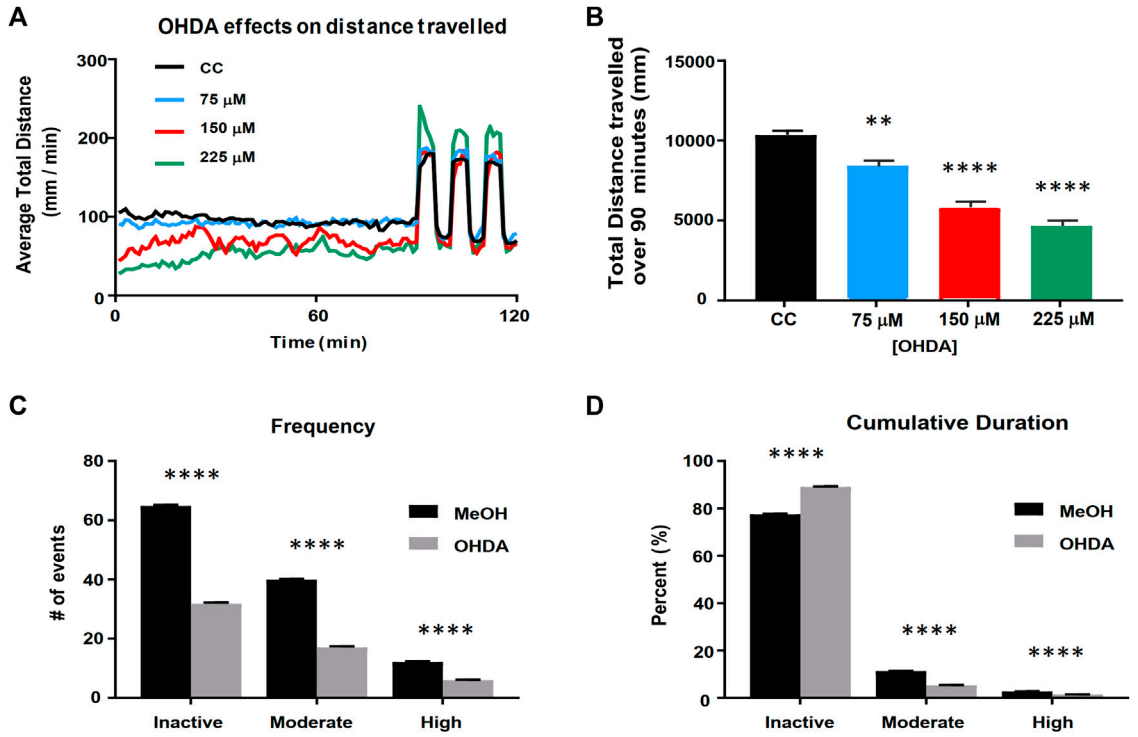

FIGURE 3
Validation of the larval zebrafish OHDA model. Panel **(A)** Behavioral profiles of total distance traveled (60 s bins) following OHDA exposure from 48 to 120 hpf. Panel **(B)** Total distance travelled during the first 90 min in the light following OHDA exposure from 48 to 120 hpf (n = 36). Advanced activity analytics **(C,D)** of Total Frequency of switching between activity states **(C)** and the nested Cumulative Duration in each activity state **(D)** (n = 48). CC vs. OHDA, ** = $p < 0.01$ **** = $p < 0.0001$.

determination of OHDA dose and time conditions. We found that larval exposure to OHDA produced a concentration-dependent decrease in the baseline activity during an initial 90-min period in the light (Figures 3A,B). It also led to a non-significant increase in the maximum response to the light/dark transition (startle response) at 225 µM. Based on these findings, we selected 150 µM OHDA as our testing model as it produced a decrease in activity during the 90-min baseline period, which can be considered a model of bradykinesia, while not impacting the startle response which suggests a minimal effect on general locomotor function (Figure 3). Visual assessment of the OHDA treated larvae appeared to show a more complex pattern of behavior than could be assessed by a simple measure of distance travelled. We observed that OHDA treated larvae, when at rest, displayed a small, periodic side-to-side movement with no velocity that may represent a 'resting tremor'. This behavior had not been previously defined and further highlights the significance of the OHDA exposure to act as a model of PD. Thus, in addition to analyzing distance travelled by the larvae as described above, larval activity was also analyzed using a % pixel-change based assessment (Figures 3C,D). The activity was divided into three types: high, moderate, and inactive states. The high and moderate activities reflect burst swimming (escape behavior) and slower speed foraging swimming respectively (Budick and O'Malley, 2000). The inactive state was set between 0 and 0.03% change as a way to quantify the 'resting tremor' as a unique phenotype in the OHDA treated zebrafish larvae. OHDA treatment caused a reduction in the frequency of all states (Figure 3C). Typically, OHDA treatment resulted in a 50–60% reduction in activity state transitions for all three states (Figure 3C). As shown in Figure 3D, all larvae spent the majority of their time in the inactive state, with untreated larvae spending ~80% of their activity in the inactive state, ~15% in the moderately active state and ~5% in the highly active state (Figure 3D). The OHDA treated larvae spent a greater fraction of their time in the inactive state (~90%) with a concomitant decrease in moderate and high activities (5 and 1% respectively).

Assessment of behavioral response to cannabinoids and equimolar MEMs

Initial experiments were conducted to determine the effective concentration ranges of each of the five pure, individual cannabinoids. In general, the cannabinoids tested acutely showed a similar effect on baseline larval behavior to that

TABLE 1 Cannabinoid dilution series testing results. The effects of purified individual cannabinoids was tested acutely on 120 hpf zebrafish larvae. Also, the pure individual cannabinoids were also evaluated for their ability to reverse OHDA-mediated hypoactivity. L/D = Light/dark startle response.

Chemical	Concentration range	Phenotype	OHDA treatment
Cannabidiol (CBD)	0.25–4 μM	Immediate increase in activity at 2 μM Sedative and abolished L/D at 2 μM	No significant change in activity 0.125–1 μM
Cannabinol (CBN)	0.25–4 μM	Immediate increase in activity at 1 μM Sedative and abolished L/D at 1 μM	No significant change in activity 0.1–1 μM
Cannabichromene (CBC)	0.1–3 μM	Immediate increase in activity at 0.5 μM Sedative and abolished L/D at 0.5 μM	No significant change in activity 0.1–0.5 μM
Cannabidivarin (CBDV)	0.25–4 μM	Immediate increase in activity at 2.5 μM Sedative and abolished L/D at 2.5 μM	No significant change in activity 0.1–0.5 μM
Cannabigerol (CBG)	0.25–3 μM	Immediate increase in activity at 2 μM Sedative and abolished L/D at 2 μM	No significant change in activity 0.25–1 μM

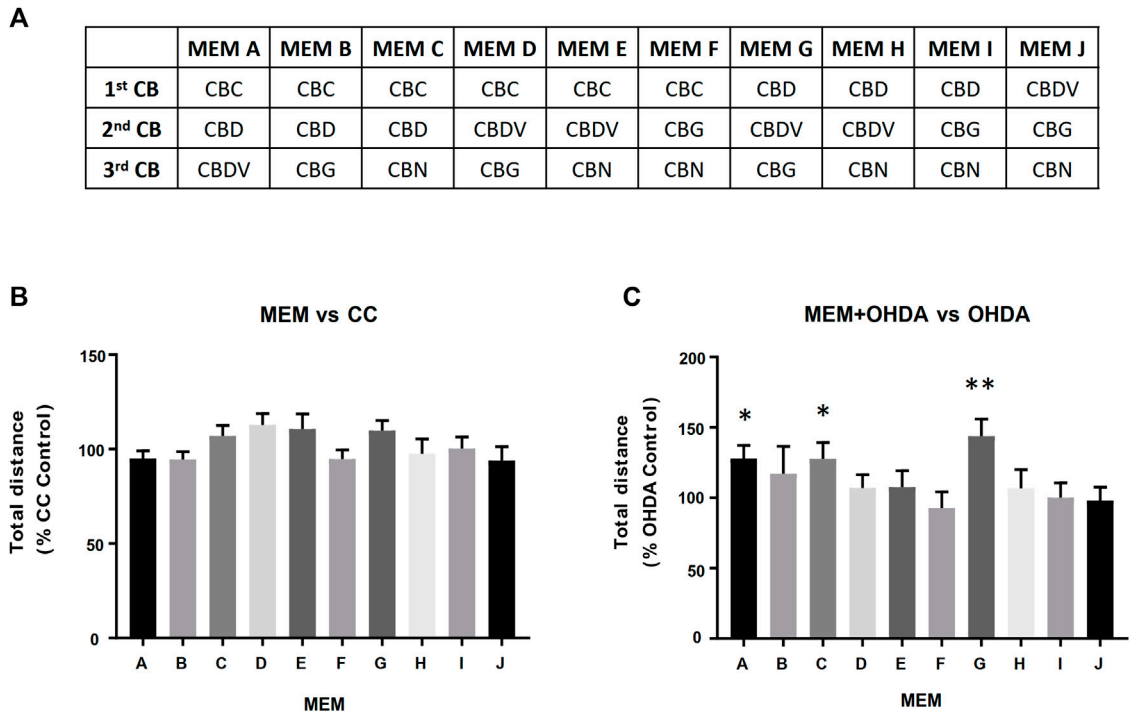

FIGURE 4
Equimolar Minimum Essential Mixtures (E-MEM) alleviate OHDA mediated hypoactivity. Panel **(A)** Five cannabinoids (CBs) were used to create the 10 possible three component equimolar mixtures. Panels **(B**,**C)** Each of the 500 nM E-MEM (166.7 nM of each cannabinoid) was assessed for its ability modify total distance travelled of **(B)** Carrier Control (CC) or **(C)** 150 μM OHDA. Data is normalized to either CC **(B)** or OHDA **(C)** (100%). MEM + OHDA vs. OHDA, * = $p < 0.05$, ** $p < 0.01$.

previously profiled for CBD (Achenbach et al., 2018). As the concentration was increased, the normal response to a light to dark transition was abolished. The effective concentration range was considered the concentrations between a no observable effect level (NOE) and a level that had a minimal statistically significant effect on behavior (Table 1). At the concentrations of the cannabinoids tested there was a slight opposition to the 150 μM OHDA induced hypoactivity, however, the effects were not significant.

In order to assess possible potentiating effects between the cannabinoids, three component, equimolar minimum essential mixtures (E-MEM) of the 5 cannabinoids were prepared (Figure 4A). Three of these E-MEMs; A, C and G showed a significant opposition to the OHDA induced

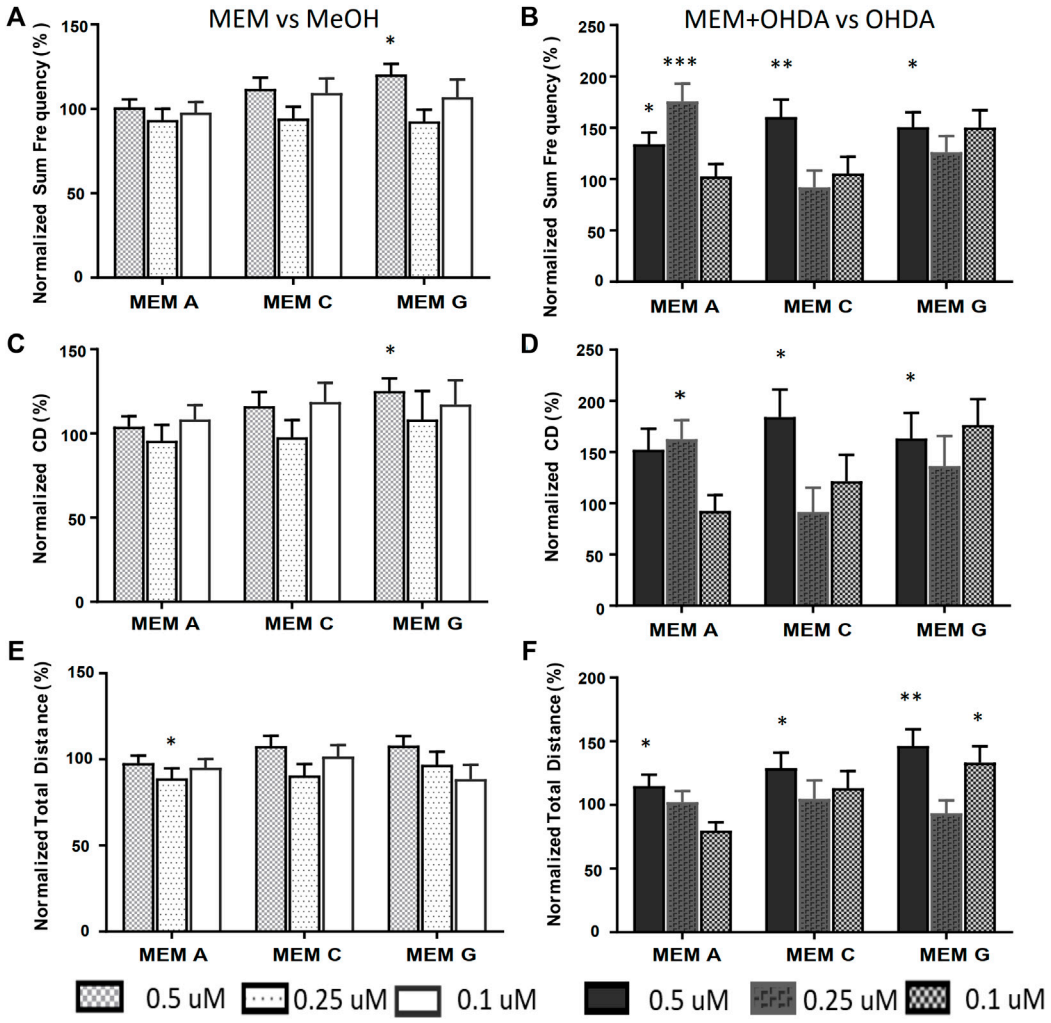

FIGURE 5
Equimolar MEMs alleviate both OHDA mediated Total Frequency and Cumulative Duration deficits. Activity metrics of Total Frequency **(A,B)**, Cumulative Duration **(C,D)** and Total Distance **(E,F)** for equimolar MEMs at 500, 250 and 100 nM (166.7, 83.3 and 33.3 nM each ingredient respectively). MEM vs. methanol carrier control **(A,C,E)**, and MEM+150 μM OHDA vs. 150 μM OHDA **(B,D,F)**. *$p < 0.05$, **$p < 0.01$, ***$p < 0.001$.

hypoactivity as measured by the total distance travelled (Figure 4C) while not displaying any effect on carrier control larvae (Figure 4B).

The equimolar MEMs (A, C and G) were further analyzed using the refined activity metrics. At 500 nM all three E-MEMs except E-MEM-C, significantly affected Frequency, Cumulative Duration (CD) and Total distance as measured using refined activity metrics vs OHDA (Figures 5B,D,F). 250 nM dilutions of the E-MEMs abolished these changes, except with relation to Frequency and CD in 250 nM E-MEM A (Figure 5B). No recovery was apparent for the 100 nM E-MEM experiments for Frequency or CD metrics. 500 nM MEM G increased the activity of MeOH treated control larvae as measured by Frequency and CD, (Figures 5A,C), but not total distance (Figure 5E).

Identification of optimal, defined cannabinoid-ratio minimum essential mixture

Based on the results from the equimolar mixture experiments, a comprehensive series of experiments were performed where one or two components of each mixture were reduced by 50% (1:2 ratio relative to the equimolar MEM) and/or 90% (1:10 ratio relative to the equimolar MEM) to produce novel molar ratios for further efficacy studies. The defined cannabinoid-ratio minimum essential mixtures (DCR-MEMs) that produced the most significant opposition to the PD-like effects of OHDA will be described herein (Figure 6) and a comprehensive summary of all of the results is included in Table 2. Optimization of all three E-MEMs

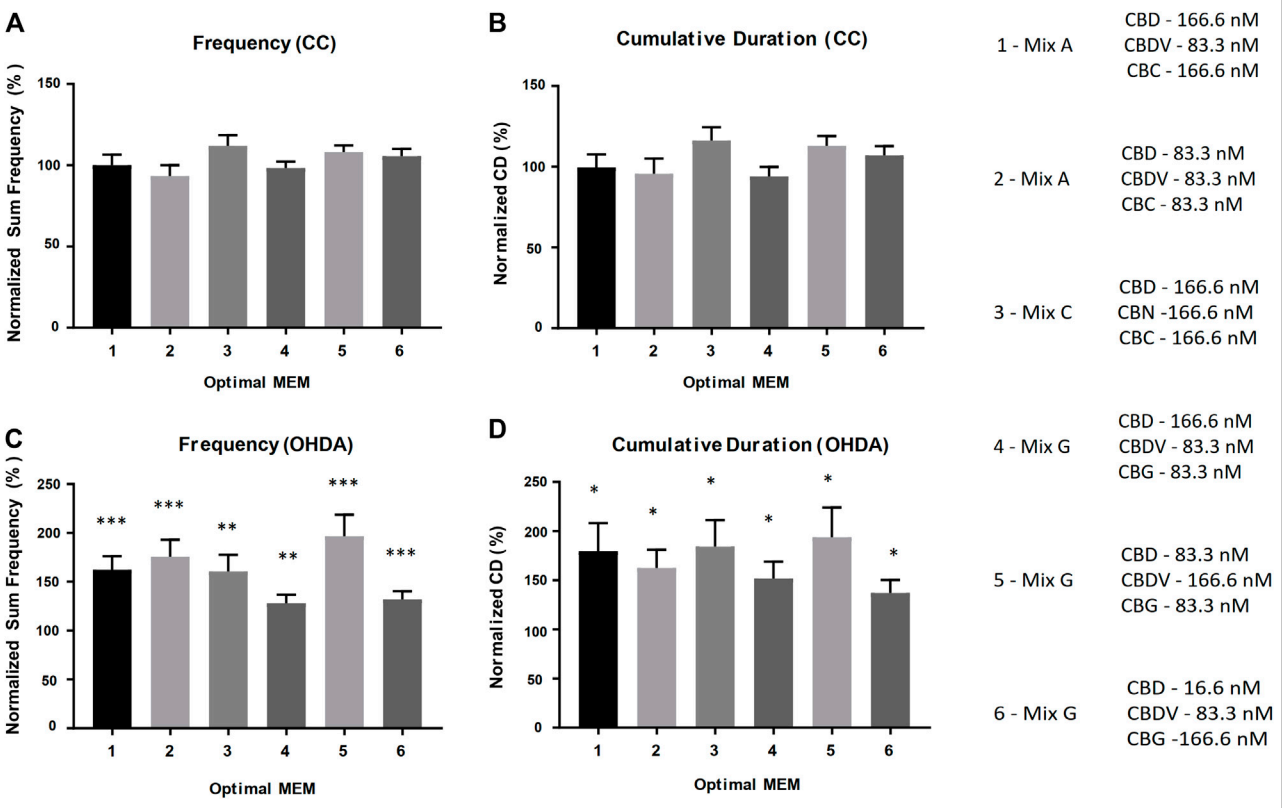

FIGURE 6
Optimal DCR-MEM ratios alleviate both OHDA mediated frequency and cumulative duration deficits. Activity metrics of Total Frequency **(A–C)** and Cumulative Duration **(B–D)**. Optimal DCR-MEM vs. methanol carrier control **(A,B)**, and Optimal DCR-MEM+150 μM OHDA vs. 150 μM OHDA **(C,D)**. * = $p < 0.05$, ** = $p < 0.01$, *** = $p < 0.001$.

led to a substantial opposition to PD-like, OHDA mediated changes in Frequency and Cumulative Duration, while having no effect on methanol treated controls (Figure 6). For E-MEM A, the 250 nM equimolar mixture performed as well as the optimized version (a 50% decrease in CBDV from the original 500 nM dilution). None of the MEM C optimized ratios were able to improve upon the 500 nM original dilution without causing increased activity against methanol controls. Several optimized ratios were developed for MEM G that improved upon the original equimolar response to OHDA, while not affecting methanol treated larvae. Specifically, ratio 5 displayed the greatest response in both the Frequency and Cumulative Duration metrics (Figure 6).

Discussion

Summary of findings: Use of the zebrafish OHDA model to reduce complexity of cannabinoid mixtures that demonstrated efficacy in cell-based MPTP-neuroprotection and dopamine release assays

Anecdotal and Patient Reported Outcomes (PRO) suggest that c Cannabis can alleviate the symptoms of several neurological disorders, including PD. Analysis of clinical meta-data offers mixed evidence in support of medical cannabis. While well tolerated, medical cannabis has been shown to have limited benefit in improving dyskinesia and motor function (Thanabalasingam et al., 2021), although patients did report improvements in sleep quality and quality of life (Urbi et al., 2022). Conversely, cannabis-derived phytocannabinoids have shown a clear neuroprotective effect in rodent models (Prakash and Carter, 2021). While these meta-analyses reveal that medicinal cannabis has therapeutic potential, in order to become a recommended intervention in the treatment of PD, more studies will be required.

However, the use of cannabis as a therapeutic is hampered by a number of factors, including the presence of psychoactive

TABLE 2 Summary of Efficacy of Defined Cannabinoid Ratio MEM activities in the OHDA assay in zebrafish. The concentrations of each of the three cannabinoids tested shown in each field of this table are shown starting with the CBD concentration (labeled in the top row). The CBD concentration is used to divide the results table into three columns. The second cannabinoid and concentration for each ratio result is in the first column of the table and is used to further divide the table into nine sets of nine results, and the last cannabinoid and concentration is above the cell in the row containing the label of the original equimolar ratio formula. Astrices (* = $p < 0.05$, ** = $p < 0.01$, *** = $p < 0.001$) on either side of the "/" represent the level of statistical significance in change in the Total Frequency of Activity State Change metric (right-side)/Cumulative Duration metric (left-side) of zebrafish exposed to the MEM + OHDA versus the OHDA-alone group. Zeroes represent no statistically-significant change in activity, "-" indicates a further reduction (increase in PD-like symptoms, $p < 0.05$)) in activity. N/A = combinations not selected because of the inactivity of their precursors. Bolded cells also showed an MEM dependant increase on methanol treated control larvae.

	166.6 nM CBD			83.3 nM CBD			16.6 nM CBD		
MIX A	**166.6 nM CBDV**	**83.3 nM CBDV**	**16.6 nM CBDV**	**166.6 nM CBDV**	**83.3 nM CBDV**	**16.6 nM CBDV**	**166.6 nM CBDV**	**83.3 nM CBDV**	**16.6 nM CBDV**
166.6 nM CBC	*/*	***/*	0/0	*/*	0/0	0/0	***/0**	0/0	0/0
83.3 nM CBC	0/0	0/0	0/0	**0/0**	***/*	N/A	0/0	N/A	N/A
16.6 nM CBC	****/0**	0/0	****/0**	0/0	N/A	N/A	0/0	N/A	0/0
MIX C	166.6 nM CBN	83.3 nM CBN	16.6 nM CBN	166.6 nM CBN	83.3 nM CBN	16.6 nM CBN	166.6 nM CBN	83.3 nM CBN	16.6 nM CBN
166.6 nM CBC	**/*	0/0	*/0	0/0	0/0	0/0	**0/0**	0/0	0/0
83.3 nM CBC	0/0	***/*	0/0	**0/0**	0/0	N/A	****/0**	N/A	N/A
16.6 nM CBC	0/0	*/0	****/0**	0/0	N/A	N/A	**0/0**	N/A	0/0
MIX G	166.6 nM CBDV	83.3 nM CBDV	16.6 nM CBDV	166.6 nM CBDV	83.3 nM CBDV	16.6 nM CBDV	166.6 nM CBDV	83.3 nM CBDV	16.6 nM CBDV
166.6 nM CBG	*/*	*/0	0/0	*/*	0/0	0/0	*/*	***/*	***/0**
83.3 nM CBG	0/0	**/*	0/-	***/*	0/0	N/A	0/0	N/A	N/A
16.6 nM CBG	**0/0**	0/0	0/0	0/0	N/A	N/A	0/0	N/A	0/*

compounds, potential negative chemical interactions, and non-standardized drug delivery methods (inhalation, edibles, dermal). Because there are hundreds of ingredients in cannabis extracts that may have therapeutic potential along with an extremely large number of possible combinations of these constituents, it may be impossible to systematically test every combination in order to identify the optimal mixture of purified components that make cannabis derived compounds good potential therapeutics. Therefore, one approach to identify the essential elements in cannabis is to logically and experimentally reduce the complexity of these mixtures while retaining as much of the original bioactivity as possible. More specifically, one may increase the probability of a positive therapeutic outcome by identifying the top performing mixture at each level of reduced complexity without exhaustively (and blindly) attempting to test every possible variation.

In this paper, we demonstrated the utility of a multitiered approach to identify minimum essential mixtures that are pharmacologically active in cell and animal models of PD. The research presented in this manuscript is predicated on a previously identified patented mixture of cannabis derived compounds (U.S. Patent Number 10,653,640). In our previous work, an *in-silico* database containing the relative percentages (% wt/wt) of the components found in extracts from different varieties of the cannabis plant (Reimann-Philipp et al., 2020) was used to identify a pool of cannabis components with therapeutic potential. The efficacy of >1,000 complex mixtures derived from this original pool of cannabis components were tested using dopaminergic cell models of PD (U.S. Patent Number 10,653,640). Based on this information, the most effective preliminary mixtures were reduced to complex mixtures derived from 10 cannabis-based compounds

containing both cannabinoids and terpenes for further testing. We used two cell models to initially reduce the complexity of this patented mixture and to define the most efficacious minimum essential mixtures in the animal model. The MPTP/MPP^+ assay used in this study models several aspects of PD pathology, including mitochondrial dysfunction and calcium dysregulation, neuronal cytotoxicity resulting from the calcium dysregulation in the mitochondria and the concomitant increase in the production of reactive oxygen and nitrogen species (Cassarino et al., 1997). For this assay we chose Cath.a cells, which are murine neurons from the Locus Coeruleus (LC), one of the earliest sites of PD neurodegeneration (Paredes-Rodriguez et al., 2020). Additionally, because cannabinoids reportedly modulate DA secretion (More and Choi, 2015), we also used dopamine-release assays to measure the ability of these compounds to supplement low dopamine production levels through increased DA secretion. PC12 cells are dopaminergic neuroendocrine cells that have been extensively characterized and are highly amenable to pharmaceutical manipulation (Zhang G. et al., 2019). The cell-based data demonstrated clearly that the cannabinoids provided both neuroprotective and dopamine secretion abilities not seen in the terpene mixtures alone (Figures 1, 2). Because PD has a complex pathology, no single cell line can recapitulate all of the mechanistic details. Thus future work will endeavor to continue to validate the cell line observations in additional animal models, potentially using *ex vivo* cultures of dopaminergic neurons. Importantly, in both of these assays, the cannabinoids demonstrated positive interactions that may be explained by the entourage effect. While more data and modeling are required to determine whether the activity of these combinations represent true synergy (Lederer et al., 2019), the maximal effects seen in the mixtures do represent more than the expected sum of their individual effects. Based on these findings, the terpenes were eliminated from the pool of compounds prior to testing the candidate Minimum Essential Mixtures (MEMs) in the zebrafish model of PD.

A larval zebrafish model was selected to assess the ability of the cannabinoid mixtures to alleviate the movement disorders associated with Parkinson's disease. When larval zebrafish are exposed to 6-hydroxydopamine (OHDA), there is a dose-dependent effect that leads to the inactivation and eventual death of DA-producing cells of the substantia nigra (Zhang W. et al., 2019). DA-producing neuronal cell loss and associated DA depletion in the striatum are correlated with altered motor behavior and changes in the movement patterns of zebrafish (Feng et al., 2014; Cronin and Grealy, 2017; Benvenutti et al., 2018). Zebrafish larval locomotion is often divided into burst swimming (high velocity) and slow swimming (lower velocity) states (Budick and O'Malley, 2000). Not surprisingly, these disparate behaviors have been mapped to multiple different regions of the brain that are enervated substantially by dopaminergic neurons (Drapeau et al., 2002; McLean and Fetcho, 2004; Severi et al., 2014).

In the current study, we observed a third activity state, characterized by a zero-velocity, tremor-like movement. Attempts to quantify this activity led us to develop advanced analytics of larval behavior, and further evaluation of the etiology of this phenotype is ongoing. The use of the zebrafish OHDA model allowed for a reduction in the complexity and a refinement of the ratios of the original cannabinoid mixtures that demonstrated efficacy in the cell-based assays. MEMs containing CBD and CBDV or CBD and CBC demonstrated the greatest therapeutic potential. These MEMs can now be tested in additional, higher-cost, preclinical model systems.

Support for evaluating the endocannabinoid system as a drug development target for Parkinson's disease

While cannabinoids have been suggested as potential agents for treating a spectrum of neurological disorders, including PD, the mechanism by which they exert these actions in unknown. *A priori*, cannabinoids would appear to be promising drugs for targeting the mechanistic pathways that underlie PD with respect to their effects on movement and potentially modifying disease progression through neuroprotective actions. The minor cannabinoids are ligands for a number of receptors, including CB1, CB2, peroxisome proliferator-activated receptors (PPARs), serotonin 5-HT1a receptors, TRPV1 and others (Walsh et al., 2021). These receptors likely play roles in a number of the known multifactorial etiologies of PD, including mitochondrial Ca2+ homeostasis, intracellular Ca2+ signaling, reactive oxygen species, and neuro-inflammatory pathways (More and Choi, 2015). Increasing evidence supports a modulatory role for the ECB system in movement and movement disorders through bi-phasic modulation of dopaminergic, glutamatergic, and GABAergic receptors within ECB retrograde-signaling systems (Catlow and Sanchez-Ramos, 2015; More and Choi, 2015). The human endocannabinoid (ECB) system is therefore an attractive target for the development of novel treatments for neurologic disorders.

Preclinical studies using exogenous cannabinoids have shown their ability to act as neuroprotectants for dopamine (DA)-producing neurons, to reduce oxidative stress and neuroinflammation, and to provide relief from the motor symptoms of PD (More and Choi, 2015; Bandres-Ciga et al., 2020). Loss of dopaminergic neurons in the substantia nigra pars compacta (SNpc) region and their projecting fibers in the striatum are one of the core pathological features of Parkinson's disease (Gonzalez-Rodriguez et al., 2020). A significant body of literature also demonstrates that cannabinoids can individually restore mitochondrial Ca2+ homeostasis, intracellular calcium signaling, and protect against cytotoxic oxidative stress that would otherwise

harm DA-producing neurons (Ryan et al., 2009; Turner et al., 2017; Peres et al., 2018). PD patients in PRO studies reported motor symptom relief from cannabis use; where they reported improvements/decreases in bradykinesia, muscle rigidity, tremor, and dyskinesia in decreasing order of significance (More and Choi, 2015). The data in this study support the idea that ECB-targeting will modify Parkinsonian movement disorders and provides a MEM for further experimentation.

In this work, cell models of PD allowed for the screening of complex mixtures of cannabis-derived ingredients and identified the cannabinoids as those being responsible for the neuroprotective (MPTP/MPP^+ assays) and dopamine secretory effects. Using the OHDA zebrafish model of Parkinsonian movement disorders, three MEMs containing equal parts of three cannabinoids each were identified that could significantly relieve the OHDA-related motor symptoms. An additional 63 variations using different ratios of the 3 original MEM were also tested, and 22 out of 63 of the defined cannabinoid ratio variations also significantly improved OHDA-related symptoms in zebrafish. Five of these 22 MEMs outperformed the original mixtures and will be further tested in more advanced animal models to develop new therapeutic options for Parkinson's patients.

Conclusions

Cannabis has therapeutic promise in PD. However, there is a need to move beyond whole plant extracts and generate safe, reproducible medicines for patients. This paper identified promising minimal essential mixtures of cannabinoids based on a step-wise, strategic approach to reducing the complexity of the plant secondary metabolome. The sequential use of *in silico*, *in vitro,* and medium throughput *in vivo* experimental systems has generated refined, de-risked, mixtures that can now be tested in additional, higher-cost, preclinical model systems of PD.

Data availability statement

The raw data supporting the conclusions of this article will be made available by the authors, without undue reservation.

Ethics statement

The animal study was reviewed and approved by Animal Care Committee, National Research Council of Canada.

Author contributions

Conceptualization, HT, AS-H, and LE; Data curation, MM, JN, and LS; Formal analysis, MM, JN, and LS; Funding acquisition, HT and LE; Methodology, MM, JN, and LS; Supervision, HT and LE; Validation, HT and LE; Visualization, MM, JN, and LS; Writing–original draft, MM; Writing–review and editing, JN, HT, AS, AS-H, and LE.

Funding

This research project was funded by GBS Global Biopharma. Grants to Chaminade University of Honolulu, Hawaii were received by HT and LS. Work between GBS and the National Research Council of Canada (Halifax, Nova Scotia, Canada) were conducted under an agreement by LE, MM and JN.

Acknowledgments

We would like to thank Christine Luckhart (Noldus Canada) for her support in development of the advanced analytics, and the zebrafish husbandry team at the NRC.

Conflict of interest

A.S.H. is employed by GBS Global Biopharma. H.T. and A.J.S. serve on the Scientific Advisory Board of GBS Global Biopharma. The funders were involved in the conceptualization of the research project, but they had no role in the design of the study; in the collection, analyses, or interpretation of data; in the writing of the manuscript, or in the decision to publish the results.

The remaining authors declare that the research was conducted in the absence of any commercial or financial relationships that could be construed as a potential conflict of interest.

Publisher's note

Supplementary material

The Supplementary Material for this article can be found online at: https://www.frontiersin.org/articles/10.3389/fphar.2022.907579/full#supplementary-material

SUPPLEMENTARY FIGURE S1
Preliminary dilution range testing of cannabinoids in MPTP/MPP$^+$ protection assay. The percent protection from MPTP/MPP$^+$ induced cytotoxicity was initially measured at 5 concentrations to establish an effective dose range. * = $p < 0.05$. See manuscript for methods.

SUPPLEMENTARY FIGURE S2
Schematic representation of exposure paradigms for cell culture MPP$^+$/MPTP survival and Dopamine release assays, and the 6-OHDA larval zebrafish assay. Test = addition of test compound or mixture. hpf = hours post-fertilization.

References

Achenbach, J. C., Hill, J., Hui, J. P. M., Morash, M. G., Berrue, F., and Ellis, L. D. (2018). Analysis of the uptake, metabolism, and behavioral effects of cannabinoids on zebrafish larvae. *Zebrafish* 15, 349–360. doi:10.1089/zeb.2017.1541

Arshad, A., Chen, X., Cong, Z., Qing, H., and Deng, Y. (2014). TRPC1 protects dopaminergic SH-SY5Y cells from MPP+, salsolinol, and N-methyl-(R)-salsolinol-induced cytotoxicity. *Acta Biochim. Biophys. Sin.* 46, 22–30. doi:10.1093/abbs/gmt127

Bandres-ciga, S., Saez-Atienzar, S., Kim, J. J., Makarious, M. B., Faghri, F., Diez-Fairen, M., et al. (2020). Large-scale pathway specific polygenic risk and transcriptomic community network analysis identifies novel functional pathways in Parkinson disease. *Acta Neuropathol.* 140, 341–358. doi:10.1007/s00401-020-02181-3

Ben-shabat, S., Fride, E., Sheskin, T., Tamiri, T., Rhee, M. H., Vogel, Z., et al. (1998). An entourage effect: Inactive endogenous fatty acid glycerol esters enhance 2-arachidonoyl-glycerol cannabinoid activity. *Eur. J. Pharmacol.* 353, 23–31. doi:10.1016/s0014-2999(98)00392-6

Benvenutti, R., Marcon, M., Reis, C. G., Nery, L. R., Miguel, C., Herrmann, A. P., et al. (2018). N-acetylcysteine protects against motor, optomotor and morphological deficits induced by 6-OHDA in zebrafish larvae. *PeerJ* 6, e4957. doi:10.7717/peerj.4957

Blasco-benito, S., Seijo-Vila, M., Caro-Villalobos, M., Tundidor, I., Andradas, C., Garcia-Taboada, E., et al. (2018). Appraising the "entourage effect": Antitumor action of a pure cannabinoid versus a botanical drug preparation in preclinical models of breast cancer. *Biochem. Pharmacol.* 157, 285–293. doi:10.1016/j.bcp.2018.06.025

Budick, S. A., and O'malley, D. M. (2000). Locomotor repertoire of the larval zebrafish: Swimming, turning and prey capture. *J. Exp. Biol.* 203, 2565–2579. doi:10.1242/jeb.203.17.2565

Cassarino, D. S., Fall, C. P., Swerdlow, R. H., Smith, T. S., Halvorsen, E. M., Miller, S. W., et al. (1997). Elevated reactive oxygen species and antioxidant enzyme activities in animal and cellular models of Parkinson's disease. *Biochim. Biophys. Acta* 1362, 77–86. doi:10.1016/s0925-4439(97)00070-7

Catlow, B., and Sanchez-ramos, J. (2015). Cannabinoids for the treatment of movement disorders. *Curr. Treat. Options Neurol.* 17, 370. doi:10.1007/s11940-015-0370-5

Cogan, P. S. (2020). The 'entourage effect' or 'hodge-podge hashish': The questionable rebranding, marketing, and expectations of cannabis polypharmacy. *Expert Rev. Clin. Pharmacol.* 13, 835–845. doi:10.1080/17512433.2020.1721281

Couch, J. R., Grimes, G. R., Green, B. J., Wiegand, D. M., King, B., and Methner, M. M. (2020). Review of NIOSH cannabis-related health hazard evaluations and research. *Ann. Work Expo. Health* 64, 693–704. doi:10.1093/annweh/wxaa013

Cronin, A., and Grealy, M. (2017). Neuroprotective and neuro-restorative effects of minocycline and rasagiline in a zebrafish 6-hydroxydopamine model of Parkinson's disease. *Neuroscience* 367, 34–46. doi:10.1016/j.neuroscience.2017.10.018

Drapeau, P., Saint-Amant, L., Buss, R. R., Chong, M., Mcdearmid, J. R., and Brustein, E. (2002). Development of the locomotor network in zebrafish. *Prog. Neurobiol.* 68, 85–111. doi:10.1016/s0301-0082(02)00075-8

Feeney, M. P., Bega, D., Kluger, B. M., Stoessl, A. J., Evers, C. M., De Leon, R., et al. (2021). Weeding through the haze: A survey on cannabis use among people living with Parkinson's disease in the US. *NPJ Park. Dis.* 7, 21. doi:10.1038/s41531-021-00165-y

Feng, C. W., Wen, Z. H., Huang, S. Y., Hung, H. C., Chen, C. H., Yang, S. N., et al. (2014). Effects of 6-hydroxydopamine exposure on motor activity and biochemical expression in zebrafish (*Danio rerio*) larvae. *Zebrafish* 11, 227–239. doi:10.1089/zeb.2013.0950

Ferber, S. G., Namdar, D., Hen-Shoval, D., Eger, G., Koltai, H., Shoval, G., et al. (2020). The "entourage effect": Terpenes coupled with cannabinoids for the treatment of mood disorders and anxiety disorders. *Curr. Neuropharmacol.* 18, 87–96. doi:10.2174/1570159X17666190903103923

Finlay, D. B., Sircombe, K. J., Nimick, M., Jones, C., and Glass, M. (2020). Terpenoids from cannabis do not mediate an entourage effect by acting at cannabinoid receptors. *Front. Pharmacol.* 11, 359. doi:10.3389/fphar.2020.00359

Gan-or, Z., Dion, P. A., and Rouleau, G. A. (2015). Genetic perspective on the role of the autophagy-lysosome pathway in Parkinson disease. *Autophagy* 11, 1443–1457. doi:10.1080/15548627.2015.1067364

Gautam, C. S., and Saha, L. (2008). Fixed dose drug combinations (FDCs): Rational or irrational: A view point. *Br. J. Clin. Pharmacol.* 65, 795–796. doi:10.1111/j.1365-2125.2007.03089.x

Gonzalez-rodriguez, P., Zampese, E., and Surmeier, D. J. (2020). Selective neuronal vulnerability in Parkinson's disease. *Prog. Brain Res.* 252, 61–89. doi:10.1016/bs.pbr.2020.02.005

Greenamyre, J. T., and Hastings, T. G. (2004). Biomedicine. Parkinson's--divergent causes, convergent mechanisms. *Science* 304, 1120–1122. doi:10.1126/science.1098966

Greene, L. A., and Tischler, A. S. (1976). Establishment of a noradrenergic clonal line of rat adrenal pheochromocytoma cells which respond to nerve growth factor. *Proc. Natl. Acad. Sci. U. S. A.* 73, 2424–2428. doi:10.1073/pnas.73.7.2424

Heblinski, M., Santiago, M., Fletcher, C., Stuart, J., Connor, M., Mcgregor, I. S., et al. (2020). Terpenoids commonly found in cannabis sativa do not modulate the actions of phytocannabinoids or endocannabinoids on TRPA1 and TRPV1 channels. *Cannabis Cannabinoid Res.* 5, 305–317. doi:10.1089/can.2019.0099

Hu, R., Cao, Q., Sun, Z., Chen, J., Zheng, Q., and Xiao, F. (2018). A novel method of neural differentiation of PC12 cells by using Opti-MEM as a basic induction medium. *Int. J. Mol. Med.* 41, 195–201. doi:10.3892/ijmm.2017.3195

Jeon, C. Y., Jin, J. K., Koh, Y. H., Chun, W., Choi, I. G., Kown, H. J., et al. (2010). Neurites from PC12 cells are connected to each other by synapse-like structures. *Synapse* 64, 765–772. doi:10.1002/syn.20789

Langston, J. W., and Palfreman, J. (2014). *The case of the frozen addicts : How the solution of a medical mystery revolutionized the understanding of Parkinson's disease*. Amsterdam, The Netherlands: IOS Press.

Lavigne, J. E., Hecksel, R., Keresztes, A., and Streicher, J. M. (2021). Cannabis sativa terpenes are cannabimimetic and selectively enhance cannabinoid activity. *Sci. Rep.* 11, 8232. doi:10.1038/s41598-021-87740-8

Lederer, S., Dijkstra, T. M. H., and Heskes, T. (2019). Additive dose response models: Defining synergy. *Front. Pharmacol.* 10, 1384. doi:10.3389/fphar.2019.01384

Lin, K. J., Lin, K. L., Chen, S. D., Liou, C. W., Chuang, Y. C., Lin, H. Y., et al. (2019). The overcrowded crossroads: Mitochondria, alpha-synuclein, and the endo-lysosomal system interaction in Parkinson's disease. *Int. J. Mol. Sci.* 20, E5312. doi:10.3390/ijms20215312

Maayah, Z. H., Takahara, S., Ferdaoussi, M., and Dyck, J. R. B. (2020). The molecular mechanisms that underpin the biological benefits of full-spectrum cannabis extract in the treatment of neuropathic pain and inflammation. *Biochim. Biophys. Acta. Mol. Basis Dis.* 1866, 165771. doi:10.1016/j.bbadis.2020.165771

Mani, S., Sevanan, M., Krishnamoorthy, A., and Sekar, S. (2021). A systematic review of molecular approaches that link mitochondrial dysfunction and neuroinflammation in Parkinson's disease. *Neurol. Sci.* 42, 4459–4469. doi:10.1007/s10072-021-05551-1

Mclean, D. L., and Fetcho, J. R. (2004). Relationship of tyrosine hydroxylase and serotonin immunoreactivity to sensorimotor circuitry in larval zebrafish. *J. Comp. Neurol.* 480, 57–71. doi:10.1002/cne.20281

Milligan, C. J., Anderson, L. L., Bowen, M. T., Banister, S. D., Mcgregor, I. S., Arnold, J. C., et al. (2022). A nutraceutical product, extracted from Cannabis sativa, modulates voltage-gated sodium channel function. *J. Cannabis Res.* 4, 30. doi:10.1186/s42238-022-00136-x

More, S. V., and Choi, D. K. (2015). Promising cannabinoid-based therapies for Parkinson's disease: Motor symptoms to neuroprotection. *Mol. Neurodegener.* 10, 17. doi:10.1186/s13024-015-0012-0

Oultram, J. M. J., Pegler, J. L., Bowser, T. A., Ney, L. J., Eamens, A. L., and Grof, C. P. L. (2021). Cannabis sativa: Interdisciplinary strategies and avenues for medical and commercial progression outside of CBD and THC. *Biomedicines* 9, 234. doi:10.3390/biomedicines9030234

Paredes-rodriguez, E., Vegas-Suarez, S., Morera-Herreras, T., De Deurwaerdere, P., and Miguelez, C. (2020). The noradrenergic system in Parkinson's disease. *Front. Pharmacol.* 11, 435. doi:10.3389/fphar.2020.00435

Patricio, F., Morales-Andrade, A. A., Patricio-Martinez, A., and Limon, I. D. (2020). Cannabidiol as a therapeutic target: Evidence of its neuroprotective and neuromodulatory function in Parkinson's disease. *Front. Pharmacol.* 11, 595635. doi:10.3389/fphar.2020.595635

Peres, F. F., Lima, A. C., Hallak, J. E. C., Crippa, J. A., Silva, R. H., and Abilio, V. C. (2018). Cannabidiol as a promising strategy to treat and prevent movement disorders? *Front. Pharmacol.* 9, 482. doi:10.3389/fphar.2018.00482

Prakash, S., and Carter, W. G. (2021). The neuroprotective effects of cannabis-derived phytocannabinoids and resveratrol in Parkinson's disease: A systematic literature review of pre-clinical studies. *Brain Sci.* 11, 1573. doi:10.3390/brainsci11121573

Qi, Y., Wang, J. K., Mcmillian, M., and Chikaraishi, D. M. (1997). Characterization of a CNS cell line, CAD, in which morphological differentiation is initiated by serum deprivation. *J. Neurosci.* 17, 1217–1225. doi:10.1523/jneurosci.17-04-01217.1997

Reimann-philipp, U., Speck, M., Orser, C., Johnson, S., Hilyard, A., Turner, H., et al. (2020). Cannabis chemovar nomenclature misrepresents chemical and genetic diversity; survey of variations in chemical profiles and genetic markers in Nevada medical cannabis samples. *Cannabis Cannabinoid Res.* 5, 215–230. doi:10.1089/can.2018.0063

Russo, E. B. (2011). Taming THC: Potential cannabis synergy and phytocannabinoid-terpenoid entourage effects. *Br. J. Pharmacol.* 163, 1344–1364. doi:10.1111/j.1476-5381.2011.01238.x

Russo, E. B. (2018). The case for the entourage effect and conventional breeding of clinical cannabis: No "strain, " No gain. *Front. Plant Sci.* 9, 1969. doi:10.3389/fpls.2018.01969

Ryan, D., Drysdale, A. J., Lafourcade, C., Pertwee, R. G., and Platt, B. (2009). Cannabidiol targets mitochondria to regulate intracellular Ca2+ levels. *J. Neurosci.* 29, 2053–2063. doi:10.1523/JNEUROSCI.4212-08.2009

Santiago, M., Sachdev, S., Arnold, J. C., Mcgregor, I. S., and Connor, M. (2019). Absence of entourage: Terpenoids commonly found in cannabis sativa do not modulate the functional activity of d9-THC at human CB1 and CB2 receptors. *Cannabis Cannabinoid Res.* 4, 165–176. doi:10.1089/can.2019.0016

Severi, K. E., Portugues, R., Marques, J. C., O'Malley, D. M., Orger, M. B., and Engert, F. (2014). Neural control and modulation of swimming speed in the larval zebrafish. *Neuron* 83, 692–707. doi:10.1016/j.neuron.2014.06.032

Stasilowicz, A., Tomala, A., Podolak, I., and Cielecka-Piontek, J. (2021). Cannabis sativa L. As a natural drug meeting the criteria of a multitarget approach to treatment. *Int. J. Mol. Sci.* 22, E778. doi:10.3390/ijms22020778

Surmeier, D. J. (2018). Determinants of dopaminergic neuron loss in Parkinson's disease. *FEBS J.* 285, 3657–3668. doi:10.1111/febs.14607

Thanabalasingam, S. J., Ranjith, B., Jackson, R., and Wijeratne, D. T. (2021). Cannabis and its derivatives for the use of motor symptoms in Parkinson's disease: A systematic review and meta-analysis. *Ther. Adv. Neurol. Disord.* 14, 17562864211018561. doi:10.1177/17562864211018561

Turner, H., Chueh, D., Ortiz, T., Stokes, A. J., and Small-Howard, A. L. (2017). Cannabinoid therapeutics in Parkinson's disease: Promise and paradox. *J. Herbs, Spices Med. Plants* 23, 231–248. doi:10.1080/10496475.2017.1312724

Urbi, B., Corbett, J., Hughes, I., Owusu, M. A., Thorning, S., Broadley, S. A., et al. (2022). Effects of cannabis in Parkinson's disease: A systematic review and meta-analysis. *J. Park. Dis.* 12, 495–508. doi:10.3233/JPD-212923

Utsumi, H., Okuma, Y., Kano, O., Suzuki, Y., Iijima, M., Tomimitsu, H., et al. (2013). Evaluation of the efficacy of pramipexole for treating levodopa-induced dyskinesia in patients with Parkinson's disease. *Intern. Med.* 52, 325–332. doi:10.2169/internalmedicine.52.8333

Venderova, K., Ruzicka, E., Vorisek, V., and Visnovsky, P. (2004). Survey on cannabis use in Parkinson's disease: Subjective improvement of motor symptoms. *Mov. Disord.* 19, 1102–1106. doi:10.1002/mds.20111

Walsh, K. B., Mckinney, A. E., and Holmes, A. E. (2021). Minor cannabinoids: Biosynthesis, molecular Pharmacology and potential therapeutic uses. *Front. Pharmacol.* 12, 777804. doi:10.3389/fphar.2021.777804

Wiseman, M. S., Bates, T., Garfinkel, A., Ocamb, C. M., and Gent, D. H. (2021). First report of powdery mildew caused by golovinomyces ambrosiae on cannabis sativa in Oregon. *Plant Dis.* 105, 2733. doi:10.1094/PDIS-11-20-2455-PDN

Yenilmez, F., Frundt, O., Hidding, U., and Buhmann, C. (2021). Cannabis in Parkinson's disease: The patients' view. *J. Park. Dis.* 11, 309–321. doi:10.3233/JPD-202260

Zagzoog, A., Mohamed, K. A., Kim, H. J. J., Kim, E. D., Frank, C. S., Black, T., et al. (2020). *In vitro* and *in vivo* pharmacological activity of minor cannabinoids isolated from Cannabis sativa. *Sci. Rep.* 10, 20405. doi:10.1038/s41598-020-77175-y

Zhang, G., Buchler, I. P., Depasquale, M., Wormald, M., Liao, G., Wei, H., et al. (2019a). Development of a PC12 cell based assay for screening catechol-O-methyltransferase inhibitors. *ACS Chem. Neurosci.* 10, 4221–4226. doi:10.1021/acschemneuro.9b00395

Zhang, W., Sun, C., Shao, Y., Zhou, Z., Hou, Y., and Li, A. (2019b). Partial depletion of dopaminergic neurons in the substantia nigra impairs olfaction and alters neural activity in the olfactory bulb. *Sci. Rep.* 9, 254. doi:10.1038/s41598-018-36538-2

Glossary

ANOVA Analysis of Variance

Ca calcium

CaCl2-2H2O Calcium chloride

CB1 Cannabinoid receptor 1

CB2 Cannabinoid receptor 2

CBC Cannabichromene

CBD Cannabidiol

CBDV Cannabidivarin

CBG Cannabigerol

CBN Cannabinol

CC Carrier Control

DA Dopamine

DCR-MEM Defined Cannabinoid-Ratios Minimal Essential Mixture

ECB Endocannabinoid

E-MEM Equimolar Minimal Essential Mixture

GABA Gamma amino Butyric Acid

h hour

HE3 HEPES buffered E3

Hpf Hours Post Fertilization

KCl Potassium chloride

LID Levodopa Induced Dyskinesia

Lim Limonene

Lin Lanalool

MEM Minimal Essential Mixture

MeOH Methanol

MgSO4-7H2O Magnesium hydrate heptahydrate

MPP 1-methyl-4-phenylpyridinium

MPTP 1-methyl-4-phenyl-1,2,3,6-tetrahydropyridine

NaCl Sodium Chloride

Nero trans nerolidol

OHDA 6-hydroxydopamine

PD Parkinson's disease

Phyt Phytol

Pin alpha pinene

PRO Patient Reported Outcomes

SNpc Substantia Nigra pars compacta

TH Tyrosine Hydroxylase

THC Δ-9 tetrahydrocannabinol

TRPV1 Transient Receptor Potential cation channel subfamily V member 1

Frontiers in Pharmacology

Explores the interactions between chemicals and living beings

The most cited journal in its field, which advances access to pharmacological discoveries to prevent and treat human disease.

Discover the latest Research Topics

See more →

Frontiers

Avenue du Tribunal-Fédéral 34
1005 Lausanne, Switzerland
frontiersin.org

Contact us

+41 (0)21 510 17 00
frontiersin.org/about/contact